

2

AD-A260 252



ESL-TR-91-34



HYDRAZINE DECAY IN THE
ATMOSPHERE: CONTROLLED-
ENVIRONMENT CHAMBER STUDIES
AND KINETIC MODELING

DANIEL A. STONE AND JAMES R. LONG

AIR FORCE CIVIL ENGINEERING
SUPPORT AGENCY
RAV
TYNDALL AFB, FL 32403-6001



93-02985

FEBRUARY 1992

FINAL REPORT

OCTOBER 1987 - SEPTEMBER 1990

DTIC
ELECTE
FEB 17 1993
S E D

APPROVED FOR PUBLIC RELEASE:
DISTRIBUTION UNLIMITED



AIR FORCE ENGINEERING & SERVICES CENTER
ENGINEERING & SERVICES LABORATORY
TYNDALL AIR FORCE BASE, FLORIDA 32403

98 2 16 077

NOTICE

PLEASE DO NOT REQUEST COPIES OF THIS REPORT FROM
HQ AFESC/RD (ENGINEERING AND SERVICES LABORATORY).

ADDITIONAL COPIES MAY BE PURCHASED FROM:

NATIONAL TECHNICAL INFORMATION SERVICE
5285 PORT ROYAL ROAD
SPRINGFIELD, VIRGINIA 22161

FEDERAL GOVERNMENT AGENCIES AND THEIR CONTRACTORS
REGISTERED WITH DEFENSE TECHNICAL INFORMATION CENTER
SHOULD DIRECT REQUESTS FOR COPIES OF THIS REPORT TO:

DEFENSE TECHNICAL INFORMATION CENTER
CAMERON STATION
ALEXANDRIA, VIRGINIA 22314

REPORT DOCUMENTATION PAGE

Form Approved
 OMB No. 0704-0188

1a. REPORT SECURITY CLASSIFICATION UNCLASSIFIED		1b. RESTRICTIVE MARKINGS	
2a. SECURITY CLASSIFICATION AUTHORITY		3. DISTRIBUTION/AVAILABILITY OF REPORT Approved for Public Release. Distribution Unlimited.	
2b. DECLASSIFICATION/DOWNGRADING SCHEDULE		4. PERFORMING ORGANIZATION REPORT NUMBER(S)	
4. PERFORMING ORGANIZATION REPORT NUMBER(S)		5. MONITORING ORGANIZATION REPORT NUMBER(S)	
6a. NAME OF PERFORMING ORGANIZATION Air Force Civil Engineering Support Agency	6b. OFFICE SYMBOL (if applicable) RAVC	7a. NAME OF MONITORING ORGANIZATION	
6c. ADDRESS (City, State, and ZIP Code) HQ AFCESA/RAVC Tyndall AFB FL 32403-6001		7b. ADDRESS (City, State, and ZIP Code)	
8a. NAME OF FUNDING/SPONSORING ORGANIZATION Air Force Civil Engineering Support Agency	8b. OFFICE SYMBOL (if applicable) RAV	9. PROCUREMENT INSTRUMENT IDENTIFICATION NUMBER In-House	
8c. ADDRESS (City, State, and ZIP Code) HQ AFCESA/RAVC Tyndall AFB FL 32403-6001		10. SOURCE OF FUNDING NUMBERS	
		PROGRAM ELEMENT NO. 6.1	PROJECT NO. 0100
		TASK NO. 8314	WORK UNIT ACCESSION NO. NA
11. TITLE (Include Security Classification) (UNCLASSIFIED) Hydrazine Decay in the Atmosphere: Controlled-Environment Chamber Studies and Kinetic Modeling			
12. PERSONAL AUTHOR(S) Daniel A. Stone and James R. Long			
13a. TYPE OF REPORT Final	13b. TIME COVERED FROM <u>Oct 87</u> TO <u>Sep 90</u>	14. DATE OF REPORT (Year, Month, Day) February 1992	15. PAGE COUNT
16. SUPPLEMENTARY NOTATION Availability of this report is specified on reverse of front cover.			
17. COSATI CODES		18. SUBJECT TERMS (Continue on reverse if necessary and identify by block number)	
FIELD	GROUP	hydrazine, controlled-environment chamber, FT-IR spectroscopy, kinetic modeling, surface-catalyzed reactions	
07	04		
12	01		
19. ABSTRACT (Continue on reverse if necessary and identify by block number)			
<p>This report documents a series of experiments conducted to shed additional light on the role of surface-catalyzed reactions on the atmospheric oxidation of hydrazine vapor. The experiments were conducted in a controlled-environment chamber consisting of a one-meter diameter stainless steel sphere which is Teflon® coated. Vapor-phase hydrazine was introduced into the chamber at the 50-100 ppm concentration level. It was combined with four different synthetic atmospheric mixtures (all at one atmosphere total pressure): (1) dry helium, (2) humid (~75 percent R.H.) helium, (3) 80 percent dry helium plus 20 percent oxygen, and (4) 80 percent humid helium plus 20 percent oxygen.</p> <p>A series of experiments were conducted, using the same four synthetic atmospheres listed above, with several types of plates which were placed into a rack in the chamber. These plates included: Teflon®-coated aluminum (TCA), black iron (BI), corroded aluminum (CA), and F-16 painted aluminum (PA). The reactivity of the plates towards hydrazine decay was: TCA < BI = PA < CA.</p>			
20. DISTRIBUTION/AVAILABILITY OF ABSTRACT <input checked="" type="checkbox"/> UNCLASSIFIED/UNLIMITED <input type="checkbox"/> SAME AS RPT. <input type="checkbox"/> DTIC USERS		21. ABSTRACT SECURITY CLASSIFICATION UNCLASSIFIED	
22a. NAME OF RESPONSIBLE INDIVIDUAL Dr Daniel A. Stone		22b. TELEPHONE (Include Area Code) (904) 283-6061	22c. OFFICE SYMBOL HQ AFCESA/RAVC

Continuation of Block 19 (Abstract)

Kinetic data were generated from FT-IR spectra which were collected by using long-path optics located within the controlled-environment chamber. The absorbance values of the species being monitored followed Beer's law at the concentration levels employed in this research, so they were used directly to indicate relative species concentrations. The data were collected and processed by the instrument software supplemented with FORTRAN programs to facilitate data reduction and absorbance value measurements.

A series of potential reaction mechanisms were also developed. The kinetic processes represented by these mechanisms were modeled mathematically by using a specially developed non-linear least squares procedure based on a modified Marquardt algorithm. Several models were developed, but those with two reactive surface sites were the most successful in reproducing the experimental data. The model mechanisms gave useful insight into the kinds of kinetic processes which might be responsible for the observed behavior of the hydrazine in the chamber.

Finally, a series of experiments were conducted, as a part of this overall effort, to determine a reproducible value for an infrared absorption coefficient for two selected water lines. The coefficient determination was reasonably successful. However, under actual experimental conditions, water concentration values fluctuated too much to be very useful in any analytical sense.

Accession For	
NTIS CRA&I	<input checked="" type="checkbox"/>
DTIC TAB	<input type="checkbox"/>
Unannounced	<input type="checkbox"/>
Justification	
By	
Distribution /	
Availability Codes	
Dist	Avail and/or Special
A-1	

DTIC QUALITY INSPECTED 3

EXECUTIVE SUMMARY

Hydrazine is used as a fuel component in the Titan missile and, in a 30 percent water mixture, as an energy source for the emergency power unit in the F-16 aircraft. The need to transport, store, load and unload hydrazine in these systems results in some leaks and minor spills. There is also the ever-present potential for a massive spill when large quantities are involved. Because hydrazine is a toxic chemical and is a suspect human carcinogen, there is great concern that it be handled and transported safely. Strict regulation have been developed to ensure maximum worker and public safety from exposure to hydrazine vapors.

This project is the final phase of a series of laboratory studies designed to assess the potential hazards of hydrazine spills or leaks by characterizing the atmospheric fate of the resulting fugitive vapors. The research has focused on the role of surface-catalyzed reactions in the natural sequence of events which is likely to occur under field conditions. Previous studies have clearly shown that heterogeneous processes control the eventual fate of hydrazine vapors in the air.

To ensure maximum control over experimental variables, a new reaction chamber was constructed for this research effort. This chamber was designed to minimize wall interactions, provide temperature control, eliminate diffusion losses, and be evacuable. These design goals were realized by constructing a spherical stainless steel chamber and having it Teflon[®] coated, surrounded by heating/cooling coils, and well insulated. Chemical species concentrations were monitored with in situ long-path infrared spectroscopy.

The stability of hydrazine in the new chamber was a factor of four better than the Teflon[®]-film chambers used in previous work. However, there was still substantial interaction with the chamber walls and mirrors especially in the presence of oxygen and under humid conditions. These effects were carefully recorded and used as a baseline for later experiments.

To characterize the reactivity of a specific type of surface, a series of plates with the surface in question were placed in a supporting rack inside the chamber. The surfaces studied included: Teflon[®]-coated aluminum plates, black iron plates, corroded aluminum plates, and F-16 painted aluminum plates. Time and resources did not permit the study of additional surfaces or the use of substituted hydrazine fuels.

As an integral part of the experimental approach used in this research, mathematical models were developed to aid in the definition of kinetic reaction pathways. These models provided a

means of evaluating different proposed reaction pathways and assisted in experimental protocol development. Earlier models which only followed the concentration of one reactant were extended to use concentration-time data from two chemical species.

The reactivities of the surfaces generally followed the patterns seen in previous studies. The addition of Teflon[®]-coated plates to the reactor resulted in a five-fold increase in hydrazine decay. This increased by another factor of two in the presence of 20 percent oxygen. These results demonstrated that the Teflon[®] coating and/or the other surfaces present in the chamber still exerted substantial influence on the chemical processes which occur therein.

The reactivities of the black iron and painted aluminum plates were about the same and were about 10 times faster than the baseline reactivity of the chamber with the additional Teflon[®]-coated aluminum plates. This result showed that more reactive surfaces did result in a substantial increase in the destruction of hydrazine vapor under simulated atmospheric conditions. These results were also reflected in the model fits to these data where key rate constants were much larger for black iron and painted aluminum plates than they were for Teflon[®]-coated aluminum plates.

The most reactive of all the plates were the corroded aluminum. This observation confirmed similar findings of earlier researchers. However, the present study differs in the proposed reaction mechanism used to explain the observed reaction intermediates.

The results of this study help to substantiate and extend the findings of previous researchers. Hydrazine vapors may be removed from the atmosphere by a number of chemical and physical processes. For each release scenario, the combination of these factors must be carefully considered. Where surfaces are prominent, as in indoor or near-earth areas, the adsorption and subsequent reactions of hydrazine are a major factor in its removal from the environment. In the open air, homogeneous processes, such as its reaction with ozone and hydroxyl radicals are most likely to be the controlling removal factors.

PREFACE

This report was prepared by the Civil Engineering Laboratory of the Air Force Civil Engineering Support Agency (AFCESA), Tyndall Air Force Base FL 32403-6001.

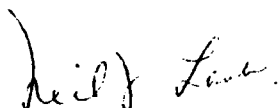
This research was sponsored by AFCESA. Dr Daniel A. Stone and Mr James R. Long (AFCESA/RAVC) were the government project officers. This report summarizes work accomplished between October 1987 and September 1990 under program element 61101F.

This report has been reviewed by the Public Affairs Office (PA) and is releasable to the National Technical Information Service (NTIS). At NTIS, it will be available to the general public, including foreign nationals.

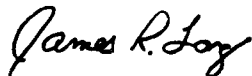
This technical report has been reviewed and is approved for publication.



DANIEL A. STONE, PhD
Project Officer



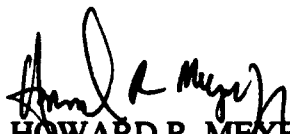
NEIL J. LAMB, Lt Col, USAF, BSC
Chief, Environics Division



JAMES R. LONG, GS-9
Project Officer



FRANK P. GALLAGHER III, Colonel, USAF
Director, Air Force Civil Engineering Laboratory



HOWARD R. MEYER, Jr. Maj, USAF
Chief, Research and Development Branch

TABLE OF CONTENTS

Section	Title	Page
I	INTRODUCTION	1
	A. OBJECTIVE	1
	B. BACKGROUND	1
	C. SCOPE	2
II	EXPERIMENTAL PROCEDURES	3
	A. SPHERICAL REACTION CHAMBER	3
	1. Design	3
	2. Construction	3
	3. Performance	4
	B. MATERIALS	6
	1. Test Plates	6
	2. Hydrazine	7
	3. Methane	7
	4. Helium	7
	5. Oxygen	7
	6. Water	7
	C. METHODS AND PROCEDURES	7
	1. Sample Preparation and Introduction	7
	2. FT-IR Spectrometer Operation	7
III	MATHEMATICAL KINETIC MODELS	9
	A. INTRODUCTION	9
	1. One-Measurement Models	9
	a. Review of Previous Studies	9
	b. Current Studies	10
	2. Model Revisions	13
	3. Model Development	14
	4. Two-Measurement Models	17
	a. MOD310	18
	b. MOD315	20
	c. MOD350	21

TABLE OF CONTENTS
(Continued)

Section	Title	Page
	d. MOD360	23
	e. MOD361	24
	f. MOD370	25
	g. MOD375	27
	h. MOD380	28
	i. MOD385	29
	j. MOD390	30
IV	RESULTS AND DISCUSSION	32
	A. NO ADDED PLATES	32
	B. TEFLON®-COATED ALUMINUM PLATES	42
	C. WATER CALIBRATION SPECTRA	43
	D. BLACK IRON PLATES	52
	E. CORRODED ALUMINUM PLATES	57
	F. ADDITIONAL BASELINE REACTIVITY RUNS (NO ADDED PLATES)	62
	G. PAINTED ALUMINUM PLATES	66
V	CONCLUSIONS AND RECOMMENDATIONS	70
	A. NO ADDED PLATES	70
	B. TEFLON®-COATED ALUMINUM PLATES	71
	C. WATER CALIBRATION SPECTRA	71
	D. BLACK IRON PLATES	72
	E. CORRODED ALUMINUM PLATES	72
	F. PAINTED ALUMINUM PLATES	73
	G. RECOMMENDATIONS FOR ADDITIONAL RESEARCH	74
VI	REFERENCES	75

TABLE OF CONTENTS
(Continued)

Section	Title	Page
APPENDIX		
A	FLOW DIAGRAM FOR DATA ACQUISITION AND ANALYSIS	76
B	SOFTWARE LISTING FOR THE PROGRAM USED FOR OVERALL CONTROL OF FT-IR DATA ACQUISITION AND STORAGE	77
C	SOFTWARE LISTINGS FOR THE FORTRAN PROGRAM USED TO CONTROL DATA ACQUISITION TIMING FROM THE 1280 DATA STATION CLOCK	79
D	SOFTWARE LISTING FOR THE FORTRAN PROGRAM USED TO READ AND REPORT THE CHAMBER TEMPERATURE	81
E	SOFTWARE LISTING FOR THE FORTRAN PROGRAM USED TO READ AND REPORT THE CHAMBER RELATIVE HUMIDITY	84
F	SOFTWARE LISTING FOR THE FORTRAN PROGRAM USED TO PROCESS AND SEND CHAMBER DATA TO AN EXTERNAL COMPUTER FOR ANALYSIS AND PLOTTING	87
G	SOFTWARE LISTING FOR THE FORTRAN PROGRAM USED TO CALCULATE THE BASELINE-CORRECTED ABSORBANCE VALUE FOR HYDRAZINE VAPOR AT 957 WAVENUMBERS	95
H	SOFTWARE LISTING FOR THE FORTRAN PROGRAM USED TO CALCULATE THE BASELINE-CORRECTED ABSORBANCE VALUES FOR METHANE VAPOR AT 3018 AND 1305 WAVENUMBERS	98
I	SOFTWARE LISTING FOR THE FORTRAN PROGRAM USED TO CALCULATE THE BASELINE-CORRECTED ABSORBANCE VALUE FOR AMMONIA VAPOR AT 967 WAVENUMBERS	104
J	SOFTWARE LISTING FOR THE FORTRAN PROGRAM USED TO CALCULATE THE BASELINE-CORRECTED ABSORBANCE VALUE FOR WATER VAPOR AT 1700 WAVENUMBERS	108

TABLE OF CONTENTS
(Concluded)

Section	Title	Page
APPENDIX		
K	WATER CALIBRATION DATA INCLUDING BOTH VAPOR AND LIQUID SAMPLES	112
L	SOFTWARE LISTING FOR THE GWBASIC PROGRAM USED TO CALCULATE ABSORBANCE VALUES AS A FUNCTION OF FIXED TIME INTERVALS	121
M	SUMMARY OF THE EXPERIMENTS CONDUCTED IN THE SPHERICAL CHAMBER	122
N	SUMMARY OF MODEL FITTING DATA FOR RUNS WITH NO ADDED PLATES	127
O	SUMMARY OF MODEL FITTING DATA FOR RUNS WITH TEFLON®-COATED ALUMINUM PLATES	145
P	SUMMARY OF MODEL FITTING DATA FOR RUNS WITH BLACK IRON PLATES	154
Q	SUMMARY OF MODEL FITTING DATA FOR RUNS WITH CORRODED ALUMINUM PLATES	164
R	SUMMARY OF MODEL FITTING DATA FOR RUNS WITH PAINTED ALUMINUM PLATES	174
S	REPRESENTATIVE MODEL FITS -- PLOTS FOR HYDRAZINE AND AMMONIA (SINGLE SELECTED RUNS)	184
T	SOFTWARE LISTING FOR FORTRAN NONLINEAR LEAST SQUARES FITTING PROGRAM	192

LIST OF FIGURES

Figure	Title	Page
1	Schematic Diagram of the Spherical Chamber Viewed from the Sample Introduction Port Side	4
2	Schematic Diagram of the Spherical Chamber Viewed from the Side Opposite the Sample Introduction Port	4
3	Schematic Drawing of the Optical Path from the FT-IR Spectrometer through the Spherical Chamber to the Detector	5
4	Representative Spectrum of 20 ppm Methane and 50 ppm Hydrazine	5
5	Plot of Normalized Methane Absorbance versus Time in the Spherical Chamber	32
6	Plots of Methane and Sulfur Hexafluoride Absorbance versus Time in the Spherical Chamber	33
7	Plots of Normalized Hydrazine Absorbance versus Time in Pure Dry Helium (No Added Plates)	34
8	Comparison of Beginning and Ending Spectra from a Hydrazine Desorption Experiment in the Spherical Chamber (No Added Plates)	35
9	Plots of Hydrazine Decay in the Spherical Chamber in Pure, Dry Helium (Series Two and Three, No Added Plates)	37
10	Plots of Hydrazine Decay in the Spherical Chamber in 80 Percent Helium and 20 Percent Oxygen (Dry Conditions, No Added Plates)	38
11	Plot of Hydrazine Decay in the Spherical Chamber Before and After Coating the Mirrors and Other Metal Surfaces with Paraffin Wax (No Added Plates)	40
12	Plot of Hydrazine Decay in Dry Helium from 20 Apr 89 to 5 May 89 (No Added Plates)	41
13	Plots of Hydrazine Decay in the Spherical Chamber with 20 FEP Teflon®-Coated Aluminum Plates	42
14	Part of the Water Vapor Infrared Spectrum Showing the Analytical Peaks Used in the Quantitative Measurements	44

LIST OF FIGURES
(Continued)

Figure	Title	Page
15	Calibration Curve for 0.0 ppm Water	46
16	Calibration Curve for 2.55 ppm Water	46
17	Calibration Curve for 5.1 ppm Water	46
18	Calibration Curve for 12.8 ppm Water	46
19	Calibration Curve for 25.5 ppm Water	46
20	Calibration Curve for Water Vapor Based on the Zero Time Intercept Data from Figures 12-16	47
21	Plot of Absorbance Versus Concentration and Measurement Time for the Water Data	49
22	Plot of Expected versus Predicted Absorbance Values Based on the Water Calibration Plan Shown in Figure 18	50
23	Hydrazine Decay in Pure, Dry Helium (No Added Plates)	53
24	Hydrazine Decay in Pure, Dry Helium with 19 Black Iron Plates	54
25	Hydrazine Decay with 19 Black Iron Plates in 80 Percent Dry Helium and 20 Percent Oxygen.	55
26	Hydrazine Decay with 19 Black Iron Plates in 80 Percent Helium and 20 Percent Oxygen with 50 Percent Relative Humidity	56
27	Comparison of Diimide Spectra from Tuazon, et. al. (Reference 8) and This Work..	56
28	Hydrazine Decay in Pure, Dry Helium with One Corroded Aluminum Plate	57
29	Hydrazine Decay in 80 Percent Helium and 20 Percent Oxygen with One Corroded Aluminum Plate	58
30	Hydrazine Decay in 80 Percent Helium and 20 Percent Oxygen (Under Humid Conditions) with One Corroded Aluminum Plate	59
31	Hydrazine Decay in 80 Percent Helium and 20 Percent Oxygen with One Corroded Aluminum Plate. Spectra were acquired at the Beginning, Middle, and End of the Run	60

LIST OF FIGURES

(Continued)

Figure	Title	Page
32	Diimide Formation in the Decay of Hydrazine in 80 Percent Humid Helium and 20 Percent Oxygen with One Corroded Aluminum Plate	61
33	Plots of Hydrazine, Diimide, and Hydrogen Peroxide Showing their Relative Band Positions for Spectral Identification	61
34	Hydrazine Decay in Pure, Dry Helium (No Added Plates)	62
35	Hydrazine Decay in Humid Helium (No Added Plates)	63
36	Hydrazine Decay in Dry Helium with 20 Percent Oxygen (No Added Plates)	64
37	Hydrazine Decay in Humid Helium with 20 Percent Oxygen (No Added Painted Aluminum Plates)	65
38	Hydrazine Decay in Dry Helium (with 20 Added Painted Aluminum Plates)	66
39	Hydrazine Decay in Dry Helium and 20 Percent Oxygen (with 20 Added Painted Aluminum Plates)	68
40	Hydrazine Decay in Humid Helium (with 20 Added Painted Aluminum Plates)	68
41	Hydrazine Decay in Humid Helium with 20 Percent Oxygen (with 20 Added Painted Aluminum Plates)	69
S1	Model (MOD361) Fits for Hydrazine and Ammonia for the Run Conducted on 18 Apr 90 (Dry Helium, no Plates)	184
S2	Model (MOD 361) Fits for Hydrazine and Ammonia for the Run Conducted on 04 May 90 (Humid Helium, no Plates)	185
S3	Model (MOD310) Fits for Hydrazine and Ammonia for the Run Conducted on 25 May 90 (80 Percent Dry Helium and 20 Percent Oxygen, No Plates)	185
S4	Model (MOD361) Fits for Hydrazine and Ammonia for the Run Conducted on 04 Jun 90 (80 Percent Humid Helium and 20 Percent Oxygen, No Plates)	186
S5	Model (MOD370) Fits for Hydrazine and Ammonia for the Run Conducted on 16 Jan 90 (80 Percent Humid Helium and 20 Percent Oxygen, with 19 Black Iron Plates)	186

LIST OF FIGURES
(Concluded)

Figure	Title	Page
S6	Model (MOD370) Fits for Hydrazine and Ammonia for the Run Conducted on 20 Jul 90 (80 Percent Dry Helium and 20 Percent Oxygen, with 20 Painted Aluminum Plates)	187
S7	Model (MOD360) Fits for Hydrazine and Ammonia for the Run Conducted on 04 Jan 90 (80 Percent Dry Helium and 20 Percent Oxygen, with 19 Black Iron Plates)	187
S8	Model (MOD350) Fits for Hydrazine and Ammonia for the Run Conducted on 11 Jan 90 (80 Percent Dry Helium and 20 Percent Oxygen, with 19 Black Iron Plates)	188
S9	Model (MOD310) Fits for Hydrazine and Ammonia for the Run Conducted on 27 Jul 90 (80 Percent Dry Helium and 20 Percent Oxygen, with 20 Painted Aluminum Plates)	188
S10	Model (MOD350) Fits for Hydrazine and Ammonia for the Run Conducted on 01 Aug 90 (Humid Helium 20 Painted Aluminum Plates)	189
S11	Model (MOD310) Fits for Hydrazine and Ammonia for the Run Conducted on 07 Aug 90 (80 Percent Humid Helium and 20 Percent Oxygen, with 20 Painted Aluminum Plates)	189
S12	Model (MOD315) Fits for Hydrazine and Ammonia for the Run Conducted on 15 Mar 90 (Dry Helium and 1 Corroded Aluminum Plate)	190
S13	Model (MOD315) Fits for Hydrazine and Ammonia for the Run Conducted on 27 Mar 90 (80 Percent Dry Helium and 20 Percent Oxygen, with 1 Corroded Aluminum Plate)	190
S14	Model (MOD375) Fits for Hydrazine and Ammonia for the Run Conducted on 29 Mar 90 (80 Percent Humid Helium and 20 Percent Oxygen, with 1 Corroded Aluminum Plate)	191

LIST OF TABLES

Table	Title	Page
1	WATER CALIBRATION DATA GENERATED FROM THE BEST FIT LINES OF ABSORBANCE-TIME PLOTS FOR EACH CONCENTRATION VALUE	48
2	WATER CALIBRATION DATA. COMPARISON OF ACTUAL CONCENTRATIONS INJECTED VERSUS CONCENTRATIONS CALCULATED FROM BEST FIT PLANE (DATA ARE FROM JULY - AUGUST 1989)	51

SECTION I

INTRODUCTION

A. OBJECTIVE

This research was conducted to extend our knowledge of the chemical and physical processes which control the eventual fate of vapor-phase hydrazine in the environment. It included both analytical measurements in a controlled-environment chamber and the use of computer models to formulate and test decay mechanisms.

Hydrazine spills can occur during both normal operations and in accidents. The vapors which escape have a finite lifetime which depends on their interactions with both surfaces and in the open atmosphere. This study was undertaken in a chamber which allowed more complete control of critical experimental variables than was previously possible.

B. BACKGROUND

Hydrazine is used extensively in small thrusters for satellites, as a fuel cell reactant, in emergency and auxiliary power generating units, and as a liquid rocket fuel component. Both routine handling and accidental spills can produce fuel vapors which constitute a substantial human health risk. Hydrazine is classified as an animal carcinogen and a suspect human carcinogen. The concern for its potential toxicity is reflected in its low threshold limit value for exposure of 100 parts-per-billion. This combination of routine use and known toxicity has prompted a number of studies of the environmental fate of hydrazine in both soil and atmospheric environments.

The relevant past research on the atmospheric fate of hydrazine vapor has been reviewed in the introduction of a previous AFESC technical report (Reference 1). Subsequent research was conducted by Stone and Wiseman (Reference 1) and by Martin, et. al. (Reference 2). The results of both research groups were summarized in another publication (Reference 3). The main conclusions of these research efforts were:

- Hydrazine decay by homogeneous (i.e., strictly gas-phase) reactions proceeds at a negligible rate under normal atmospheric conditions.

- Hydrazine interacts strongly with many surfaces including Teflon[®] film. These interactions are enhanced by the presence of water vapor and are only partially reversible.
- Kinetic models which include second-order adsorption processes can successfully describe the decay of hydrazine as observed in the Teflon[®]-film chambers including the conditioning which occurs in sequential experimental runs..
- Products formed from the atmospheric (surface-catalyzed) oxidation of hydrazine were mainly water and (by inference) nitrogen. Small amounts of ammonia were also formed under some conditions. Diimide (N₂H₂) was detected in small amounts as a reactive intermediate with some of the high-surface area samples added to the chambers.

These previous studies showed that both permeation and adsorption were important processes in the decay of hydrazine vapor. The current study was undertaken to see if a solid chamber could give more complete mechanistic and kinetic results by enabling a greater degree of control over experimental conditions.

C. SCOPE

This study included the design and construction of a new controlled-environment chamber and the subsequent characterization and calibration of this chamber. The baseline stability of hydrazine in the chamber was determined. Then the effects of added surfaces (in the form of thin metal plates set inside the chamber in a special rack) were determined. Finally, additional efforts were devoted to the development of improved computer models to define potential reaction mechanisms.

SECTION II

EXPERIMENTAL PROCEDURES

A. SPHERICAL REACTION CHAMBER

1. Design. To overcome some experimental difficulties encountered with the 320-liter, Teflon[®]-film reaction chamber used in earlier laboratory studies (Reference 1), a new controlled-atmosphere environmental simulation chamber was constructed. The design and construction details for this chamber have been previously described (References 4 and 5) and will only be briefly outlined here.

The primary design consideration for this chamber was to minimize surface interactions. To this end, a spherical design was adopted giving the lowest surface-to-volume ratio of any simple geometrical solid. The chamber was also coated with a 10-mil thick layer of FEP Teflon[®]. The size of the chamber was chosen to give a reasonable tradeoff between optical path length and internal volume. The choice of a 1-meter diameter sphere gave a working optical path length of 106 meters while maintaining a manageable volume of about 525 liters.

2. Construction. The chamber was constructed of 3/16-in stainless steel hemispheres welded together. Three 12-inch circular ports are welded to corresponding openings in the chamber wall. Two are diametrically opposed across the horizontal diameter. These contain mounts for the long-path infrared optics. The third port is placed at right angles to the line joining the other two. It is used for introducing surface samples into the chamber. There are several other ports in the chamber wall. One 4-inch optical view ports is placed above each of the 12-inch mirror mounting ports. These facilitate mirror alignment. There are additional ports for pressure measuring devices, a temperature/humidity probe, a stirring fan, and a high-vacuum pumping station. The chamber is shown schematically in Figure 1.

The chamber has copper coils welded to its outer surface for temperature control. It is also surrounded by 1.5 inches of Rubatex[®] high-density foam insulation. With the heating/cooling recirculation unit operating, the chamber temperature can be varied from 6.4 °C to 46.6 °C.

A control panel and glass sample introduction manifold are mounted on an aluminum frame which is attached to the chamber on the side opposite the sample introduction port. The control panel provides a mount for the temperature gauge and for two different pressure gauges. The chamber is shown schematically from this viewpoint in Figure 2.

The optical system for the chamber was designed to provide the maximum possible pathlength within the 1-meter mirror separation constraint. This was

accomplished by using a modification of the basic White (Reference 6) 3-mirror system as suggested by Olson (Reference 7). The chamber optical system is interfaced to a Nicolet Model 160-SX Fourier transform infrared (FT-IR) spectrometer. The optical interface is diagrammed in Figure 3. The entire optical path is purged with pure, dry air provided by an in-house system (Reference 4).

3. Performance. Typical performance of the chamber optical system is shown in a representative spectrum of hydrazine vapor with methane as an internal standard in one atmosphere of dry helium. This spectrum was acquired under the following conditions: a path length of 106 meters, a resolution of 1.0 cm^{-1} , and 256 scans. Signal-to-noise levels drop beyond $2,000\text{ cm}^{-1}$, but useable spectra can be obtained at frequencies beyond $4,000\text{ cm}^{-1}$.

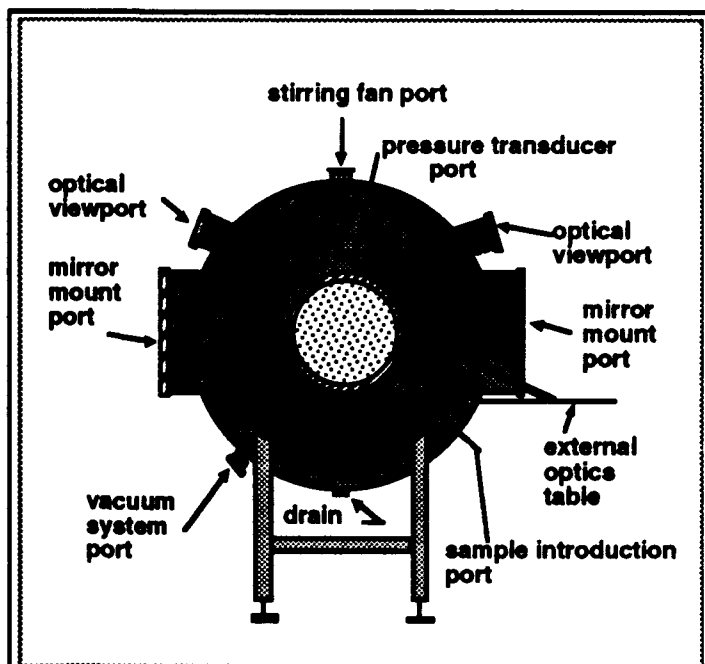


Figure 1. Schematic Diagram of the Spherical Chamber Viewed from the Sample Introduction Port Side.

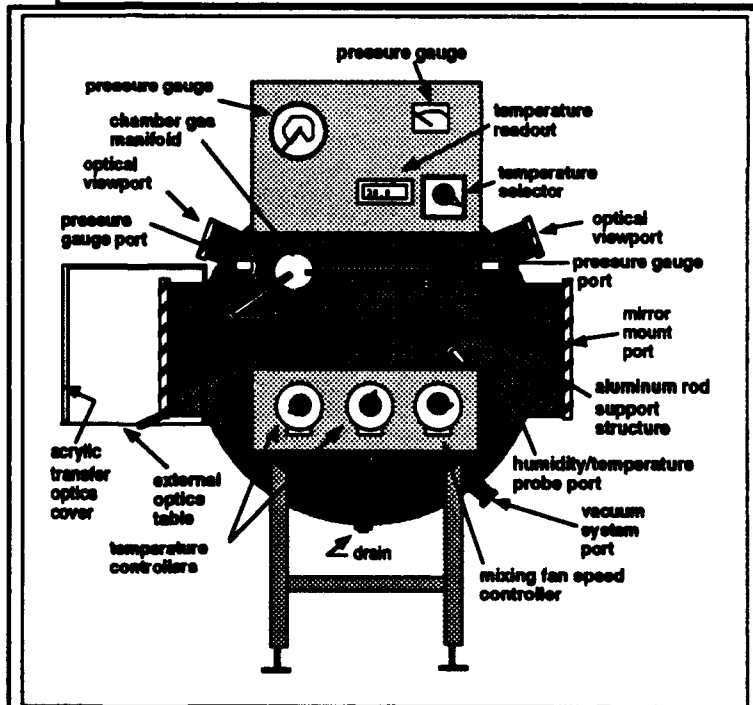


Figure 2. Schematic Diagram of the Spherical Chamber Viewed from the Side Opposite the Sample Introduction Port.

TOP VIEW

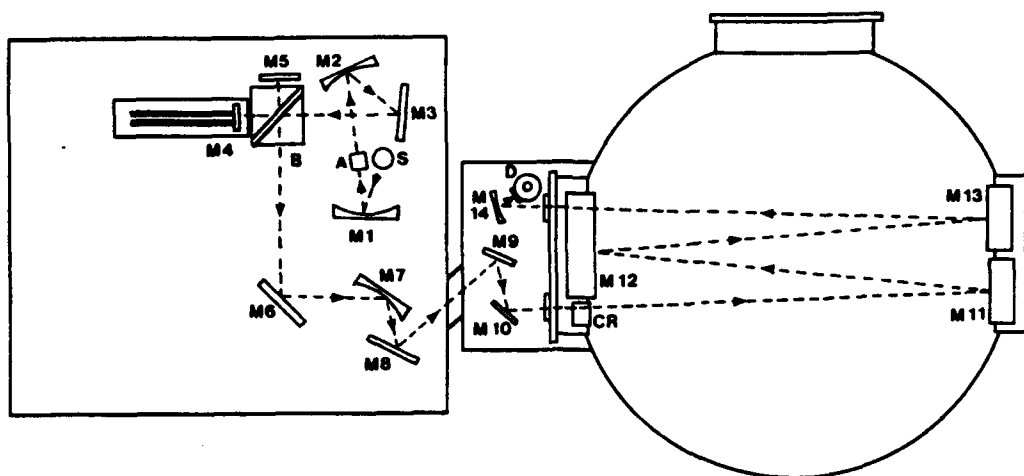


Figure 3. Schematic Drawing of the Optical Path from the FT-IR Spectrometer, through the Long Path Chamber to the Detector.

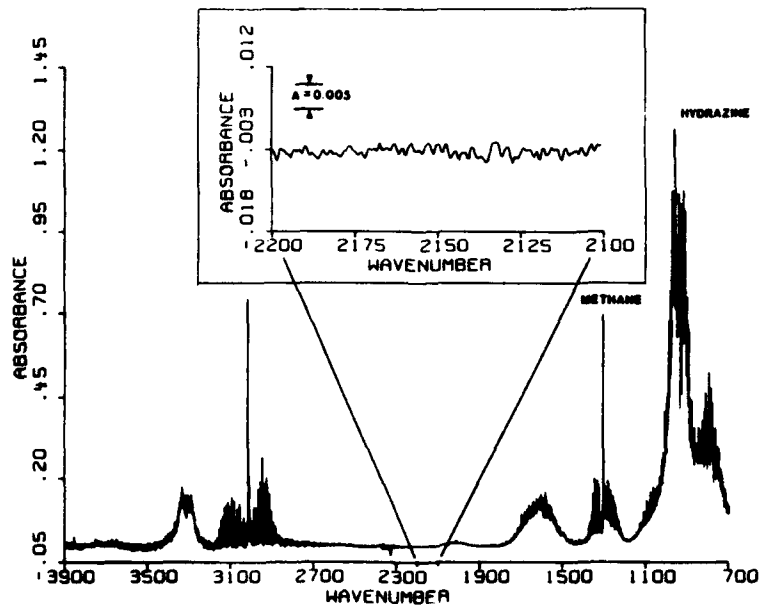


Figure 4. Representative Spectrum of 20 ppm Methane and 50 ppm Hydrazine. Conditions were: resolution, 1.0 cm^{-1} ; 256 coadded scans; path length 106 meters. The Inset Shows an Expansion of the $2200\text{-}2100 \text{ cm}^{-1}$ Region Demonstrating the Low Peak-to-Peak Noise Level.

B. MATERIALS

1. Test Plates. To characterize the effects of different 'operational' surfaces on the air oxidation rate and kinetics of hydrazine vapor, several sets of metal plates were obtained. These plates were sized to (a) fit into a Teflon[®]-coated rack which was placed inside the chamber, and (b) have approximately the same surface area as the interior of the chamber. To achieve these design goals, 20 plates were fabricated which were 35.5 cm long by 20.2 cm wide. The total surface area of each plate was 0.143 meter², giving a total surface area of 2.87 meter². The interior surface area of the chamber was about 3.14 meter². The following types of plates were used:

•Teflon[®]-coated aluminum. These plates were coated with the same FEP Teflon[®] as the interior of the chamber. They were used to evaluate the reactivity of the Teflon[®] coating in the chamber. The plates were washed in a 2 percent solution of Micro[®] liquid laboratory cleaner (International Products Corp, Trenton, NJ), rinsed with hot tap water, then distilled water, and finally with a 50 percent methanol - 50 percent acetone solution. They were then kept wrapped in clean paper towels covered with aluminum foil until they were placed in the chamber.

•black iron. These plates were used to evaluate the reactivity of hydrazine vapor in contact with iron surfaces. The plates were scrubbed with fine steel wool and then cleaned and stored as described above.

•corroded aluminum. To verify the results from a parallel study at the NASA White Sands Test Facility, funded by AFESC (Reference 2), corroded aluminum plates were prepared. Twenty plates were supported upright, spaced 1/2 inch apart, in a Teflon[®] holder then covered with about 45 liters of tap water in a deep sink. Then about 250 grams of solid calcium hypochlorite were added. Finally, a stream of air was bubbled through the water at about 15 liters/min. The plates were kept in the water for about 6 weeks. During this time, a grey-white, gelatinous material (probably Bayerite [Reference 8]) formed on the surfaces of the plates. The plates were removed from the water and air-dried, causing a rather coarse white powder to form on the surfaces. The excess was removed by tapping the plates gently against a table top. Then they were stored as described above.

•painted aluminum. These plates were used to characterize the reactivity of the surface of an F-16 aircraft. Twenty plates were primed and painted by the aircraft maintenance personnel at Tyndall AFB with the type of painted used in the F-16. These were washed and rinsed and stored for use as described above.

2. Hydrazine. The hydrazine used in this study (Aldrich, 98 percent pure) was transferred under argon to a distillation apparatus, refluxed over reagent grade NaOH for 4 hours and then distilled. The fraction collected at 113.5 °C was transferred under argon and stored in a Pyrex® flask with a Teflon® vacuum valve.

3. Methane. The methane used in this study was Fisher high-purity grade (99.99 percent).

4. Helium. The helium used was high-purity grade (99.995 percent).

5. Oxygen. The oxygen used was ultra-high-purity (99.99 percent).

6. Water. The water used was laboratory distilled water.

C. METHODS AND PROCEDURES

1. Sample Preparation and Introduction. Samples of hydrazine vapor were prepared on the portable vacuum system described previously (Reference 4, pp. 20-21). A 5-liter Pyrex® flask with Teflon® vacuum valves (Kontes, Cat. No. 826600-004) at both ends was filled to 8 Torr with hydrazine vapor, then flushed into the chamber with helium. For runs conducted under simulated atmospheric conditions, 150 Torr of oxygen were added to 610 Torr of helium. The mixing fan was operated during the filling process. All runs were made at 760 Torr total pressure in the chamber and at 20 °C (unless otherwise noted)..

Methane was added to some runs as an internal standard. It was added as a 10 cc sample from a gas syringe (1 atmosphere sample pressure) injected into the chamber sample manifold during the chamber fill procedure.

Water was added to the chamber to create 'humid' conditions, i.e., approximately 50 percent relative humidity. This was accomplished by injecting 5 mL of liquid water into the chamber sample manifold, then heating and evaporating the water into the chamber.

2. FT-IR Spectrometer Operation. The FT-IR spectrometer used in this study was a Nicolet model 6000C which had been upgraded to model 160SX specifications. It includes a 1280 processor with coprocessor, 256K of 20-bit word memory, 24Mbyte hard drive, 1 Mbyte (8-in) floppy drive, and a Write Once Read Many optical storage accessory (Nicolet Maxtor Model RXT-800S). Unless otherwise noted, spectra were run at 1.0 cm⁻¹ resolution using a specially-

fabricated mercury-cadmium-telluride A (MCT-A) detector (Infrared Associates Model NB FTIR). The number of coadded scans per spectrum varied from 16 to 256 with 128 being the most common. Spectra were acquired under instrument control using the Nicolet FT-IR control language and the MACRO commands it provides.

Molecular species of interest were monitored by recording their absorption spectra as a function of time. A pathlength of 106 meters was used for most of the study, however, this was shortened to 50 meters toward the end of the experiments because of mirror surface degradation.

A background spectrum for a particular experiment was obtained by co-adding 1024 instrument scans and storing the result. Subsequently acquired sample spectra were ratioed against this stored background spectrum to give absorbance spectra. A typical experimental run was conducted as follows. Immediately after the chamber was filled to begin an experimental run, the FT-IR spectrometer was placed under software control for automatic data acquisition, processing, storage and plotting. The initial spectrum was acquired within 3-5 minutes after the chamber was filled. Then spectra were acquired at regular intervals thereafter as set by the system control software. The resulting data, including time, species absorbance values, humidity, and temperature, were sent to an open computer file and stored in ASCII format for offline processing and plotting. All of these operations and calculations were handled automatically by the instrument's MACRO software. (See Appendix A for a data acquisition flow diagram, and Appendix B-I for data acquisition and processing software program listings.)

SECTION III

MATHEMATICAL KINETIC MODELS

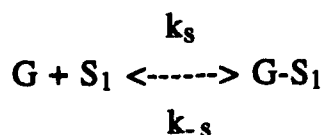
A. INTRODUCTION

1. One-Measurement Models

a. Review of Previous Studies

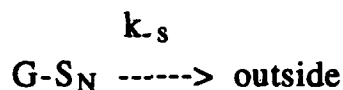
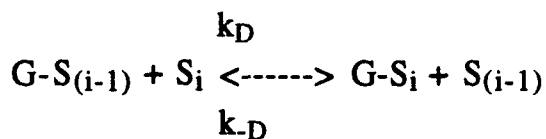
Prior to the work described in this report, research was conducted to investigate and characterize the decay and/or disappearance of hydrazine in an environmental chamber. (Reference 3) The study employed two fluorocarbon-film environmental chambers. The chambers were of different size with one having a surface to volume (S/V) ratio of 8.9 m^{-1} and the other a S/V ratio of 3.4 m^{-1} . The first chamber had a capacity of 320 L and the second had a capacity of 6520 L. Each of these chambers were enclosed in a larger chamber such that the external environment could be controlled in terms of temperature and humidity. The appropriate IR bands were monitored to follow the decay processes of hydrazine and some of its derivatives which were also studied.

A modified Marquardt algorithm using an Euler method of numeric integration was used to estimate the parameters of proposed models which characterized the loss processes. There were two types of models investigated. The first model was a permeation model which treated the fluorocarbon film as a series of permeable pore layers. With this approach the first expression in the model was,



where G was the gas, k_s and k_{-s} were the adsorption and desorption rate constants S_1 was the inside pore layer of the chamber wall. Since the film had an associated thickness, it was possible for there to be N pore layers with S_N being the outside layer. As molecules were adsorbed into the inside layer, the molecule could then diffuse to other pore layers within the wall until it moved to outside of the film and was lost to the external environment. Incorporation of N pore layers into the model resulted in the addition of the following expressions:

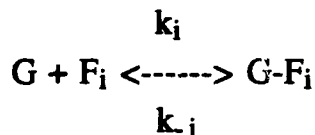
for $i = 2$ to N



where k_D was the rate constant for diffusion between two adjacent pore layers and k_{-s} was the desorption rate constant as in the first expression.

The second model was an adsorption model whereby the hydrazine adsorbed onto nonpermeable sites. The expression for this process was given by the following:

for $i = 1$ to f



where k_i and k_{-i} are the adsorption and desorption rate constants at the nonpermeable site i with f being the number of different types of nonpermeable adsorption sites.

The overall loss process was governed primarily by the S/V ratio of the chamber. Autoxidation did not appear to be a significant factor since the presence of oxygen in the matrix gas had little effect on the rate of disappearance. Chamber conditions which altered the chamber surface such as humidity and previous decay runs also had significant effects on the rate of disappearance. The models used to fit the data worked well to quantitatively and qualitatively characterize the physical loss process.

b. Current Studies

Following the work described above, a new environmental chamber was constructed. (References 4 and 5) It consisted of a spherical stainless steel chamber coated internally with Teflon.[®] Pressure and temperature within the 500-L chamber were regulated and the S/V ratio

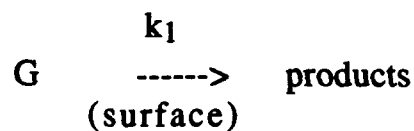
was minimized in comparison to cylindrical and cube chambers with the S/V ratio for the spherical chamber being equal to 4.836 m⁻¹.

In subsequent studies, data from the spherical chamber were analyzed with more one-measurement models. (Reference 11) Models based on fitting one measurement through time were used with the Marquardt algorithm (Reference 12) being incorporated with a least-squares differential corrector (LSDC) as well as fourth-order Runge-Kutta numeric integration. The signal used was the FT-IR absorbance band for hydrazine at 958 cm⁻¹.

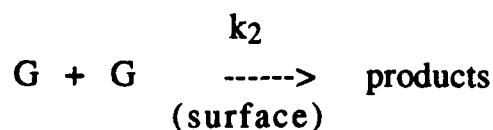
This study resulted in an implementation of the Marquardt algorithm which was approximately 1000 times faster than previous versions. (Reference 3) The speed enhancement was due to the optimization of software through the use of a FORTRAN program in place of the previously used BASIC version as well improvements to the implementation of the algorithm. Also, the use of more advanced computer hardware played a vital role in the speed increase.

Several models were proposed and tested with hydrazine decay data collected from the environmental chamber. The atmosphere within the chamber consisted of 80 percent helium and 20 percent oxygen. Also included in the chamber were 20 Teflon[®]-coated aluminum plates so that the effect of an increased S/V ratio within the chamber could be studied.

The first model tested was a first-order linear model. In this model, the loss process is described as a first-order reaction at a surface site expressed as:

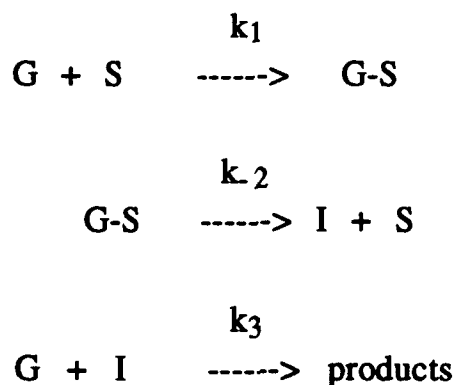


where G is the concentration of the hydrazine gas and k₁ is the reaction rate constant. The second model tested was a first-order nonlinear model. This model characterized the loss process as a bimolecular reaction at a surface site.



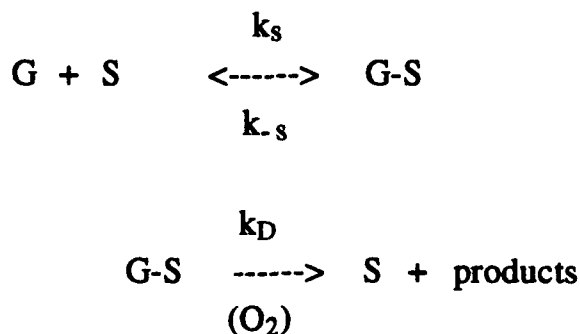
Again G is the concentration of the hydrazine gas and k_2 is the reaction rate constant.

A more complicated model was evaluated with the creation of a third-order irreversible oxidation model. In the model, irreversible adsorption of the gas onto a surface site was followed by the formation of an intermediate product which then went on to react with hydrazine to give a final product. The surface site used in the reaction was returned following the formation of the intermediate. Three expressions were generated to describe this process and were as follows:



where G was the concentration of hydrazine, S was a surface site, and G-S was the hydrazine adsorbed onto the surface. The rate constant for the adsorption onto the surface was given by k_1 with k_2 being the rate constant of the formation of an intermediate, S. The intermediate then reacted with hydrazine to form products with the reaction rate constant being given by k_3 .

Another model tested was a second-order catalytic adsorption model. This model incorporated reversible adsorption of hydrazine, G, onto a surface site, S, with the adsorbed species, G-S, then undergoing catalytic oxidation to yield products. The two equations used were:



where k_s and k_{-s} are the rate constants for the adsorption and desorption of hydrazine onto a surface site and k_D is the rate of catalytic oxidation. In the current studies, the third-order irreversible oxidation model consistently gave the best fits overall compared with to other models tested.

2. Model Revisions

Another aspect of this work was to update and optimize the algorithm used for the parameter estimation as well as incorporate data from the newly constructed environmental chamber. The work was successful on both counts and paved the way for the work described below.

The models used during this project have undergone extensive modifications from previous versions. Modifications made include changes to the kinetic models themselves as well as changes in the implementation of the Marquardt algorithm. The current implementation of the algorithm is believed to be the most optimal configuration thus far for this work.

A brief summary of the changes that have been made are as follows. One of the major changes made includes the utilization of two-measurement models as opposed to using only one measurement for the purpose of fitting. With this, it became necessary to modify the kinetic models proposed in order to incorporate the second measurement into the model scheme. Another major change was a modification to the program logic. As the parameter estimation program iterates and attempts to converge down to an error surface minimum, a decision process was implemented after each calculation loop to determine the degree of the gradient and least squares solution present in the move down the error surface.

The value of the FORTRAN program parameter known as MarqLambda controlled how gradient or least square the solution for a particular iteration would be. After convergence of the loop, a decision was made as to how MarqLambda should be modified. Lower values made the solution more least square (larger move) and a higher value made the solution more gradient (smaller move). It was necessary to make modifications to this parameter to optimize the search down the error surface.

During the first step of a loop, the nominal value of MarqLambda was used. It was generally initialized in the initial conditions file as 0.01. After the first step, the sum of the square of the error (SOS) as well as the root mean square (RMS) error were calculated for the fit. Once this was

done, MarqLambda was scaled down by a factor of ten to give a more least square solution. The SOS and RMS errors were again calculated. The nominal value for MarqLambda was then scaled up by a factor of ten to give a more gradient solution. The SOS and RMS error values for this solution were also calculated. The program then made a comparison to see which value of MarqLambda resulted in the smallest SOS and RMS error value. That value then became the next nominal value for MarqLambda. If none of the results yielded improvement, the original nominal value of MarqLambda was retained.

In past versions of the program, the Jacobian was reevaluated for each new value of MarqLambda tested within the outer loop. To optimize the program, the Jacobian is now evaluated only once at the start of the loop. Another switch was used to scale the Jacobian matrix. When the data was ill conditioned, this option was used to scale the columns of the Jacobian matrix, A, by the norms of the columns. This helped prevent the routine from running out of significant digits when the values in the matrix spanned several orders of magnitude.

Within the initial conditions file, a boolean switch could be set to force nonnegative parameters since negative values do not have any physically meaningful value for concentration.

3. Model Development

Over the course of this project, one of the primary goals was to develop kinetic models which could meet certain criteria. The criteria were based on real world limitations which had to be taken into consideration. In doing so, the results from the analysis remained physically meaningful and efficiently performed.

The first criterion, though not the most significant, was that of computation time. The models that were constructed consisted of, in general, no more than six or seven differential equations. Due to the computer hardware at our disposal, models that contained more than six differential equations required a large amount of time to converge to a solution. Because of the enormous amount of data generated from the environmental chamber, computation time had to be controlled so that all data sets could be analyzed thoroughly.

The next criterion was based on the kinetic model itself. It would have been quite difficult to express fully the complexity of the system under study. Instead, empirical models were created in an attempt to describe the major processes which were believed to be responsible for the observed optical response measured by the FT-IR signal. Since the FT-IR signal was a cumulative

response representing several physical/chemical (P/C) processes, the empirical models were an attempt to simplify and mathematically represent these processes.

The third criterion was model performance. If the model adequately represented the P/C processes, a small value for the root mean square (RMS) error would be expected between the actual and the fitted data points. In the event that the data set contained a high level of noise (which would have resulted in a higher than expected RMS error value), plots of the fitted data revealed in part the source of some of the model error. Plots of the fitted data and of the residuals along with the RMS value were excellent indicators of how well a model fitted the data set and were useful for comparison with other models.

Quite often, the second and third criteria became the pivotal points of the analysis. Superior performance in terms of the P/C processes represented by a model coincided with poor model performance in terms of mathematical indicators for these models.

The original source code for these was written in FORTRAN by Dr. W. P. Mounfield at Louisiana State University. The source code for the parameter estimation program including applicable library routines contained over 10,000 lines of code. A listing of the program (excluding the library routines) is given in Appendix T. The library routines were called directly from commercially available software programs (Reference 13).

The creation of a new model involved the modification of the source code of an existing program to reflect the pertinent model changes. There were six steps necessary to implement a new model into the source code copied from an existing program:

[1. Header] The first step was to edit the comment section at the top of the code. The model being implemented and its differential equations were listed here to give the user a record of what the program contained. Also listed here were any substitutions that were made when the user attempted to reduce the differential equations into common terms.

[2. Matrix dimensions] The second step was to edit the variable initialization section at the top of the program. The values of five variables were modified to accommodate both the new model and the data set. The variables to be modified are listed below.

- NUM_STATE = the number of state variables in the model
- NUM_PARAM = the number of parameter variables in the model

- $M = \text{NUM_STATE} + \text{NUM_PARAM}$
- $N = M + 1$
- MAX_POINTS = the maximum number of data points allowed in a data set minus one
(this is critical when working on a computer system with limited memory such as a DOS system)

[3. Subroutine EXTRACT_A2] In the subroutine extract_a2, the user defined the equation which was used to define the matrix A, the Jacobian. The matrix A was based upon the partial of the measurement values with respect to the states.

[4. Subroutine FORM_ERROR] In the subroutine form_error, the user defined the matrix YHAT in the same terms as those used to define the matrix A. This matrix was then used to calculate the error between the actual and calculated measurement values.

[5. Function FUNCOFX] In this function, the user defined the differential equations proposed for the model and was required for explicit model calculations. The equations defined the matrix X in the program.

[6. Initial conditions file] An external initial conditions ASCII file was required to initialize state and parameter startup values. This file had to be edited to reflect the proper number of states and parameters and had to be in the proper format for input into the program. In this file the user also set toggle switches that controlled certain features in the program as well as edit certain computational parameters.

Below is an example of an initial conditions file used for MOD380. Certain parameters and switches were included in prior work or experimentation and are no longer utilized for this study. Parameters no longer utilized are denoted by "*".

```

FALSE Scale the Jacobian? false = no, use levenberg lamda
TRUE  NON-NEGATIVE PARAMETER, true = yes force all par to be non-neg
76    Number of data points (-1) in data set
FALSE If explicit partials are defined, true = yes *
20    Max number of iterations before stopping unless converged
10.0  MarqV, a number to increase/decrease lamda by at each iteration
1.0E-2 MarqLambda, a number to add to AtA in  $(ATA + \text{lamda } I)x = b$ 
1.0E-5 MarqEpsilon(case 1), a convergence criterion
1.0E-5 MarqEpsilon(case 2), a convergence criterion

```

FALSE With SVD? TRUE = yes, takes precedence over inversion *
 FALSE With added noise? TRUE = the program will ADD noise to data *
 0.00 Added noise mean, if we add noise *
 0.01 Added noise standard deviation, if we add noise *
 FALSE With weights on meas.'s? i.e., . do you know the var of the noise? *
 FALSE With inversion?, true = yes, use inversion, no= solve $ax=b$ *
 1.18 Maximum delta time between steps
 0.5 Initial concentration of HZ (not used if $s=0$.i.e., . HZ estimated) *
 0.05 Standard deviation of measurement noise, if known and used *
 0.001 Init. state 1
 0.001 Init. state 2, or I
 0.001 Init. state 3, or NH_3
 0.5 Init. state 4, or estimated hydrazine concentration
 0.5 k_1
 1.3 k_2
 0.2 k_3
 0.4 S, empirical quantitative value for surface site abundance
 FALSE If run has sequential injections of HZ, true = yes *
 2 Number of sequential runs, must exist if seq = true *
 10.5 Time values for injection of HZ *
 1.05 Concentration at injection time *

4. Two-Measurement Models

After the completion of the initial one-measurement model studies described above, the next step was to incorporate a second measurement into the model. This was an attempt to improve on the second criterion described above. In characterizing a system, it was a natural extension of the single measurement work to simultaneously utilize a second FT-IR band signal which more completely defined the P/C processes being considered. The benefit was the utilization of more information during the analysis of the system under question.

With the use of a second measurement, certain difficulties made it seem counterproductive to our attempt to improve on the second criterion. One difficulty was that since the second measurement was directly associated with a minor product in the decay process, the kinetic model must then reflect that product in the differential equations. Initially this appeared to

be beneficial, but in practice, it resulted in overly restrictive models. With the emphasis on the creation of models with realistic P/C processes, forcing certain empirical species through specific decompositions generally caused difficulties in finding an acceptable numeric solution to the problem. This procedure also restricted the types of kinetic schemes which could be tested.

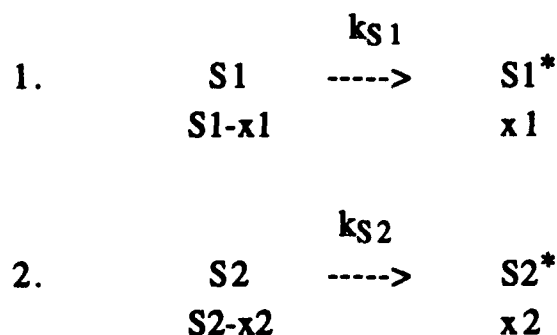
During the model development stage of this project, several models were proposed and tested. Only a select few were able to give fair to good results. Below is a description of the models utilized in this study. The complexity of each model varied according to the scope of the P/C processes it attempted to simulate. In some cases, simple models served as tools to test data sets to see if a solution, though not physically meaningful, could be found. The simplest models almost always converged to a good numerical solution.

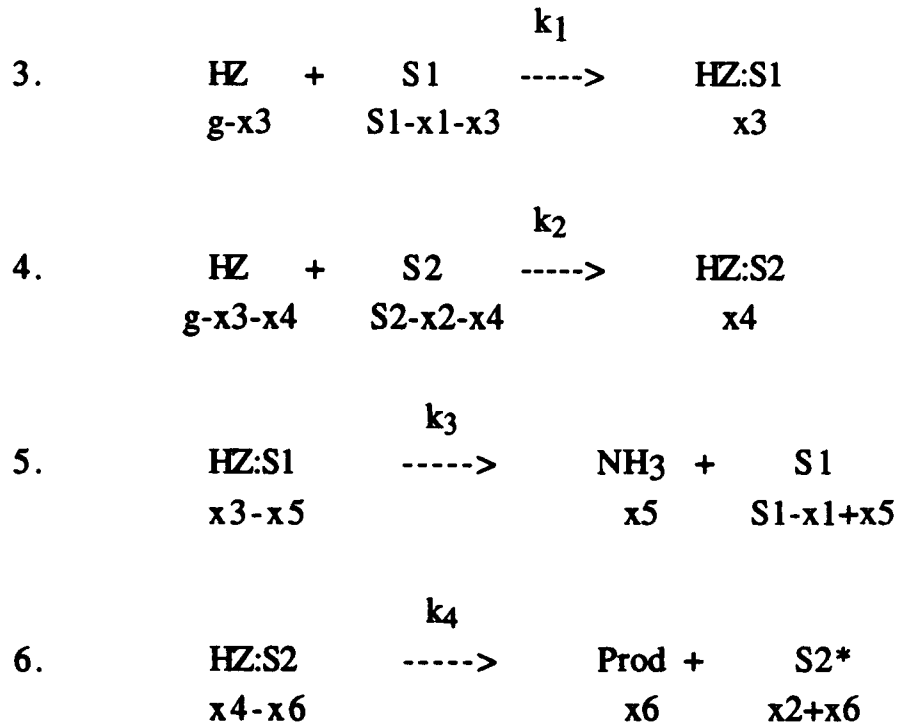
For all of the models presented below, all second measurements used represent the ammonia band in the IR spectrum. The band for water was available but proved to be of limited use since it was very difficult to stabilize and reproduce at times and generally could not be fit in any meaningful fashion.

The data sets used above required a specific file format. The data had to be in a column format with the first column being the time measurement. The second column was the absorbance measurement of hydrazine and the third column was the ammonia measurement.

Below are descriptions of the models used consistently for these studies. Not all of the models listed always gave a good fit, but by experimenting with all of them, a good fit could often be achieved for a given data set. The names given to the models are empirical in nature.

a. MOD310





$$y1 = x7 - x3 - x4 - x5 - x6$$

$$y2 = x5$$

$$x1 = 0.001 \text{ (S1*)}$$

$$dx1/dt = k_{s1} (S1-x1-x3+x5)$$

$$x2 = 0.001 \text{ (S2*)}$$

$$dx2/dt = k_{s2} (S2-x2-x4)$$

$$x3 = x3$$

$$dx3/dt = k_1 (g-x3-x4) (S1-x1-x3+x5)$$

$$x4 = x4$$

$$dx4/dt = k_2 (g-x3-x4) (S2-x2-x4)$$

$$x5 = 0.001 \text{ (NH}_3\text{)}$$

$$dx5/dt = k_3 (x3-x5)$$

$$x6 = 0.001 \text{ (prod)}$$

$$dx6/dt = k_4 (x4-x6)$$

$$x7 = g$$

$$x8 = S1$$

$$e1 = x8 - x1 - x3 + x5$$

$$x9 = S2$$

$$e2 = x9 - x2 - x4$$

$$x10 = k_{s1}$$

$$e3 = x7 - x3 - x4$$

$$x11 = k_{s2}$$

$$x12 = k_1$$

$$dx1/dt = x10 * e1$$

$$x13 = k_2$$

$$dx2/dt = x11 * e2$$

$$x14 = k_3$$

$$dx3/dt = x12 * e3 * e1$$

$$x15 = k_4$$

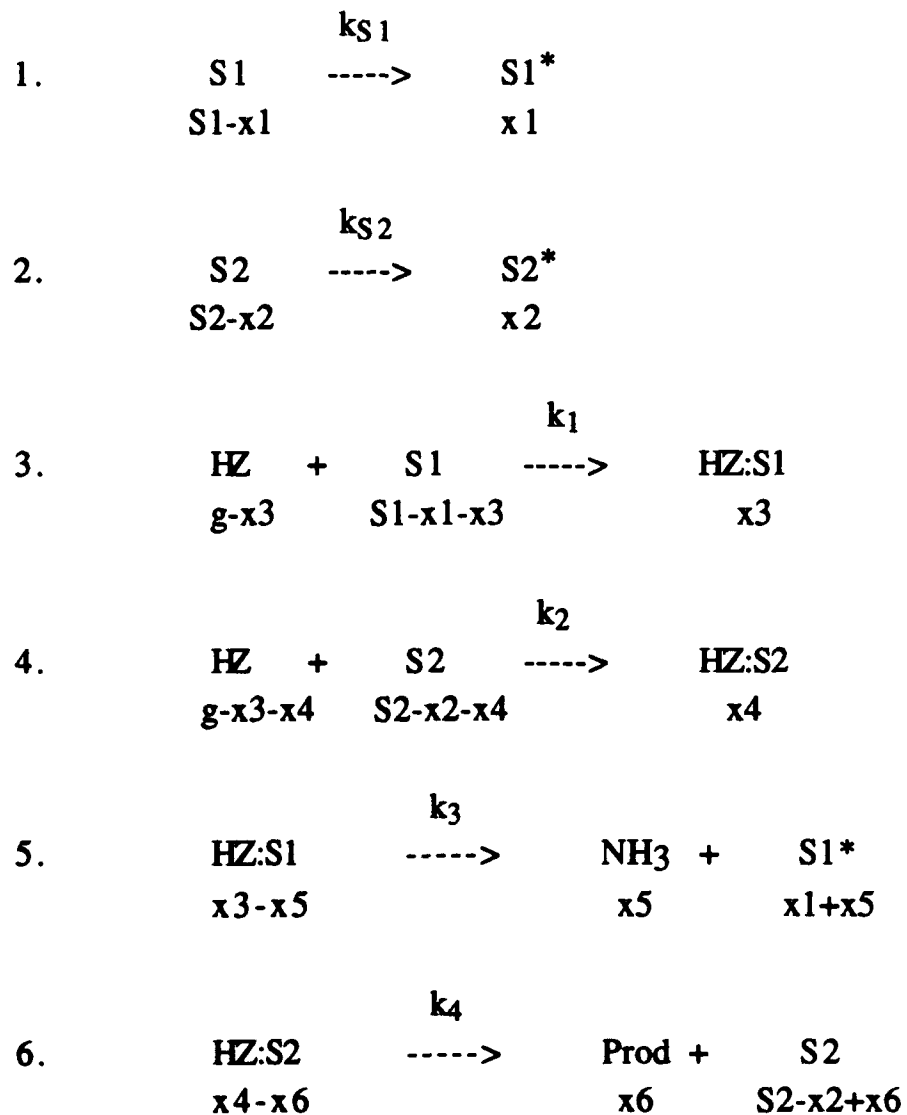
$$dx4/dt = x13 * e3 * e2$$

$$dx5/dt = x14 * (x3-x5)$$

$$dx6/dt = x15 * (x4-x6)$$

MOD310 incorporated two measurements, one being hydrazine and the other being ammonia. This model included two types of surface sites for reactions to occur. Both sites undergo a poisoning effect whereby the surface site becomes unusable. This is represented in the first and second equation. There are six equations in all. This helped take into account the "chamber conditioning" (Reference 1-2) effect which appeared after repetitive decay runs. The reactants in the third and fourth equations represented hydrazine binding to the surfaces where they may then undergo a decomposition reaction whereby ammonia and some unspecified products were formed. The formation of the unspecified products returns an unusable site.

b. MOD315



$$y1 = x7 - x3 - x4 - x5 - x6$$

$$y2 = x5$$

$$x1 = 0.001 \text{ (S1*)}$$

$$dx1/dt = k_{s1} (S1 - x1 - x3 + x5)$$

$$x2 = 0.001 \text{ (S2*)}$$

$$dx2/dt = k_{s2} (S2 - x2 - x4)$$

$$x3 = x3$$

$$dx3/dt = k_1 (g - x3 - x4) (S1 - x1 - x3 + x5)$$

$$x4 = x4$$

$$dx4/dt = k_2 (g - x3 - x4) (S2 - x2 - x4)$$

$$x5 = 0.001 \text{ (NH}_3\text{)}$$

$$dx5/dt = k_3 (x3 - x5)$$

$$x6 = 0.001 \text{ (prod)}$$

$$dx6/dt = k_4 (x4 - x6)$$

$$x7 = g$$

$$x8 = S1$$

$$e1 = x8 - x1 - x3 + x5$$

$$x9 = S2$$

$$e2 = x9 - x2 - x4$$

$$x10 = k_{s1}$$

$$e3 = x7 - x3 - x4$$

$$x11 = k_{s2}$$

$$x12 = k_1$$

$$dx1/dt = x10 * e1$$

$$x13 = k_2$$

$$dx2/dt = x11 * e2$$

$$x14 = k_3$$

$$dx3/dt = x12 * e3 * e1$$

$$x15 = k_4$$

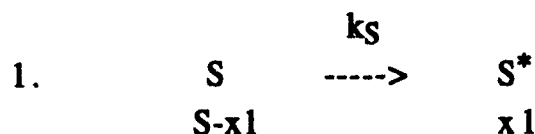
$$dx4/dt = x13 * e3 * e2$$

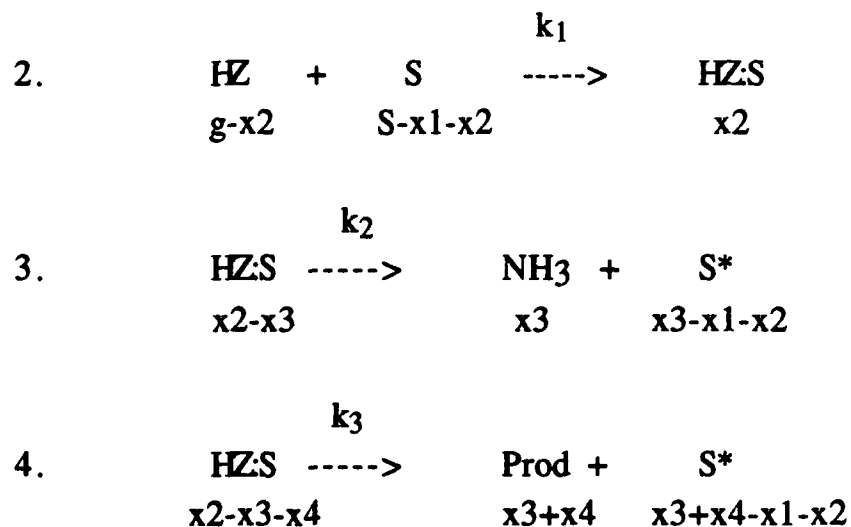
$$dx5/dt = x14 * (x3 - x5)$$

$$dx6/dt = x15 * (x4 - x6)$$

MOD315 is a two-measurement model, one being hydrazine and the other being ammonia. This model also included two types of surface sites for reactions to occur. The first and second equations represent "chamber conditioning." There are six equations in all. The reactants in the third and fourth equations represent hydrazine binding to the surfaces where they may then undergo a decomposition reaction whereby ammonia and some unspecified products are formed. The formation of the ammonia returns an unusable site.

c. MOD350





$$y_1 = g - x_2 - x_3 - x_4$$

$$y_2 = x_3$$

$$x_1 = 0.001 (S^*)$$

$$x_2 = x_2$$

$$x_3 = x_3 (\text{NH}_3)$$

$$x_4 = 0.001(\text{prod})$$

$$x_5 = g$$

$$x_6 = S$$

$$x_7 = k_5$$

$$x_8 = k_1$$

$$x_9 = k_2$$

$$dx_1/dt = k_5 (S-x_1-x_2)$$

$$dx_2/dt = k_1 (g-x_2) (S-x_1-x_2)$$

$$dx_3/dt = k_2 (x_2-x_3-x_4)$$

$$dx_4/dt = k_3 (x_2-x_3-x_4)$$

$$e_1 = x_6 - x_1 - x_2$$

$$e_2 = x_5 - x_2$$

$$e_3 = x_2 - x_3 - x_4$$

$$dx_1/dt = x_7 * e_1$$

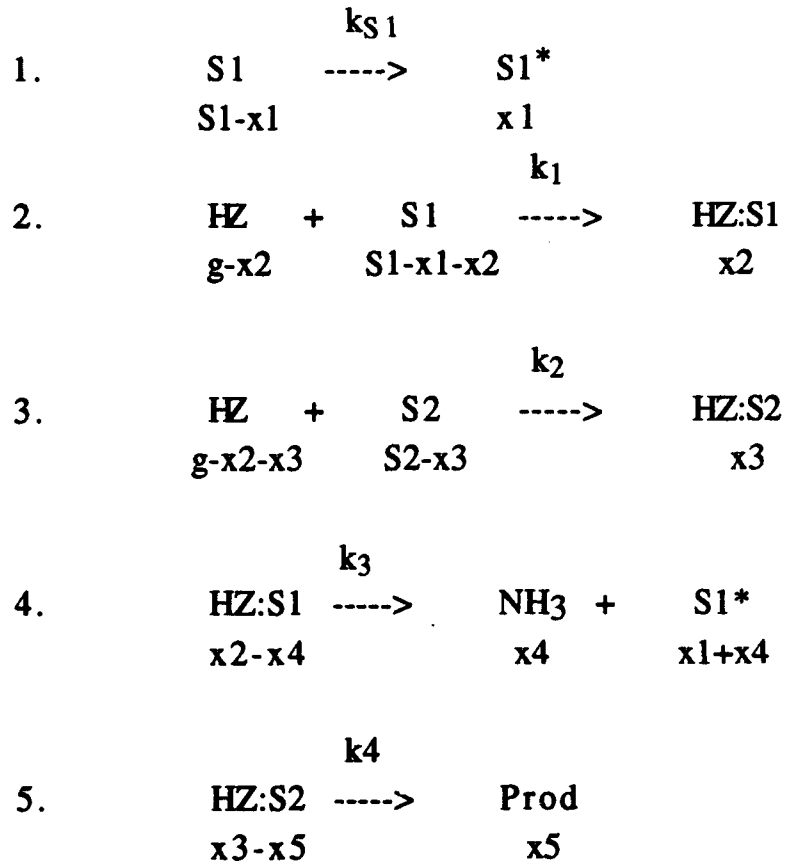
$$dx_2/dt = x_8 * e_2 * e_1$$

$$dx_3/dt = x_9 * e_3$$

$$dx_4/dt = x_{10} * e_3$$

MOD350 represents a simplification of MOD310 and MOD315 with only four equations. In this model there is only one type of surface site available for reaction. It too undergoes a conditioning effect (Equation (1)) and the formation of unspecified products and ammonia yields unusable sites.

d. MOD360



$$y1 = x6 - x2 - x3 - x4 - x5$$

$$y2 = x4$$

$$x1 = 0.001 (S1^*)$$

$$x2 = x2$$

$$x3 = x3$$

$$x4 = x4 (NH_3)$$

$$x5 = x5 (prod)$$

$$x6 = g$$

$$x7 = S1$$

$$x8 = S2$$

$$x9 = k_{S1}$$

$$x10 = k_1$$

$$x11 = k_2$$

$$x12 = k_3$$

$$dx1/dt = k_{S1} (S1 - x1 - x2)$$

$$dx2/dt = k_1 (g - x2 - x3) (S1 - x1 - x2)$$

$$dx3/dt = k_2 (g - x2 - x3) (S2 - x3)$$

$$dx4/dt = k_3 (x2 - x4)$$

$$dx5/dt = k_4 (x3 - x5)$$

$$e1 = x7 - x1 - x2$$

$$e2 = x6 - x2 - x3$$

$$e3 = x2 - x4$$

$$e4 = x3 - x5$$

$$e5 = x8 - x3$$

$$x_{13} = k_4$$

$$dx_1/dt = x_9 * e_1$$

$$dx_2/dt = x_{10} * e_2 * e_1$$

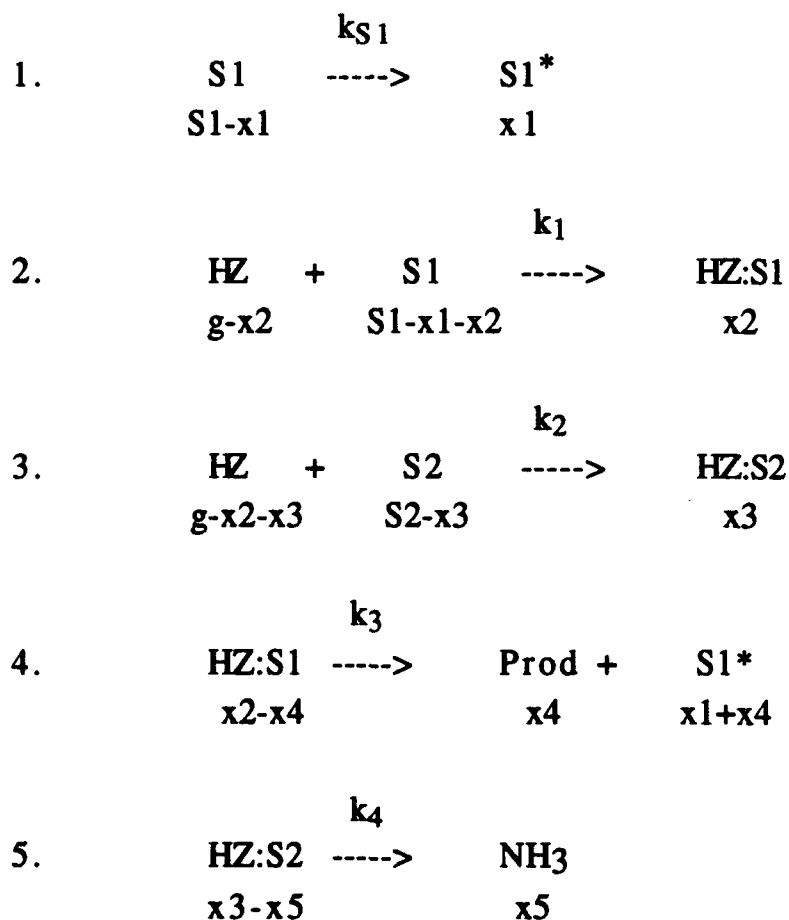
$$dx_3/dt = x_{11} * e_2 * e_5$$

$$dx_4/dt = x_{12} * e_3$$

$$dx_5/dt = x_{13} * e_4$$

MOD360 contains five differential equations (numbered to the left, above). This model incorporates two types of surface sites with only one of them becoming poisoned. Equation (4) represents the formation of ammonia resulting in an unusable site. Equation (5) shows the formation of unspecified products on the second type of surface site. The products in Equation (5) do not take into account the fate of the surface site; it is essentially "consumed."

e. MOD361



$$y_1 = x_6 - x_2 - x_3 - x_4 - x_5$$

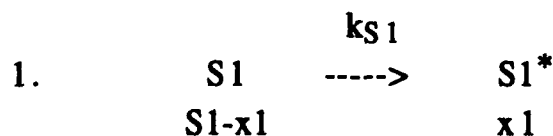
$$y_2 = x_5$$

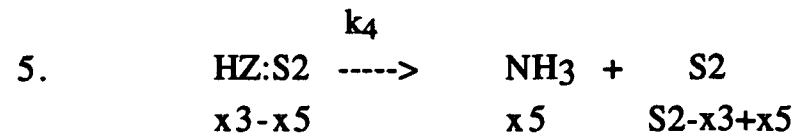
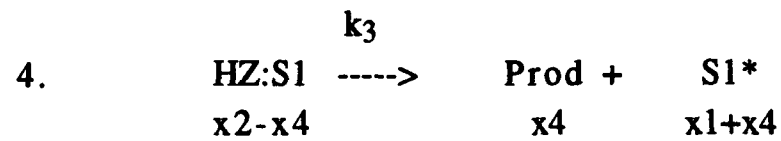
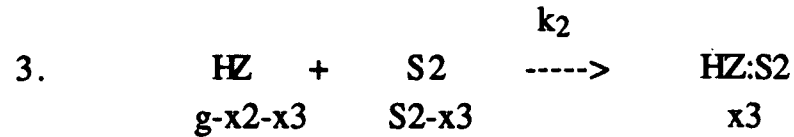
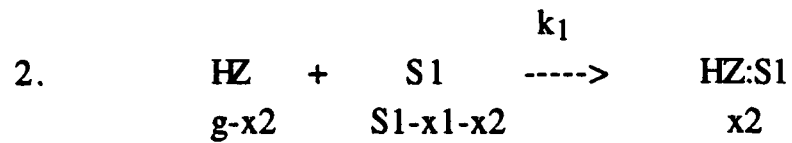
$x_1 = 0.001 (S_1^*)$	$dx_1/dt = k_{S_1}(S_1 - x_1 - x_2)$
$x_2 = x_2$	$dx_2/dt = k_1 (g - x_2 - x_3) (S_1 - x_1 - x_2)$
$x_3 = x_3$	$dx_3/dt = k_2 (g - x_2 - x_3) (S_2 - x_3)$
$x_4 = x_4 \text{ (prod)}$	$dx_4/dt = k_3 (x_2 - x_4)$
$x_5 = x_5 \text{ (NH}_3\text{)}$	$dx_5/dt = k_4 (x_3 - x_5)$
$x_6 = g$	
$x_7 = S_1$	$e_1 = x_7 - x_1 - x_2$
$x_8 = S_2$	$e_2 = x_6 - x_2 - x_3$
$x_9 = k_{S_1}$	$e_3 = x_2 - x_4$
$x_{10} = k_1$	$e_4 = x_3 - x_5$
$x_{11} = k_2$	$e_5 = x_8 - x_3$
$x_{12} = k_3$	
$x_{13} = k_4$	
	$dx_1/dt = x_9 * e_1$
	$dx_2/dt = x_{10} * e_2 * e_1$
	$dx_3/dt = x_{11} * e_2 * e_5$
	$dx_4/dt = x_{12} * e_3$
	$dx_5/dt = x_{13} * e_4$

MOD361 also contains five differential equations (numbered to the left, above). One of the two surface sites in this model becomes. Equation (4) represents the formation of unspecified products resulting in an unusable site. Equation (5) shows the formation of ammonia on the second type of surface site. As with MOD360, the products in Equation (5) do not take into account the fate of the surface site.

MOD360 and MOD361 are not physically meaningful because of Equations (5) and their insufficient characterization of surface site 2. These two models were prototypes for the next models to be developed.

f. MOD370





$$y_1 = x_6 - x_2 - x_3 - x_4 - x_5$$

$$y_2 = x_5$$

$$x_1 = 0.001 (\text{S1}^*)$$

$$x_2 = x_2$$

$$x_3 = x_3$$

$$x_4 = x_4 (\text{prod})$$

$$x_5 = x_5 (\text{NH}_3)$$

$$x_6 = g$$

$$x_7 = \text{S1}$$

$$x_8 = \text{S2}$$

$$x_9 = k_{S1}$$

$$x_{10} = k_1$$

$$x_{11} = k_2$$

$$x_{12} = k_3$$

$$x_{13} = k_4$$

$$\frac{dx_1}{dt} = k_{S1} (\text{S1}-x_1-x_2)$$

$$\frac{dx_2}{dt} = k_1 (g-x_2-x_3) (\text{S1}-x_1-x_2)$$

$$\frac{dx_3}{dt} = k_2 (g-x_2-x_3) (\text{S2}-x_3+x_5)$$

$$\frac{dx_4}{dt} = k_3 (x_2-x_4)$$

$$\frac{dx_5}{dt} = k_4 (x_3-x_5)$$

$$e_1 = x_7 - x_1 - x_2$$

$$e_2 = x_6 - x_2 - x_3$$

$$e_3 = x_2 - x_4$$

$$e_4 = x_3 - x_5$$

$$e_5 = x_8 - x_3 + x_5$$

$$\frac{dx_1}{dt} = x_9 * e_1$$

$$\frac{dx_2}{dt} = x_{10} * e_2 * e_1$$

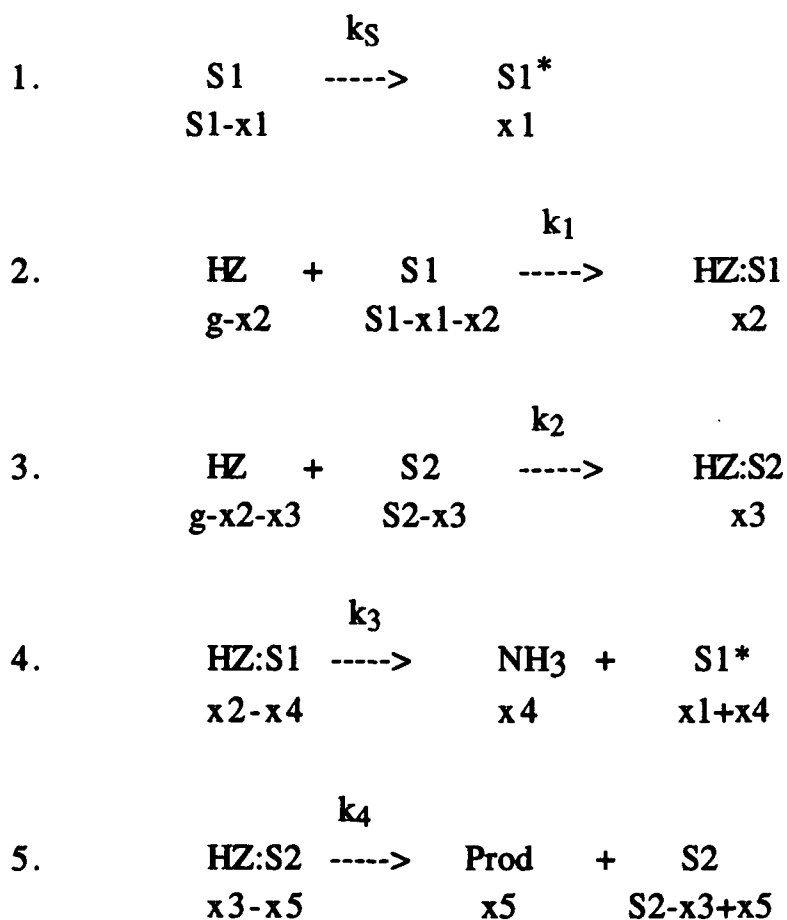
$$\frac{dx_3}{dt} = x_{11} * e_2 * e_5$$

$$\frac{dx_4}{dt} = x_{12} * e_3$$

$$dx5/dt = x13 * e4$$

MOD370 is an extension of MOD360. It has two surface sites with the first one undergoing the poisoning process. Hydrazine binds to both surface types and undergoes a decomposition reaction to yield unspecified products and ammonia. Upon formation of the unspecified products, an unusable surface site is returned. After the formation of ammonia, a usable surface site is returned.

g. MOD375



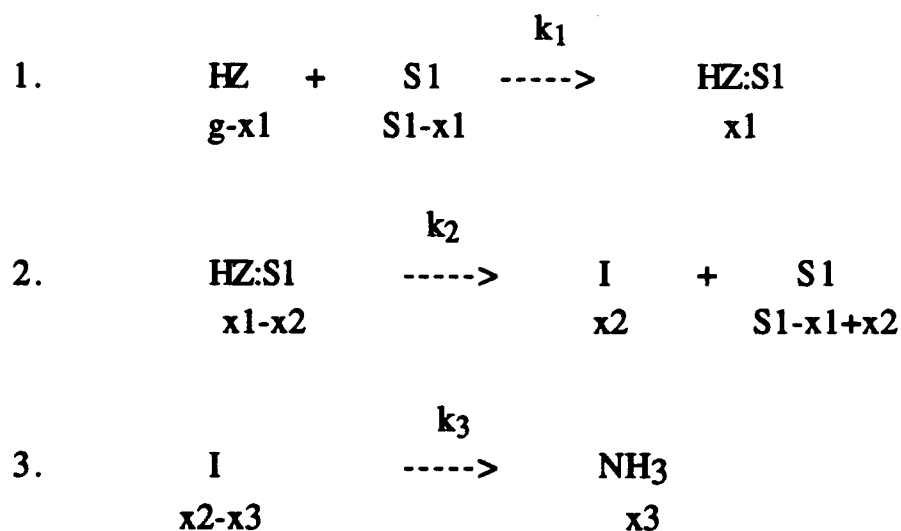
$$\begin{aligned}
 y1 &= x6 - x2 - x3 - x4 - x5 \\
 y2 &= x4
 \end{aligned}$$

$$\begin{aligned}
 x1 &= 0.001 (S1^*) & dx1/dt &= k_s1 (S1-x1-x2) \\
 x2 &= x2 & dx2/dt &= k_1 (g-x2-x3) (S1-x1-x2) \\
 x3 &= x3 & dx3/dt &= k_2 (g-x2-x3) (S2-x3+x5)
 \end{aligned}$$

$$\begin{array}{ll}
x_4 = x_4 \text{ (NH}_3\text{)} & dx_4/dt = k_3 (x_2 - x_4) \\
x_5 = x_5 \text{ (prod)} & dx_5/dt = k_4 (x_3 - x_5) \\
x_6 = g & \\
x_7 = S_1 & e_1 = x_7 - x_1 - x_2 \\
x_8 = S_2 & e_2 = x_6 - x_2 - x_3 \\
x_9 = k_{S_1} & e_3 = x_2 - x_4 \\
x_{10} = k_1 & e_4 = x_3 - x_5 \\
x_{11} = k_2 & e_5 = x_8 - x_3 + x_5 \\
x_{12} = k_3 & \\
x_{13} = k_4 & dx_1/dt = x_9 * e_1 \\
& dx_2/dt = x_{10} * e_2 * e_1 \\
& dx_4/dt = x_{12} * e_3 \\
& dx_5/dt = x_{13} * e_4
\end{array}$$

MOD375 also has two surface sites with the first one undergoing a conditioning process. Hydrazine binds to both surface types and decomposes forming ammonia and unspecified products. In this model, the formation of ammonia returns an unusable surface site while the formation of the unspecified product returns a usable site.

h. MOD380



$$y_1 = x_4 - x_1 - x_2 - x_3$$

$$y_2 = x_3$$

$$x1 = \text{HZ:S1}$$

$$x2 = \text{I}$$

$$x3 = x3$$

$$x4 = g$$

$$x5 = k_1$$

$$x6 = k_2$$

$$x7 = k_3$$

$$x8 = S_1$$

$$dx1/dt = k_1 (g-x1) (S_1-x1+x2)$$

$$dx1/dt = x5 * (x4-x1) * e1$$

$$dx2/dt = k_2 (x1-x2)$$

$$dx2/dt = x6 * (x1-x2)$$

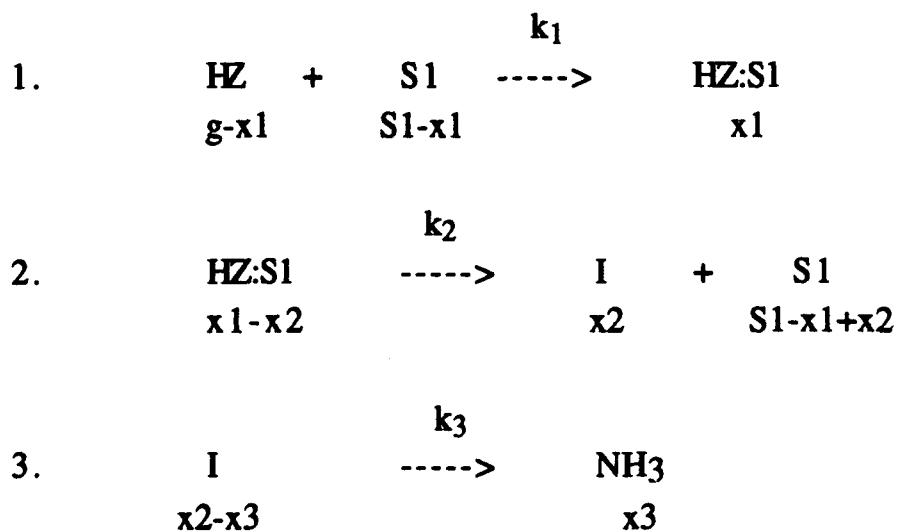
$$dx3/dt = k_3 (\text{I})$$

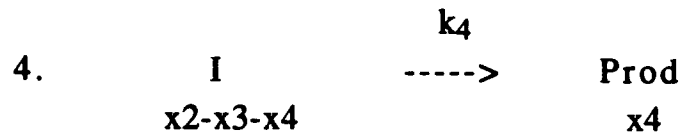
$$dx3/dt = x7 * (x2-x3)$$

$$e1 = x8-x1-x2$$

MOD380 is a very simple model (three differential equations) with very little physically significant meaning. The model incorporates one surface site which binds with hydrazine to then forms an intermediate which then goes to ammonia. Even though the model is overly simple it was useful as a data set feasibility model. If it was uncertain whether a solution to any model could be obtained with a particular data set, this model was used to find out whether the data was capable of producing a solution. The solution for this model was quite easy to find and was relatively quick in terms of computation time.

i. MOD385





$$y1 = x5 - x1 - x1 - x2 - x4$$

$$y2 = x3$$

$$x1 = \text{HZ:S1}$$

$$x2 = \text{I}$$

$$x3 = x3$$

$$x4 = x4$$

$$x5 = g$$

$$x6 = k_1$$

$$x7 = k_2$$

$$x8 = k_3$$

$$x9 = \text{S1}$$

$$x10 = k_4$$

$$dx1/dt = k_1 (g-x1) (\text{S1}-x1+x2)$$

$$dx1/dt = x6 * (x4-x1) * e1$$

$$dx2/dt = k_2 (x1-x2)$$

$$dx2/dt = x7 * e1$$

$$dx3/dt = k_3 (\text{I})$$

$$dx3/dt = x8 * e2$$

$$dx4/dt = k_4 (\text{I})$$

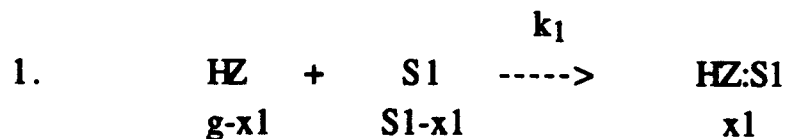
$$dx4/dt = x9 * e2$$

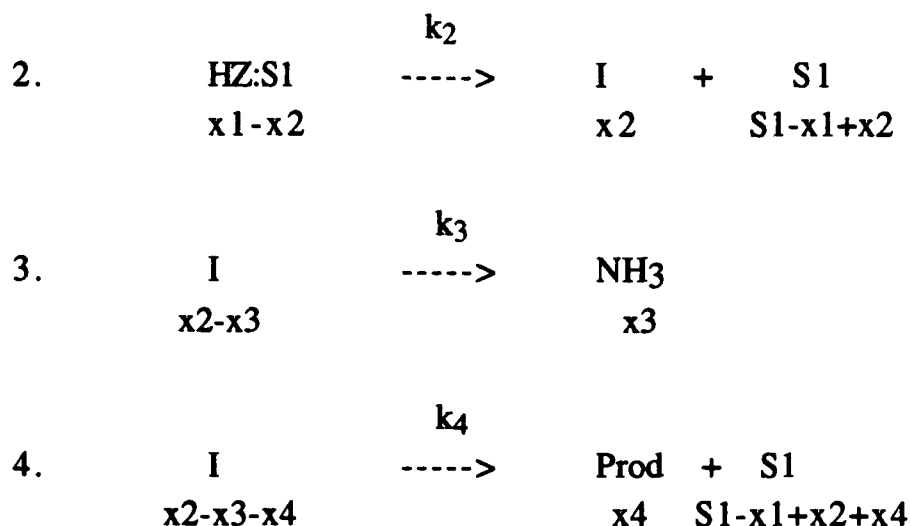
$$e1 = x1-x2$$

$$e2 = x2 - x3 - x4$$

MOD385 is an extension of MOD380. It too binds to a surface which then yields an intermediate and an available surface site. This intermediate then forms ammonia and unspecified products.

j. MOD390





$$y_1 = x_5 - x_1 - x_1 - x_2 - x_4$$

$$y_2 = x_3$$

$$x_1 = \text{HZ:S1}$$

$$x_2 = \text{I}$$

$$x_3 = x_3$$

$$x_4 = x_4$$

$$x_5 = g$$

$$x_6 = \text{S1}$$

$$x_7 = k_1$$

$$x_8 = k_2$$

$$x_9 = k_3$$

$$x_{10} = k_4$$

$$dx_1/dt = k_1 (g - x_1) (x_6 - x_1 + x_2 + x_4)$$

$$dx_1/dt = x_7 * (x_5 - x_1) * (x_6 - e_1)$$

$$dx_2/dt = k_2 (x_1 - x_2 - x_4)$$

$$dx_2/dt = x_8 * e_1$$

$$dx_3/dt = k_3 (x_2 - x_3)$$

$$dx_3/dt = x_9 * (x_2 - x_3)$$

$$dx_4/dt = k_4 (x_1 - x_2 - x_4)$$

$$dx_4/dt = x_{10} * e_1$$

$$e_1 = x_1 - x_2 - x_4$$

In MOD390, hydrazine binds to a surface site. The bound hydrazine then takes one of two paths. One path is the formation of an intermediate and the return of the surface site. The intermediate then goes on to form ammonia. The second path is for the bound hydrazine to form unspecified products and return a surface site.

Representative models fits for selected chamber data are shown in Appendix S.

SECTION IV

RESULTS AND DISCUSSION

A. NO ADDED PLATES

1. Inert Gas Stability Runs

The first set of experiments which were conducted in the chamber was designed to test the stability of inert gases. The initial run used 21 ppm methane (CH_4) in one atmosphere (760 Torr) of dry, ultra-pure helium. This was followed by a run with both CH_4 (at 19.3 ppm) and sulfur hexafluoride (SF_6) (at 0.58 ppm) in dry, ultra-pure helium. These runs were followed for 800 and 300 hours respectively. Generally, there was a slight decrease in species concentration in the first run (Figure 5), but the CH_4 - SF_6 plots showed essentially constant absorbance values (Figure 6). Thus, inert gases appear to be stable in the chamber, as anticipated.

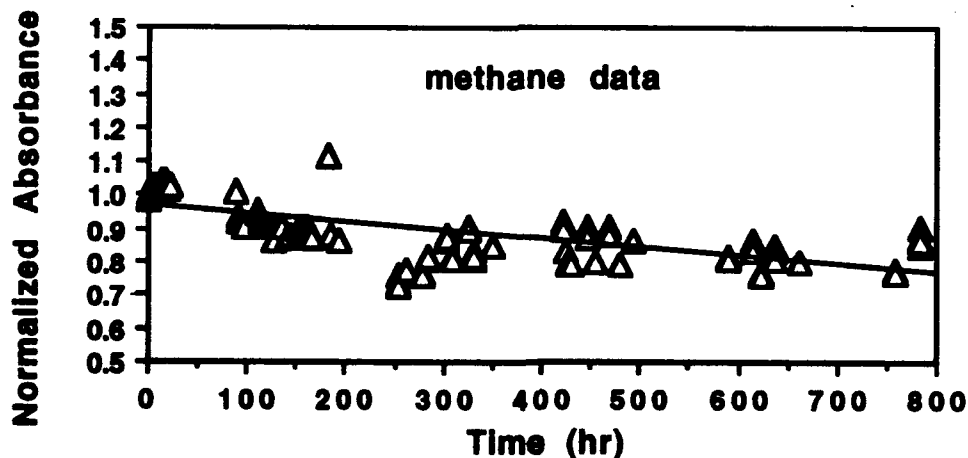


Figure 5. Plot of Normalized Methane Absorbance versus Time in the Spherical Chamber.

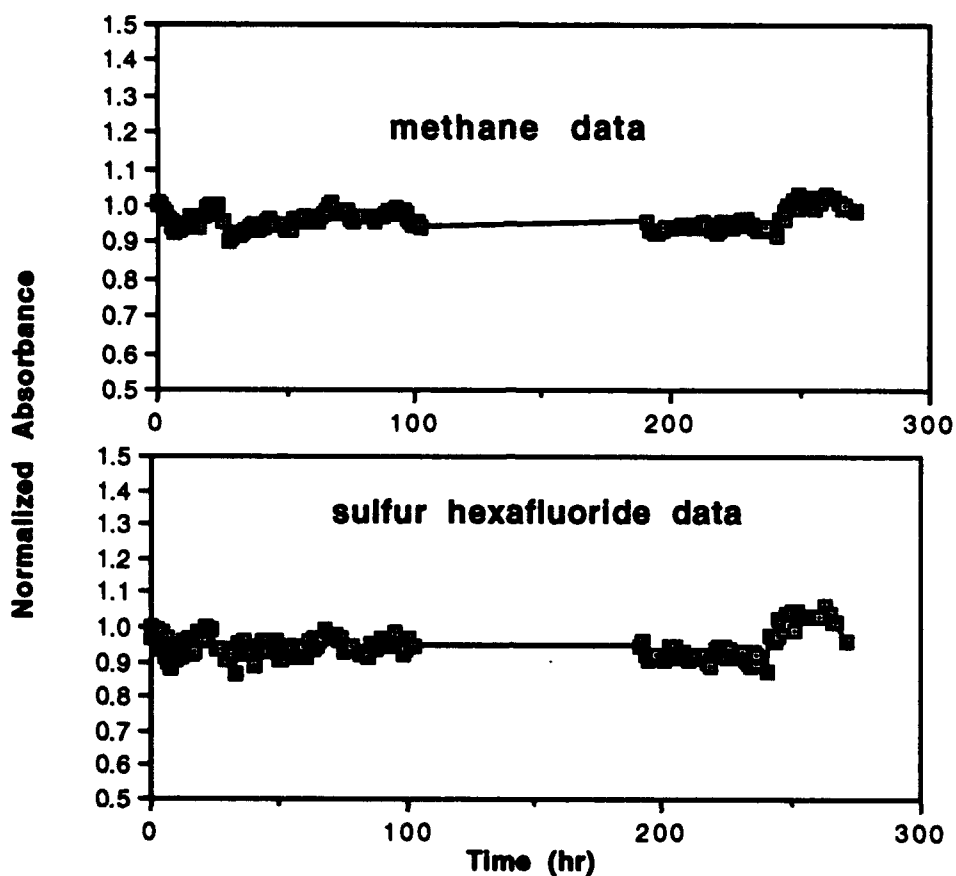


Figure 6. Plots of Methane and Sulfur Hexafluoride Absorbance versus Time in the Spherical Chamber.

2. Hydrazine Stability in Helium - Series 1

These inert gas stability experiments were followed by a series of experiments to determine the stability of vapor-phase hydrazine in the chamber. The initial set of hydrazine (HZ) experiments were conducted in pure, dry helium. The set consisted of four separate runs. The first run consisted of 50 ppm HZ with 20 ppm CH₄ as an internal standard in dry, pure helium. At the conclusion of the first run, the chamber was pumped down to 685 Torr and a new reference spectrum was recorded. Then another 50 ppm HZ were added and its decay was followed. This procedure was repeated for a total of four runs.

The results of this initial HZ stability test were disappointing. Although care was taken to minimize the surface-to-volume ratio in the chamber design and to coat all possible interior surfaces with Teflon[®], the half-life of HZ in the initial test was only 10.5 hours. However, in the subsequent runs in the first sequence, this increased considerably so that by the fourth run the half-life was about 100 hours. These data are plotted in Figure 7.

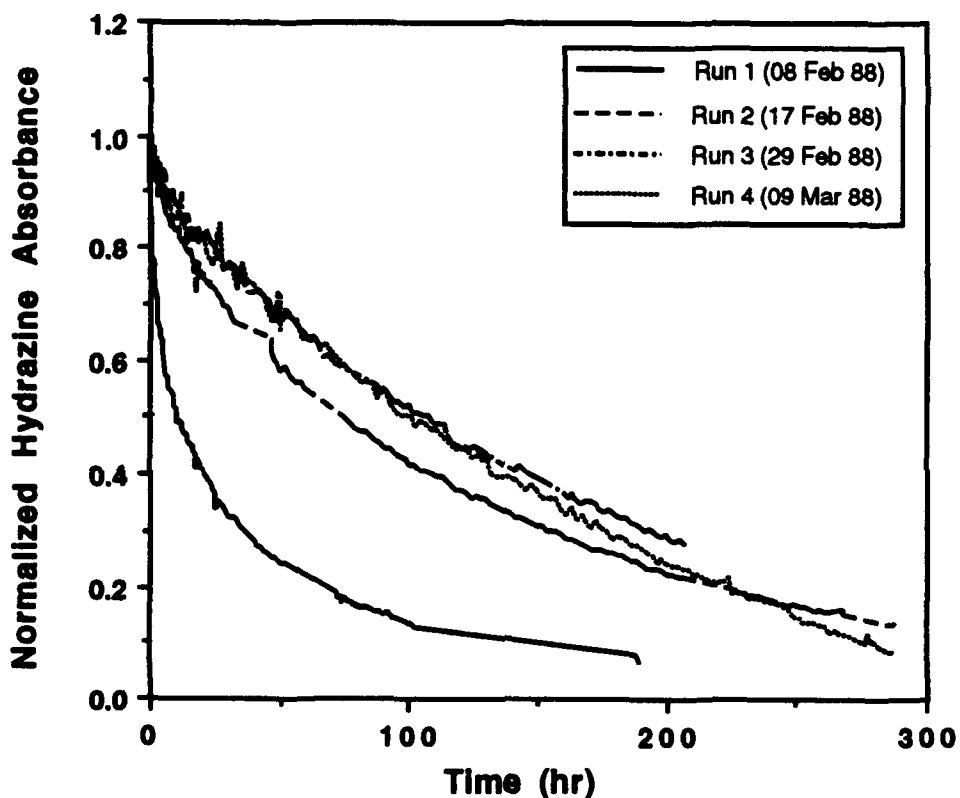


Figure 7. Plots of Normalized Hydrazine Absorbance versus Time in Pure, Dry Helium (No Added Plates).

The conditioning effect noted in this series of runs was quite dramatic. It was noted in most runs conducted in the chamber. Indeed, this type of behavior is quite common for molecules (like water and hydrazine) which have a strong affinity for most surfaces.

Methane was used in these runs, and in many subsequent runs, as an internal standard to determine long-term stability in the chamber. Over the course of many runs, it was determined that

there was no observed loss of methane, so its use was eventually discontinued. No further methane plots are included in this report.

3. Desorption Experiments

After this first series of runs, two experiments were conducted to determine the desorption behavior of any surface-bound HZ. In the first, the chamber was pumped down to 10 millitorr (after concluding Run 4 above) and then filled to 760 Torr with pure, dry helium. Then it was monitored for 90 hours.

At the end of this time, a small amount (about 2 ppm) of HZ had appeared along with a small amount (about 1 ppm) of ammonia (NH_3). Species concentrations were calculated by measuring the absorbance values at specific analytical peaks and using Beer's law with absorption coefficients from earlier works: $\text{HZ} = 4.6 \text{ cm}^{-1}\text{atm}^{-1}$, base e^* and $\text{NH}_3 = 35 \text{ cm}^{-1}\text{atm}^{-1}$, base e (Reference 10). The spectrum of the chamber contents at the beginning of this experiment and at the end are compared in Figure 8.

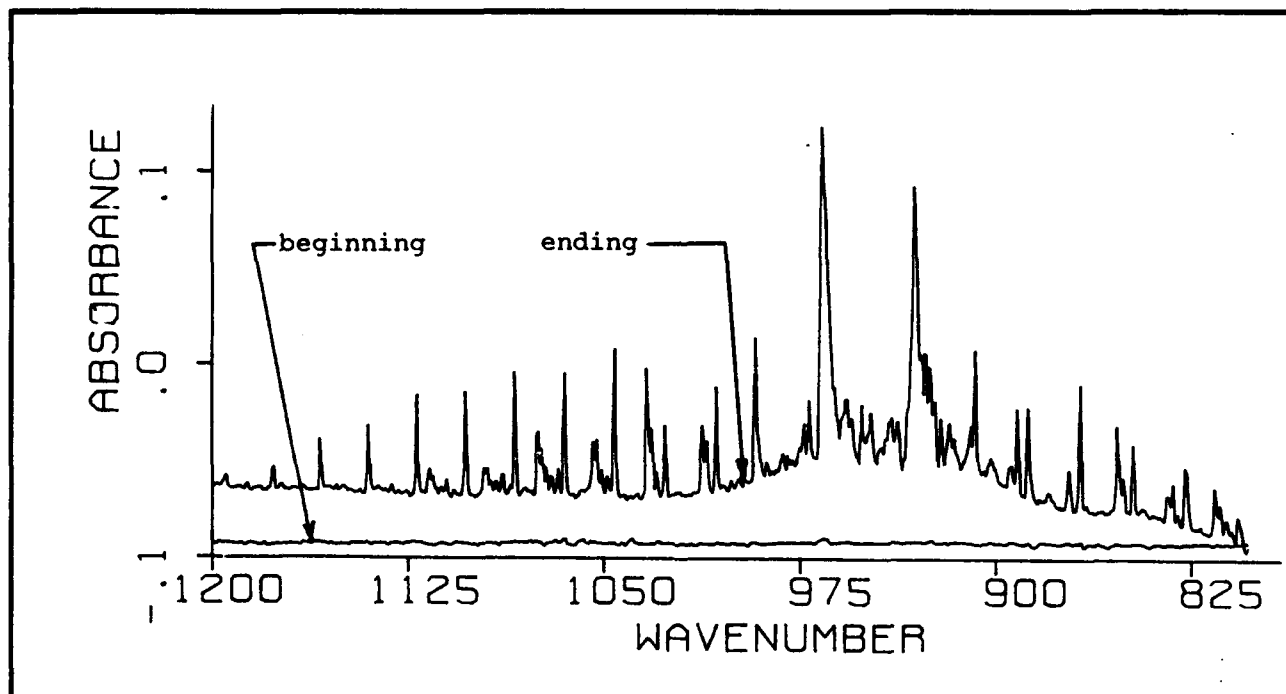


Figure 8. A Comparison of the Chamber Contents at the Beginning and Ending of a Desorption Experiment (No Added Plates).

*Unpublished value from earlier work in a Teflon[®]-film reaction chamber. This value is also consistent with the observed absorbance values used in this study based on a concentration of 50 or 100 ppm and a path length of 100 or 50 meters.

Then the chamber was pumped down to 200 milliTorr and filled with humid helium. The humidity was supplied by injecting 8 milliliters (mL) of water into the chamber manifold, then heating the manifold and vaporizing the water into the chamber while filling it with helium. Once the total pressure was 760 Torr, the chamber contents were again monitored, this time for 240 hours. At the end of this experiment, there was no evidence of any HZ but about 3 ppm of NH₃ had formed.

4. Hydrazine Stability in Helium - Series 2 and 3

Next, a second series of runs were made to evaluate the stability of HZ vapor in the chamber and to characterize chamber conditioning processes. These runs were conducted in pure, dry helium. The results were similar to the first series of runs.

Following the second series of runs, the chamber was heated to 45 °C and pumped out overnight. Then it was cooled to 20 °C in preparation for the third series of runs. The third series of runs was cut short and consisted of a single run. This run was somewhat unusual in that it did not decay as rapidly as previous runs. There was no humid desorption run between Series 2 and 3 of the HZ stability runs as there had been between Series 1 and 2. This may have caused the chamber to have remained in a more 'conditioned' state for the series 3 run. The results of the runs made in Series 2 and 3 are shown in Figure 9.

5. Hydrazine Stability in 20 percent Oxygen - 80 percent Helium

Following the series 3 run described in para III.A.4 above, another desorption run was conducted. In this instance, 7.8 mL of distilled water were vaporized into the chamber in one atmosphere of helium. The system was monitored for 5 days (20-24 Jun 88). At the end of this time there was again about 2 ppm NH₃ produced but no additional HZ. The chamber then sat idle for about 2 months before experiments resumed.

The initial runs with HZ in a 20 percent oxygen - 80 percent helium atmosphere were conducted between 23 Aug 88 and 30 Aug 88. The hydrazine was introduced as a vapor from the portable vacuum system (using the 516.3 mL sample bulb, four 10-Torr aliquots) and flushed into the chamber (with the mixing fan running) with pure, dry helium to 610 Torr. Then ultra-pure oxygen was introduced to bring the total pressure to 760 Torr. Then species concentration monitoring was begun.

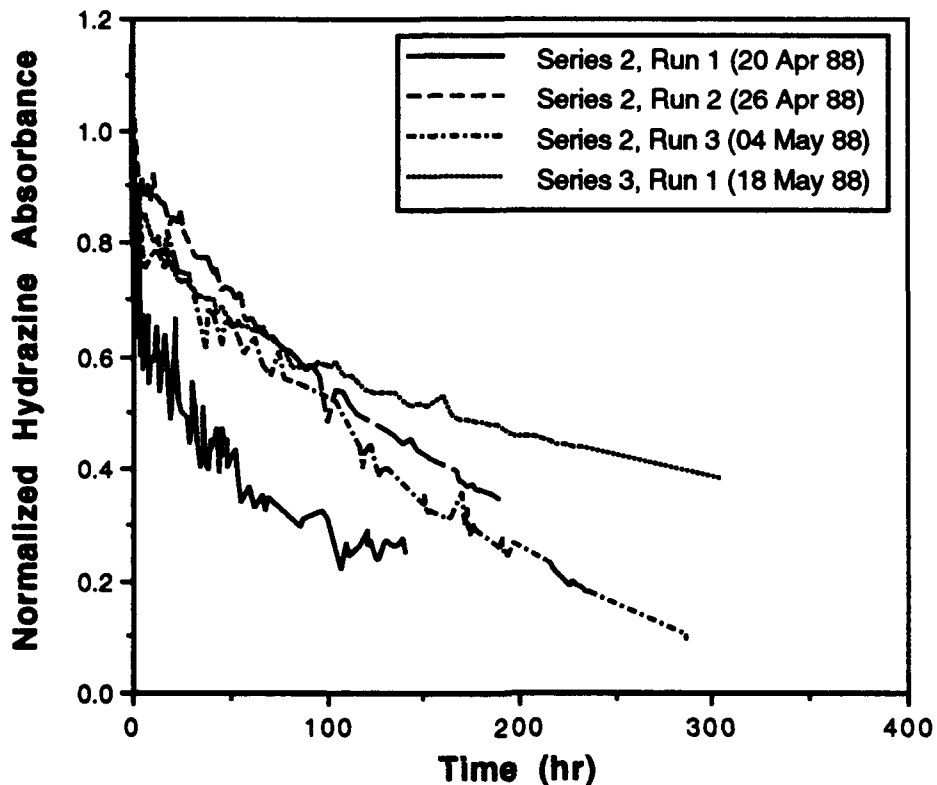


Figure 9. Plots of Hydrazine Decay in the Spherical Chamber (Series 2 and 3, No Added Plates).

The initial results were disappointing. The half-lives were less than 10 hours although care had been taken to minimize surface catalysis effects. The decay curves are plotted in Figure 10. The seven runs in this series were sequential, but not identical in their preparation. After Runs 1 and 2, the chamber was pumped down to 0.1 Torr in preparation for the next run. After Runs 3-6, the chamber was pumped down to 700 Torr in preparation for the next run.

Some mild chamber conditioning was evident in the first three runs. However, the final four runs showed no additional conditioning effects and were closely grouped together.

A small amount of ammonia formed in these runs (about 2 ppm). Some water was also formed; however, no attempt was made to quantify the water until later in this research.

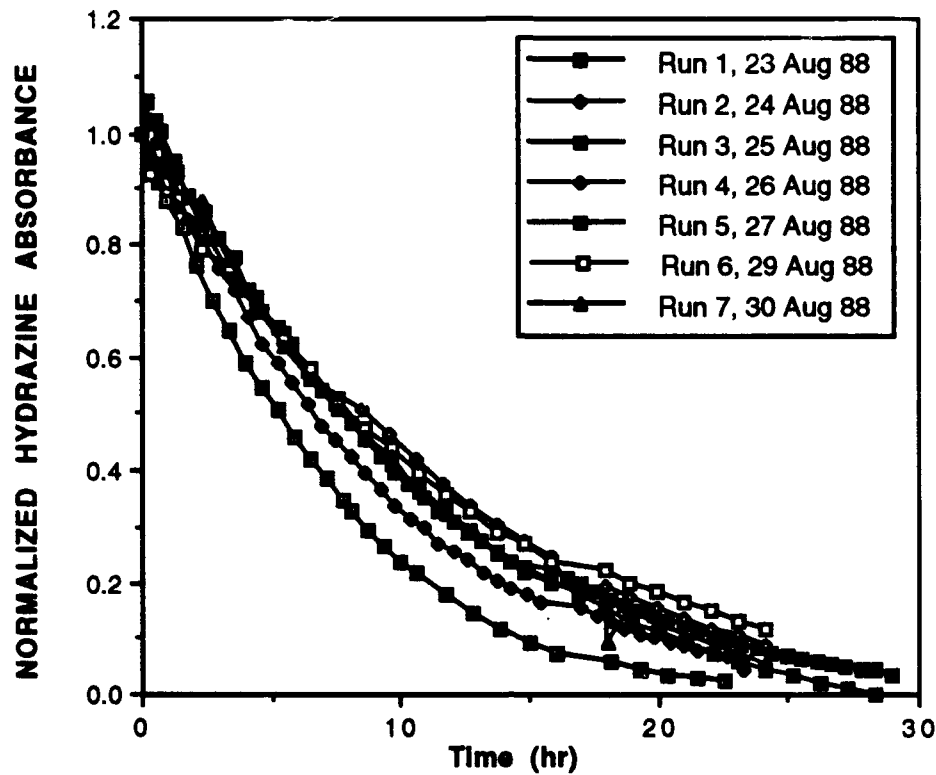


Figure 10. Plots of Hydrazine Decay in 80 Percent Helium - 20 Percent Oxygen in the Spherical Chamber (Dry Conditions, No Added Plates).

6. Additional Chamber Characterization and Conditioning Runs

Following the initial HZ plus 20 percent oxygen runs, the chamber was not used for about three months. This was followed by another set of HZ decay runs in dry helium. The first run was from 25 Nov 88 to 06 Dec 88. Another objective of this run was to obtain spectra with increased time resolution. This was done to test the sampling period in a numerical model being developed to describe HZ decay in the chamber. The spectra were collected as interferograms with 60 co-added scans and then processed off line.

One additional run was made to test the model, this time using 256 co-added scans in the data acquisition. This run went from 06 Jan 89 to 09 Jan 89. Both of these runs in dry helium produced a HZ decay curve which was about the same as the earlier runs under the same conditions. The HZ half-life was again about 70-80 hours. As before under these conditions, a small amount of ammonia was produced.

Following these two runs, it was decided to test the behavior of HZ in the chamber with pure air from the Aadco unit. The objective of this run was to see if perhaps the rapid decay of HZ in the 20 percent oxygen runs had been caused by some impurity in the oxygen itself. The run in pure air had the same increased decay rate as previous runs in synthetic air.

Because of concern over the increased decay rate of HZ when oxygen was present, it was decided to coat all possible surfaces inside the chamber (which were not Teflon[®] coated) with paraffin wax. To accomplish this, the mirrors were removed from the chamber. They were pre-heated with a heat gun and then brushed on their sides with melted paraffin wax. The wax coating was also applied to the brass shaft of the mixing fan and to the interior of the KF elbows used to connect to external vacuum gauges. It was hoped that this treatment would remove potential catalytic surfaces.

The interior chamber walls were also cleaned by rubbing them with a laboratory wipe soaked in acetone/methanol. This produced a brown deposit on the wipe indicating that surface reactions had been occurring.

Having completed these attempts to passivate and clean the chamber surfaces, another series of runs was made with pure air from the Aadco unit. These runs did show some improvement; the half-life of the HZ decay increased by a factor of about two. A comparison of HZ decay behavior before and after the wax coating is shown in Figure 11. One final attempt was made to decrease the reactivity of the interior, non-Teflon-coated surfaces by coating the two 4-in Pyrex[®] view ports with paraffin wax. This, however, had no effect on the decay of HZ in air and the wax was later removed from these view ports.

One final attempt was made to passivate the chamber and decrease surface-catalyzed decay processes. This was to expose the chamber to a large concentration of HZ vapor, about 1000 ppm, then pump it out. The hope was that this large dose of HZ would cover all the reactive surface sites and prevent them from further reactions later on. The high HZ

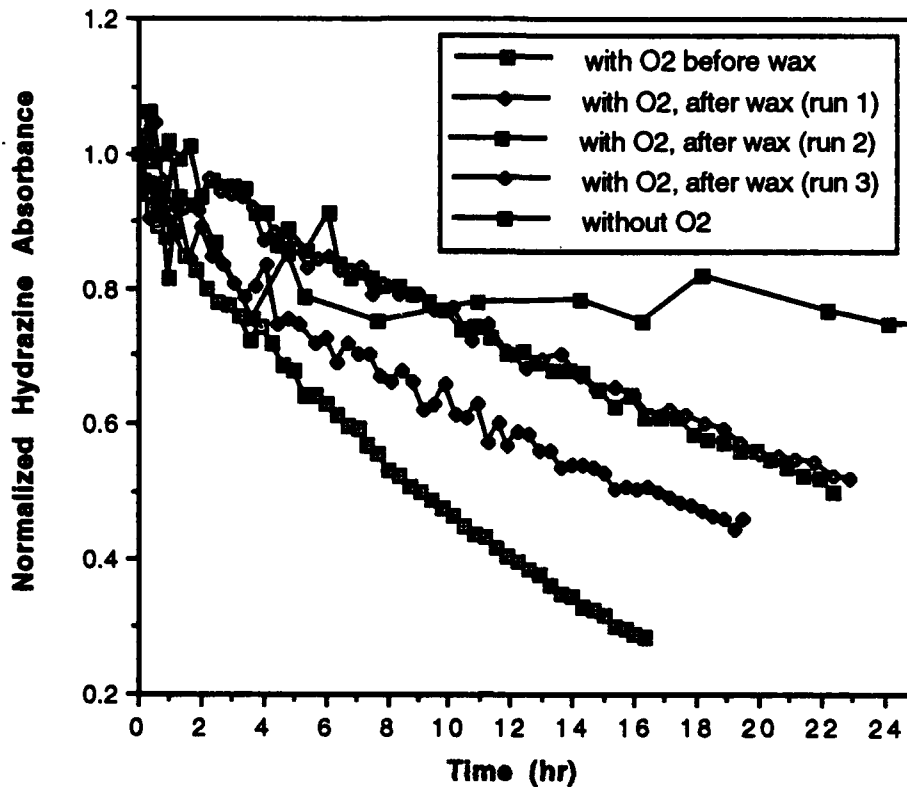


Figure 11. Plot of Hydrazine Decay in the Spherical Chamber Before and After Coating the Mirrors and Other Metal Surfaces with Paraffin Wax (No Added Plates)

concentration was allowed to set overnight. Then the chamber was pumped out and a 'normal' run was conducted with 50 ppm HZ in pure air. The resulting decay curve was essentially identical to the one labeled 'with O₂, after wax (run 3)' in Figure 11. In other words, the high HZ treatment had no observable effect on the surface activity of the chamber.

After this, one additional run was completed to characterize the stability of HZ in dry helium after the wax and passivation treatments. This run was followed for 15 days. The decay pattern was about the same as earlier runs under similar conditions. This run is shown in Figure 12.

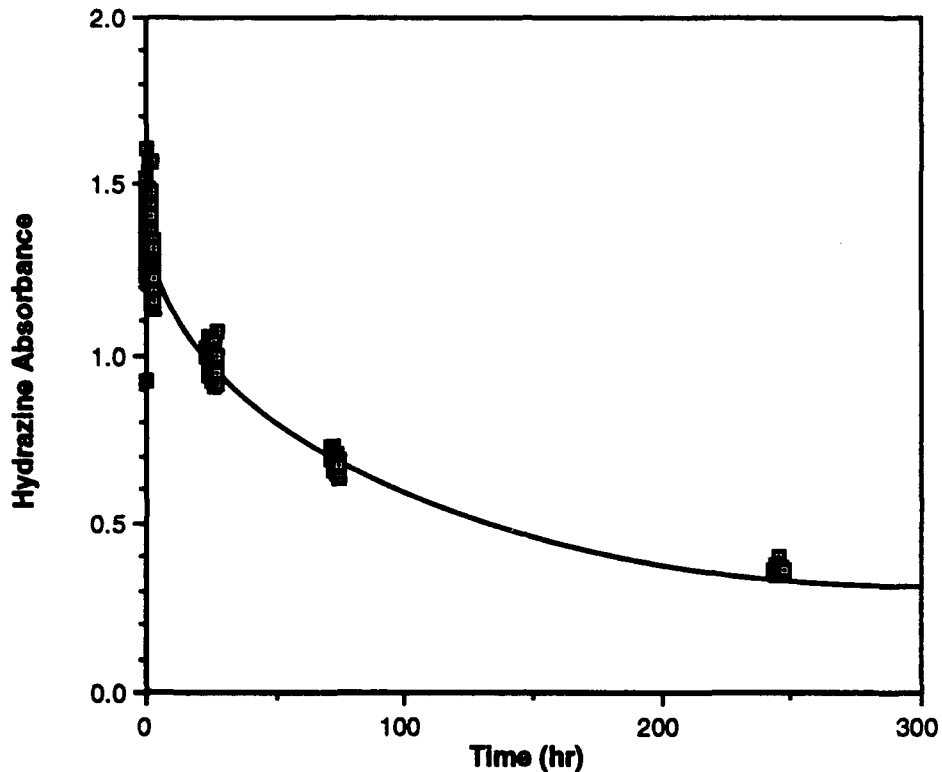


Figure 12. Plot of HZ decay in dry helium from 20 Apr - 5 May 89. (Connecting line is only a visual, not a model, fit.)

The data from the runs with pure, dry helium were fit best with the model MOD361. Even though this is a developmental model, it shows that a two-site mechanism provides an appropriate basis for a kinetic reaction mechanism under these reaction conditions. Other models gave poorer to much poorer fits.

No runs were conducted with humid helium in this initial series of characterization experiments.

In an 80 percent helium and 20 percent oxygen atmosphere, most of the models (with the exception of those with intermediate formation) gave very good fits. The MOD361 model has slightly better fits than the others. This two-site approach also appears to cover the case of added oxygen.

A summary of the model fits for the experiments with no plates present is given in Appendix N.

B. TEFLON®-COATED ALUMINUM PLATES

To characterize the reactivity of the Teflon® surface of the chamber, several runs were conducted where 20 Teflon®-coated aluminum plates were placed inside the chamber. This had the effect of doubling the surface area while maintaining the same volume.

The initial run was conducted in pure, dry helium. The approximate HZ half-life was 45 hours. This was two to three times faster than previous runs without plates under similar conditions and gave strong evidence that the Teflon®-coated surfaces are providing sites for hydrazine sorption.

This run was followed by a series of three runs in 80 percent dry helium and 20 percent oxygen. Again, the effects of the added Teflon® surfaces were evident. The half-life of the HZ under these conditions was about 10 hours, whereas it had been about 22 hours before the plates were added. These runs are plotted in Figure 13.

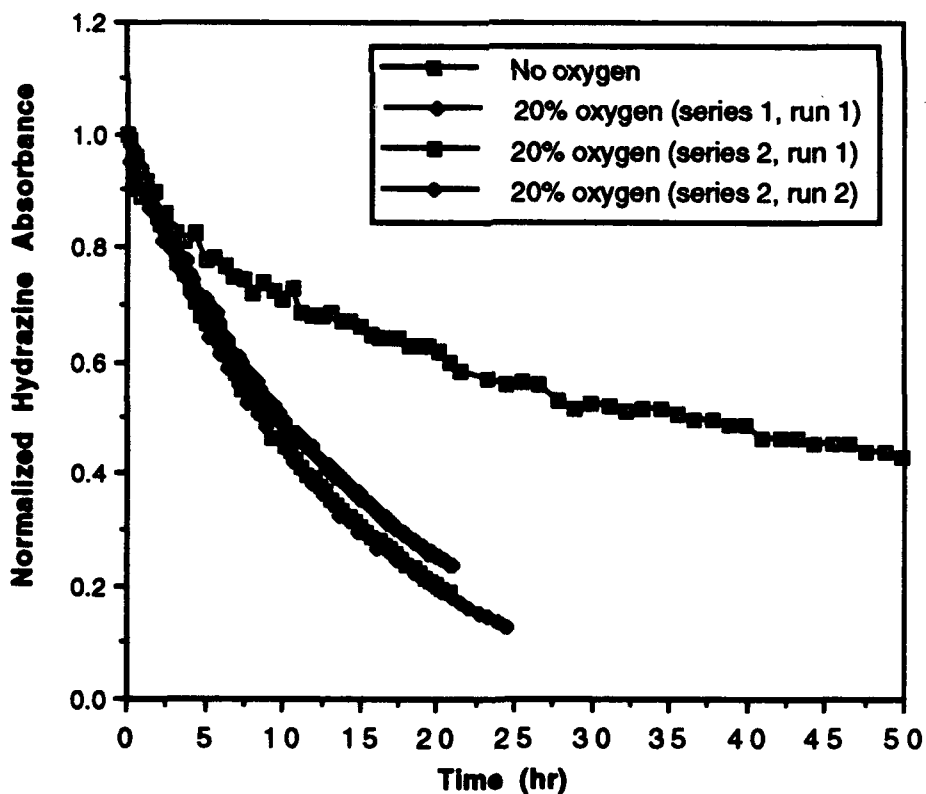


Figure 13. Plots of HZ Decay in Spherical Chamber with 20 FEP-Teflon®-Coated Aluminum Plates.

Ammonia formation was enhanced by the presence of this added surface area in the case of the run with no oxygen (about twice as much was produced). However, when oxygen was added, there was no increase in ammonia production over 20 percent oxygen runs without the added plates.

For runs both without and with 20 percent oxygen, model MOD360 gave the best fits. Other two-site models also gave good fits with one or two exceptions on individual runs. The one-site models with intermediates gave poor fits. The similarity of models MOD 360 and MOD361 shows that a two-site approach is a good description of the processes which occur when only Teflon[®] surfaces are present. These are both working models, however, and additional refinements can probably be made.

A summary of model fits to these runs with FEP-Teflon[®]-coated aluminum plates, present is given in Appendix O.

C. WATER CALIBRATION SPECTRA

The tests on the surface reactivity of different materials were interrupted so that quantitative water reference spectra could be obtained for use in monitoring HZ decay runs. Since the entire optical system of the spectrometer and chamber coupling area were purged with dry, pure air, there was reasonable expectation that reference spectra of water could be obtained by calibrated sampling in the chamber.

First, the vapor transfer method was tried. Water vapor was expanded into an evacuated sample bulb to a known pressure and then flushed into the chamber with dry helium. Water has a rich rotational structure within its three primary vibrational bands. The ν_2 bending region from 1300-2000 cm^{-1} was examined for an area which would not be affected by HZ absorption bands. Two rotational bands were selected, one at 1700.362 cm^{-1} and the other at 1652.817 cm^{-1} . Both of these bands were monitored to see how linear they were as a function of concentration. They are shown in Figure 14.

The initial results confirmed that water will adsorb onto most surfaces available to it in a given experimental apparatus. Thus, the samples first prepared in a 2.0-Liter glass sampling bulb were later tried in a 0.125-Liter glass bulb. However both showed an unacceptable amount of variation in absorbance from one sample to succeeding duplicate samples.

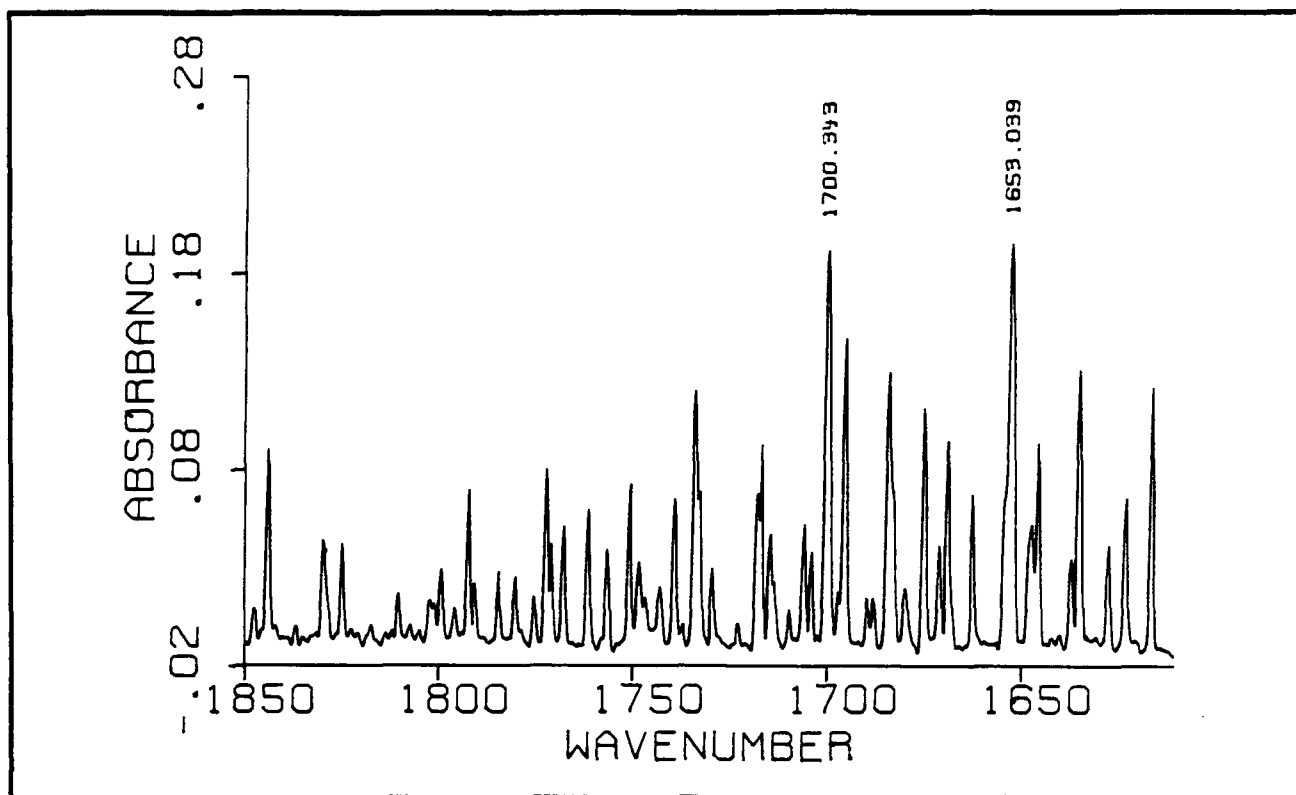


Figure 14. Part of the Water Vapor Infrared Spectrum Showing the Analytical Peaks Used in the Quantitative Measurements.

Liquid sampling was used to address this problem. Water samples in microliter (μL) quantities were injected into the heated chamber sample manifold and vaporized then flushed into the chamber with dry helium. This techniques proved somewhat more reproducible. However, further experiments showed that the eventual magnitude of the absorbance value at any given infrared peak was determined not only by the amount of sample injected, but also by the time after the injection when the spectrum was recorded.

Because of this time-varying behavior, the normal concentration versus absorbance calibration curve would not work for water. The first approach to deal with this problem was to obtain data on the absorbance of water samples at set concentrations as a function of time. Then plot the absorbance values versus time and use the intercept as the 'zero time' value. Then these intercept ('i.e., 'zero time') values could be plotted against sample concentration to give a valid calibration curve. The data necessary to complete this analysis were obtained by recording a series of infrared spectra from samples of different concentration levels (0.0, 2.55, 5.1, 12.8, and 25.5 ppm) as a function of time. At each time interval, four spectra were acquired with each consisting of 512 co-added scans. The spectra were acquired at a resolution of 1.0 cm^{-1} . These sets of spectra were

acquired over periods of time ranging from 25 to over 100 hours. Each concentration level was repeated at least two times. Methane was used as a calibration gas in these experiments.

These initial calibration curves were generated by the following procedure. The absorbance values from four separate experimental runs at the two analytical wavelengths (1653 cm^{-1} and 1700 cm^{-1}) were averaged. The four methane absorbance values at its analytical peak (1306 cm^{-1}) were also averaged. This average methane value was then normalized to a set value of 0.800. The correction factor necessary to make this adjustment was then applied to each of the averaged values for the water peaks. This gave the 'corrected average' values for the water peaks. These 'corrected averages' were then plotted versus the concentration of the water samples to give a calibration curve.

The data for these analyses are listed in Appendix K. An example calculation will serve to demonstrate the process.

1. Obtain and average the analytical peak data.

spectrum	water absorbance		methane absorbance
	1700 cm^{-1}	1653 cm^{-1}	1306 cm^{-1}
1	0.295	0.278	0.724
2	0.296	0.279	0.726
3	0.293	0.274	0.724
4	0.295	0.278	0.718
(ave)	$\overline{0.295}$	$\overline{0.278}$	$\overline{0.723}$

2. Normalize the methane peak to the reference value of 0.800

$$0.800/0.723 = 1.107$$

3. Apply this 'correction factor' to the water peaks.

$$0.295 \times 1.107 = 0.326 \text{ and } 0.278 \times 1.107 = 0.308$$

The data for the 1700 cm^{-1} peak were used to determine the eventual calibration curve. Plots of the individual curves used to define the 'zero time' absorbance values are shown in Figures 15 - 19.

As previously noted, the intercept values for these plots were plotted against the concentrations to form the calibration curve for water (at 1700 cm^{-1}). This plot is shown in Figure

20. The slope of this curve can be used to determine the absorption coefficient for water (base e) at 1700 cm^{-1} (base e) for water vapor at 1700 cm^{-1} . The calculations are shown below.

Beer's law (base e) can be expressed as

$$\ln(10)A = \epsilon l c$$

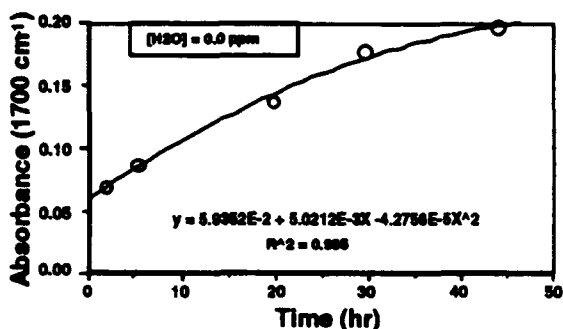


Figure 15. Calibration Curve for 0.0 ppm Water.

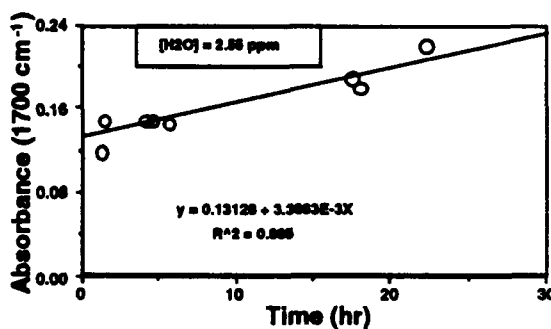


Figure 16. Calibration Curve for 2.55 ppm Water.

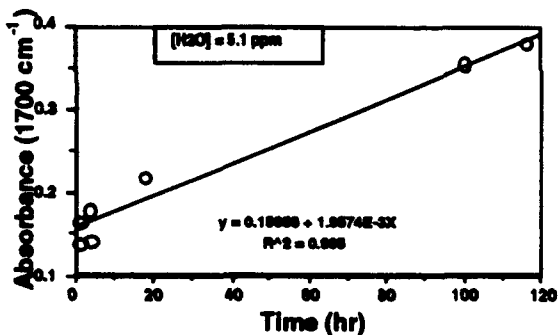


Figure 17. Calibration Curve for 5.1 ppm Water.

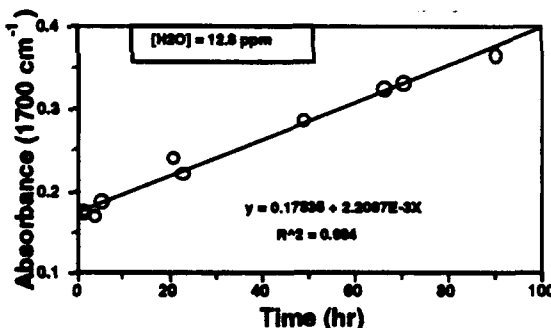


Figure 18. Calibration Curve for 12.8 ppm Water.

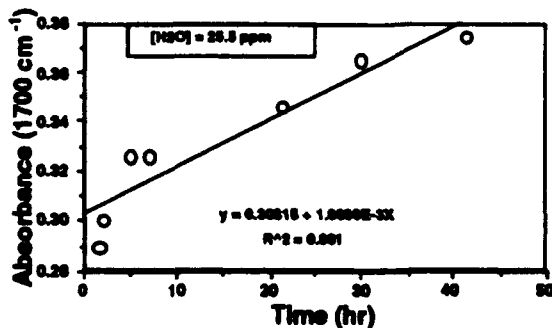


Figure 19. Calibration Curve for 25.5 ppm Water.

Where A is the absorbance (base 10), l is the path length (cm), ϵ is the extinction coefficient (base e) and c is the concentration (atm). The above expression may be rearranged slightly to give,

$$A = [l/\ln(10)] \epsilon c$$

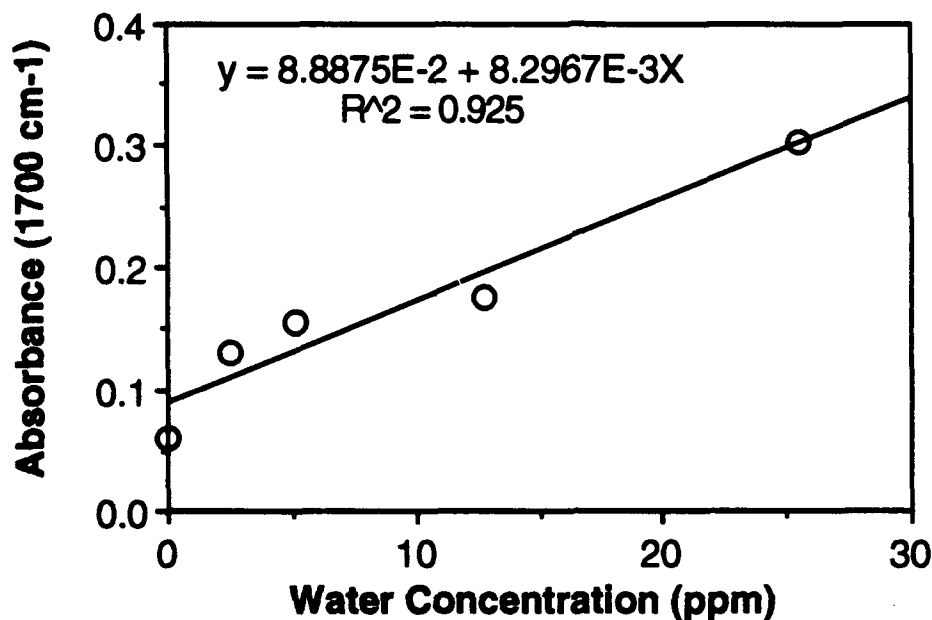


Figure 20. Calibration Curve for Water Vapor Based on the 'Zero Time Intercept Data from Figures 15-19 above.

Thus, if absorbance is plotted against concentration (i.e., Figure 20), the slope is $[l/\ln(10)]\epsilon$, or $\epsilon = [\ln(10)/l]$ (slope). Substituting the value of the slope from Figure 20 and the pathlength (106 meters) gives,

$$\epsilon = [(2.303)/(1.06 \times 10^4 \text{ cm})](8.297 \times 10^{-3})(10^6 \text{ atm}^{-1})$$

$$\epsilon = 1.8 \text{ cm}^{-1} \text{ atm}^{-1}$$

This is a relatively weak band.

Further consideration of the time varying nature of the water absorbance versus concentration curve, resulted in the decision to consider a 3-dimensional calibration curve, or, more precisely, a calibration plane. The first attempt was made by simply performing an analysis (using the program

STATGRAPHICS®, V 4.0, STSC, Inc., Rockville, MD) on the absorbance, time, concentration data as obtained. This gave an initial plane with absorbance as the dependent variable and time and concentration as the independent variables. The equation of the plane was,

$$A = 0.007169(\text{conc.}) + 0.002001(\text{time}) + 0.109257$$

with a fitting parameter, $R^2 = 0.943$.

In an attempt to improve the fit somewhat, the following was tried. Each set of measurement time versus absorbance data (for the 1700 cm^{-1} line) was plotted and fit with the best straight line (i.e., the fits from Figures 15-19 above). Then the equation for each line was used to generate absorbance values for an arbitrary set of measurement times from 0 - 100 hours at 5-hour intervals. This was accomplished by using a short computer program written in GWBASIC (Appendix L).

The results of this program are listed in Table 1. It was clear that there were problems with the values for 0.0 ppm and 2.55 ppm. The parabolic fit for the 0.00 ppm data caused the calculated absorbance value to peak at 60 hours, then decline. Thus, only the data points from 0 - 60 hours were used. In the case of the 2.55 ppm data, the values were larger than the 5.1 ppm data after the 20 hour point. Therefore, the 2.55 ppm data were dropped entirely. The remaining data points were plotted in three dimensions with absorbance as the dependent variable by using the STATGRAPHICS program. The results were somewhat improved. The improved equation for the best fit plane was:

$$A = 0.0074403 (\text{conc}) + 0.002075 (\text{time}) + 0.100147$$

The fitting coefficient was 0.984. This calibration plane is shown in Figure 21.

Table 1. WATER CALIBRATION DATA GENERATED FROM THE BEST FIT LINES OF ABSORBANCE - TIME PLOTS FOR EACH CONCENTRATION VALUE.

Time (hr)	0.0 ppm	2.55 ppm	5.1 ppm	12.8 ppm	25.5 ppm
0	0.059	0.131	0.157	0.175	0.303
5	0.083	0.148	0.166	0.186	0.313
10	0.105	0.165	0.176	0.197	0.322
15	0.125	0.182	0.186	0.209	0.332

Table 1. WATER CALIBRATION DATA GENERATED FROM THE BEST FIT LINES OF ABSORBANCE - TIME PLOTS FOR EACH CONCENTRATION VALUE. (CONCLUDED)

Time (hr)	0.0 ppm	2.55 ppm	5.1 ppm	12.8 ppm	25.5 ppm
20	0.143	0.199	0.196	0.22	0.341
25	0.158	0.216	0.206	0.231	0.35
30	0.172	0.233	0.215	0.242	0.36
35	0.183	0.25	0.225	0.253	0.369
40	0.192	0.267	0.235	0.264	0.379
45	0.199	0.284	0.245	0.275	0.388
50	0.204	0.301	0.255	0.286	0.398
55	0.206	0.318	0.264	0.297	0.407
60	0.207	0.335	0.274	0.308	0.417
65	0.205	0.351	0.284	0.319	0.426
70	0.201	0.368	0.294	0.33	0.435
75	0.195	0.385	0.303	0.341	0.445
80	0.187	0.402	0.313	0.352	0.454
85	0.177	0.419	0.323	0.363	0.464
90	0.165	0.436	0.333	0.374	0.473
95	0.151	0.453	0.343	0.385	0.483
100	0.134	0.47	0.352	0.396	0.492

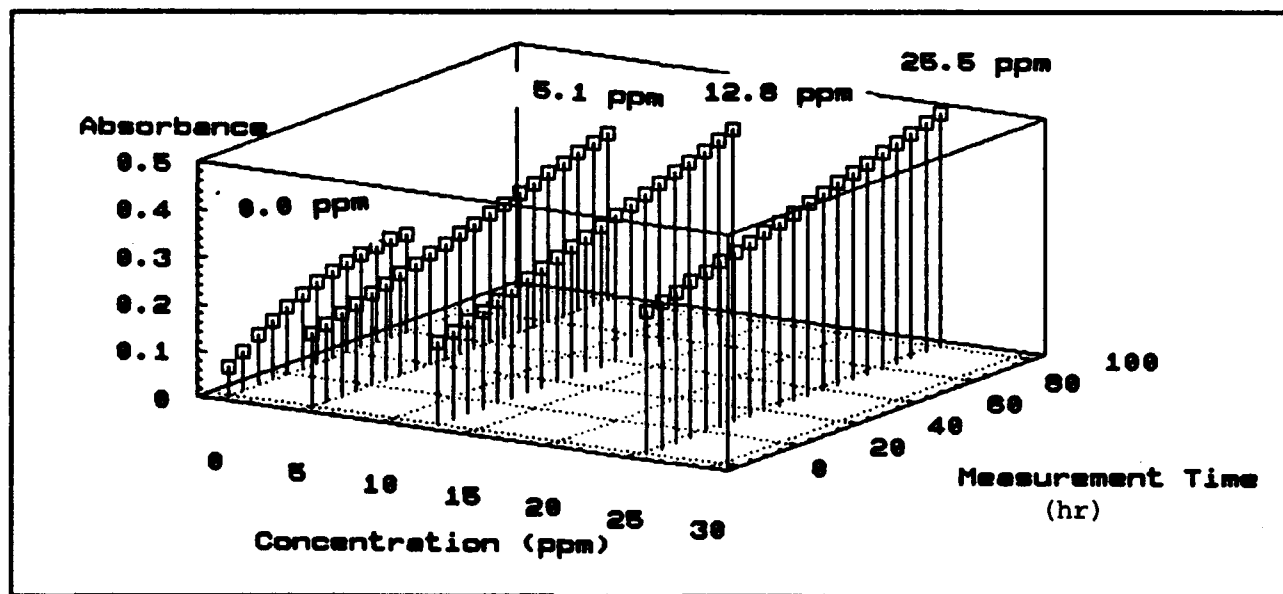


Figure 21. Plot of Absorbance Versus Concentration and Measurement Time for the Water Data

The plot of the expected absorbance values versus the predicted values (based on the best fit plane equation) are shown in Figure 22. To test the ability of this equation to find an unknown concentration value from an absorbance - time value, a series of calculations were done comparing measured concentrations with concentrations calculated from the best fit plane equation. The results are shown in Table 2.

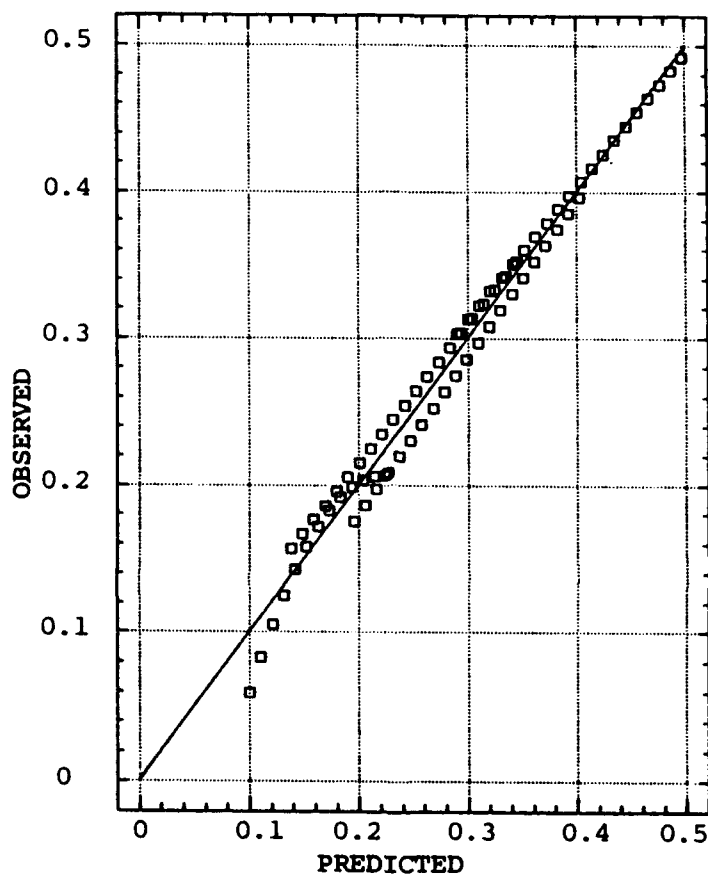


Figure 22. Plot of Expected versus Predicted Absorbance Values Based on the Water Calibration Plane Shown in Figure 21.

The results show that the calibration plane values were generally quite good at the upper concentration range, but too high at the lower concentrations. This best-fit plane equation was subsequently used for calculating the water concentration values from the measurement time and absorbance values of the FT-IR data. This was accomplished by simply including the best-fit plane equation in the spreadsheet calculations which were made on the raw data from the chamber (see Appendix A).

Table 2. WATER CALIBRATION DATA. COMPARISON OF ACTUAL CONCENTRATIONS INJECTED VERSUS CONCENTRATIONS CALCULATED FROM BEST FIT PLANE (DATA ARE FROM JULY - AUGUST 1989).

[H ₂ O] injected (ppm)	[H ₂ O] calc. (ppm)	Measurement Time (hr)	Absorbance	Run No.
0.00	-4.732	1.958	0.069	2
0.00	-3.367	5.254	0.086	2
0.00	-0.666	19.666	0.136	2
0.00	1.949	29.567	0.176	2
0.00	0.631	43.933	0.196	2
0.00	1.180	1.482	0.112	3
0.00	2.079	8.861	0.134	3
0.00	1.570	22.734	0.159	3
0.00	2.112	32.358	0.183	3
0.00	2.708	46.607	0.217	3
0.00	3.514	56.729	0.244	3
0.00	2.565	70.735	0.266	3
0.00	2.540	80.946	0.287	3
0.00	-4.355	166.879	0.414	3
0.00	-8.267	238.743	0.534	3
2.55	1.920	1.236	0.117	1
2.55	4.608	5.576	0.146	1
2.55	9.900	22.262	0.220	1
2.55	6.058	1.340	0.148	2
2.55	5.136	4.164	0.147	2
2.55	6.920	17.526	0.188	2
2.55	5.922	1.346	0.147	3
2.55	5.032	4.538	0.147	3
2.55	5.549	18.106	0.179	3
5.10	8.271	1.114	0.164	1
5.10	9.566	3.700	0.179	1
5.10	11.171	17.706	0.220	1
5.10	4.628	1.167	0.137	2
5.10	4.343	4.114	0.141	2
5.10	6.162	100.250	0.354	2
5.10	5.090	116.624	0.380	2
12.80	9.949	1.362	0.177	1
12.80	10.476	5.256	0.189	1

Table 2. WATER CALIBRATION DATA. COMPARISON OF ACTUAL CONCENTRATIONS INJECTED VERSUS CONCENTRATIONS CALCULATED FROM BEST FIT PLANE (DATA ARE FROM JULY - AUGUST 1989). [CONCLUDED]

[H ₂ O] injected (ppm)	[H ₂ O] calc. (ppm)	Measurement Time (hr)	Absorbance	Run No.
12.80	13.321	20.599	0.242	1
12.80	9.440	1.261	0.173	2
12.80	8.480	3.739	0.171	2
12.80	9.997	22.879	0.222	2
12.80	11.601	48.938	0.288	2
12.80	11.748	66.241	0.325	2
12.80	11.560	70.288	0.332	2
12.80	10.496	90.010	0.365	2
25.50	26.343	1.857	0.300	1
25.50	29.004	4.845	0.326	1
25.50	27.241	29.963	0.365	1
25.50	25.244	41.461	0.374	1
25.50	24.925	1.639	0.289	2
25.50	28.405	6.995	0.326	2
25.50	27.125	21.222	0.346	2

D. BLACK IRON PLATES

In preparation for a series of runs with hydrazine and black iron plates, the chamber was heated to 45 °C, and pumped out with the mechanical pump. This produced an obvious new set of aliphatic C-H bands in the 2700-3100 cm⁻¹ and 1450-1470 cm⁻¹ regions. These have clearly resulted from paraffin wax vapors depositing on the mirror and window surfaces. They detract somewhat from the overall sensitivity of the IR signal, but are ratioed out in any subsequent spectra and so pose no significant problem.

Following the above procedure, two hydrazine stability runs in pure, dry helium were conducted, the first for 6 days and the second for 14 days. There was considerable conditioning noted in these runs as seen in Figure 23.

Following these characterization runs, 19 black iron plates were placed into the chamber. Two baseline hydrazine decay runs in pure, dry helium were conducted. Between the two runs,

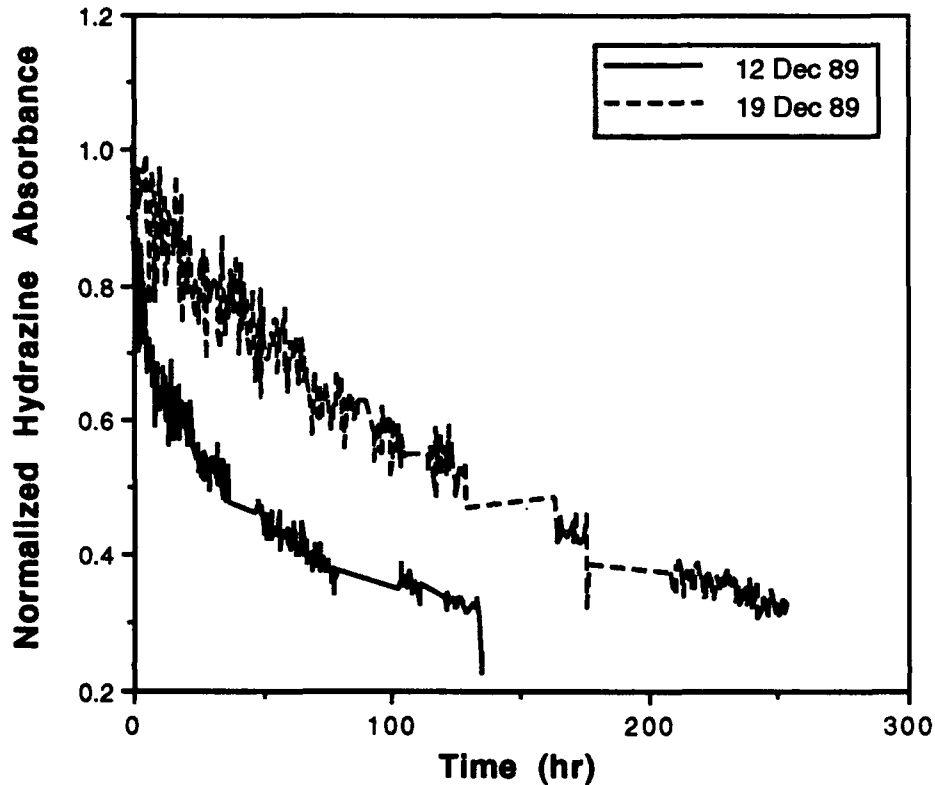


Figure 23. Hydrazine Decay in Pure, Dry Helium (No Added Plates)

the chamber was evacuated overnight with the turbopump. In spite of this, there was a substantial conditioning effect evident from the first to the second run as shown in Figure 24. Traces of ammonia were evident after the second run.

When the first decay run (4 Jan 90) was modeled, the fits were about the same for all the models except those which invoked a reaction intermediate (MOD385 and MOD390); these gave a significantly poorer fit. This is reasonable in terms of the expected reactivity of this system in the absence of oxygen. Model MOD360 gave the best fit by a slight margin.

The second decay run (5 Jan 90) gave somewhat different model fit results. The single-site model (MOD350) gave a slightly better fit than the two-site model (MOD360), which could be a reflection of the conditioning process. However, the overall magnitude of the fit (as measured by

the sum of squares of the residuals) was about a factor of 10 worse than the fit for Run 1. This is

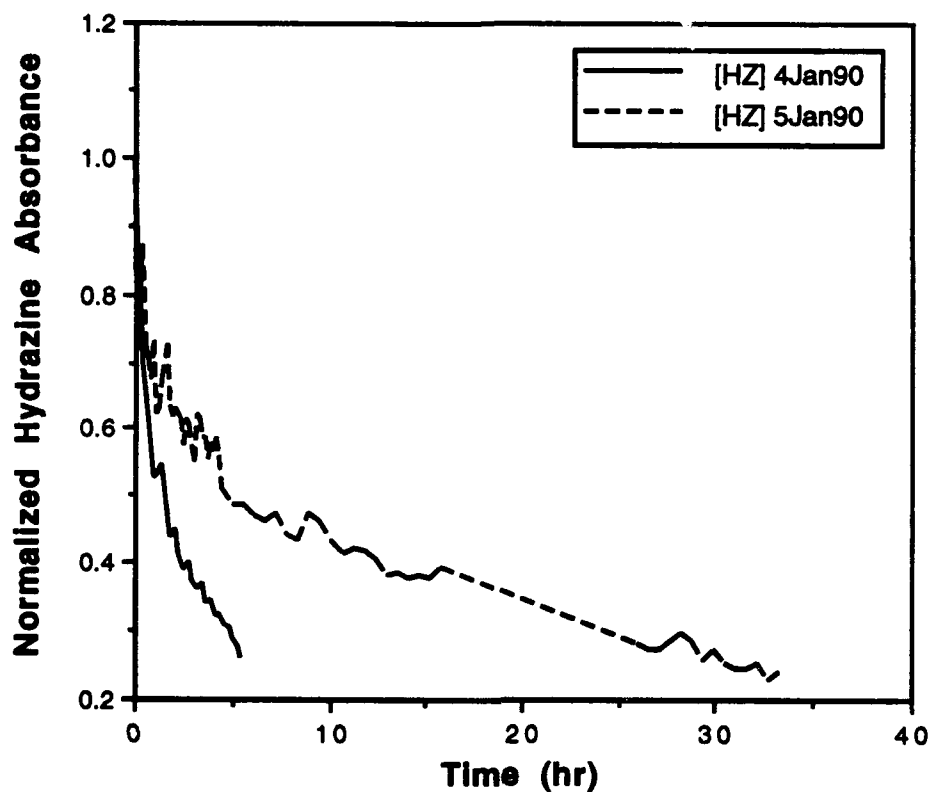


Figure 24. Hydrazine Decay in Pure, Dry Helium with 19 Black Iron Plates.

partly due to a decrease in S/N in Run two. The other models all gave similar, though somewhat poorer fits except for MOD370 and MOD385 which gave very poor fits.

Following these baseline decay runs, several runs were made with 80 percent dry helium and 20 percent oxygen. These runs showed an overall conditioning effect, even when the chamber was thoroughly pumped out between runs. The decay times were much faster in the presence of oxygen, with half lives of one hour or less. This indicates that the black iron plates exhibit a significant degree of catalytic activity with respect to hydrazine oxidation in synthetic air. The runs conducted under these conditions are shown in Figure 25. Ammonia was a minor product in these runs as well. About twice as much was produced as in the runs with no oxygen, but this still amounted to only 2-4 ppm.

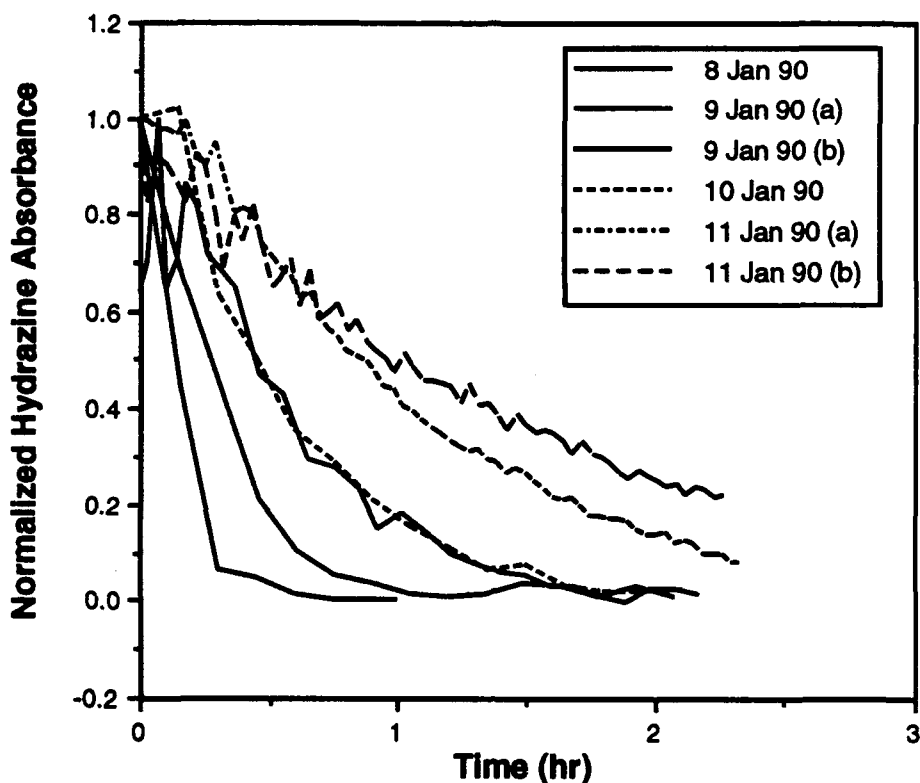


Figure 25. Hydrazine Decay with 19 Black Iron Plates in 80 Percent Dry Helium and 20 Percent Oxygen.

The 8 Jan 90 and the 9(b) Jan 90 runs could not be modeled because of the poor quality of the data. The remaining runs were most closely modeled by the single-site model MOD350, although again, the differences with the other models were small. As before, MOD385 and MOD390 were significantly worse.

Finally, two sets of runs were conducted in humid, synthetic air. There was less conditioning evident, and the decay rate was increased by about a factor of four over the runs in dry synthetic air. These runs produced the most ammonia, about 25 percent more than the runs in dry synthetic air. The hydrazine decay curves are shown in Figure 26.

The 16(a) Jan 90 data were too sparse to permit modeling. The other three runs were fit best by the two-site model MOD370. In the presence of high concentrations of water vapor, this model suggests that two types of active sites are participating in the decay kinetics. The relatively poor fits provided by the models which produce intermediate species is supported by the fact that there was only a very small quantity of diimide observed in these runs.

A summary of the model fits for all of the black iron data is given in Appendix P.

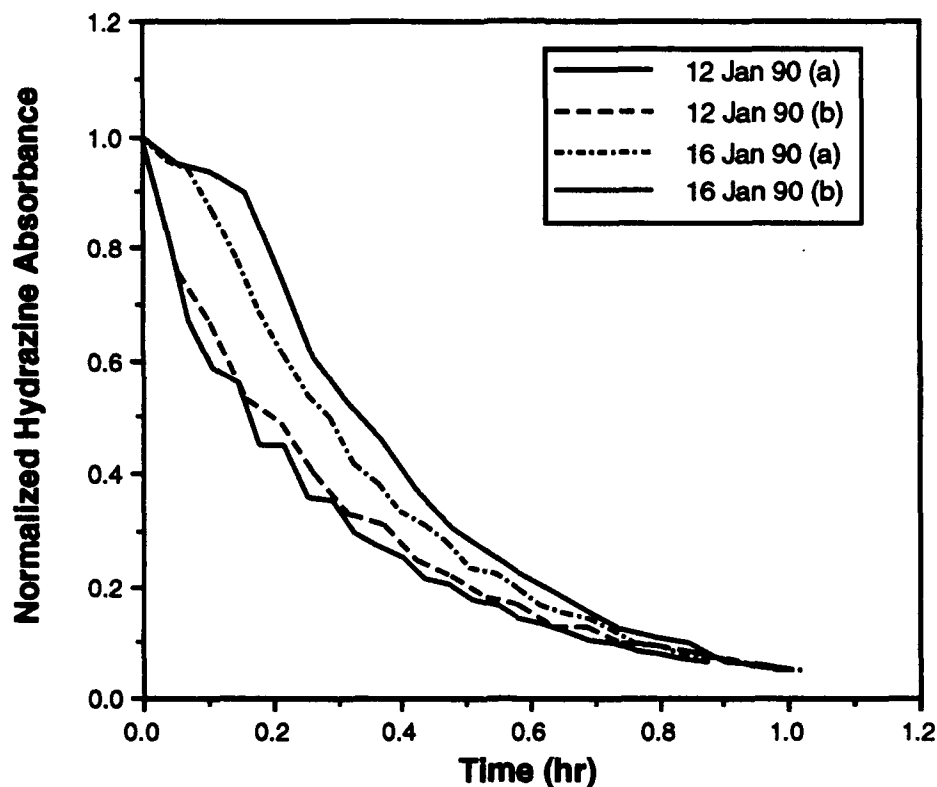


Figure 26. Hydrazine Decay with 19 Black Iron Plates in 80 Percent Helium and 20 Percent Oxygen with 50 Percent Relative Humidity.

Because the mechanism proposed for the catalytic oxidation of hydrazine involved diimide ($\text{HN}=\text{NH}$) as an intermediate (Reference 2), an attempt was made to see if any of this material could be seen in the decay spectra with black iron plates present. In the presence of oxygen, there was indeed a small amount found as verified by peak comparison with an infrared spectrum taken by Tuazon and co-workers (Reference 9). These spectra are shown in Figure 27.

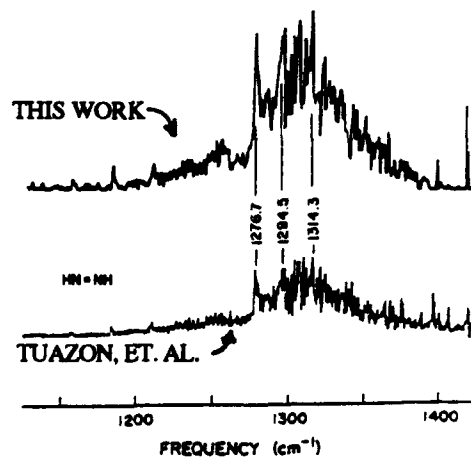


Figure 27. Comparison of Diimide Spectra from Tuazon, et. al. (Reference 9) and This Work.

E. CORRODED ALUMINUM PLATES

Following the observation by researchers at NASA/WSTF that corroded aluminum plates were very reactive with respect to heterogeneous hydrazine vapor oxidation, plates of this type were evaluated in the RDVC chamber. At first, 20 of the plates which had been synthetically corroded as described earlier (see Section II. B. 1.) were placed in the chamber. However, when hydrazine vapor was added in the usual manner, it decayed so rapidly that no useable spectra as a function of time could be obtained. The number of plates was cut to four, and the chamber was "conditioned" with a large excess of hydrazine vapor, still the reaction was too rapid to follow. Finally, three of the remaining plates were removed, leaving only one plate in the chamber. This single plate proved very reactive, but at least it was possible to follow the reactions of hydrazine and oxygen in synthetic air.

With the single plate in the chamber, two runs were made in pure, dry helium to establish the baseline reactivity of the system. After the first run, the chamber was pumped out to 10 microns pressure with the turbopump. There was still a significant conditioning effect evident between the two runs as shown in Figure 28.

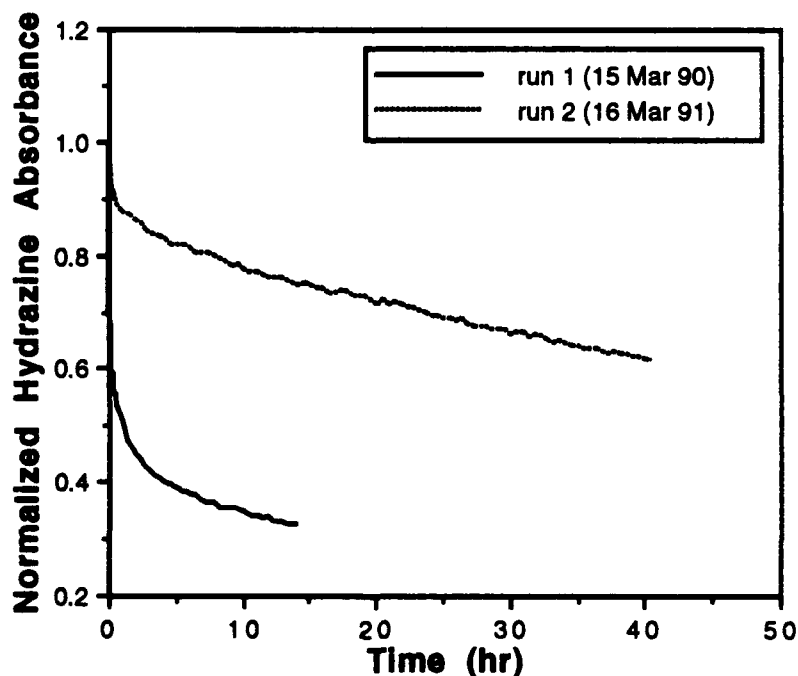


Figure 28. Hydrazine Decay in Pure, Dry Helium with One Corroded Aluminum Plate.

Model MOD310 gave very good fits for these two runs, although most of the other models gave fits which were almost as good. This provides some substance to the assumption that the reaction involves two surface sites both of which are susceptible to poisoning by reactions with vapor-phase species.

These baseline reactivity runs were followed by a series of six runs with 80 percent helium and 20 percent oxygen (dry conditions). The decay was very rapid in these runs with half lives of 1 hour or less. There was the usual conditioning effect from one run to the next. These runs are shown in Figure 29. Some diimide formation was also evident in these runs. It built up to a maximum at about 1/2 an hour then decayed slowly down from there. This is typical behavior for an intermediate in an oxidation reaction of this type.

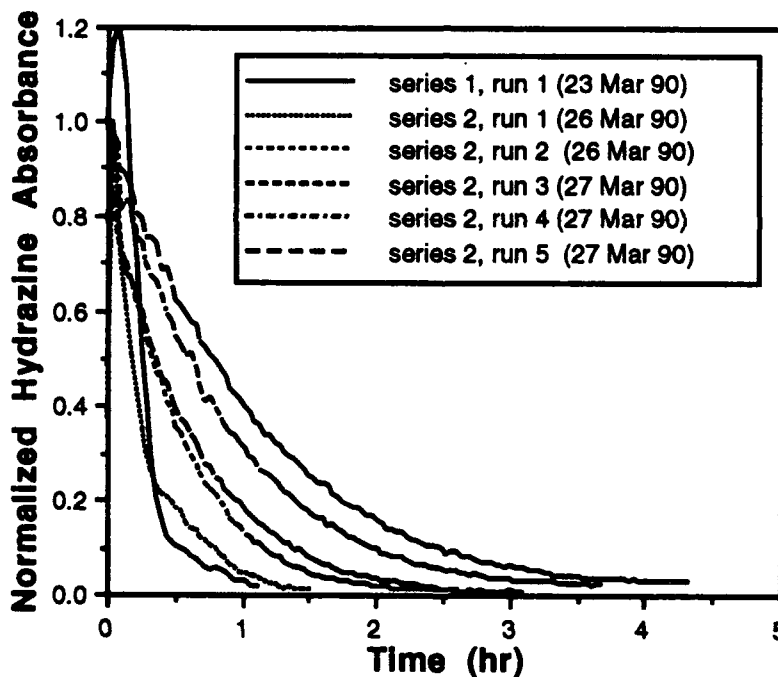


Figure 29. Hydrazine Decay in 80 Percent Helium and 20 Percent Oxygen with One Corroded Aluminum Plate.

Because of the obvious formation of the diimide intermediate, the feeling was that models which explicitly incorporated an intermediate (i.e., MOD385 and MOD390) would provide the best fits to these data. However, this proved not to be the case. In fact, these models provided the worst fits, by far. Of the other models, MOD375 provided the best fit. This is a two-site model

with no explicit intermediate formation. This leads to the conclusion that neither MOD385 nor MOD390 have sufficient information to account for the intermediate properly, i.e., they need to be expanded, or intermediate concentration data need to be directly incorporated into their fitting runs.

Finally, two experimental runs were made under humid conditions with 20 percent oxygen present. Under these conditions, the reactivity was greatest. About twice as much diimide intermediate was produced as was the case under dry conditions. Also, about twice as much ammonia was produced, although both of these compounds were produced in amounts less than 5 ppm. The hydrazine half-life was less than 1/4 hour in these runs. They are plotted in Figure 30.

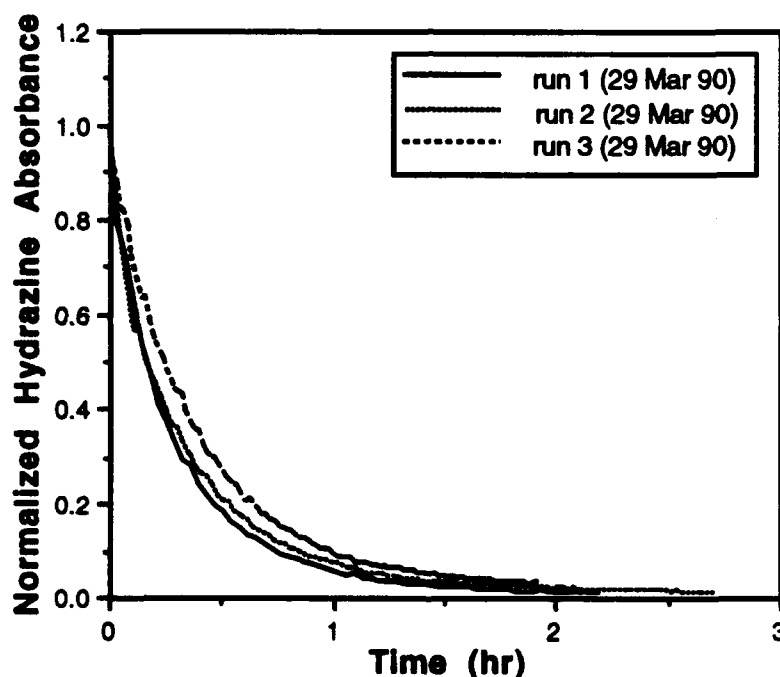


Figure 30. Hydrazine Decay in 80 Percent Helium and 20 Percent Oxygen (Under Humid Conditions) with One Corroded Aluminum Plate.

A similar situation occurred in this case [i.e., decay in 80 percent humid helium and 20 percent oxygen] when the models were applied. The two models which specifically include an intermediate gave very poor fits. The best fit for these reaction conditions was provided by MOD315. This two site model handles the data well in spite of the lack of an explicit intermediate being formed. This again leads to the conclusion that the models which do have an intermediate must need some additional measurement information or mechanistic adjustments.

The spectra of hydrazine decay under the conditions of 80 percent humid helium and 20 percent oxygen (Figure 31) show the formation of diimide and ammonia very clearly. In these time-sequence spectra, the build up and subsequent decay of diimide is evident as is the formation of ammonia.

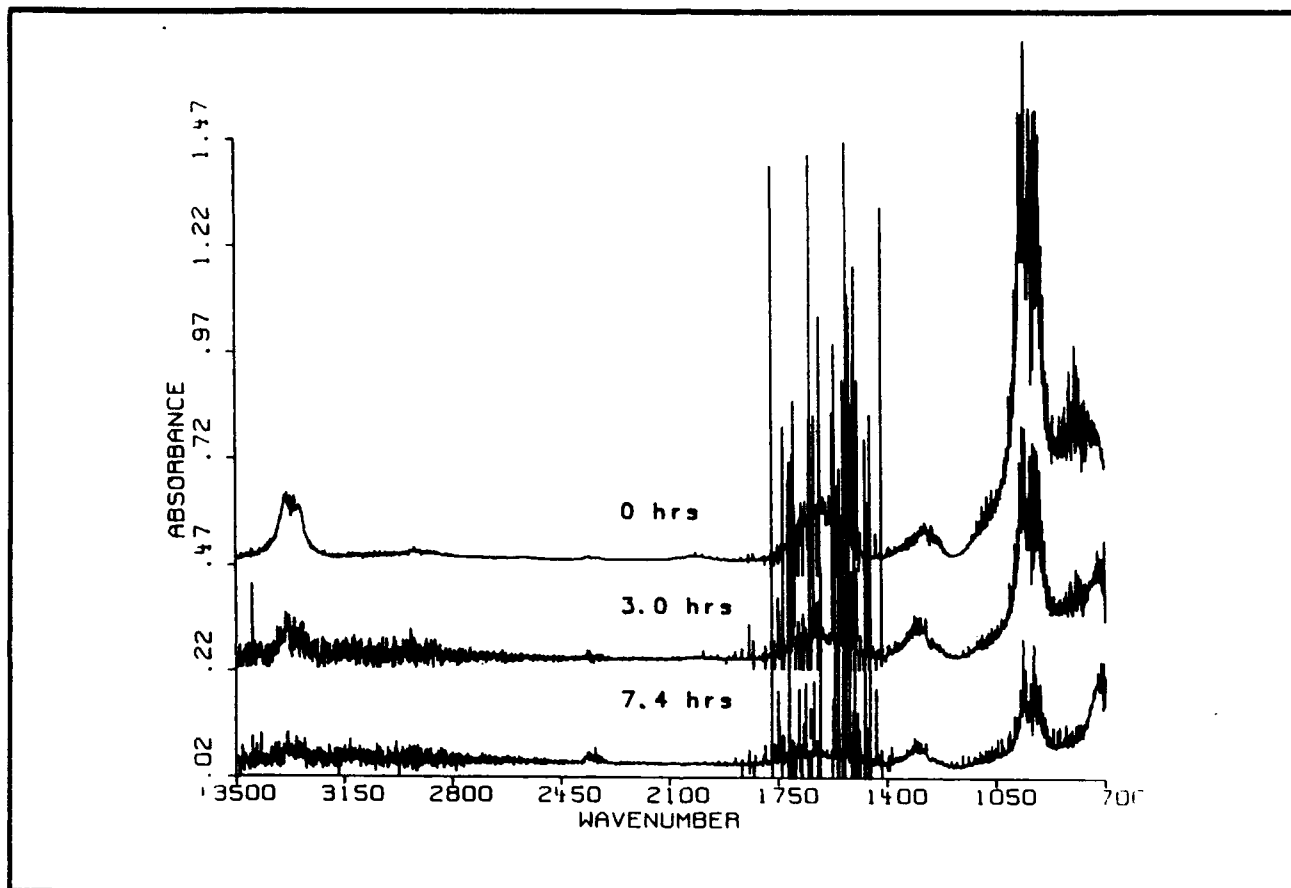


Figure 31. Hydrazine Decay in 80 Percent Helium and 20 Percent Oxygen with One Corroded Aluminum Plate. Spectra were acquired at the Beginning, Middle, and End of the Run.

The concentration of diimide was monitored in many of these runs because of the near coincidence of one of its principal bands with the methane analytical band at 1306 cm^{-1} (i.e., the software used to automatically acquire a band at the methane location produced, in the absence of methane, values which were absorbances for diimide). The diimide concentration as a function of time in the humid helium plus oxygen run is shown in Figure 32 as an example.

Finally, a comparison was made between the observed spectral bands in the hydrazine decay plots and bands from diimide and hydrogen peroxide. These are shown in Figure 33. It is clear

that in these spectra at least, no hydrogen peroxide is apparent as a reaction intermediate in these hydrazine decay reactions.

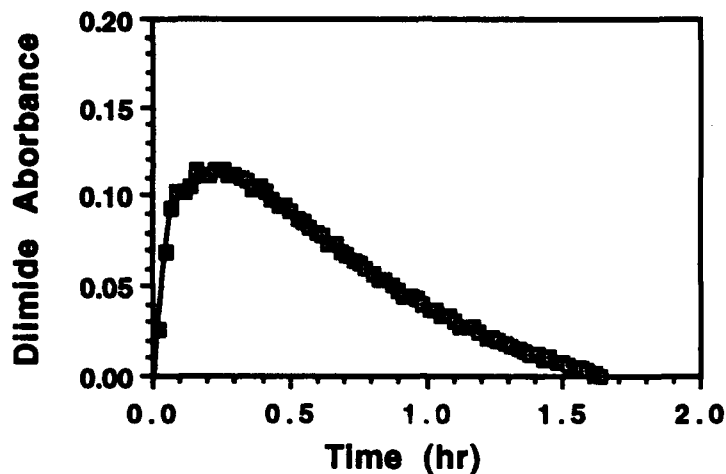


Figure 32. Diimide Formation in the Decay of Hydrazine in 80 Percent Humid Helium and 20 Percent Oxygen with One Corroded Aluminum Plate.

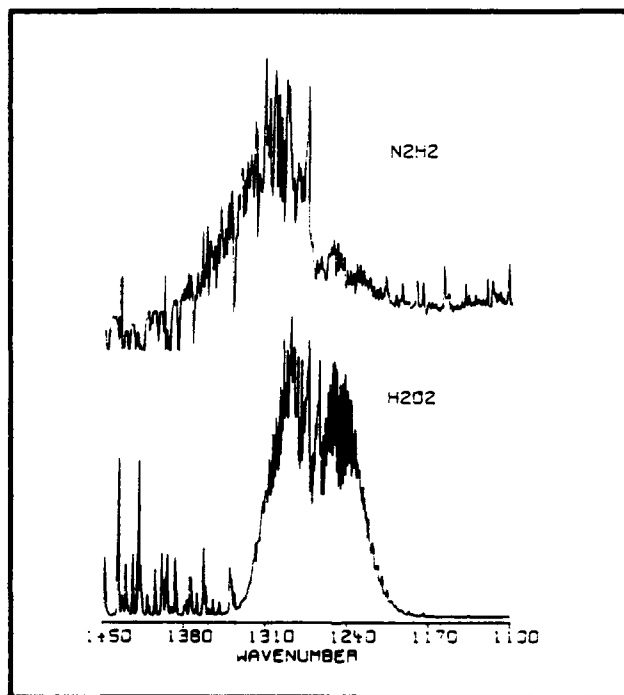


Figure 33. Plots of Hydrazine, Diimide, and Hydrogen Peroxide Showing their Relative Band Positions for Spectral Identification.

A summary of all the model fits for the experiments with corroded aluminum plates is given in Appendix Q.

F. ADDITIONAL BASELINE REACTIVITY RUNS (NO ADDED PLATES)

At the conclusion of the experiments with the corroded aluminum plates, the chamber was opened and the plates were removed. The chamber was cleaned by vacuuming the interior bottom section and wiping as much of the interior as possible with a 50-50 mixture of acetone and methanol. Then the chamber was closed up and pumped down overnight.

The first run in this series was a hydrazine decay run in pure, dry helium. 100 ppm HZ were flushed into the chamber and the decay was followed for an extended period of time. The results were typical of earlier runs, indicating no drastic change in the chamber's basic characteristics had occurred. The decay of hydrazine in this run is shown in Figure 34.

Models which did not incorporate intermediates gave good fits. Models MOD361 and MOD360 gave the best fits; but both of these have insufficient site 2 characterization.

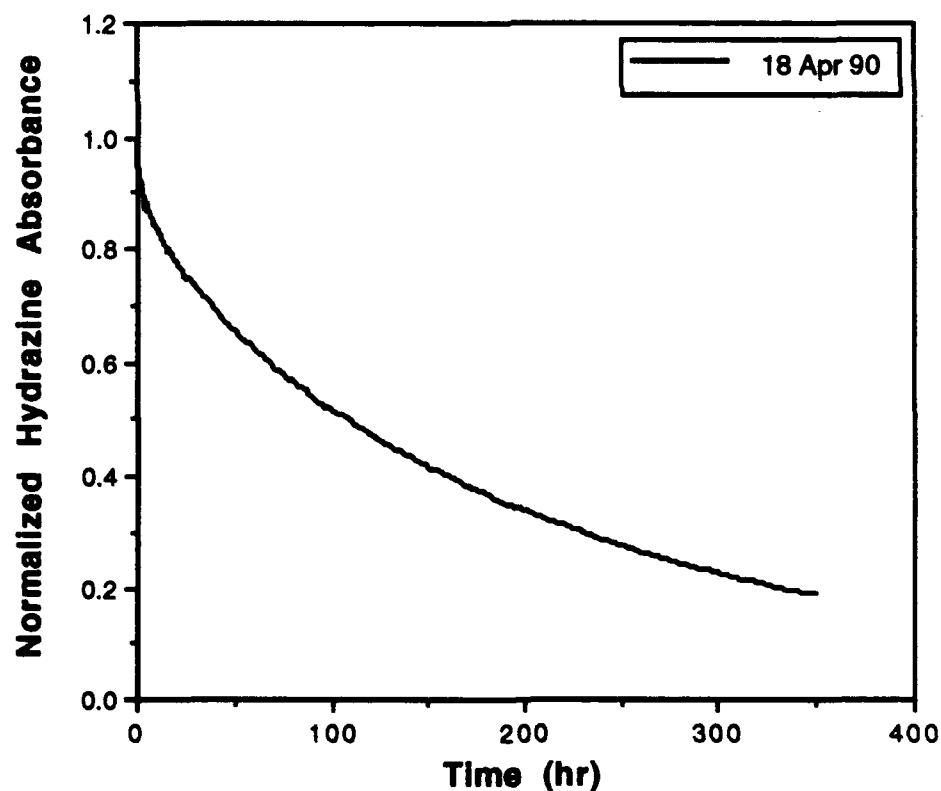


Figure 34. Hydrazine Decay in Pure, Dry Helium with No Added Plates.

Of the remaining models, only MOD310 and MOD370 gave reasonable values. MOD310 incorporates two surface sites, both of which can become contaminated. It produces ammonia from site 1 and product from site 2. This gave a somewhat better fit than model MOD370 which allows only one site to become contaminated and produces ammonia from site 2 and product from site 1.

Following this run, an experiment was conducted where 100 ppm HZ were flushed into the chamber in humid helium. In this case, the expected increase in decay rate was observed, as in earlier trials under these conditions. The decay is shown in Figure 35.

For the humid helium run, the best fit was given by model MOD361. This model

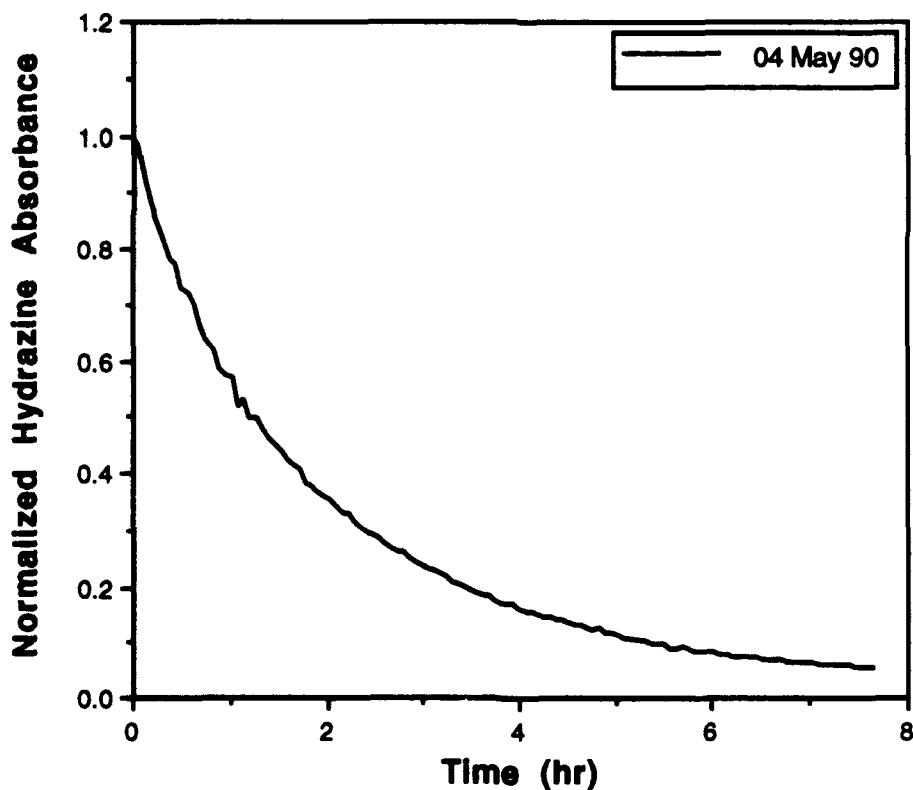


Figure 35. Hydrazine Decay in Humid Helium (No Added Plates).

is of limited utility because it does not account for the fate of the second type of surface sites. It may, however, serve as a guide for improved attempts to model this particular system.

Next a series of four runs was used to test the behavior of hydrazine in the presence of oxygen, under dry conditions. The decay patterns were interesting. They were considerably faster than the run with no oxygen present (Fig. 34 above), but not quite as fast as the pure, humid helium run. Also, there was no evidence for conditioning in these runs. They are shown in Figure 36 below.

Model MOD310 provided the most consistently good fits to this series of runs. The other models all had difficulty with the 25 May 90 run, but the reason for this is not clear.

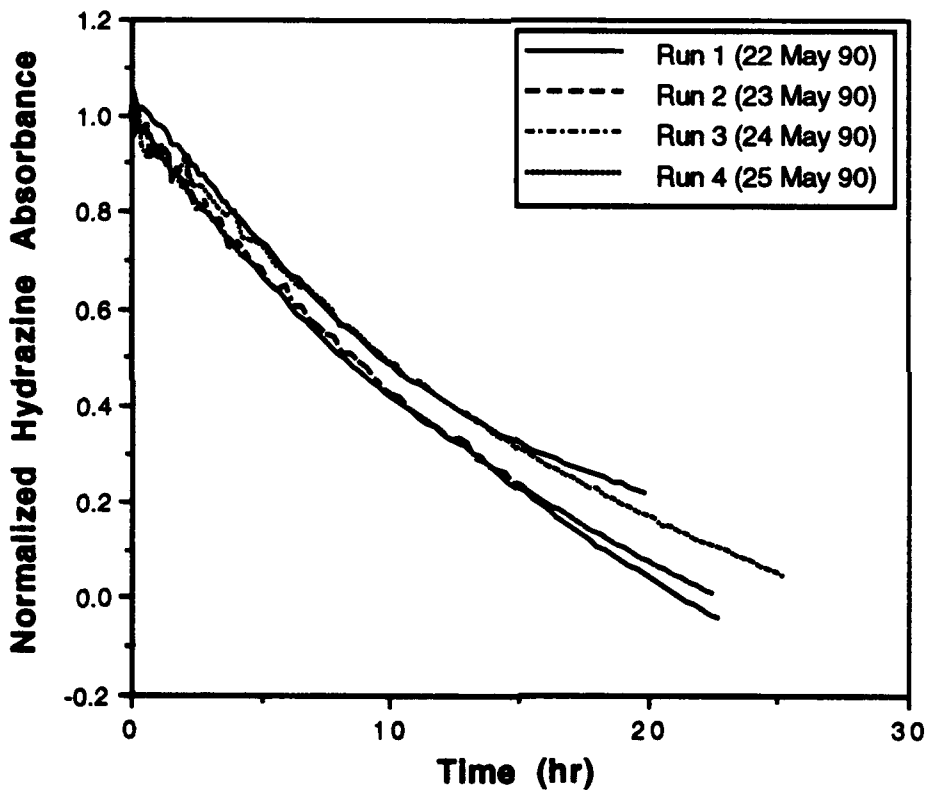


Figure 36. Hydrazine Decay in Dry Helium with 20 Percent Oxygen (with No Added Plates).

The general approach followed by MOD310 shows a good deal of flexibility since it can handle both the dry and humid conditions under which these runs were conducted.

Following the humid helium runs, a final set of characterization runs was made with humid helium and 20 percent oxygen. In this case, three runs were made and a definite conditioning effect was observed. However, the decay rate was no more rapid than in the humid helium run

with no added oxygen. These conditions also produced the highest levels of ammonia and diimide. The results of these three runs are shown in Figure 37.

For this final series of runs, the only models which could successfully handle all three runs (the 1 Jun 90 run diverged for all other models) were MOD380 and MOD385. These models include intermediates specifically and provide the first case where they gave the best fits. This has some significance since diimide production in these runs was among the highest of any experiment in the entire study.

Appendix N summarizes the model fits for all of the experiments described in this section.

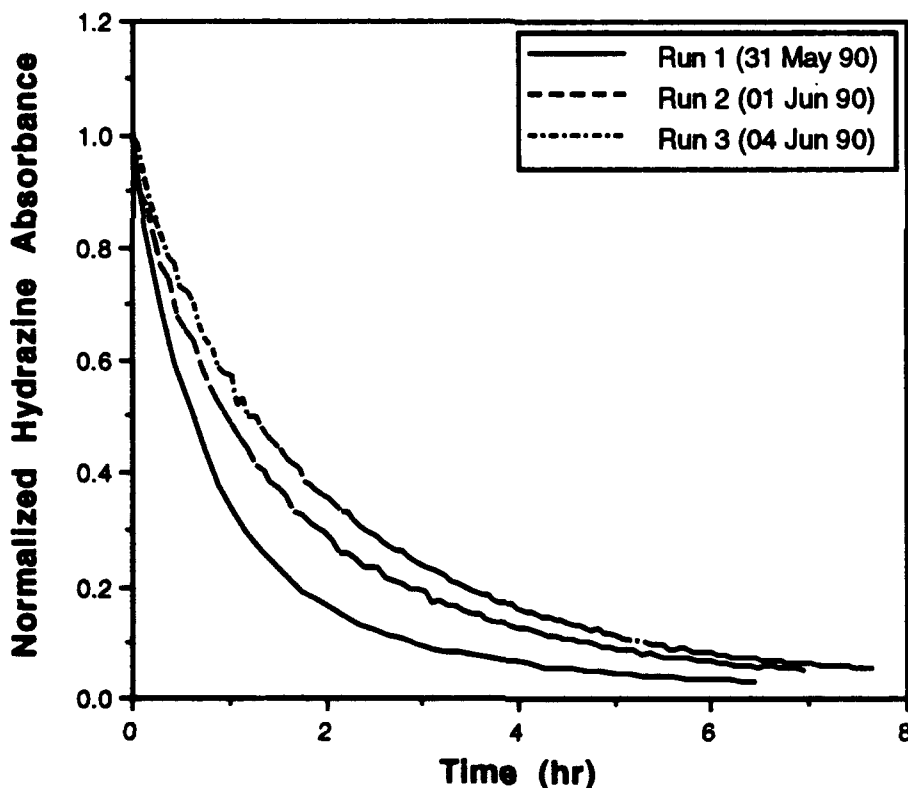


Figure 37. Hydrazine Decay in Humid Helium with 20 Percent Oxygen (with No Added Plates).

G. PAINTED ALUMINUM PLATES

The final set of experiments on added surfaces was conducted with 20 aluminum plates which were painted in the same manner as an F-16 aircraft. The plates were placed in the holder inside the chamber after they had been rinsed carefully with a 50-50 mixture of acetone and methanol. The chamber was pumped down to 5×10^{-6} Torr and left overnight.

The first set of three runs was carried out by flushing 50 ppm HZ vapor into the chamber with dry helium. The decay was fairly rapid with a half life of about 2-3 hours. Two subsequent sequential runs showed the familiar conditioning effect with half lives increasing to about 5 and 7 hours respectively. These decay curves are shown in Figure 38.

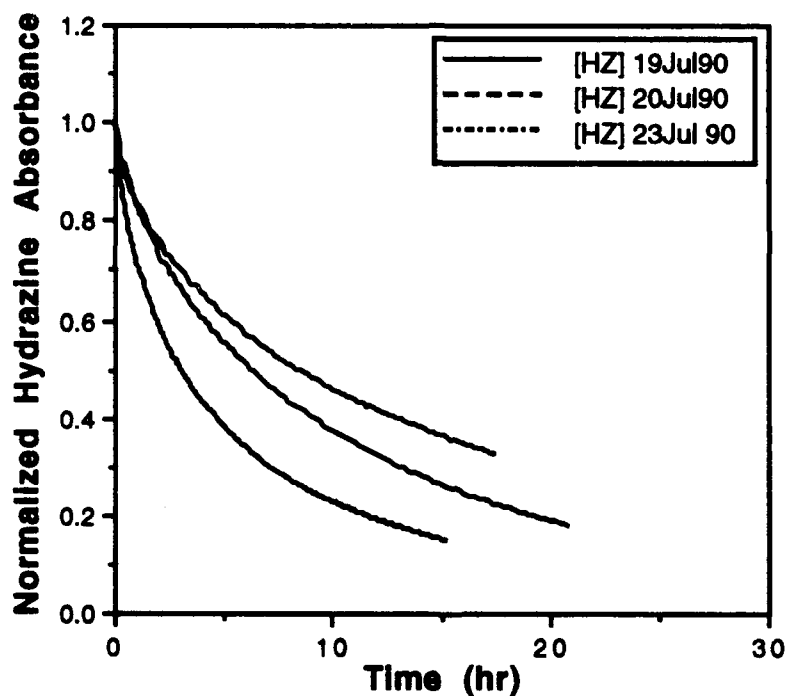


Figure 38. Hydrazine Decay in Dry Helium with 20 Added Painted Aluminum Plates.

A small amount of ammonia was formed in the initial run in this sequence and a trace was produced in the second run. The third run produced none at all. No diimide was formed during any of the three runs.

The third run could not be modeled with the two-parameter model because of the negative (i.e., zero) ammonia values. For the other two runs, all of the models, except those which include intermediates, gave very good fits. Model MOD370 gave a slightly better fit than the others. This two-site model predicts ammonia formation, but the values of the rate constant suggest it would be low. This is what is observed experimentally.

Following this first set of runs, a second set was made where 20 percent oxygen was added to the helium, again under dry conditions. There was a somewhat unusual pattern in the three runs in this set of experiments. They actually decayed somewhat faster with each run, i.e., a kind of 'reverse conditioning' effect. This is shown in Figure 39. The reason for this behavior is not known, but there may have been some unusual experimental conditions which were not noted or planned.

Under these experimental conditions, model MOD310 gave a somewhat better fit than other models. Again, models with intermediates did poorly. The model results had no clearly discernable trends which might give indications for the 'reverse conditioning' which was observed.

The next set of experiments were conducted to test the effects of humidity on the decay processes. Liquid water was flushed into the chamber with helium to give a humidity of 50 percent. Then 50 ppm hydrazine vapor was swept into the chamber with some additional helium. The resulting decay pattern followed the more familiar pattern of earlier runs. There was a definite conditioning effect as shown in Figure 40. However, there was very little difference between these runs and the runs in dry helium. Somewhat more ammonia was produced under these humid conditions, but no diimide was observed.

The nonintermediate models all generally fit the data quite well. Model MOD370 gave slightly better overall fits. This supports the experimental observation that these runs behaved almost the same as the earlier runs without water added.

The final set of runs was done under humid conditions with 20 percent oxygen added to the helium. This resulted in the most rapid hydrazine decay with half lives of two hours or less. It also gave the highest ammonia production of these runs with painted aluminum plates. Finally, there was some diimide produced as well. The hydrazine decay is shown in Figure 41.

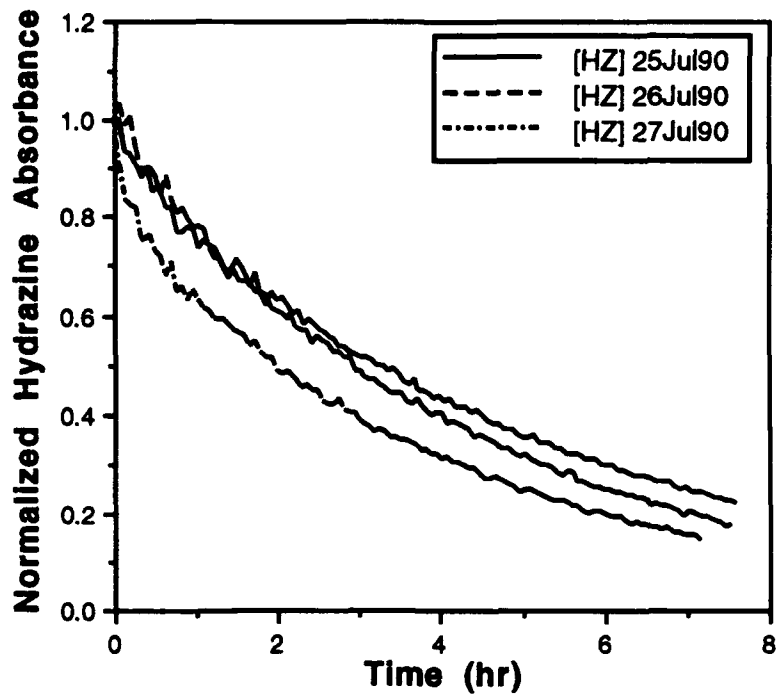


Figure 39. Hydrazine Decay in Dry Helium with 20 Percent Oxygen (with 20 Added Painted Aluminum Plates).

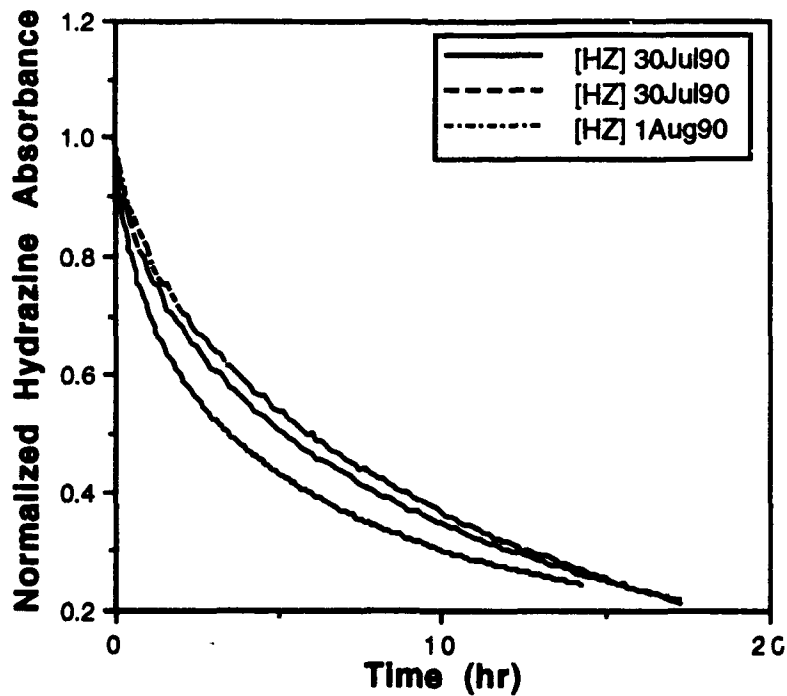


Figure 40. Hydrazine Decay in Humid Helium (with 20 Added Painted Aluminum Plates).

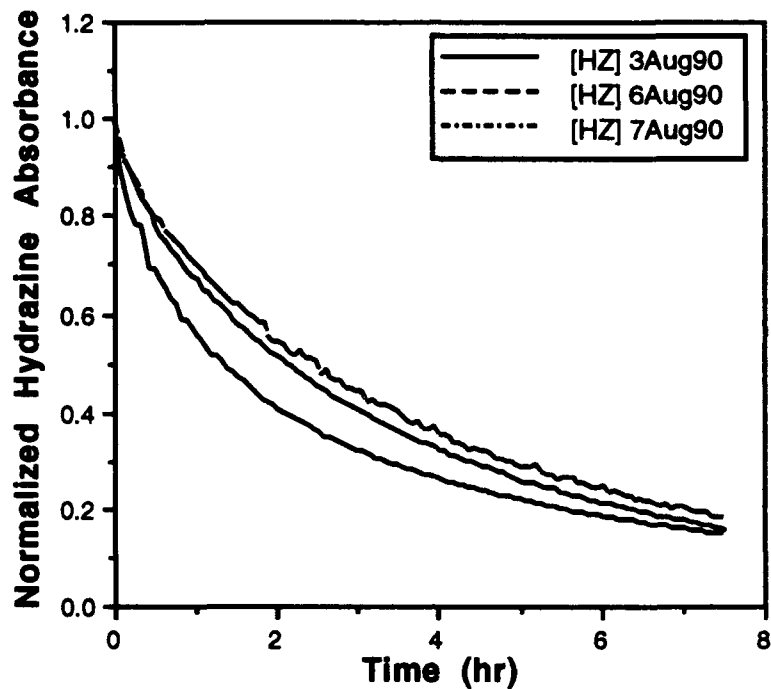


Figure 41. Hydrazine Decay in Humid Helium with 20 Percent Oxygen (with 20 Added Aluminum Plates).

Modeling of these runs showed a similar pattern to earlier runs, i.e., the nonintermediate models gave good fits, but MOD310 was the best. This is the same model which gave the best fit for the run with 20 percent oxygen and no humidity. This consistency supports the idea that water interactions are small with the painted aluminum plates.

A summary of the model fits for all of the experiments with painted aluminum plates is given in Appendix R.

SECTION V

CONCLUSIONS AND RECOMMENDATIONS

A. NO ADDED PLATES

Hydrazine decay in the spherical chamber in the absence of any added test surfaces is still controlled entirely by the chamber walls (and the mirrors, viewports, and other non-Teflon[®]-coated surfaces present). The reactivity of hydrazine can be lowered substantially by the use of inert surfaces, but interactions still occur. The use of a solid chamber did remove losses due to permeation through the walls which was an important loss mechanism in studies conducted in Teflon[®]-film chambers. Half lives in the spherical chamber, in the absence of oxygen, were about four times longer than those in the Teflon[®]-film chambers.

When oxygen is added to the system, the decay rate increases by a factor of ten. This indicates a strong interaction between the hydrazine adsorbed on the surfaces inside the chamber and the oxygen.

In the presence of large water concentrations (i.e., runs conducted under humid conditions), the decay of hydrazine is not greatly affected unless oxygen is also present. However, the production of ammonia is increased over that observed under dry conditions. The most rapid decay of hydrazine occurs under humid conditions with oxygen present. The water plays an important role in facilitating surface-catalyzed reactions. The reactive intermediate diimide is also produced under these conditions, however, there is no evidence for any hydrogen peroxide formation.

The models presented in this report generally give very good fits to the observed experimental data. These models all include two types of surface sites, indeed, earlier attempts at model fits with a single type of site were not nearly as successful. However, the models cannot identify the sites as being on the Teflon[®] surface or on some other chamber surface. The models also provide a functional description of ammonia formation, although, again, the specific formation site(s) cannot be identified with certainty.

The formation of ammonia in these runs was somewhat unexpected. The chamber is almost entirely Teflon[®] coated and the remaining surfaces are mostly Pyrex[®] glass. The ammonia

formation mechanism proposed by Martin, et. al. (Reference 2) invokes the use of a metal surface and the presence of water. The amount of ammonia produced depended on the water present, but the very small surface area of exposed metal leads to the conclusion that the same type of reaction may be possible on glass or even Teflon[®] surfaces (or on the metal beneath the Teflon[®]-coated surfaces). The same argument holds for diimide production. Further experiments will be necessary to address these mechanistic questions.

B. TEFLON-COATED ALUMINUM PLATES

Experiments with these plates were designed to determine the effects of adding additional Teflon[®]-coated surface area. The addition of the plates nearly doubled the interior surface area of the chamber, thus doubling the S/V ratio. The additional surface area decreased the half life of the pure helium runs by about a factor of four and the helium plus oxygen runs by a factor of two. There was some evidence of Teflon[®] film surface area dependence in one earlier study (Reference 1), but this was not observed when a much larger Teflon[®]-film chamber was used in a subsequent study (Reference 2).

During the course of the experiments with the Teflon[®]-coated aluminum plates, an additional group of experiments was conducted with no plates in the chamber. These runs showed that the baseline chamber reactivity in the absence of oxygen was about the same as it had been when the first group of runs with no plates present had been made. However, the decay rate in the presence of oxygen had decreased by a factor of two indicating some type of long-term conditioning effect.

These observations show that it is not yet entirely clear how the available Teflon[®] surface area is related to the observed hydrazine decay rate. The functional relationship is apparently fairly complicated, although it can be adequately modeled by a two-site approach.

C. WATER CALIBRATION SPECTRA

The decision to conduct specific experiments to determine one or more accurate analytical absorption coefficients for water was made in the hope of using this information as input to the mathematical models which were used to assist in data interpretation. It quickly became evident, however, that the task was not going to be an easy one.

The first problem was that vapor samples gave very poor reproducibility. They were also difficult to prepare accurately because of the constant adsorption of vapor samples on the vacuum lines and sample bulb. The use of liquid samples which were injected and then vaporized alleviated this problem. However, it was soon noted that the absorbance of the liquid samples was a function of time. So the data had to be gathered as a function of time and a calibration plane became necessary instead of the usual calibration line. Because of these experimental difficulties, the water calibration runs took much longer than expected.

The eventual water concentration data turned out to be less useful than anticipated. At least with the current models, it is difficult to include water into a decay mechanism in a way which produces meaningful results. Additional modeling effort will be necessary to realize the anticipated benefit of the water concentration data.

D. BLACK IRON PLATES

As noted by Martin and co-workers (Reference 2), iron and its oxides are good catalysts for hydrazine oxidation, thus it was expected that these plates would be quite reactive when exposed to hydrazine. This was borne out by subsequent observations. In the absence of oxygen, the decay rate increased by a factor of about 20 over the empty chamber. In the presence of oxygen, it was increased by an additional factor of about ten. The addition of humidity further increased the decay rates by a factor of two.

There was some ammonia formed in these runs, but only about two times the amount observed in the absence of the plates. Also, some diimide was observed, but only in small quantities. These observations lead to the conclusion that the dominant interaction mechanism in the presence of black iron plates is concerted oxidation of the hydrazine to water and nitrogen with the concomitant reduction of iron oxides present on the surface of the plates.

E. CORRODED ALUMINUM PLATES

The corroded aluminum plates were by far the most reactive plates studied during these experiments. The primary reason for this, as noted by Martin and co-workers (Reference 2), is the large surface area of the bayerite which forms on the surface during the corrosion process. Even

taking this into account, the corroded aluminum was the most reactive surface in terms of the amount of ammonia and diimide which were formed during hydrazine decay experiments. Indeed, a series of experiments were conducted with 10 of these plates in the chamber to see if a relatively large amount of diimide could be produced for additional study. This proved mostly unsuccessful for reasons which are not entirely clear.

A comparison of the same model (e.g., MOD370) for black iron runs and corroded aluminum runs suggests that one of the surface site concentrations is higher for the corroded aluminum. This result appears to indicate that the models do give an indication of the validity of a given reaction mechanism.

The high reactivity of bayerite towards hydrazine oxidation suggests its possible use as a catalyst in some type of system used to scrub hydrazine vapors. This would, of course, require substantial additional testing to validate.

One other observation of note with the corroded aluminum plates is the lack of any observed hydrogen peroxide formation during hydrazine decay runs. In similar experiments in a Teflon[®]-film chamber, Martin and co-workers (Reference 2) reported that a mixture of diimide and hydrogen peroxide formed during the reaction of hydrazine vapor with air. In this work, only diimide could be identified. This finding suggests that the reaction mechanism proposed by these researchers (Reference 2) would have to be modified somewhat to preclude the formation of hydrogen peroxide.

F. PAINTED ALUMINUM PLATES

The final set of experimental runs were designed to simulate spills which contact the surface of F-16 aircraft. The painted aluminum plates were quite reactive with respect to hydrazine decay. In the absence of oxygen, the half life for hydrazine was about the same as the black iron plates. When oxygen was added, it decreased by about a factor of two. Under humid conditions and in the absence of oxygen, there was an additional decrease in half life by a factor of two; while the addition of humidity to the 20 percent oxygen runs showed little effect over the runs with no humidity present.

Ammonia and diimide formation were, somewhat surprisingly, lower than in the chamber runs with no plates present.

G. RECOMMENDATIONS FOR ADDITIONAL RESEARCH

While progress has been made in understanding the factors which control the surface-catalyzed reactions of hydrazine fuel vapors, there are several areas which need additional research. These include, but are not necessarily limited to the following:

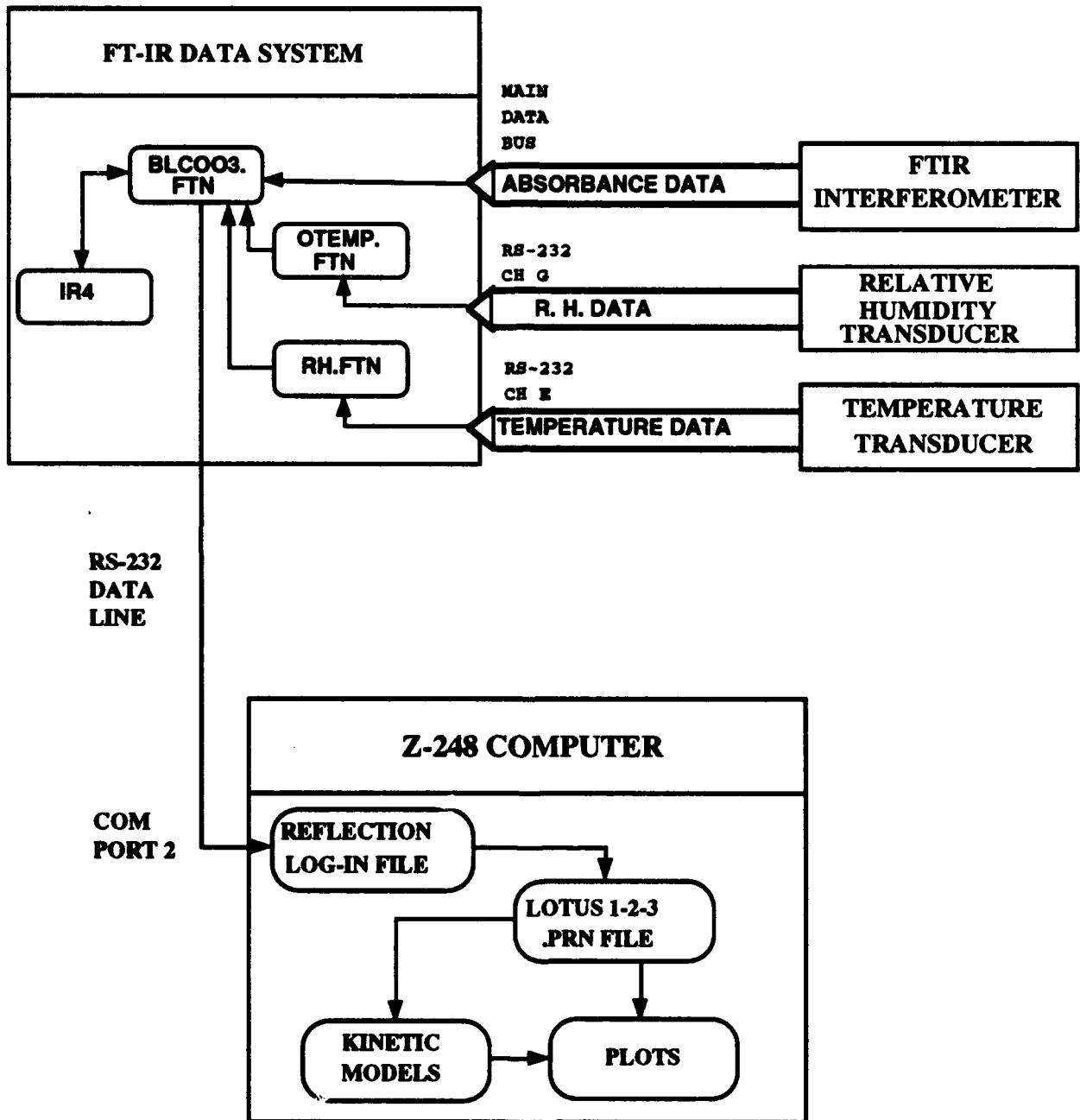
- separate characterizations of the surfaces used in these studies with specific surface composition/area analysis techniques.
- additional experiments with Pyrex[®] glass plates to determine the role of mirror and viewport surfaces in hydrazine decay reactions.
- experiments with substituted hydrazines to compare their reactivities and product distributions.
- experiments at reduced pressure to define the role of diffusion in the decay processes observed.
- more extensive 'interactive' modeling efforts to derive the maximum amount of information from the models developed.

REFERENCES

1. D. A. Stone and F.L. Wiseman, Hydrazine Loss Processes in a Teflon Film Reaction Chamber: Laboratory Results and Kinetic Models, ESL-TR-87-68, Engineering and Services Laboratory, Air Force Engineering and Services Center, Tyndall Air Force Base, FL , March 1988.
2. N.B. Martin, D.D. Davis, J.E. Kilduff, and W.C. Mahone, Environmental Fate of Hydrazines, ESL-TR-89-32, Engineering and Services Laboratory, Air Force Engineering and Services Center, Tyndall Air Force Base, FL , December 1989.
3. D.A. Stone, F.L. Wiseman, J.E. Kilduff, S.L. Koontz, and D.D. Davis, "The Disappearance of Fuel Hydrazine Vapors in Fluorocarbon-Film Environmental Chambers. Experimental Observations and Kinetic Modeling," Environmental Science & Technology, Vol. 23, pp. 328-333, 1989.
4. D. A. Stone, A Controlled-Environment Chamber for Atmospheric Chemistry Studies Using FT-IR Spectroscopy, ESL-TR-89-44, Engineering and Services Laboratory, Air Force Engineering and Services Center, Tyndall Air Force Base, FL , June 1990.
5. D. A. Stone, "A Controlled-Environment Chamber for Atmospheric Chemistry Studies Using FT-IR Spectroscopy", Applied Spectroscopy, Vol. 44, pp. 945-950, 1990.
6. J. U. White, "Long Optical Paths of Large Aperture," Optical Society of America, Vol. 32, pp. 285-288, 1942.
7. W. B. Olson, "Minimization of Volume and Astigmatism in White Cells for Use with Circular Sources and Apertures," Applied Optics, Vol. 23, pp. 1580-1585, 1984.
8. K. Wefers and C. Misra, Oxides and Hydroxides of Aluminum, Alcoa Technical Paper No. 19 (Revised), Alcoa Laboratories, 1987.
9. E.C. Tuazon, W.P.L. Carter, R.V. Brown, R. Atkinson, A.M. Winer, and J.N. Pitts, Jr., Atmospheric Reaction Mechanisms of Amine Fuels, ESL-TR-82-17, Engineering and Services Laboratory, Air Force Engineering and Services Center, Tyndall Air Force Base, FL, March 1982.
10. P.L. Hanst, W.E. Wilson, R.K. Patterson, B.W. Gay, Jr., A Spectroscopic Study of California Smog, EPA Report No. 650/4-75-006, February 1975.
11. W.P. Mounfield, Jr. and D.A. Stone, "Computer Modeling as an Aid to the Analysis of Kinetic Data," Applied Spectroscopy, 44, 679-686 (1990).
12. D.W. Marquardt, J. Soc. Industr. Appl. Math., Vol. II, 431 (1963).
13. J.J. Dongarra, C.B. Moler, J.R. Bunch, and G.W. Stewart, LINPACK Users' Guide, SIAM, Philadelphia, 1979.

APPENDIX A

FLOW DIAGRAM FOR DATA ACQUISITION AND ANALYSIS



APPENDIX B

SOFTWARE LISTING FOR THE PROGRAM USED FOR OVERALL CONTROL OF FT-IR DATA ACQUISITION AND STORAGE

This program is called IR4. It was written in the Nicolet MACRO language by using the text editor called TED. It was then compiled into a form compatible with the FT-IR software by using a Nicolet program called MACCRT. The use of the text editor allows comments to be included in a MACRO program for documentation and user assistance.

The main MACRO program (IR4) calls other SUB-MACRO programs. These were written and compiled as subsections of IR4. Each program ends with the statement END. Each new subsection begins with "!" followed by the program name.

```
!IR4
\
\      ACQUIRES, BASELINE CORRECTS, AND PRINTS OR
\      SENDS SPECTRAL DATA TO A PRINTER OR OPEN
\      COMPUTER FILE. (USES BLC003.FTN FOR
\      BASELINE CORRECTION AND TIME3.FTN FOR
\      CONTROLLING THE SAMPLING INTERVAL)
\
BFN
DFN
NSD
OMD
ENTER LOTUS-FORMAT DATA (E.G., 1 JUN 89 = 32660)
RTP
OMD
ENTER THE SPECIES TO MEASURE, YES=1, NO=0
OMD
SPECIES FLAGS ARE: HZ=WTY, MMH=SMN, UDMH=SIZ, CH4=ITR, H2O=MNT
OMD
                NH3=RTO

WTY
SMN
SIZ
ITR
MNT
RTO
OMD
ENTER THE DELAY TIME (IN MIN) BETWEEN SPECTRA
VI3
OMD
PRESS "RETURN" TO BEGIN
PAU
VI0=0
TS2
END
!TS2                \MACRO TO PERFORM THE DATA ACQUISITION
\                AND PROCESSING
```

```

\
FOR AAA=1 TIL 120\      LOOP TO ACQUIRE AND PROCESS 120 FILES
PRN DFN
AQ6\                   MACRO TO ACQUIRE AND PRINT DATA
DFN=DFN+1
DCL=204445             \SET COLOR PARAMETERS FOR DELAY PERIOD
DCX                   \EXECUTE COLOR CHANGE
GFN
TIME3.FTN             FORTTRAN PROGRAM TO EXECUTE THE
\                     DESIRED DELAY BETWEEN SETS OF SCANS
FRN
DCL=210414            \SEC COLOR PARAMETERS FOR SCAN PERIOD
DCX                   \EXECUTE COLOR CHANGE
NXT AAA
END
!AQ6                  \MACRO TO ACQUIRE, COMPUTE, AND PRINT OUT A
\                     BASELINE-CORRECTED ABSORBANCE VALUE FOR ANY OF THE
\                     SPECIES CHOSEN FOR MONITORING.  MODIFICATION OF AQ4
\                     TO INCLUDE FORTTRAN PROGRAM OTEMP.FTN AND RH.FTN
\
TEM=4\                SET TEM TO TOGGLE PRINTER ON
NPR\                  TURN ON PRINTER
SCD
GFN
OTEMP.FTN
FRN
GFN
RH.FTN
FRN
OFN=DFN
MOS
RAS
ABS
XSP=4000
XEP=700
YSP=-.25
YEP=1.25
DSS
XEP=0
DFN=SFN
GFN
BLC003.FTN
FRN
TEM=4\SET TEM TO TOGGLE PRINTER OFF
NPR\TURN PRINTER OFF
DFN=OFN
END
!!

```

APPENDIX C

SOFTWARE LISTINGS FOR FORTRAN PROGRAM USED TO CONTROL DATA ACQUISITION TIMING FROM 1280 DATA SYSTEM CLOCK

This program is called TIME3.ASC. It was written with the text editor TED and compiled using Nicolet FORTRAN 77 (V8.06; L1-067-030486). The compiled version of the program has the .FTN extension. The program reads the system clock and counts elapsed time until an interval equal to the user input value for the delay between sets of scans is reached.

```
CCCCCCCCCCCCCCCCCCCCCCCCCCCCCCCCCCCCCCCCCCCCCCCCCCCCCCCCCCCC
C
C TIME3.ASC          PROGRAM TO RETRIEVE TIME (IN SEC FROM      C
C                   MIDNIGHT) FROM LOCATION 071 OF PAGE ZERO  C
C                   MEMORY AND USE IT TO CONTROL THE          C
C                   INTERVAL BETWEEN SETS OF FT-IR SCANS.     C
C
C
CCCCCCCCCCCCCCCCCCCCCCCCCCCCCCCCCCCCCCCCCCCCCCCCCCCCCCCCCCCC
C
```

C234567

```
      INTVL=IRVAL(13765,0)
      ICOUNT=60*INTVL
      IFLAG=0
      IFLAG2=0
      ISUM=0
      ITEMP=0
C      PRINT*, 'ICOUNT= ', ICOUNT
C      PRINT*, 'IFLAG= ', IFLAG
C      PRINT*, 'IFLAG2= ', IFLAG2
C      PRINT*, ' '
      30  CONTINUE
C
C READ THE TIME VALUE (IN SEC SINCE MIDNIGHT) FROM PAGE 0
C MEMORY
C
A .ZERADD IS3 71
A MEMA IS3
C      PRINT*, 'IS3=', IS3
      IF (IS3 .EQ. ITEMP) GOTO 30
      IF (IS3 .EQ. 0 .AND. IFLAG2 .EQ. 0) GOTO 50
      IF (IFLAG .EQ. 0) ISUM=IS3+ICOUNT
C      PRINT*, '          ISUM=', ISUM
      IF ((ISUM-IS3) .LE. 0) GOTO 100
      IFLAG=1
C      PRINT*, 'IS3= ', IS3
```

```
      ITEMP=IS3
C     PRINT*, 'ITEMP= ', ITEMP
      GOTO 30
    50  IFLAG2=1
      ISUM=ISUM-86400
C     PRINT*, 'IS3=0', 'ISUM=', ISUM
      GOTO 30
    100 IFLAG2=0
      CALL EXIT

      END
```

BATCH FILE USED TO COMPILE THE ABOVE PROGRAM.

NAME: TIME3.BAT

LISTING

```
RUN FORTRAN
TIME3.ASC:L
RUN RELOAD
:B=1000-53777
TIME3.REL:L
IRVAL.REL [ROOT,HLIB]:L
FORRUN.LIB [ROOT,HLIB]:R
NICAPL.LIB [ROOT,HLIB]:R
DPSYS.LIB [ROOT,HLIB]:R
FIOS.LIB [ROOT,HLIB]:R
NICSYS.LIB [ROOT,HLIB]:R
/-TT:U
/TIME3.FTN:S
DEL TIME3.REL
DEL TIME3.TMP
```

APPENDIX D

SOFTWARE LISTING FOR FORTRAN PROGRAM USED TO READ AND REPORT THE CHAMBER TEMPERATURE

This program is called OTEMP.ASC. It was written with the text editor TED and compiled using Nicolet FORTRAN 77 (V8.06; L1-057-030486). The compiled version of the program has the .FTN extension. The program requests data from an Omega Model 680 temperature sensing module. The temperature data are read as a series of ASCII numbers through the Nicolet 1280 computer RS-232 port G and stored in the FT-IR file status block in the area normally used for a spectrum title.

```

C
CCCCCCCCCCCCCCCCCCCCCCCCCCCCCCCCCCCCCCCCCCCCCCCCCCCCCCCCCCCC
C
C PROGRAM OTEMP.ASC C
C
C THIS IS A PROGRAM TO READ ASCII TEMPERATURE DATA C
C FROM AN OMEGA MODEL 680 THERMOCOUPLE THERMOMETER C
C INTO THE FT-IR DATA SYSTEM AND STORE THE RESULT IN C
C EACH SCRATCH FILE STATUS BLOCK IN LOCATIONS 68-71. C
C
CCCCCCCCCCCCCCCCCCCCCCCCCCCCCCCCCCCCCCCCCCCCCCCCCCCCCCCCCCCC
C
C DEFINE VARIABLES
      INTEGER CHANNEL, BAUDRATE, BIT, BAUDVAL, DELAY, IOUT, I,
      1DELTA, VALUE
      LOGICAL VALID
      CHARACTER*10 TMP(10), WT, CONC
      CHARACTER*1 CHR, T1, T2, T3, T4, T5, T6, T7, T8
C SET BAUDRATE AT 1200, CHANNEL=2 (I.E., CHANNEL G)
C AND CALL SUBROUTINE BAUDSET
      BAUDRATE=1200
      CHANNEL=2
      VALID = .TRUE.
C PRINT *, 'CALLING BAUDSET'
      CALL BAUDSET(CHANNEL, BAUDRATE, VALID)

C SEND CHARACTER "R" TO REQUEST DATA TRANSMISSION FROM THE
C OMEGA UNIT
      VALUE = 82
C PRINT *, 'CALLING CHWRITE'
      CALL CHWRITE (CHANNEL, VALUE, VALID)

C RECEIVE THE CHARACTERS TRANSMITTED BY THE OMEGA UNIT
      DELAY=0
      DO 10 I=1, 8
          CALL CHREAD (CHANNEL, DELAY, CHR, VALID)
C PRINT *, 'I=', I
          TMP(I)=CHR
C PRINT *, 'TEMP=', TMP(I)
10 CONTINUE

```

```

C      DO 20 I=1,8
C      WRITE(3,100) I,TMP(I)
C100  FORMAT(' ', 'I=', I2, 2X, 'TEMP=', I4)
C20   CONTINUE

      T1=TMP(1)
      T2=TMP(2)
      T3=TMP(3)
      T4=TMP(4)
      T5=TMP(5)
      T6=TMP(6)
      T7=TMP(7)
C      T8=TMP(8)
      WT=T1 // T2 // T3 // T4 // T5 // T6 // T7
C      PRINT *, 'T=', WT, ' DEG C'
      TEMP=REAL(WT)
      RETURN
      END

```

BATCH FILE USED TO COMPILE THE ABOVE PROGRAM.

NAME: OTEMP.BAT

LISTING

```

RUN FORTRAN
OTEMP.ASC:L
RUN FORTRAN
BAUDSET.ASC:L
RUN FORTRAN
CHWRITE.ASC:L
RUN FORTRAN
CHREAD.ASC:L
RUN RELOAD
:B=1000-53777
OTEMP.REL:L
BAUDSET.REL:L
CHWRITE.REL:L
CHREAD.REL:L
IRVAL.REL [ROOT,HLIB]:L
FORRUN.LIB [ROOT,HLIB]:R
NICAPL.LIB [ROOT,HLIB]:R
DPSYS.LIB [ROOT,HLIB]:R
FIOS.LIB [ROOT,HLIB]:R
NICSYS.LIB [ROOT,HLIB]:R
/-TT:U
/OTEMP.FTN:S
DEL OTEMP.REL
DEL OTEMP.TMP
DEL BAUDSET.REL
DEL BAUDSET.TMP
DEL CHWRITE.REL
DEL CHWRITE.TMP

```

DEL CHREAD.REL
DEL CHREAD.TMP

APPENDIX E

SOFTWARE LISTING FOR FORTRAN PROGRAM USED TO READ AND REPORT THE CHAMBER RELATIVE HUMIDITY

This program is called RH.ASC. It was written with the text editor TED and compiled using Nicolet FORTRAN 77 (V8.06; L1-067-030486). The compiled version of the program has the .FTN extension. The program requests data from a Vaisala Model HMP 114Y humidity/temperature transducer. The humidity data are read as DC volts using a Goerz Model M2110 digital VOM with an RS-232 output port. The output from this unit was read as a series of ASCII numbers through the Nicolet 1280 computer RS-232 port E and stored in the FT-IR file status block in an area not used by the FT-IR software.

```
C
CCCCCCCCCCCCCCCCCCCCCCCCCCCCCCCCCCCCCCCCCCCCCCCCCCCCCCCCCCCC
C
C PROGRAM RH.ASC
C
C THIS IS A PROGRAM TO READ ASCII RELATIVE HUMIDITY
C INTO THE FT-IR DATA SYSTEM AND STORE THE RESULT IN
C EACH SCRATCH FILE STATUS BLOCK IN LOCATIONS 238-243.
C
CCCCCCCCCCCCCCCCCCCCCCCCCCCCCCCCCCCCCCCCCCCCCCCCCCCCCCCCCCCC
C
C DEFINE VARIABLES
  INTEGER CHANNEL, BAUDRATE, BIT, BAUDVAL, DELAY, IOUT, I,
  1DELTA, VALUE
  INTEGER IDATA(512), IH3, IH4, IH5, IH6, IH7
  LOGICAL VALID
  REAL R1
  CHARACTER*6 H
  CHARACTER*10 HUMID(10)
  CHARACTER*1 CHR, RH1, RH2, RH3, RH4, RH5, RH6, RH7

  FLASER=15798.2
  NPMAX=22528

C
C READ FT-IR PARAMETERS FOR DATA RETRIEVAL
C
  IDFN=IRVAL(14022,0)
  NSECS=IRVAL(14001,0)
  INODE=IRVAL(13004,0)
  NDPW=IRVAL(14000,0)
  IXSP=IRVAL(14025,0)
  IENP=IRVAL(14026,0)

C
C LOCATE SECTORS TO BE READ USING THE FOLLOWING INDEX
C
  IDFSEC=(IDFN+1)*NSECS+87

C
C READ HEADER BLOCK INFORMATION USING IRTISK. STORE
C RESULTS IN AN ARRAY CALLED IDATA.
```

```

C      CALL IRTISK(IDATA,512,IDFSEC,INODE)
C
C  SET BAUDRATE AT 1200, CHANNEL=1 (I.E., CHANNEL E)
C  AND CALL SUBROUTINE BAUDSET
      BAUDRATE=1200
      CHANNEL=1
      VALID =.TRUE.
C      PRINT *,'CALLING BAUDSET'
      CALL BAUDSET(CHANNEL, BAUDRATE, VALID)

C  SEND CHARACTER "ENQ" TO REQUEST DATA TRANSMISSION FROM THE
C  M2110 UNIT
      VALUE = 5
      CALL CHWRITE (CHANNEL,VALUE,VALID)

C  RECEIVE THE CHARACTERS TRANSMITTED BY THE M2110 UNIT
      DELAY=0
      DO 10 I=1,7
        CALL CHREAD(CHANNEL,DELAY,CHR,VALID)
        HUMID(I)=CHR
10     CONTINUE

      RH1=HUMID(1)
      RH2=HUMID(2)
      RH3=HUMID(3)
      RH4=HUMID(4)
      RH5=HUMID(5)
      RH6=HUMID(6)
      RH7=HUMID(7)
      H= RH1 // RH4 // RH5 // RH3 // RH6 // RH7
C      PRINT*,H
C
C  WRITE THE INDIVIDUAL TEMPERATURE CHARACTERS TO LOCATIONS
C  238-243 OF THE IDATA ARRAY
C
      IDATA(238)=ICHR(RH1)
      IDATA(239)=ICHR(RH4)
      IDATA(240)=ICHR(RH5)
      IDATA(241)=ICHR(RH3)
      IDATA(242)=ICHR(RH6)
      IDATA(243)=ICHR(RH7)

      CALL IWTISK(IDATA,512,IDFSEC,INODE)
      CALL EXIT
      END

```

BATCH FILE USED TO COMPILE THE ABOVE PROGRAM.

NAME: RH.BAT

LISTING

```
RUN FORTRAN
RH.ASC:L
RUN FORTRAN
BAUDSET.ASC:L
RUN FORTRAN
CHWRITE.ASC:L
RUN FORTRAN
CHREAD.ASC:L
RUN RELOAD
:B=1000-53777
RH.REL:L
BAUDSET.REL:L
CHWRITE.REL:L
CHREAD.REL:L
IRVAL.REL [ROOT,HLIB]:L
FORRUN.LIB [ROOT,HLIB]:R
NICAPL.LIB [ROOT,HLIB]:R
DPSYS.LIB [ROOT,HLIB]:R
FIOS.LIB [ROOT,HLIB]:R
NICSYS.LIB [ROOT,HLIB]:R
/-TT:U
/RH.FTN:S
DEL RH.REL
DEL RH.TMP
DEL BAUDSET.REL
DEL BAUDSET.TMP
DEL CHWRITE.REL
DEL CHWRITE.TMP
DEL CHREAD.REL
DEL CHREAD.TMP
```

APPENDIX F

SOFTWARE LISTING FOR FORTRAN PROGRAM USED TO PROCESS AND SEND CHAMBER DATA TO AN EXTERNAL COMPUTER FOR ANALYSIS AND PLOTTING

```
CCCCCCCCCCCCCCCCCCCCCCCCCCCCCCCCCCCCCCCCCCCCCCCCCCCCCCCCCCCC
C                                                                 C
C PROGRAM BLC003.ASC                                          C
C                                                                 C
C THIS PROGRAM RETRIEVES DATA FROM FT-IR SCRATCH FILES,    C
C AND CALCULATES BASELINE-CORRECTED ABSORBANCE VALUES     C
C FOR ANALYTICAL PEAKS. THERE IS A SUBROUTINE FOR EACH     C
C SPECIES OF INTEREST. THERE ARE ALSO SUBROUTINES FOR     C
C TEMPERATURE AND RELATIVE HUMIDITY DETERMINATIONS.       C
C                                                                 C
C THE PROGRAM IS CALLED WITH MACRO IR4 AND FEEDS DATA     C
C DIRECTLY TO A LOGGING FILE (USING REFLECTIONS WITH A     C
C Z-248 COMPUTER OR USING ADVANCE LINK WITH AN HP-150     C
C COMPUTER) OVER AN RS-232 LINE. THE OUTPUT DATA HAS     C
C THE FORM:                                                C
C                                                                 C
C 32665 09 15 41 20.3 1.023 .897 .235 05.17              C
C                                                                 C
C WHERE THE DATA ARE (IN ORDER) - LOTUS-FORMAT DATE, TIME OF C
C ACQUISITION OF THE FT-IR FILE (HH MM SS), TEMPERATURE   C
C (DEG C), ABSORBANCE VALUES (3 ARE SHOWN), AND %RH.     C
C                                                                 C
CCCCCCCCCCCCCCCCCCCCCCCCCCCCCCCCCCCCCCCCCCCCCCCCCCCCCCCCCCCC
C234567
C PROGRAM DIMENSIONED FOR 1.0 CM-1 SPECTRA
C
REAL Y(16384),BP1,LBP,PXA,PYA,CABS,XDIF,XDIF2,YDIF,
1FAC1,FAC2,EP,SP,A1,A2,A3,A4,A5,A6
INTEGER IDATA(512),IDA(22528),COUNT,DP1,DP2,TFLAG,LDATE
CHARACTER*2 HH,NN,SS
CHARACTER*1 CT1,CT2,CT3,CT4
CHARACTER*1 H1,H2,N1,N2,S1,S2
CHARACTER*1 RH1,RH2,RH3,RH4,RH5,RH6
CHARACTER*4 CTEMP
CHARACTER*6 HUMID

FLASER = 15798.2
NPMAX = 22528
SN = 0
C
C *****
C READ FTIR PARAMETERS FOR DATA RETRIEVAL:
C
IDFN = IRVAL(14022,0)
NSECS = IRVAL(14001,0)
INODE = IRVAL(13004,0)
```

```
NDPW = IRVAL(14000,0)
IXSP = IRVAL(14025,0)
IXEP = IRVAL(14026,0)
```

```
C
C THESE IRVAL FUNCTIONS READ THE MEMORY LOCATIONS
C CORRESPONDING TO THESE PARAMETERS (ALL ARE INTEGERS):
```

```
C
C (OCTAL) LOCATION PARAMETER
C 13004 INODE NO.
C 14000 NDP (=INTEGER/256)
C 14001 FSZ (=INTEGER/512)
C 14022 DFN
C 14025 XSP
C 14026 XEP
```

```
C *****
```

```
C READ FTIR PARAMETERS FOR SETTING SUBROUTINE FLAGS:
C (1=HZ, 2=MMH, 3=UDMH, 4=CH4, 5=H2O, 6=NH3)
```

```
IFLAG1 = IRVAL(13710,0)
IFLAG2 = IRVAL(13713,0)
IFLAG3 = IRVAL(13714,0)
IFLAG4 = IRVAL(13715,0)
IFLAG5 = IRVAL(13731,0)
IFLAG6 = IRVAL(13750,0)
```

```
C
C PRINT 501,IFLAG1,IFLAG2,IFLAG3,IFLAG4,IFLAG5
C 501 FORMAT(' ',IFLAG1= ',I4,2X,IFLAG2= ',I4,2X,IFLAG3= '
C 1,I4,2X,/,IFLAG4= ',I4,2X,IFLAG5= ',I4,2X,IFLAG6= ',I4,
C 1/)
```

```
C THESE IRVAL FUNCTIONS READ THE MEMORY LOCATIONS
C CORRESPONDING TO THESE PARAMETERS (ALL ARE INTEGERS):
```

```
C
C (OCTAL) LOCATION PARAMETER
C 13710 WTY
C 13713 SMN
C 13714 SIZ
C 13715 ITR
C 13731 MNT
C 13750 RTO
```

```
C *****
```

```
C THE FIRST 88 SECTORS OF THE SCRATCH AREA (I.E., SECTORS 0-87)
C CONTAIN MISCELLANEOUS INFORMATION. SCRATCH FILE 0 BEGINS
C AT SECTOR 88 AND OCCUPIES FSZ/512 SECTORS. ALL SUBSEQUENT
C FILES ARE THE SAME SIZE AS FILE 0.
```

```
C THE LAST SECTOR OF EACH FILE IS THE FILE STATUS BLOCK. THERE
C ARE A CONSIDERABLE NUMBER OF SECTORS BETWEEN THE END OF THE
C DATA AND THE BEGINNING OF THE FILE STATUS BLOCK. IT IS NOT
```

```

C CLEAR WHAT THESE EXTRA SECTORS ARE USED FOR.
C *****
C
C LOCATE SECTORS TO BE READ USING THE FOLLOWING INDEX.
C
C     IDFSEC=(IDFN+1)*NSECS+87
C     PRINT 998, IDFSEC
C 998   FORMAT(' ', 'IDFSEC= ', I6, '/')
C *****
C
C READ HEADER BLOCK INFORMATION USING IRTISK.  STORE RESULTS
C IN AN ARRAY CALLED IDATA.
C
C     CALL IRTISK(IDATA, 512, IDFSEC, INODE)
C     DO 10 I=1, 17
C     PRINT 1000, I, IDATA(I)
C1000  FORMAT(' ', 'IDATA', I2, 2X, ' = ', I6)
C 10    CONTINUE
C
C NOW, FILE STATUS INFO CAN BE DETERMINED FROM THE ELEMENTS
C OF IDATA:
C
C     IABS = ABSORBANCE FLAG, 0 IF ABSORBANCE
C     IPTS = NO. OF DATA POINTS
C     FEXP = EXPONENT FOR FILE SCALING
C     FXAX = DATA POINT SPACING ON X AXIS
C
C     IABS = IDATA(10)
C     IF (IABS.NE.0) GOTO 900
C     IPTS = IDATA(15)*128
C     FEXP = 2**(19-IDATA(6))
C     FXAX = FLASER/(IPTS*IDATA(17))
C     PRINT 980, IPTS, FEXP, FXAX
C 980  FORMAT(' ', '/', ' IPTS= ', I8, 2X, ' FEXP= ', E10.4, 2X, ' FXAX= ',
C 1F10.5, /)
C -----
C
C NOW DETERMINE THE STARTING AND ENDING POINTS FOR THE FILE TO
C BE READ.  THIS IS DONE BY TWO SEQUENTIAL IF - ENDIF LOOPS.
C THE FIRST SETS ISTEP EQUAL TO THE LESSER OF XSP AND XEP
C (WHICH ARE READ FROM THE FT-IR SCRATCH FILE HEADER BLOCK).
C THE SECOND LOOP CONVERTS THE XSP AND XEP VALUES FROM CM-1
C TO SCRATCH FILE DATA POINT VALUES.  THE 0.5 FACTOR WHICH IS
C ADDED ENSURES THAT INTEGER ISTEP AND IENP VALUES ARE ROUNDED
C CORRECTLY.
C
C     IF (IXSP.LE.IXEP) THEN
C         ISTEP = IXSP
C         IENP = IXEP
C     ELSE
C         ISTEP = IXEP
C         IENP = IXSP
C     ENDIF
C     IF (IXSP.GT.IXEP) THEN
C         ISTEP = IXEP/FXAX+0.5

```

```

        IENP = IXSP/FXAX+0.5
    ELSE
        ISTP = IXSP/FXAX+0.5
        IENP = IXEP/FXAX+0.5
    ENDIF
    NP = IENP-ISTP+1
C     PRINT 850, ISTP,IENP,NP
C 850 FORMAT(' ',/, ' ISTP= ',I6,2X, 'IENP= ',I6,2X, 'NP= ',I6,/)
C
C     CHECK FOR A REASONABLE NO. OF PTS. IN NP
C
C     IF (NP.GT.NPMAX) THEN
C         WRITE(2,901) NPMAX,NP
C     ELSEIF (NP.LT.5) THEN
C         WRITE(2,902) NP
C     ENDIF
C
C NOW READ DATA FROM SCRATCH FILE DFN INTO ARRAY IDA
C
C IN IS A COUNTER. NDONE TAKES THE DATA POINT VALUE OF ISTP AND
C CONVERTS IT TO SECTORS. NSKIP TAKES THE STARTING DATA POINT
C VALUE (ISTP) AND SUBTRACTS AN INTEGER NO. OF DATA POINTS, BY
C SECTOR, FROM IT, LEAVING THE POINT IN THE SELECTED SECTOR
C WHERE DATA REPRESENTING THE INTERVAL ISTP - IENP BEGIN.
C
C     IN = 1
C     NDONE = ISTP/512
C     NSKIP = ISTP-NDONE*512
C     PRINT 400, NDONE,NSKIP
C 400 FORMAT(' ',/, ' NDONE= ',I8,2X, 'NSKIP= ',I8,/)
C
C IF THE SCRATCH FT-IR FILE HAD XSP=0 OR XEP=0, THEN DATA CAN
C BE READ DIRECTLY, ONCE THE PROPER BEGINNING SECTOR IS
C SPECIFIED. IF XSP OR XEP WERE NOT ZERO, THEN NDONE SECTORS
C PLUS NSKIP POINTS MUST BE SKIPPED OVER TO BEGIN READING DATA.
C
C RESET FLAG FOR BASELINE CORRECTION ROUTINE
C
C     IFLAG=0
C     IF (NSKIP.GT.0) THEN
C
C SET FLAG FOR BASELINE CORRECTION ROUTINE
C
C     IFLAG=1
C     CALL IRTISK(IDA,512,88+IDFN*NSECS+NDONE,INODE)
C     DO 20 I=NSKIP+1,512
C         IDA(IN) = IDA(I)
C         IN = IN + 1
C 20 CONTINUE
C     NDONE = NDONE + 1
C     ENDIF
C
C NPREM IS A COUNTER WHICH TELLS HOW MANY DATA POINTS TO READ
C FROM THE FT-IR SCRATCH FILE TO COVER THE INTERVAL SPECIFIED

```

```

C BY ISTEP AND IENP.
C
      NPREM = NP-IN+1
C      PRINT 402, IN, NPREM
C 402  FORMAT(' ', 'IN= ', I6, 2X, 'NPREM= ', I10, /)
      IF (NPREM.GT.0) THEN
          CALL IRTISK(IDA(IN), NPREM, 88+IDFN*NSECS+NDONE, INODE)
      ENDIF
C
C NOW THE POINTS IN THE INTEGER ARRAY IDA ARE CONVERTED TO REAL
C VALUES BY DIVIDING EACH ONE BY FEXP (SEE FT-IR SOFTWARE
C MANUAL, P. 18-5 FOR AN EXPLANATION). NOTE THAT ANY TOTALLY
C ABSORBING DATA POINTS HAVE THE VALUE -524288 AND THESE ARE
C SET EQUAL TO ZERO IN THE REAL DATA ARRAY.
C
      DO 50 I = 1, NP
          IDAS = IDA(I)
          IF (IDAS.EQ.-524288) IDAS = 0
          Y(I) = IDAS/FEXP
C      PRINT 403, I, Y(I)
C 403  FORMAT(' ', 'X(', I3, ')=' , F6.3)
      50  CONTINUE
C      DO 51 I=1980, 2032
C          WN=(I-1)*FXAX
C          PRINT 71, WN, Y(I)
C 71   FORMAT(' ', 'WN=' , F8.3, 2X, 'Y=' , F8.3)
C 51   CONTINUE
C
C *****
C NOW THAT THE DATA POINTS ARE AVAILABLE, BASELINE CORRECTION
C CAN BE MADE. THE CORRECTION WILL BE MADE IN THE SAME MANNER
C IT WOULD BE DONE BY HAND. A POINT ON ONE SIDE OF THE
C ANALYTICAL PEAK WILL BE CHOSEN BY AVERAGING THE ABSORBANCE
C VALUES OVER A CERTAIN PORTION OF THE X-AXIS. FOR SPECIES
C WHICH HAVE HIGHLY STRUCTURED PEAKS, THIS MAY BE A VERY SHORT
C DISTANCE (E.G., METHANE USES A 2 CM-1 ON ONE SIDE OF THE
C ANALYTICAL PEAK AND A 1.0 CM-1 INTERVAL ON THE OTHER. THESE
C INTERVALS ARE BASED ON EXPANDED PLOTS AND ARE CHOSEN TO GIVE
C POINTS CLOSE TO THOSE ONE WOULD CHOOSE IF DOING THE BASELINE
C CORRECTION BY HAND). THE SAME THING IS DONE ON THE OTHER
C SIDE OF THE ANALYTICAL PEAK. THESE POINTS WILL BE DEFINED
C WITHIN THE SUBROUTINE FOR EACH SEPARATE SPECIES.
C *****
C
C
C TO CONFORM WITH LOTUS 1-2-3 DATE FORMAT, READ THE VALUE OF
C RTP, THEN PRINT THIS AS LDATE
C
      LDATE = IRVAL(13751, 0)
C
C TO AVOID EXTRA CHARACTERS IN THE TIME PRINTOUT,
C PICK OUT THE CHARACTERS NEEDED FROM THE IDATA ARRAY AND
C CONCATENATE THEM INTO THE NECESSARY OUTPUT.
C

```

```

DO 25 I=58,65
  IF (I.EQ.58) THEN
    H1=CHAR(IDATA(I))
  ELSEIF (I.EQ.59) THEN
    H2=CHAR(IDATA(I))
  ELSEIF (I.EQ.61) THEN
    N1=CHAR(IDATA(I))
  ELSEIF (I.EQ.62) THEN
    N2=CHAR(IDATA(I))
  ELSEIF (I.EQ.64) THEN
    S1=CHAR(IDATA(I))
  ELSE (I.EQ.65)
    S2=CHAR(IDATA(I))
  ENDIF
25 CONTINUE
C
C CONCATENATE THE APPROPRIATE IDATA ELEMENTS TO FORM TIME
C CHARACTERS WHICH CAN BE PRINTED.
C
      HH = H1 // H2
      NN = N1 // N2
      SS = S1 // S2
C
C RETRIEVE THE TEMPERATURE CHARACTERS FROM THE IDATA ARRAY
C (THESE CHARACTERS ARE WRITTEN TO THE IDATA ARRAY DURING DATA
C ACQUISITION UNDER THE MACRO AQ6 WITH THE FORTRAN PROGRAM
C OTEMP.FTN)
C
      CT1=CHAR(IDATA(68))
      CT2=CHAR(IDATA(69))
      CT3=CHAR(IDATA(70))
      CT4=CHAR(IDATA(71))
C
C NOW, CONCATENATE THESE CHARACTERS TO FORM THE TEMPERATURE
C
      CTEMP=CT1 // CT2 // CT3 // CT4
C
C RETRIEVE THE RELATIVE HUMIDITY CHARACTERS FROM THE IDATA
C ARRAY (THESE CHARACTERS ARE WRITTEN TO THE IDATA ARRAY
C DURING DATA ACQUISITION UNDER THE MACRO AQ6 WITH THE
C FORTRAN PROGRAM RH.FTN)
C
      RH1=CHAR(IDATA(238))
      RH2=CHAR(IDATA(239))
      RH3=CHAR(IDATA(240))
      RH4=CHAR(IDATA(241))
      RH5=CHAR(IDATA(242))
      RH6=CHAR(IDATA(243))
C
C NOW, CONCATENATE THE %RH DATA INTO FINAL FORM
C
      HUMID= RH1 // RH2 // RH3 // RH4 // RH5 // RH6

```

```

C
C DETERMINE WHICH SPECIES ARE TO BE ANALYZED.
C
844  IF (IFLAG1.EQ.1) CALL HZ(Y,FXAX,CABS)
      A1=CABS
C     IF (IFLAG2.EQ.1) CALL MMH(Y,FXAX,CABS)
C     A2=CABS
C     IF (IFLAG3.EQ.1) CALL UDMH(Y,FXAX,CABS)
C     A3=CABS
      IF (IFLAG4.EQ.1) CALL CH4(Y,FXAX,CABS)
      A4=CABS
      IF (IFLAG5.EQ.1) CALL H2O(Y,FXAX,CABS)
      A5=CABS
      IF (IFLAG6.EQ.1) CALL NH3(Y,FXAX,CABS)
      A6=CABS
C
850  PRINT 150,LDATE,HH,NN,SS,CTEMP,A1,A4,A5,A6,HUMID
150  FORMAT(' ',I5,2X,3(A2,2X),A4,2X,4(F6.3),2X,A6)
C
      GOTO 999
C
C FORMAT STATEMENTS
C
900  WRITE(2,990) IDATA(10)
901  FORMAT(' ',/, ' ONLY DIMENSIONED TO ',I6, ' PTS', 'NOT ',I6
1,/,)
902  FORMAT(' ', 'WHY ARE THERE ONLY ',I6, 'PTSREQUESTED?',/,)
990  FORMAT(' ',//, ' ABSORBANCE FLAG = ',I2,2X, 'NOT AN
      ABSORBANCE FILE',//)
999  CONTINUE
      CALL EXIT
      END

```

BATCH FILE USED TO COMPILE THE ABOVE PROGRAM.

NAME: BLC003.BAT

LISTING

```

RUN FORTRAN
BLC003.ASC:L
RUN FORTRAN
HZ.ASC:L
RUN FORTRAN
CH4.ASC:L
RUN FORTRAN
NH3.ASC:L
RUN FORTRAN
H2O.ASC:L
RUN RELOAD
:B=1000-53777
BLC003.REL:L

```

HZ.REL:L
CH4.REL:L
NH3.REL:L
H2O.REL:L
IRVAL.REL [ROOT,HLIB]:L
FORRUN.LIB [ROOT,HLIB]:R
NICAPL.LIB [ROOT,HLIB]:R
DPSYS.LIB [ROOT,HLIB]:R
FIOS.LIB [ROOT,HLIB]:R
NICSYS.LIB [ROOT,HLIB]:R
/-TT:U
/BLC003.FTN:S
DEL BLC003.REL
DEL BLC003.TMP
DEL HZ.REL
DEL HZ.TMP
DEL CH4.REL
DEL CH4.TMP
DEL NH3.REL
DEL NH3.TMP
DEL H2O.REL
DEL H2O.TMP

APPENDIX G

SOFTWARE LISTING FOR FORTRAN PROGRAM USED TO CALCULATE THE BASELINE-CORRECTED ABSORBANCE VALUE FOR HYDRAZINE VAPOR AT 957 CM-1

```

CCCCCCCCCCCCCCCCCCCCCCCCCCCCCCCCCCCCCCCCCCCCCCCCCCCCCCCCCCCC
C                                                                 C
C  SUBROUTINE HZ (Y, FXAX, CABS)                                  C
C                                                                 C
C  CALCULATES THE BASELINE BY TAKING THE AVERAGE OF POINTS    C
C  ON ONE SIDE OF THE ANALYTICAL PEAK (1180 - 1160 CM-1) FOR THE C
C  BEGINNING POINT.  THEN TAKING THE AVERAGE OF POINTS ON     C
C  THE OTHER SIDE OF THE ANALYTICAL PEAK (860 - 846) FOR THE   C
C  ENDING POINT.  A LINE CONNNECTING THESE TWO POINTS FORMS   C
C  THE BASELINE.  THE ABSORBANCE VALUE AT THE ANALYTICAL      C
C  PEAK (957 CM-1) IS THEN CORRECTED TO THIS MEASURED BASELINE. C
C                                                                 C
CCCCCCCCCCCCCCCCCCCCCCCCCCCCCCCCCCCCCCCCCCCCCCCCCCCCCCCCCCCC

      REAL  Y(22528), BP1, LBP, PXA, PYA, CABS, XDIF, XDIF2, YDIF,
      1FAC1, FAC2, EP, SP, IC
      INTEGER COUNT

C
C  DEFINE THE BASELINE POINTS FOR THE HYDRAZINE ANALYTICAL PEAK
C
      IPT1=1180/FXAX
      IPT2=1160/FXAX
      IPT3=860/FXAX
      IPT4=846/FXAX

C
C      PRINT 35, IPT1, IPT2, IPT3, IPT4
C 35  FORMAT(' ', 'IPT1=', I4, 2X, 'IPT2=', I4, 2X, 'IPT3=', I4, 2X,
C      1'IPT4=', I4, /)
C
C  AVERAGE THE POINTS FOR THE 1ST BASELINE VALUE
C
      SP = 0
      BP1= 0
      COUNT = 0
      IFIRST=IPT1
      ILAST =IPT2

C
C  NOW CALCULATE FIRST BASELINE POINT
C
      PRINT 36, IFIRST, ILAST
C 36  FORMAT(' ', 'IFIRST=', I4, 2X, 'ILAST=', I4, /)
      DO 70 I=ILAST, IFIRST
          SP=SP+Y(I)
          COUNT=COUNT+1

C
C  CALCULATE WAVENUMBER VALUES FOR PRINTOUT

```

```

C
C      WN=(I-1)*FXAX
C      PRINT 37,WN,Y(I),SP,COUNT
C 37   FORMAT(' ','WN=',F8.3,2X,'Y(I)=',F8.3,2X,'SP=',F8.3,
C      12X,'COUNT=',I6)
C      70   CONTINUE
C          BP1=SP/COUNT
C
C AVERAGE THE POINTS FOR THE 2ND BASELINE VALUE
C
C      EP = 0
C      LBP = 0
C      COUNT = 0
C      IFIRST=IPT3
C      ILAST =IPT4
C
C NOW CALCULATE THE SECOND BASELINE POINT
C
C      DO 80 I=ILAST,IFIRST
C          EP=EP+Y(I)
C          COUNT=COUNT+1
C 80   CONTINUE
C      LBP=EP/COUNT
C
C PRINT OUT THE BASELINE DETERMINING POINTS
C
C      PRINT 85, BP1,LBP
C 85   FORMAT(' ','BP1=',F9.4,2X,'LBP=',F9.4,/)
C
C DETERMINE THE X,Y VALUES (CM-1 AND ABS.) FOR THE
C ANALYTICAL PEAK (957 CM-1) BY FINDING THE MAXIMUM Y VALUE
C IN THE INTERVAL FOR THIS PEAK WHICH IS: 959 CM-1 TO 956
C CM-1 (OR IN DATA POINT VALUES: 1989 TO 1982).
C
C      PXA=0
C      PYA=0
C      DO 82 I=1982,1989
C          IF (Y(I).GT.Y(I-1)) THEN
C              PYA=Y(I)
C              IC=I-1
C              PXA=IC*FXAX
C          ENDIF
C      PRINT 299,I,Y(I),PYA,IC,PXA
C 299   FORMAT(' ','I=',I4,2X,'Y=',F8.3,2X,'PYA=',F8.3,2X,
C      1'IC=',F8.3,2X,'PXA=',F8.3)
C      82   CONTINUE
C      PRINT 86,PXA,PYA
C 86   FORMAT(' ','PXA=',F8.3,2X,'PYA=',F8.3,/)
C
C CALCULATE THE BASELINE CORRECTION. THERE ARE TWO POSSIBLE
C CASES: (A) POSITIVE SLOPING BASELINE, OR (B) NEGATIVE
C SLOPING BASELINE.
C
C      CASE (A) - POSITIVE SLOPING BASELINE (BP1 < LBP)

```

```

C
C SKIP TO CASE (B) IF BASELINE SLOPE IS NEGATIVE
C
C     IF(BP1.GT.LBP) GOTO 3000
C
C OTHERWISE PROCEED WITH THE CORRECTION
C
C     DP1=(1180+1160)/2
C     DP2=(860+846)/2
C     YDIF=LBP-BP1
C     XDIF=DP1-DP2
C     XDIF2=DP1-PXA
C     FAC1=XDIF2/XDIF
C     FAC2=FAC1*YDIF
C     FAC2=FAC2+BP1
C     PRINT 87, DP1,DP2,YDIF,XDIF,XDIF2,FAC1,FAC2
C 87  FORMAT(' ', 'DP1=', F8.3, 2X, 'DP2=', F8.3, 2X, 'YDIF=', F9.4, 2X,
C     1'XDIF=', F9.4, 2X, 'XDIF2=', F9.4, 2X, /, 'FAC1=', F9.4, 2X, 'FAC2=',
C     2F9.4, /)
C     GOTO 3500
C
C     CASE (B) - NEGATIVE SLOPING BASELINE (BP1 > LBP)
C
C 3000 CONTINUE
C     DP1=(1180+1160)/2
C     DP2=(860+846)/2
C     YDIF=BP1-LBP
C     XDIF=DP1-DP2
C     XDIF2=PXA-DP2
C     FAC1=XDIF2/XDIF
C     FAC2=FAC1*YDIF
C     FAC2=FAC2+LBP
C     PRINT 57, DP1,DP2,YDIF,XDIF,XDIF2,FAC1,FAC2
C 57  FORMAT(' ', 'DP1=', F8.3, 2X, 'DP2=', F8.3, 2X, 'YDIF=', F9.4, 2X,
C     1'XDIF=', F9.4, 2X, 'XDIF2=', F9.4, 2X, /, 'FAC1=', F9.4, 2X, 'FAC2=',
C     2F9.4, /)
C 3500 CONTINUE
C
C APPLY THE CORRECTION TO THE ABSORBANCE VALUE FROM PPK
C
C     CABS=PYA-FAC2
C
C PRINT OUT CORRECTED ABSORBANCE VALUE
C
C     PRINT 88, CABS
C 88  FORMAT(' ', F4.3)
C     135('-'), /)
C
C END THE SUBROUTINE
C
C     RETURN
C     END [NOTE: this program was compiled and linked as a
C         subroutine of BLC003.ASC. See Appendix F for the
C         applicable batch file listing.]

```

APPENDIX H

SOFTWARE LISTING FOR FORTRAN PROGRAM USED TO CALCULATE THE BASELINE-CORRECTED ABSORBANCE VALUES FOR METHANE VAPOR AT 3018 CM-1 AND 1305 CM-1

```

CCCCCCCCCCCCCCCCCCCCCCCCCCCCCCCCCCCCCCCCCCCCCCCCCCCCCCCCCCCC
C                                                                 C
C  SUBROUTINE CH4 (Y, FXAX, CABS)                                C
C                                                                 C
C  CALCULATES THE BASELINE BY TAKING THE AVERAGE OF POINTS     C
C  ON ONE SIDE OF THE ANALYTICAL PEAK (3026 - 3023 CM-1) FOR THE C
C  BEGINNING POINT. THEN TAKING THE AVERAGE OF POINTS ON       C
C  THE OTHER SIDE OF THE ANALYTICAL PEAK (2996 - 2992) FOR THE  C
C  ENDING POINT. A LINE CONNNECTING THESE TWO POINTS FORMS     C
C  THE BASELINE. THE ABSORBANCE VALUE AT THE FIRST ANALYTICAL  C
C  PEAK (3018 CM-1) IS THEN CORRECTED TO THIS MEASURED BASELINE. C
C  THE SECOND ANALYTICAL PEAK AT 1305 CM-1 IS CORRECTED        C
C  SIMILARLY. (ONLY THE 1305 CM-1 PEAK WAS USED IN THIS STUDY.) C
C                                                                 C
CCCCCCCCCCCCCCCCCCCCCCCCCCCCCCCCCCCCCCCCCCCCCCCCCCCCCCCCCCCC

      SUBROUTINE CH4 (X, FXAX)
      REAL  X(22528), BP1, LBP, PXA, PYA, CABS, XDIF, XDIF2, YDIF,
      1FAC1, FAC2, EP, SP, IC
      INTEGER COUNT

C
C  DEFINE THE BASELINE POINTS FOR METHANE
C  -- FIRST: THE PEAK AT 3018 CM-1 --
C
      IPT1=3026/FXAX
      IPT2=3023/FXAX
      IPT3=2996/FXAX
      IPT4=2992/FXAX

C
C  -- SECOND: THE PEAK AT 1305 CM-1 --
C
      IPT5=1310/FXAX
      IPT6=1308/FXAX
      IPT7=1280/FXAX
      IPT8=1279/FXAX

C
C  PRINT 35, IPT1, IPT2, IPT3, IPT4
C 35  FORMAT(' ', 'IPT1=', I4, 2X, 'IPT2=', I4, 2X, 'IPT3=', I4, 2X,
C      1'IPT4=', I4, /)
C
C  AVERAGE THE POINTS FOR THE 1ST BASELINE VALUE, 3018 CM-1 PEAK
C
      SP = 0
      BP1= 0
      COUNT = 0
      IFIRST=IPT1

```

```

        ILAST =IPT2
C
C NOW CALCULATE FIRST BASELINE POINT
C
C      PRINT 36, IFIRST, ILAST
C 36   FORMAT(' ', 'IFIRST=', I4, 2X, ' ILAST=', I4, /)
      DO 70 I=ILAST, IFIRST
        SP=SP+X(I)
        COUNT=COUNT+1
C
C CALCULATE WAVENUMBER VALUES FOR PRINTOUT
C
C      WN=(I-1)*FXAX
C      PRINT 37, WN, X(I), SP, COUNT
C 37   FORMAT(' ', 'WN=', F8.3, 2X, ' X(I)=', F8.3, 2X, ' SP=', F8.3, 2X,
C 1'COUNT=', I6)
      70 CONTINUE
        BP1=SP/COUNT
C
C AVERAGE THE POINTS FOR THE 2ND BASELINE VALUE, 3018 CM-1 PEAK
C
      EP = 0
      LBP = 0
      COUNT = 0
      IFIRST=IPT3
      ILAST =IPT4
C
C NOW CALCULATE THE SECOND BASELINE POINT
C
      DO 80 I=ILAST, IFIRST
        EP=EP+X(I)
        COUNT=COUNT+1
      80 CONTINUE
        LBP=EP/COUNT
C
C PRINT OUT THE BASELINE DETERMINING POINTS
C
C      PRINT 85, BP1, LBP
C 85   FORMAT(' ', 'BP1= ', F9.4, 2X, ' LBP= ', F9.4, /)
C
C DETERMINE THE X, Y VALUES (CM-1 AND ABS.) FOR THE FIRST
C ANALYTICAL PEAK (3018 CM-1) BY FINDING THE MAXIMUM Y VALUE
C IN THE INTERVAL FOR THIS PEAK WHICH IS: 3020 CM-1 TO 3010
C CM-1 (OR IN DATA POINT VALUES: 6263 TO 6243).
C
      PXA=0
      PYA=0
      DO 82 I=6243, 6263
        IF (X(I).GT.X(I-1)) THEN
          PYA=X(I)
          IC=I-1
          PXA=IC*FXAX
        ENDIF
C      PRINT 299, I, X(I), PYA, IC, PXA

```

```

C 299          FORMAT(' ', 'I=', I4, 2X, 'X=', F8.3, 2X, 'PYA=', F8.3, 2X,
C 1 'IC=', F8.3, 2X, 'PXA=', F8.3)
C 82          CONTINUE
C           PRINT 86, PXA, PYA
C 86          FORMAT(' ', 'PXA= ', F8.3, 2X, 'PYA= ', F8.3, /)
C
C CALCULATE THE BASELINE CORRECTION.  THERE ARE TWO POSSIBLE
C CASES:  (A) POSITIVE SLOPING BASELINE, OR (B) NEGATIVE
C SLOPING BASELINE.
C
C           CASE (A) - POSITIVE SLOPING BASELINE (BP1 < LBP)
C
C SKIP TO CASE (B) IF BASELINE SLOPE IS NEGATIVE
C
C           IF(BP1.GT.LBP) GOTO 3000
C
C OTHERWISE PROCEED WITH THE CORRECTION
C
C           DP1=(3026+3023)/2
C           DP2=(2996+2992)/2
C           YDIF=LBP-BP1
C           XDIF=DP1-DP2
C           XDIF2=DP1-PXA
C           FAC1=XDIF2/XDIF
C           FAC2=FAC1*YDIF
C           FAC2=FAC2+BP1
C           PRINT 87, DP1, DP2, YDIF, XDIF, XDIF2, FAC1, FAC2
C 87          FORMAT(' ', 'DP1=', F8.3, 2X, 'DP2=', F8.3, 2X, 'YDIF=', F9.4, 2X,
C 1 'XDIF=', F9.4, 2X, 'XDIF2=', F9.4, 2X, /, 'FAC1=', F9.4, 2X, 'FAC2=',
C 2F9.4, /)
C           GOTO 3500
C
C           CASE (B) - NEGATIVE SLOPING BASELINE (BP1 > LBP)
C
C 3000        CONTINUE
C           DP1=(3026+3023)/2
C           DP2=(2996+2992)/2
C           YDIF=BP1-LBP
C           XDIF=DP1-DP2
C           XDIF2=PXA-DP2
C           FAC1=XDIF2/XDIF
C           FAC2=FAC1*YDIF
C           FAC2=FAC2+LBP
C           PRINT 57, DP1, DP2, YDIF, XDIF, XDIF2, FAC1, FAC2
C 57          FORMAT(' ', 'DP1=', F8.3, 2X, 'DP2=', F8.3, 2X, 'YDIF=', F9.4, 2X,
C 1 'XDIF=', F9.4, 2X, 'XDIF2=', F9.4, 2X, /, 'FAC1=', F9.4, 2X, 'FAC2=',
C 2F9.4, /)
C 3500        CONTINUE
C
C APPLY THE CORRECTION TO THE ABSORBANCE VALUE FROM PPK
C
C           CABS=PYA-FAC2
C
C PRINT OUT CORRECTED ABSORBANCE VALUE

```

```

C
C      PRINT 88, CABS
C 88   FORMAT(35('-',),/, ' ', 'PEAK ABS(CH4, 3018 CM-1)= ',F6.3)
C
C AVERAGE THE POINTS FOR THE 1ST BASELINE VALUE, 1305 CM-1 PEAK
C
C      SP = 0
C      BP1= 0
C      COUNT = 0
C      IFIRST=IPT5
C      ILAST =IPT6
C
C NOW CALCULATE FIRST BASELINE POINT
C
C      PRINT 38, IFIRST, ILAST
C 38   FORMAT(' ', 'IFIRST=', I4, 2X, ' ILAST=', I4, /)
C      DO 72 I=ILAST, IFIRST
C          SP=SP+X(I)
C          COUNT=COUNT+1
C
C CALCULATE WAVENUMBER VALUES FOR PRINTOUT
C
C      WN=(I-1)*FXAX
C      PRINT 39, WN, X(I), SP, COUNT
C 39   FORMAT(' ', 'WN=', F8.3, 2X, ' X(I)=', F8.3, 2X, ' SP=', F8.3, 2X,
C 1'COUNT=', I6)
C 72   CONTINUE
C      BP1=SP/COUNT
C
C AVERAGE THE POINTS FOR THE 2ND BASELINE VALUE, 3018 CM-1 PEAK
C
C      EP = 0
C      LBP = 0
C      COUNT = 0
C      IFIRST=IPT7
C      ILAST =IPT8
C
C NOW CALCULATE THE SECOND BASELINE POINT
C
C      DO 83 I=ILAST, IFIRST
C          EP=EP+X(I)
C          COUNT=COUNT+1
C 83   CONTINUE
C      LBP=EP/COUNT
C
C PRINT OUT THE BASELINE DETERMINING POINTS
C
C      PRINT 67, BP1, LBP
C 67   FORMAT(' ', 'BP1= ', F9.4, 2X, ' LBP= ', F9.4, /)
C
C DETERMINE THE X, Y VALUES (CM-1 AND ABS.) FOR THE FIRST
C ANALYTICAL PEAK (1305 CM-1) BY FINDING THE MAXIMUM Y VALUE
C IN THE INTERVAL FOR THIS PEAK WHICH IS: 1307 CM-1 TO 1304
C CM-1 (OR IN DATA POINT VALUES: 2710 TO 2704).

```

```

C
    PXA=0
    PYA=0
    DO 84 I=2704,2710
        IF (X(I).GT.X(I-1)) THEN
            PYA=X(I)
            IC=I-1
            PXA=IC*FXAX
        ENDIF
C      PRINT 399,I,X(I),PYA,IC,PXA
C 399      FORMAT(' ','I=',I4,2X,'X=',F8.3,2X,'PYA=',F8.3,2X,
C      1'IC=',F8.3,2X,'PXA=',F8.3)
C 84      CONTINUE
C      PRINT 89,PXA,PYA
C 89      FORMAT(' ','PXA=',F8.3,2X,'PYA=',F8.3,/)
C
C CALCULATE THE BASELINE CORRECTION.  THERE ARE TWO POSSIBLE
C CASES: (A) POSITIVE SLOPING BASELINE, OR (B) NEGATIVE
C SLOPING BASELINE.
C
C      CASE (A) - POSITIVE SLOPING BASELINE (BP1 < LBP)
C
C SKIP TO CASE (B) IF BASELINE SLOPE IS NEGATIVE
C
C      IF(BP1.GT.LBP) GOTO 3100
C
C OTHERWISE PROCEED WITH THE CORRECTION
C
    DP1=(1310+1308)/2
    DP2=(1280+1279)/2
    YDIF=LBP-BP1
    XDIF=DP1-DP2
    XDIF2=DP1-PXA
    FAC1=XDIF2/XDIF
    FAC2=FAC1*YDIF
    FAC2=FAC2+BP1
C      PRINT 187, DP1,DP2,YDIF,XDIF,XDIF2,FAC1,FAC2
C 187      FORMAT(' ','DP1=',F8.3,2X,'DP2=',F8.3,2X,'YDIF=',F9.4,2X,
C      1'XDIF=',F9.4,2X,'XDIF2=',F9.4,2X,/, 'FAC1=',F9.4,2X,'FAC2=',
C      2F9.4,/)
C      GOTO 4500
C
C      CASE (B) - NEGATIVE SLOPING BASELINE (BP1 > LBP)
C
C 3100      CONTINUE
    DP1=(1310+1308)/2
    DP2=(1280+1279)/2
    YDIF=BP1-LBP
    XDIF=DP1-DP2
    XDIF2=PXA-DP2
    FAC1=XDIF2/XDIF
    FAC2=FAC1*YDIF
    FAC2=FAC2+LBP
C 4500      CONTINUE

```

```
C
C APPLY THE CORRECTION TO THE ABSORBANCE VALUE FROM PPK
C
      CABS=PYA-FAC2
C
C PRINT OUT CORRECTED ABSORBANCE VALUE
C
      PRINT 188, CABS
C 188      FORMAT(' ', 'PEAK ABS(CH4, 1305 CM-1)= ', F6.3, '/', 35('-'),
C          1/)
C
C END THE SUBROUTINE
C
      RETURN
      END
```

[NOTE: this program was compiled and linked as a subroutine of BLC003.ASC. See Appendix F for the applicable batch file listing.]

APPENDIX I

SOFTWARE LISTING FOR FORTRAN SUBROUTINE USED TO CALCULATE THE BASELINE-CORRECTED ABSORBANCE VALUE FOR AMMONIA VAPOR AT 967 CM-1

```

CCCCCCCCCCCCCCCCCCCCCCCCCCCCCCCCCCCCCCCCCCCCCCCCCCCCCCCCCCCC
C
C   SUBROUTINE NH3 (Y,FXAX,CABS)
C
C   AMMONIA AND HYDRAZINE ABSORBANCE BANDS HAVE ALMOST
C   COMPLETE OVERLAP IN THE 700 - 1000 CM-1 REGION. TO MEASURE
C   THE AMMONIA ABSORBANCE IN THIS REGION, THEREFORE, IT IS
C   NECESSARY TO FIRST SUBTRACT OUT THE CONTRIBUTION FROM THE
C   HYDRAZINE. THIS WAS DONE BY RECORDING A REFERENCE
C   HYDRAZINE SPECTRUM AND THEN DOING A SCALED, POINT-BY-POINT
C   SUBTRACTION OF THE HYDRAZINE FROM THE MIXTURE SPECTRUM.
C   THE HYDRAZINE REFERENCE SPECTRUM IS STORED AS A DATA
C   STATEMENT IN THE BEGINNING OF THE PROGRAM.
C
C   ONCE THE HYDRAZINE CONTRIBUTION IS SUBTRACTED, OUT THIS
C   SUBROUTINE CALCULATES THE BASELINE BY TAKING THE AVERAGE
C   OF POINTS ON ONE SIDE OF THE ANALYTICAL PEAK (980 - 975 CM-1)
C   FOR THE BEGINNING POINT. THEN TAKING THE AVERAGE OF POINTS
C   ON THE OTHER SIDE OF THE ANALYTICAL PEAK (957 - 955) FOR THE
C   ENDING POINT. A LINE CONNNECTING THESE TWO POINTS FORMS
C   THE BASELINE. THE ABSORBANCE VALUE AT THE ANALYTICAL
C   PEAK (967 CM-1) IS THEN CORRECTED TO THIS MEASURED BASELINE.
C
CCCCCCCCCCCCCCCCCCCCCCCCCCCCCCCCCCCCCCCCCCCCCCCCCCCCCCCCCCCC
C
C   SUBROUTINE NH3 (Y,FXAX,CABS)
C
C   REAL  Y(22528),BP1,LBP, PXA, PYA, CABS, XDIF, XDIF2, YDIF,
1FAC1, FAC2, EP, SP, IC, REF(100), SCALE, TEM
C   INTEGER COUNT
C   DATA REF/.942,1.005,.871,.852,.919,.952,1.031,1.024,.923,
1.812,.725,.588,.585,.715,.712,.668,.745,.813,.819,.828,
2.802,.853,.940,.910,.789,.809,.823,.664,.585,.626,.643,
3.609,.628,.661,.706,.824,.738,.605,.712,.890,.818,.651,
4.639,.658,.557,.521,.495,.466,.516,.522,.456,.500,.597/
C
C   DEFINE THE BASELINE POINTS FOR THE AMMONIA ANALYTICAL PEAK
C
C   IPT1=980/FXAX
C   IPT2=975/FXAX
C   IPT3=957/FXAX
C   IPT4=955/FXAX
C
C   PRINT 35, IPT1,IPT2,IPT3,IPT4
C 35  FORMAT(' ', 'IPT1=', I4, 2X, 'IPT2=', I4, 2X, 'IPT3=', I4, 2X,
C 1 'IPT4=', I4, /)

```

```

C
C FIND THE SCALE FACTOR FOR SUBTRACTING OUT HYDRAZINE
C
      SCALE=ABS(Y(1987)/REF(7))
C      PRINT *, 'Y(1987)=' ,Y(1987), 'REF(7)=' ,REF(7), 'SCALE=' ,
C      1SCALE
C
C SUBTRACT OUT THE HYDRAZINE CONTRIBUTION TO THE ABSORBANCE
C FROM 955 TO 980 CM-1 SO THAT AMMONIA ABSORBANCE CAN BE
C COMPUTED ACCURATELY
C
      DO 40 I= IPT4,IPT1
          J=I+1-IPT4
          TEM=Y(I)
          REF(J)=SCALE*REF(J)
          Y(I)=Y(I)-REF(J)
C          PRINT 42, I, TEM, Y(I), REF(J), J
C 42      FORMAT(' ', 'I=' ,I6, 2X, 'Y(I)=' ,F6.3, 2X, 'Y(I) CORR.=' ,
C      1F6.3, 2X, 'REF(J)=' ,F6.3, 2X, 'J=' ,I4)
C 40      CONTINUE
C
C AVERAGE THE POINTS FOR THE 1ST BASELINE VALUE
C
      SP = 0
      BP1= 0
      COUNT = 0
      IFIRST=IPT1
      ILAST =IPT2
C
C NOW CALCULATE FIRST BASELINE POINT
C
      PRINT 36, IFIRST, ILAST
C 36      FORMAT(' ', 'IFIRST=' ,I4, 2X, 'ILAST=' , I4, /)
      DO 70 I=ILAST, IFIRST
          SP=SP+Y(I)
          COUNT=COUNT+1
C
C CALCULATE WAVENUMBER VALUES FOR PRINTOUT
C
      WN=(I-1)*FXAX
      PRINT 37, WN, Y(I), SP, COUNT
C 37      FORMAT(' ', 'WN=' ,F8.3, 2X, 'Y(I)=' ,F8.3, 2X, 'SP=' ,F8.3,
C      12X, 'COUNT=' , I6)
C 70      CONTINUE
          BP1=SP/COUNT
C
C AVERAGE THE POINTS FOR THE 2ND BASELINE VALUE
C
      EP = 0
      LBP = 0
      COUNT = 0
      IFIRST=IPT3
      ILAST =IPT4
C

```

```

C NOW CALCULATE THE SECOND BASELINE POINT
C
      DO 80 I=ILAST,IFIRST
        EP=EP+Y(I)
        COUNT=COUNT+1
80    CONTINUE
      LBP=EP/COUNT
C
C PRINT OUT THE BASELINE DETERMINING POINTS
C
      PRINT 85, BP1,LBP
C 85    FORMAT(' ', 'BP1= ',F9.4,2X, 'LBP= ',F9.4,/)
C
C DETERMINE THE X,Y VALUES (CM-1 AND ABS.) FOR THE
C ANALYTICAL PEAK (967 CM-1) BY FINDING THE MAXIMUM Y VALUE
C IN THE INTERVAL FOR THIS PEAK WHICH IS: 970 CM-1 TO 960
C CM-1 (OR IN DATA POINT VALUES: 2011 TO 1991).
C
      PXA=0
      PYA=0
      DO 82 I=1991,2011
        IF (Y(I).GT.Y(I-1)) THEN
          PYA=Y(I)
          IC=I-1
          PXA=IC*FXAX
        ENDIF
      PRINT 299, I, Y(I), PYA, IC, PXA
C 299    FORMAT(' ', 'I=', I4,2X, 'Y=', F8.3,2X, 'PYA=', F8.3,2X,
C 1' IC=', F8.3,2X, 'PXA=', F8.3)
C 82    CONTINUE
      PRINT 86, PXA, PYA
C 86    FORMAT(' ', 'PXA= ',F8.3,2X, 'PYA= ',F8.3,/)
C
C CALCULATE THE BASELINE CORRECTION. THERE ARE TWO POSSIBLE
C CASES: (A) POSITIVE SLOPING BASELINE, OR (B) NEGATIVE
C SLOPING BASELINE.
C
      CASE (A) - POSITIVE SLOPING BASELINE (BP1 < LBP)
C
C SKIP TO CASE (B) IF BASELINE SLOPE IS NEGATIVE
C
      IF(BP1.GT.LBP) GOTO 3000
C
C OTHERWISE PROCEED WITH THE CORRECTION
C
      DP1=(980+975)/2
      DP2=(957+955)/2
      YDIF=LBP-BP1
      XDIF=DP1-DP2
      XDIF2=DP1-PXA
      FAC1=XDIF2/XDIF
      FAC2=FAC1*YDIF
      FAC2=FAC2+BP1
C PRINT 87, DP1, DP2, YDIF, XDIF, XDIF2, FAC1, FAC2

```

```

C 87   FORMAT(' ', 'DP1=', F8.3, 2X, 'DP2=', F8.3, 2X, 'YDIF=', F9.4, 2X,
C     1'XDIF=', F9.4, 2X, 'XDIF2=', F9.4, 2X, /, 'FAC1=', F9.4, 2X, 'FAC2=',
C     2F9.4, /)
      GOTO 3500
C
C     CASE (B) - NEGATIVE SLOPING BASELINE (BP1 > LBP)
C
C 3000  CONTINUE
      DP1=(980+975)/2
      DP2=(957+955)/2
      YDIF=BP1-LBP
      XDIF=DP1-DP2
      XDIF2=PXA-DP2
      FAC1=XDIF2/XDIF
      FAC2=FAC1*YDIF
      FAC2=FAC2+LBP
C     PRINT 57, DP1, DP2, YDIF, XDIF, XDIF2, FAC1, FAC2
C 57   FORMAT(' ', 'DP1=', F8.3, 2X, 'DP2=', F8.3, 2X, 'YDIF=', F9.4, 2X,
C     1'XDIF=', F9.4, 2X, 'XDIF2=', F9.4, 2X, /, 'FAC1=', F9.4, 2X, 'FAC2=',
C     2F9.4, /)
C 3500  CONTINUE
C
C APPLY THE CORRECTION TO THE ABSORBANCE VALUE FROM PPK
C
      CABS=PYA-FAC2
C
C PRINT OUT CORRECTED ABSORBANCE VALUE
C
      PRINT 88, CABS
C 88   FORMAT(35('-'), /, ' ', 'PEAK ABS (NH3, 967 CM-1)= ', F6.3, /,
C     135('-'), /)
C
C END THE SUBROUTINE
C
      RETURN
      END

```

[NOTE: this program was compiled and linked as a subroutine of BLC003.ASC. See Appendix F for the applicable batch file listing.]

APPENDIX J

SOFTWARE LISTING FOR FORTRAN PROGRAM USED TO CALCULATE THE BASELINE-CORRECTED ABSORBANCE VALUE FOR WATER VAPOR AT 1700 CM-1

```

CCCCCCCCCCCCCCCCCCCCCCCCCCCCCCCCCCCCCCCCCCCCCCCCCCCCCCCCCCCC
C
C   SUBROUTINE H2O(Y,FXAX,CABS)
C
C   CALCULATES THE BASELINE BY TAKING THE AVERAGE OF POINTS
C   ON ONE SIDE OF THE ANALYTICAL PEAK (1703 - 1702 CM-1) FOR THE
C   BEGINNING POINT. THEN TAKING THE AVERAGE OF POINTS ON
C   THE OTHER SIDE OF THE ANALYTICAL PEAK (1694 - 1691 CM-1) FOR
C   THE ENDING POINT. A LINE CONNECTING THESE TWO POINTS
C   FORMS THE BASELINE. THE ABSORBANCE VALUE AT THE
C   ANALYTICAL PEAK (1700 CM-1) IS THEN CORRECTED TO THIS
C   MEASURED BASELINE.
C
CCCCCCCCCCCCCCCCCCCCCCCCCCCCCCCCCCCCCCCCCCCCCCCCCCCCCCCCCCCC
C
C   SUBROUTINE H2O(Y,FXAX,CABS)
C
C   REAL   Y(22528),BP1,LBP,PXA,PYA,CABS,XDIF,XDIF2,YDIF,
1FAC1,FAC2,EP,SP,IC
C   INTEGER COUNT
C
C   DEFINE THE BASELINE POINTS FOR THE WATER ANALYTICAL PEAK
C
C   IPT1=1703/FXAX
C   IPT2=1702/FXAX
C   IPT3=1694/FXAX
C   IPT4=1691/FXAX
C
C   PRINT 35, IPT1,IPT2,IPT3,IPT4
C 35   FORMAT(' ', 'IPT1=', I4, 2X, 'IPT2=', I4, 2X, 'IPT3=', I4, 2X,
C   1' IPT4=', I4, /)
C
C   AVERAGE THE POINTS FOR THE 1ST BASELINE VALUE
C
C   SP = 0
C   BP1= 0
C   COUNT = 0
C   IFIRST=IPT1+1
C   ILAST =IPT2
C
C   NOW CALCULATE FIRST BASELINE POINT
C
C   PRINT 36, IFIRST,ILAST
C 36   FORMAT(' ', 'IFIRST=', I4, 2X, 'ILAST=', I4, /)
C   DO 70 I=ILAST,IFIRST

```

```

        SP=SP+Y(I+1)
        COUNT=COUNT+1
C
C CALCULATE WAVENUMBER VALUES FOR PRINTOUT
C
C         WN=(I)*FXAX
C         PRINT 37, WN,Y(I+1),SP,COUNT
C 37      FORMAT(' ', 'WN=', F8.3, 2X, 'Y(I)=' , F8.3, 2X, 'SP=' , F8.3,
C         12X, 'COUNT=' , I6)
C 70      CONTINUE
        BP1=SP/COUNT
C
C AVERAGE THE POINTS FOR THE 2ND BASELINE VALUE
C
C         EP = 0
C         LBP = 0
C         COUNT = 0
C         IFIRST=IPT3+1
C         ILAST =IPT4
C
C NOW CALCULATE THE SECOND BASELINE POINT
C
C         DO 80 I=ILAST,IFIRST
C           EP=EP+Y(I+1)
C           COUNT=COUNT+1
C
C CALCULATE WAVENUMBER VALUES FOR PRINTOUT
C
C         WN=(I)*FXAX
C         PRINT 140
C140      FORMAT(' ')
C         PRINT 137, WN,Y(I+1),SP,COUNT
C137      FORMAT(' ', 'WN=', F8.3, 2X, 'Y(I)=' , F8.3, 2X, 'SP=' , F8.3,
C         12X, 'COUNT=' , I6)
C 80      CONTINUE
        LBP=EP/COUNT
C
C PRINT OUT THE BASELINE DETERMINING POINTS
C
C         PRINT 85, BP1,LBP
C 85      FORMAT(' ', 'BP1= ', F9.4, 2X, 'LBP= ', F9.4, /)
C
C DETERMINE THE X,Y VALUES (CM-1 AND ABS.) FOR THE
C ANALYTICAL PEAK (1700 CM-1) BY FINDING THE MAXIMUM Y VALUE
C IN THE INTERVAL FOR THIS PEAK WHICH IS: 1702 CM-1 TO 1699
C CM-1 (OR IN DATA POINT VALUES: 3530 TO 3523).
C
C         PXA=0
C         PYA=0
C         DO 82 I=3523,3530
C           IF (Y(I).GT.Y(I-1)) THEN
C             PYA=Y(I)
C             IC=I-1
C             PXA=IC*FXAX

```

```

        ENDIF
C          PRINT 299, I, Y(I), PYA, IC, PXA
C 299      FORMAT(' ', 'I=', I4, 2X, 'Y=', F8.3, 2X, 'PYA=', F8.3, 2X,
C 1'IC=', F8.3, 2X, 'PXA=', F8.3)
C 82      CONTINUE
C          PRINT 86, PXA, PYA
C 86      FORMAT(' ', 'PXA= ', F8.3, 2X, 'PYA= ', F8.3, /)
C
C CALCULATE THE BASELINE CORRECTION.  THERE ARE TWO POSSIBLE
C CASES: (A) POSITIVE SLOPING BASELINE, OR (B) NEGATIVE
C SLOPING BASELINE.
C
C          CASE (A) - POSITIVE SLOPING BASELINE (BP1 < LBP)
C
C SKIP TO CASE (B) IF BASELINE SLOPE IS NEGATIVE
C
C          IF(BP1.GT.LBP) GOTO 3000
C
C OTHERWISE PROCEED WITH THE CORRECTION
C
C          DP1=(1703+1702)/2
C          DP2=(1694+1691)/2
C          YDIF=LBP-BP1
C          XDIF=DP1-DP2
C          XDIF2=DP1-PXA
C          FAC1=XDIF2/XDIF
C          FAC2=FAC1*YDIF
C          FAC2=FAC2+BP1
C          PRINT 87, DP1, DP2, YDIF, XDIF, XDIF2, FAC1, FAC2
C 87      FORMAT(' ', 'DP1=', F8.3, 2X, 'DP2=', F8.3, 2X, 'YDIF=', F9.4, 2X,
C 1'XDIF=', F9.4, 2X, 'XDIF2=', F9.4, 2X, /, 'FAC1=', F9.4, 2X, 'FAC2=',
C 2F9.4, /)
C          GOTO 3500
C
C          CASE (B) - NEGATIVE SLOPING BASELINE (BP1 > LBP)
C
C 3000    CONTINUE
C          DP1=(1703+1702)/2
C          DP2=(1694+1691)/2
C          YDIF=BP1-LBP
C          XDIF=DP1-DP2
C          XDIF2=PXA-DP2
C          FAC1=XDIF2/XDIF
C          FAC2=FAC1*YDIF
C          FAC2=FAC2+LBP
C          PRINT 57, DP1, DP2, YDIF, XDIF, XDIF2, FAC1, FAC2
C 57      FORMAT(' ', 'DP1=', F8.3, 2X, 'DP2=', F8.3, 2X, 'YDIF=', F9.4, 2X,
C 1'XDIF=', F9.4, 2X, 'XDIF2=', F9.4, 2X, /, 'FAC1=', F9.4, 2X, 'FAC2=',
C 2F9.4, /)
C 3500    CONTINUE
C
C APPLY THE CORRECTION TO THE ABSORBANCE VALUE FROM PPK
C
C          CABS=PYA-FAC2

```

```
C
C PRINT OUT CORRECTED ABSORBANCE VALUE
C
C PRINT 88, CABS
C 88 FORMAT(' ', 'CABS=', F4.3, '/')
C
C
C END THE SUBROUTINE
C
C RETURN
C END
```

[NOTE: this program was compiled and linked as a subroutine of BLC003.ASC. See Appendix F for the applicable batch file listing.]

APPENDIX K

LISTING OF ALL WATER CALIBRATION RUNS SHOWING BOTH VAPOR
AND LIQUID SAMPLES. FOR LIQUID SAMPLES, ABSORBANCE AVERAGES
AND NORMALIZATION RESULTS ARE SHOWN ALONG WITH TOTAL
ELAPSED TIME FROM SAMPLE INJECTION.

DATE	SAMPLE	RUN	WATER		TIME (hrs)	CH4 abs	PEAK 1 ave	PEAK 2 ave	DESCRIPTION
			PEAK 1	PEAK 2					
25-Jul-89	1	1	0.381	0.339		0.840			15.0 Torr H2O (in 2-liter bulb)
		2	0.384	0.333					
		3	0.384	0.339					
		4	0.390	0.333					
25-Jul-89	2	1	0.372	0.330		0.828			15.0 Torr H2O (in 2-liter bulb)
		2	0.378	0.318					
		3	0.372	0.324					
		4	0.372	0.324					
24-Jul-89	1	1	0.300	0.252		0.732			10.0 Torr H2O (in 2-liter bulb)
		2	0.306	0.258					
		3	0.300	0.258					
		4	0.312	0.258					
25-Jul-89	2	1	0.342	0.288		0.836			10.0 Torr H2O (in 2-liter bulb)
		2	0.354	0.282					
		3	0.354	0.288					
		4	0.354	0.294					
25-Jul-89	1	1	0.183	0.132		0.828			5.0 Torr H2O (in 2-liter bulb)
		2	0.189	0.144					
		3	0.192	0.150					
		4	0.198	0.147					
26-Jul-89	2	1	0.198	0.132		0.828	(data invalid FTIR purge off)		5.0 Torr H2O (in 2-liter bulb)
		2	0.198	0.162					
26-Jul-89	3	1	0.192	0.150		?			5.0 TORR (in 2-liter bulb)
		2	0.186	0.144					
		3	0.186	0.144					
		4	0.180	0.138					
26-Jul-89	1	1	0.029	0.026		?			1.0 Torr H2O (in 2-liter bulb)
		2	0.029	0.025					
		3	0.031	0.025					
		4	0.032	0.026					
27-Jul-89	3	1	0.099	0.096		0.828			1.0 Torr H2O (in 2-liter bulb)
		2	0.099	0.096					
		3	0.102	0.099					
		4	0.105	0.099					

DATE	SAMPLE	RUN	WATER		TIME (hrs)	CH4 abs	PEAK 1 ave	PEAK 2 ave	DESCRIPTION
			PEAK 1	PEAK 2					
(normalized to CH4= 0.800)									
27-Jul-89	4	1	0.105	0.099		0.828			1.0 Torr H2O (in 2-liter bulb)
		2	0.108	0.102					
		3	0.108	0.102					
		4	0.111	0.105					
28-Jul-89	1	1	0.117	0.117		0.828			8.0 Torr H2O (in 2-liter bulb)
		2	0.117	0.117					
		3	0.117	0.117					
		4	0.117	0.117					
31-Jul-89	1	1	0.390	0.360		0.804			20 ul H2O (in 760 Torr helium)
		2	0.384	0.354					
		3	0.384	0.360					
			0.386	0.358			0.384	0.356	
31-Jul-89	2	1	0.408	0.378		0.780			20 ul H2O (in 760 Torr helium)
		2	0.402	0.378					
		3	0.408	0.378					
		4	0.402	0.378					
			0.404	0.378		0.414	0.388		
31-Jul-89	1	1	0.192	0.186		0.836			5 ul H2O (in 600 Torr helium)
		2	0.192	0.180					
		3	0.192	0.180					
		4	0.192	0.186					
			0.192	0.182		0.184	0.174		
1-Aug-89	1	1	0.240	0.228		0.864			above run with helium to 760 Torr
		2	0.234	0.228					
		3	0.240	0.228					
		4	0.240	0.228					
			0.238	0.228		0.220	0.211		
1-Aug-89	1	1	0.294	0.276		0.828			above run after sitting overnight (ref. file #58)
		2	0.294	0.282					
		3	0.300	0.276					
		4	0.294	0.276					
			0.296	0.278		0.286	0.269		
1-Aug-89	1	1	0.294	0.270		0.876			above run after sitting overnight (ref. file #84)
		2	0.294	0.276					
		3	0.294	0.276					
		4	0.294	0.276					
			0.294	0.276		0.268	0.252		
1-Aug-89	2	1	0.162	0.159		0.792			5 ul H2O (in 600 Torr helium)
		2	0.165	0.159					
		3	0.165	0.159					
		4	0.165	0.162					
			0.165	0.160		0.167	0.162		
1-Aug-89	2	1	0.168	0.165		0.792			above run after 90 min
		2	0.168	0.165					

DATE	SAMPLE	RUN	WATER		TIME (hrs)	CH4 abs	PEAK 1 ave	PEAK 2 ave	DESCRIPTION
			PEAK 1	PEAK 2					

(normalized to
CH4= 0.800)

			3	0.168	0.165				
			4	0.171	0.168				
				0.169	0.166		0.171	0.168	
1-Aug-89	2	1	0.201	0.192		0.816			above run with helium to 760 Torr after 30 min
		2	0.204	0.195					
		3	0.204	0.198					
		4	0.204	0.195					
				0.204	0.196		0.200	0.192	
1-Aug-89	2	1	0.210	0.201		0.816			above run after 3 hrs
		2	0.210	0.201					
		3	0.207	0.204					
		4	0.210	0.204					
				0.209	0.203		0.205	0.199	
2-Aug-89	2	1	0.264	0.249		0.828			above run after sitting overnight
		2	0.264	0.252					
		3	0.264	0.246					
		4	0.270	0.252					
				0.266	0.250		0.257	0.242	
2-Aug-89	3	1	0.180	0.174		0.840			5 ul H2O (in 760 Torr helium)
		2	0.186	0.180					
		3	0.186	0.180					
		4	0.186	0.180					
		(avg's)	0.186	0.180	1.362		0.177	0.171	
3-Aug-89	3	1	0.192	0.186		0.840			above run after 3 hrs
		2	0.198	0.192					
		3	0.198	0.192					
		4	0.198	0.192					
		(avg's)	0.198	0.192	5.256		0.189	0.183	
3-Aug-89	3	1	0.252	0.240		0.840			above run after sitting overnight
		2	0.252	0.234					
		3	0.252	0.240					
		4	0.258	0.240					
		(avg's)	0.254	0.238	20.599		0.242	0.227	
3-Aug-89	1	1	0.117	0.120		0.828			1 ul H2O (in 760 Torr helium)
		2	0.120	0.123					
		3	0.120	0.120					
		4	0.123	0.123					
		(avg's)	0.121	0.122	1.236		0.117	0.118	
3-Aug-89	1	1	0.147	0.147		0.820			above run after 3 hrs
		2	0.147	0.147					
		3	0.150	0.150					
		4	0.153	0.153					
		(avg's)	0.150	0.150	5.756		0.146	0.146	
4-Aug-89	1	1	0.234	0.222		0.828			above run after

DATE	SAMPLE	RUN	WATER		TIME (hrs)	CH4 abs	PEAK 1 ave	PEAK 2 ave	DESCRIPTION
			PEAK 1	PEAK 2					

(normalized to
CH4= 0.800)

			2	0.228	0.222				sitting overnight
			3	0.228	0.222				
			4	0.228	0.222				
		(avg's)		0.228	0.222	22.262	0.220	0.214	
4-Aug-89	1	1	0.177	0.162		0.816			5 ul H2O (in 760 Torr helium)
		2	0.177	0.162					
		3	0.177	0.159					
		4	0.174	0.162					
		(avg's)		0.176	0.161	1.261	0.173	0.158	
4-Aug-89	1	1	0.171	0.159		0.816			above run after 3 hrs
		2	0.174	0.159					
		3	0.174	0.162					
		4	0.174	0.162					
		(avg's)		0.174	0.161	3.739	0.171	0.158	
5-Aug-89	1	1	0.225	0.204		0.828			above run after sitting overnight
		2	0.228	0.210					
		3	0.228	0.210					
		4	0.234	0.204					
		(avg's)		0.230	0.208	22.897	0.222	0.201	
6-Aug-89	1	1	0.300	0.264		0.828			above run after 48 hrs
		2	0.294	0.264					
		3	0.300	0.264					
		4	0.300	0.264					
		(avg's)		0.298	0.264	48.938	0.288	0.255	
7-Aug-89	1	1	0.336	0.300		0.828			above run after 72 hrs
		2	0.336	0.300					
		3	0.336	0.300					
		4	0.336	0.306					
		(avg's)		0.336	0.302	66.241	0.325	0.292	
7-Aug-89	1	1	0.342	0.312		0.828			above run after 78 hrs
		2	0.342	0.306					
		3	0.348	0.312					
		4	0.342	0.306					
		(avg's)		0.344	0.308	70.288	0.332	0.298	
8-Aug-89	1	1	0.378	0.342		0.828			above run after 96 hrs
		2	0.378	0.348					
		3	0.378	0.348					
		4	0.378	0.348					
		(avg's)		0.378	0.348	90.010	0.365	0.336	
8-Aug-89	1	1	0.060	0.060		---			760 Torr helium
		2	0.065	0.063					
		3	0.063	0.065					
		4	0.066	0.065					
		(avg's)		0.065	0.064	0.078			

DATE	SAMPLE	RUN	WATER		TIME (hrs)	CH4 abs	PEAK 1 ave	PEAK 2 ave	DESCRIPTION
			PEAK 1	PEAK 2					
(normalized to CH4= 0.800)									
8-Aug-89	1	1	0.078	0.077	3.097	---			above run after 3 hrs
		2	0.075	0.077					
		3	0.075	0.074					
		4	0.075	0.074					
		(avg's)	0.075	0.075					
9-Aug-89	1	1	0.126	0.123	21.471	---			above run after sitting overnight
		2	0.129	0.126					
		3	0.126	0.126					
		4	0.126	0.126					
		(avg's)	0.127	0.126					
9-Aug-89	1	1	0.141	0.138	26.789	---			above run after 27 hrs
		2	0.141	0.138					
		3	0.141	0.138					
		4	0.141	0.138					
		(avg's)	0.141	0.138					
10-Aug-89	1	1	0.174	0.165	45.163	---			above run after 45 hrs
		2	0.174	0.168					
		3	0.174	0.168					
		4	0.174	0.165					
		(avg's)	0.174	0.167					
10-Aug-89	2	1	0.138	0.138	1.114				2 ul H2O (in 760 Torr helium)
		2	0.141	0.138					
		3	0.138	0.138					
		4	0.141	0.141					
		(avg's)	0.140	0.139					
10-Aug-89	2	1	0.144	0.144	3.700				above run after 3 hrs
		2	0.153	0.147					
		3	0.150	0.150					
		4	0.153	0.150					
		(avg's)	0.152	0.149					
11-Aug-89	1	1	0.186	0.180	17.706	0.696			above run after sitting overnight
		2	0.192	0.186					
		3	0.192	0.186					
		4	0.189	0.186					
		(avg's)	0.191	0.186					
11-Aug-89	2	1	0.138	0.138	1.167	0.804			2 ul H2O (in 760 Torr helium)
		2	0.138	0.141					
		3	0.138	0.141					
		4	0.138	0.141					
		(avg's)	0.138	0.141					
11-Aug-89	2	1	0.139	0.141	4.114	0.784			above run after 4 hrs
		2	0.139	0.141					
		3	0.138	0.141					
		4	0.142	0.143					
		(avg's)	0.140	0.142					

DATE	SAMPLE	RUN	WATER		TIME (hrs)	CH4 abs	PEAK 1 ave	PEAK 2 ave	DESCRIPTION
			PEAK 1	PEAK 2					
(normalized to CH4= 0.800)									
15-Aug-89	1	1	0.343	0.317		0.777			above run after 100 hrs
		2	0.345	0.321					
		3	0.343	0.319					
		4	0.344	0.323					
		(avg's)		0.344	0.321	100.250		0.354	
16-Aug-89	1	1	0.367	0.340		0.767			above run after 116 hrs
		2	0.368	0.341		0.767			
		3	0.369	0.342		0.777			
		4	0.363	0.341		0.771			
		(avg's)		0.367	0.341	116.624	0.772	0.380	
16-Aug-89	2	1	0.152	0.149		0.783			1 ul H2O (in 760 Torr helium)
		2	0.146	0.141		0.781			
		3	0.143	0.138		0.781			
		4	0.143	0.136		0.779			
		(avg's)		0.144	0.138	1.340	0.780	0.148	
16-Aug-89	2	1	0.142	0.135		0.811			above run after 4 hrs
		2	0.142	0.137		0.781			
		3	0.143	0.136		0.771			
		4	0.144	0.136		0.779			
		(avg's)		0.143	0.136	4.164	0.777	0.147	
17-Aug-89	1	1	0.179	0.169		0.770			above run after 18 hrs
		2	0.181	0.171		0.774			
		3	0.181	0.170		0.774			
		4	0.182	0.172		0.772			
		(avg's)		0.181	0.171	17.526	0.773	0.188	
17-Aug-89	2	1	0.141	0.140		0.756			1 ul H2O (in 760 Torr helium)
		2	0.141	0.141		0.756			
		3	0.140	0.140		0.754			
		4	0.136	0.136		0.758			
		(avg's)		0.139	0.139	1.346	0.756	0.147	
17-Aug-89	2	1	0.145	0.145		0.788			above run after 5 hrs
		2	0.147	0.145		0.785			
		3	0.144	0.143		0.796			
		4	0.144	0.140		0.786			
		(avg's)		0.145	0.143	4.538	0.789	0.147	
17-Aug-89	2	1	0.178	0.174		0.794			above run after 18 hrs
		2	0.178	0.173		0.794			
		3	0.178	0.175		0.794			
		4	0.177	0.176		0.794			
		(avg's)		0.178	0.175	18.106	0.794	0.179	
18-Aug-89	1	1	0.297	0.280		0.790			10 ul H2O (in 760 Torr helium)
		2	0.292	0.278		0.785			
		3	0.295	0.277		0.783			
		4	0.293	0.277		0.779			
		(avg's)		0.293	0.277	1.857	0.782	0.300	

DATE	SAMPLE	RUN	WATER		TIME (hrs)	CH4 abs	PEAK 1 ave	PEAK 2 ave	DESCRIPTION
			PEAK 1	PEAK 2					
19-Aug-89	1	1	0.322	0.305		0.776			above run after 5 hrs
		2	0.313	0.305		0.790			
		3	0.320	0.311		0.778			
		4	0.322	0.310		0.776			
		(avg's)		0.318	0.309	4.845	0.781	0.326	
20-Aug-89	1	1	0.351	0.333		0.778			above run after 30 hrs
		2	0.354	0.337		0.774			
		3	0.355	0.337		0.774			
		4	0.352	0.333		0.776			
		(avg's)		0.354	0.336	29.963	0.775	0.365	
21-Aug-89	1	1	0.367	0.344		0.790			above run after 41 hrs
		2	0.365	0.342		0.781			
		3	0.367	0.346		0.777			
		4	0.368	0.343		0.794			
		(avg's)		0.367	0.344	41.461	0.784	0.374	
21-Aug-89	2	1	0.292	0.276		0.802			10 ul H2O (In 760 Torr helium)
		2	0.291	0.275		0.802			
		3	0.290	0.274		0.802			
		4	0.289	0.275		0.804			
		(avg's)		0.290	0.275	1.639	0.803	0.289	
21-Aug-89	2	1	0.295	0.278		0.724			above run after 7 hrs
		2	0.296	0.279		0.726			
		3	0.293	0.281		0.724			
		4	0.295	0.274		0.718			
		(avg's)		0.295	0.278	6.995	0.723	0.326	
22-Aug-89	1	1	0.315	0.297		0.728			above run after 21 hrs
		2	0.313	0.297		0.727			
		3	0.314	0.295		0.728			
		4	0.315	0.298		0.726			
		(avg's)		0.314	0.297	21.222	0.727	0.346	
22-Aug-89	2	1	0.062	0.070		0.735			dry helium + CH4 (760 Torr)
		2	0.065	0.071		0.737			
		3	0.065	0.071		0.735			
		4	0.061	0.072		0.735			
		(avg's)		0.064	0.071	1.958	0.736	0.069	
22-Aug-89	2	1	0.084	0.088		0.779			above run after 5 hrs
		2	0.082	0.088		0.783			
		3	0.084	0.090		0.777			
		4	0.084	0.090		0.774			
		(avg's)		0.083	0.089	5.254	0.778	0.086	
23-Aug-89	1	1	0.134	0.138		0.800			above run after 20 hrs
		2	0.135	0.139		0.800			
		3	0.136	0.139		0.798			
		4	0.136	0.140		0.798			
		(avg's)		0.136	0.139	19.666	0.799	0.136	

DATE	SAMPLE	RUN	WATER		TIME (hrs)	CH4 abs	PEAK 1 ave	PEAK 2 ave	DESCRIPTION
			PEAK 1	PEAK 2					
23-Aug-89	1	1	0.159	0.158	29.567	0.728	0.176	0.175	above run after 30 hrs
		2	0.158	0.157		0.718			
		3	0.159	0.158		0.722			
		4	0.160	0.160		0.728			
		(avg's)	0.159	0.158		0.723			
24-Aug-89	1	1	0.193	0.193	43.933	0.783	0.196	0.195	above run after 44 hrs
		2	0.193	0.193		0.794			
		3	0.195	0.192		0.792			
		4	0.195	0.195		0.788			
		(avg's)	0.194	0.193		0.791			
29-Aug-89	1	1	0.083	0.081	1.482	0.612	0.112	0.106	dry helium + CH4 (760 Torr)
		2	0.084	0.080		0.614			
		3	0.088	0.086		0.612			
		4	0.083	0.077		0.600			
		(avg's)	0.085	0.081		0.609			
29-Aug-89	1	1	0.098	0.090	8.861	0.597	0.134	0.124	above run after 9 hrs
		2	0.095	0.090		0.587			
		3	0.097	0.088		0.576			
		4	0.098	0.091		0.571			
		(avg's)	0.097	0.090		0.578			
30-Aug-89	1	1	0.119	0.109	22.734	0.600	0.159	0.145	above run after 23 hrs
		2	0.118	0.110		0.600			
		3	0.121	0.109		0.600			
		4	0.119	0.108		0.600			
		(avg's)	0.119	0.109		0.600			
30-Aug-89	1	1	0.133	0.120	32.358	0.597	0.183	0.169	above run after 32 hrs
		2	0.133	0.121		0.594			
		3	0.132	0.123		0.563			
		4	0.132	0.123		0.576			
		(avg's)	0.132	0.122		0.578			
31-Aug-89	1	1	0.159	0.143	46.607	0.598	0.217	0.198	above run after 47 hrs
		2	0.163	0.151		0.592			
		3	0.163	0.145		0.597			
		4	0.159	0.147		0.598			
		(avg's)	0.162	0.148		0.596			
31-Aug-89	1	1	0.175	0.156	56.729	0.572	0.244	0.221	above run after 57 hrs
		2	0.173	0.155		0.570			
		3	0.171	0.152		0.558			
		4	0.167	0.156		0.548			
		(avg's)	0.170	0.154		0.559			
1-Sep-89	1	1	0.194	0.174	70.735	0.587	0.266	0.240	above run after 71 hrs
		2	0.194	0.174		0.587			
		3	0.193	0.176		0.581			
		4	0.196	0.176		0.586			
		(avg's)	0.194	0.175		0.585			

DATE	SAMPLE	RUN	WATER		TIME (hrs)	CH4 abs	PEAK 1 ave	PEAK 2 ave	DESCRIPTION
			PEAK 1	PEAK 2					
(normalized to CH4= 0.800)									
1-Sep-89	1	1	0.206	0.190		0.586			above run after 81 hrs
			0.206	0.189		0.587			
			0.204	0.184		0.560			
			0.205	0.186		0.568			
			(avg's)		0.205	0.186	80.946	0.572	0.287
5-Sep-89	1	1	0.300	0.268		0.582			above run after 167 hrs
			0.297	0.264		0.579			
			0.299	0.269		0.576			
			0.301	0.272		0.578			
			(avg's)		0.299	0.268	166.879	0.578	0.414
8-Sep-89	1	1	0.462	0.454		0.718			above run after 239 hrs
			0.429	0.402		0.644			
			0.407	0.381		0.618			
			0.403	0.371		0.595			
			(avg's)		0.413	0.385	238.743	0.619	0.534

APPENDIX L

PROGRAM TO CALCULATE ABSORBANCE VALUES AS A FUNCTION OF FIXED TIME INTERVALS (WRITTEN IN GWBASIC)

```

10 REM   LPRINT "                               WATER CALIBRATION DATA"
20 REM   LPRINT "                               "
30 DIM A(50),B(50),C(50),D(50),E(50),H(50),P(5)
40 P(1)=0
42 P(2)=1.4
44 P(3)=3.5
46 P(4)=7
50 REM   LPRINT
60 K=1
70 REM   LPRINT "mtime 0.0 ppm  1.55 ppm 5.5 ppm 12.8 ppm 25.5ppm"
80 REM   LPRINT "===== ===== ===== ===== ====="
90 FOR I=0 TO 100 STEP 5
100 H(K)=I
110   A(K)=-4.27562E-05*I^2 + 5.02122E-03*I + .0593525
120   B(K)=3.38794E-03*I + .131176
130   C(K)=1.95744E-03*I + .156582
140   D(K)=2.20969E-03*I + .175349
150   E(K)=1.88885E-03*I + .303148
160 REM   LPRINT USING "####.####";H(K),A(K),B(K),C(K),D(K),E(K)
170 K=K+1
180 NEXT I
190 OPEN "O",#1,"H2ODATA"
200 FOR J=1 TO 21
210 PRINT#1,USING"####.####";P(1),H(J),A(J)
220 NEXT J
230 FOR J=1 TO 21
240 PRINT#1,USING"####.####";P(2),H(J),C(J)
250 NEXT J
260 FOR J=1 TO 21
270 PRINT#1,USING"####.####";P(3),H(J),D(J)
280 NEXT J
290 FOR J=1 TO 21
300 PRINT#1,USING"####.####";P(4),H(J),E(J)
310 NEXT J
320 CLOSE#1
330 END

```

APPENDIX M

SUMMARY OF EXPERIMENTS CONDUCTED IN THE SPHERICAL CHAMBER

Date	Sequential Run No.	Conditions			File Name	Comments
		Plates	water	O2		
3-Dec-87		none	none	none	SC03DC87.PRN	initial run, CH4 in dry helium [before run: chamber pumped to 10 microns with mechanical pump] [after run: chamber pumped to 5E-6 Torr, filled to 760 Torr with helium, pumped to 300 Torr, then filled again to 760 Torr with helium as CH4 and SF6 were flushed in]
11-Jan-88		none	none	none	SC11JA88.PRN	CH4 + SF6 in dry helium [before run: chamber pumped to 5E-6 Torr, filled to 760 Torr with helium, pumped to 300 Torr, then filled again to 760 Torr with helium as CH4 and SF6 were flushed in]
8-Feb-88	ser. 1, run 1	none	none	none	SC08FB88.PRN	HZ in 100% DRY HELIUM, 1st series [before run: chamber pumped with turbo pump and LN2 trap for 90 min]
17-Feb-88	ser. 1, run 2	none	none	none	SC17FB88.PRN	HZ in 100% DRY HELIUM, 1st series [before run: chamber pumped to 680 Torr, then more HZ flushed in]
29-Feb-88	ser. 1, run 3	none	none	none	SC29FB88.PRN	HZ in 100% DRY HELIUM, 1st series [before run: chamber pumped to 700 Torr, then more HZ flushed in]
9-Mar-88	ser. 1, run 4	none	none	none	SC09MF88.PRN	HZ in 100% DRY HELIUM, 1st series [before run: chamber pumped to 700 Torr, then more HZ flushed in]
21-Mar-88		none	none	none	SC21MR88.PRN	dry desorption run [before run: chamber pumped to 10 microns, then filled with dry helium with CH4]
25-Mar-88		none	none	none	SC25MF88.PRN	wet desorption run [before run: chamber pumped to 200 millitorr, then filled with humid helium (7.5 ml water vaporized and flushed in) to 760 Torr]
20-Apr-88	ser. 2, run 1	none	none	none	SC20AP88.PRN	HZ in 100% DRY HELIUM, 2nd series [before run: chamber pumped to 7E-6 Torr and held for 10 days. The temp. of the chamber was raised to 45 deg C for two days. Then HZ was flushed in with dry He to 760 Torr]
26-Apr-88	ser. 2, run 2	none	none	none	SC26AP88.PRN	HZ in 100% DRY HELIUM, 2nd series [before run: chamber pumped to 700 Torr, then more HZ flushed in]
4-May-88	ser. 2, run 3	none	none	none	SC04MY88.PRN	HZ in 100% DRY HELIUM, 2nd series [before run: chamber pumped to 700 Torr, then more HZ flushed in]
18-May-88	ser. 3, run 1	none	none	none	SC18MY88.PRN	HZ in 100% DRY HELIUM, 3rd series [before run: chamber pumped to 5E-5 Torr with LN2 trap and turbo pump, heated to 45 deg C, cooled to 19 deg C and filled with dry helium with 50 ppm HZ]
20-Jun-88		none	none	none	SC20JN88.PRN	wet desorption run [before run: chamber pumped to 10 microns with mechanical pump, then 7.8 ml of water were vaporized into the chamber with helium to 760 Torr]
23-Aug-88	ser. 1, run 1	none	none	20%	SC23AG88.PRN	HZ+20% O2 in dry helium [before run: chamber pumped to 100 microns with mechanical pump then HZ was flushed in with helium to 610 Torr, finally oxygen was added to 760 Torr]
24-Aug-88	ser. 1, run 2	none	none	20%	SC24AG88.PRN	HZ+20% O2 in dry helium [before run: chamber pumped to 100 microns with mechanical pump then HZ was flushed in with helium to 610 Torr, finally oxygen was added to 760 Torr]
25-Aug-88	ser. 1, run 3	none	none	20%	SC25AG88.PRN	HZ+20% O2 in dry helium [before run: chamber pumped to 100 microns with mechanical pump then HZ was flushed in with helium to 610 Torr, finally oxygen was added to 760 Torr]
26-Aug-88	ser. 1, run 4	none	none	20%	SC26AG88.PRN	HZ+20% O2 in dry helium [before run: chamber pumped to 700 Torr, then more HZ and more O2 added]
27-Aug-88	ser. 1, run 5	none	none	20%	SC27AG88.PRN	HZ+20% O2 in dry helium [before run: chamber pumped to 700 Torr, then more HZ and more O2 added]

Date	Sequential Run No.	Conditions			File Name	Comments
		Plates	water	O2		
29-Aug-88	ser. 1, run 6	none	none	20%	SC29AG88.PRN	HZ+20% O2 in dry helium [before run: chamber pumped to 700 Torr, then more HZ and more O2 added]
30-Aug-88	ser. 1, run 7	none	none	20%	SC30AG88.PRN	HZ+20% O2 in dry helium [before run: chamber pumped to 700 Torr, then more HZ and more O2 added]
25-Nov-88		none	none	none	SC25NV88.PRN	HZ+dry helium, rapid data collect (60 scns) [before run: the chamber sat for about 3 months filled with dry helium, then it was pumped to 1E-5 Torr and HZ was flushed in with dry helium to 760 Torr]
28-Nov-88		none	none	none	SC28NV88.PRN	(continuation of 25 Nov 88 run)
6-Dec-88		none	none	none	SC06DC88.PRN	(continuation of 25 Nov 88 run)
6-Jan-89		none	none	none	SC06JA89.PRN	HZ+dry helium, rapid data collect (256 scns) [before run: chamber evacuated to 10 microns, then HZ was flushed in with dry helium to 760 Torr]
9-Jan-89		none	none	none	SC09JA89.PRN	(continuation of 6 Jan 89 run)
19-Jan-89		none	none	20%	SC19JA89.PRN	HZ+pure air (Aedco unit) [before run: chamber pumped to 10 microns, then filled to 750 Torr with pure air then HZ was flushed in with pure air to 760 Torr]
23-Jan-89	ser. 1, run 1	none	none	20%	SC23JA89.PRN	HZ+pure air after wax coating mirrors [before run: chamber opened and mirrors, etc. coated with paraffin wax, chamber walls wiped down with acetone/methanol mix, chamber closed up and pumped to 10 microns with mechanical pump, then filled to 745 Torr with pure air, finally HZ flushed in with pure air to 760 Torr]
24-Jan-89	ser. 1, run 2	none	none	20%	SC24JA89.PRN	HZ+pure air after wax coating mirrors [before run: chamber pumped to 745 Torr and more HZ added with pure air to 760 Torr]
25-Jan-89	ser. 1, run 3	none	none	20%	SC25JA89.PRN	HZ+pure air after wax coating mirrors [before run: chamber pumped to 745 Torr and more HZ added with pure air to 760 Torr]
30-Jan-89		none	none	20%	SC30JA89.PRN	HZ+pure air after all surfaces wax coated [before run: chamber opened and view ports coated with paraffin wax, chamber closed up, pumped to 10 microns, filled to 745 Torr with pure air then HZ flushed in with pure air to 760 Torr]
31-Jan-89		none	none	none	SC31JA89.PRN	1000 ppm HZ conditioning run [before run: chamber pumped to 100 microns, then 700 microliters HZ flushed in with dry helium]
1-Feb-89		none	none	20%	SC01FB89.PRN	HZ+pure air after conditioning run [before run: 1000 ppm HZ from above run sat in chamber for 22 hrs, then chamber was pumped to 50 microns, then filled to 745 Torr with pure air, then HZ was flushed in to 760 Torr with pure air]
20-Apr-89		none	none	none	SC20AP89.PRN	HZ+dry helium, rapid data collect (60 scns) [before run: chamber rough pumped for 60 days]
21-Apr-89		none	none	none	SC21AP89.PRN	(continuation of 20 Apr 89 run)
24-Apr-89		none	none	none	SC24AP89.PRN	(continuation of 20 Apr 89 run)
1-May-89		none	none	none	SC01MY89.PRN	(continuation of 20 Apr 89 run)
5-May-89		none	none	none	SC05MY89.PRN	(continuation of 20 Apr 89 run)
9-May-89		Teflon-coated Al	none	none	SC09MY89.PRN	HZ in pure, dry helium [before run: chamber pumped to 10 microns with mechanical pump]
18-May-89		Teflon-coated Al	none	20%	SC18MY89.PRN	HZ+20% O2 in dry helium [before run: chamber pumped to 10 microns with mechanical pump]
1-Jun-89	run 1	Teflon-coated Al	none	20%	SC01JN89.PRN	HZ+20% O2 in dry helium [before run: chamber pumped to 10 microns with mechanical pump]
2-Jun-89	run 2	Teflon-coated Al	none	20%	SC02JN89.PRN	HZ+20% O2 in dry helium [before run: chamber pumped to 745 Torr, then additional HZ was flushed in with dry helium to 760 Torr]

Date	Sequential Run No.	Conditions			File Name	Comments
		Plates	water	O2		

7-Jul-89 Teflon-coated Al 56% 20% SC07JN89.PRN well desorption run with room air [before run: chamber pumped to 100 microns, then opened to room air -56% R.H. to 760 Torr]

19-Jul-89 Chrom-Plated-steel none none SC19JL89.PRN (only this run was made) HZ + pure, dry helium [before run: chamber pumped to 3E-5 Torr]

27-Jul-89 none none SC27JL89.PRN water calibration runs - vapor samples
 28-Jul-89 none none SC28JL89.PRN water calibration runs - vapor samples
 31-Jul-89 none none SC31JL89.PRN water calibration runs - liquid samples
 1-Aug-89 none none SC01AG89.PRN water calibration runs - liquid samples
 2-Aug-89 none none SC02AG89.PRN water calibration runs - liquid samples
 4-Aug-89 none none SC04AG89.PRN water calibration runs - liquid samples
 7-Aug-89 none none SC07AG89.PRN water calibration runs - liquid samples
 8-Aug-89 none none SC08AG89.PRN water calibration runs - liquid samples
 11-Aug-89 none none SC11AG89.PRN water calibration runs - liquid samples
 16-Aug-89 none none SC16AG89.PRN water calibration runs - liquid samples
 17-Aug-89 none none SC17AG89.PRN water calibration runs - liquid samples
 19-Aug-89 none none SC19AG89.PRN water calibration runs - liquid samples
 22-Aug-89 none none SC22AG89.PRN water calibration runs - liquid samples
 24-Aug-89 none none SC24AG89.PRN water calibration runs - liquid samples
 29-Aug-89 none none SC29AG89.PRN water calibration runs - liquid samples
 31-Aug-89 none none SC31AG89.PRN water calibration runs - liquid samples

12-Dec-89 none none SC12DC89.PRN HZ+dry helium [before run: chamber pumped for 7 weeks with mechanical pump]
 19-Dec-89 none none SC19DC89.PRN HZ+dry helium [before run: chamber pumped overnight @ 30 deg C]

4-Jan-80 run 1 black iron (19) none none SC04JA80.PRN HZ+dry helium+ 19 black iron plates [before run: chamber pumped overnight to 3E-5 Torr]
 5-Jan-80 run 2 black iron (19) none none SC05JA80.PRN HZ+dry helium+ 19 black iron plates [before run: chamber pumped overnight to 3E-5 Torr]
 8-Jan-80 black iron (19) none 20% SC08JA80.PRN HZ+dry helium+ 19 black iron plates [before run: chamber pumped to 3E-5 Torr for 3 days, heated to 30 deg C, then cooled to 20 deg C for this run]
 9-Jan-80 run 1 black iron (19) none 20% CA09JA80.PRN HZ+dry helium+ 19 black iron plates [before run: chamber heated to 30 deg C, and pumped overnight to 3E-5 Torr, then cooled to 20 deg C for this run]
 9-Jan-80 run 2 black iron (19) none 20% CB09JA80.PRN HZ+dry helium+ 19 black iron plates [before run: chamber pumped to 740 Torr, then additional HZ was added with 80% helium and 20% oxygen to 760 Torr]
 10-Jan-80 black iron (19) none 20% SC10JA80.PRN HZ+dry helium+ 19 black iron plates [before run: chamber heated to 35 deg C, and pumped to 10 microns, then returned to 20 deg C for this run]
 11-Jan-80 run 1 black iron (19) none 20% CA11JA80.PRN HZ+dry helium+ 19 black iron plates [before run: chamber pumped overnight to 10 microns]
 11-Jan-80 run 2 black iron (19) none 20% CB11JA80.PRN HZ+dry helium+ 19 black iron plates [before run: chamber pumped to 730 Torr, then additional HZ was flushed in with 80% helium and 20% oxygen]
 12-Jan-80 run 1 black iron (19) 6 ml 20% CA12JA80.PRN HZ+humid helium+20% O2+black iron plates [before run: chamber heated to 35 deg C and pumped to 3E-5 Torr overnight, then returned to 20 deg C for this run]
 12-Jan-80 run 2 black iron (19) 6 ml 20% CB12JA80.PRN HZ+humid helium+20% O2+black iron plates [before run: chamber pumped to 735 Torr, then additional HZ was flushed in with 80% helium and 20% oxygen]

Date	Sequential		Conditions			File Name	Comments
	Run No.	Plates	water	O2			
16-Jan-90	run 1	black iron (19)	6 ml	20%		CA16JA90.PRN	HZ-humid helium+20% O2+black iron plates [before run: chamber heated to 35 deg C and pumped to 3E-5 Torr for 3 days, then cooled to 20 deg C for this run]
16-Jan-90	run 2	black iron (19)	6 ml	20%		CB16JA90.PRN	HZ-humid helium+20% O2+black iron plates [before run: chamber pumped to 730 Torr, then additional HZ flushed in with 80% helium and 20% oxygen]
6-Mar-90	run 1	corroded Al (20)	none	none		SC06MR90.PRN	HZ-dry helium+20 corroded aluminum plates [before run: chamber sat for 10 weeks filled with pure air, then it was closed up, pumped to 10 microns for 3 days, then heated to 35 deg C and pumped to 3E-5 Torr, then returned to 20 deg C for this run]
7-Mar-90	run 2	corroded Al (20)	none	none		SC07MR90.PRN	HZ-dry helium+20 corroded aluminum plates [before run: chamber pumped to 100 microns]
14-Mar-90	run 3	corroded Al (20)	none	none		SC14MR90.PRN	HZ-dry helium+20 corroded aluminum plates [before run: chamber heated to 35 deg C and pumped to 10 microns for 3 days, then returned to 20 deg C for this run]
15-Mar-90		corroded Al (4)	none	none		CA15MR90.PRN	HZ-dry helium+4 corroded aluminum plates [before run: 16 of the plates were removed, chamber pumped to 5E-4 Torr]
15-Mar-90	run 1	corroded AL (1)	none	none		CB15MR90.PRN	HZ-dry helium+1 corroded aluminum plate [before run: 3 more plates removed, chamber pumped to 100 microns]
16-Mar-90	run 2	corroded AL (1)	none	none		SC16MR90.PRN	HZ-dry helium+1 corroded aluminum plate [before run: chamber pumped to 5E-4 Torr]
23-Mar-90	run 1	corroded AL (1)	none	20%		SC23MR90.PRN	HZ-dry helium+1 corroded aluminum plate [before run: chamber pumped to 5E-4 Torr]
26-Mar-90	run 1	corroded AL (1)	none	20%		CA26MR90.PRN	HZ-dry helium+1 corroded aluminum plate [before run: chamber pumped to 10 microns for 2 days, then to 5E-4 Torr for 2 hours, then O2 was added to 150 Torr, then helium to 725 Torr, then HZ was flushed in with helium to 760 Torr]
26-Mar-90	run 2	corroded AL (1)	none	20%		CB26MR90.PRN	HZ-dry helium+1 corroded aluminum plate [before run: chamber pumped to 730 Torr, then additional HZ was flushed in with 80% helium and 20% oxygen]
27-Mar-90	run 3	corroded AL (1)	none	20%		CA27MR90.PRN	HZ-dry helium+1 corroded aluminum plate [before run: chamber pumped to 730 Torr, then additional HZ was flushed in with 80% helium and 20% oxygen]
27-Mar-90	run 4	corroded AL (1)	none	20%		CB27MR90.PRN	HZ-dry helium+1 corroded aluminum plate [before run: chamber pumped to 730 Torr, then additional HZ was flushed in with 80% helium and 20% oxygen]
27-Mar-90	run 5	corroded AL (1)	none	20%		CC27MR90.PRN	HZ-dry helium+1 corroded aluminum plate [before run: chamber pumped to 730 Torr, then additional HZ was flushed in with 80% helium and 20% oxygen]
28-Mar-90	run 1	corroded AL (1)	6 ml H2O	20%		CB28MR90.PRN	HZ-dry helium+1 corroded aluminum plate [before run: chamber pumped to 5E-4 overnight]
29-Mar-90	run 2	corroded AL (1)	6 ml H2O	20%		CB29MR90.PRN	HZ-dry helium+1 corroded aluminum plate [before run: chamber pumped to 730 Torr, then additional HZ was flushed in with 80% helium and 20% oxygen]
29-Mar-90	run 3	corroded AL (1)	6 ml H2O	20%		CC29MR90.PRN	HZ-dry helium+1 corroded aluminum plate [before run: chamber pumped to 730 Torr, then additional HZ was flushed in with 80% helium and 20% oxygen]
9-Apr-90		corroded AL (10)	none	20%		SC09AP90.PRN	HZ-dry helium+10 corroded aluminum plates [before run: sample port cover removed and 9 plates added for attempted dimide production]
10-Apr-90		corroded AL (10)	none	20%		SC10AP90.PRN	HZ-dry helium+20 corroded aluminum plates [continued attempts at dimide spectra]
18-Apr-90		none	none	none		SC18AP90.PRN	HZ-dry helium (cal spectra) [before run: chamber pumped to 1 micron with mechanical pump]
4-May-90		none	6 ml H2O	none		SC04MY90.PRN	HZ-humid helium (cal spectra) [before run: chamber pumped to 9E-5 Torr]

Date	Sequential Run No.	Conditions			File Name	Comments
		Plates	water	O2		
22-May-90	run 1	none	none	20%	SC22MY90.PRN	HZ+dry helium +20% oxygen [before run: chamber heated to 35 deg C and pumped for 20 hrs at 1E-4 Torr, then returned to 20 deg C for this run]
23-May-90	run 2	none	none	20%	SC23MY90.PRN	HZ+dry helium +20% oxygen [before run: chamber pumped to 745 Torr, then additional HZ was flushed in with 80% helium and 20% oxygen]
24-May-90	run 3	none	none	20%	SC24MY90.PRN	HZ+dry helium +20% oxygen [before run: chamber pumped to 740 Torr, then additional HZ was flushed in with 80% helium and 20% oxygen]
25-May-90	run 4	none	none	20%	SC25MY90.PRN	HZ+dry helium +20% oxygen [before run: chamber pumped to 740 Torr, then additional HZ was flushed in with 80% helium and 20% oxygen]
31-May-90	run 1	none	6 ml H2O	20%	SC31MY90.PRN	HZ+humid helium+20%oxygen [before run: chamber pumped to 5E-5 Torr for 2 days]
1-Jun-90	run 2	none	6 ml H2O	20%	SC01JN90.PRN	HZ+humid helium+20%oxygen [before run: chamber pumped to 745 Torr then sat overnight, then additional HZ was flushed in with 80% helium and 20% oxygen]
4-Jun-90	run 3	none	6 ml H2O	20%	SC04JN90.PRN	HZ+humid helium+20%oxygen [before run: chamber pumped to 745 Torr then sat for 2 days, then additional HZ was flushed in with 80% helium and 20% oxygen]
19-Jul-90	run 1	painted alum. (20)	none	none	SC19JL90.PRN	HZ + dry helium [before run: chamber sat for 6 weeks filled with dry air, then 20 painted aluminum plates were placed inside and the chamber was pumped to 6E-5 Torr for 60 hours]
20-Jul-90	run 2	painted alum. (20)	none	none	SC20JL90.PRN	HZ + dry helium [before run: chamber pumped to 745 Torr then additional HZ was flushed in with helium]
23-Jul-90	run 3	painted alum. (20)	none	none	SC23JL90.PRN	HZ + dry helium [before run: chamber contents from previous run sat over the weekend, then the chamber was pumped to 745 Torr and additional HZ was flushed in with helium]
25-Jul-90	run 1	painted alum. (20)	none	20%	SC25JL90.PRN	HZ + dry helium + 20% oxygen [before run: chamber heated to 35 deg C and pumped to 6E-5 Torr for 2 hrs, then returned to 20 deg C for this run]
26-Jul-90	run 2	painted alum. (20)	none	20%	SC26JL90.PRN	HZ + dry helium + 20% oxygen [before run: chamber pumped to 745 Torr, then additional HZ was flushed in with 80% helium and 20% oxygen]
27-Jul-90	run 3	painted alum. (20)	none	20%	SC27JL90.PRN	HZ + dry helium + 20% oxygen [before run: chamber pumped to 745 Torr, then additional HZ was flushed in with 80% helium and 20% oxygen]
30-Jul-90	run 1	painted alum. (20)	none	none	SC30JL90.PRN	HZ + humid helium [chamber pumped to 10 microns for 2 days]
31-Jul-90	run 2	painted alum. (20)	none	none	SC31JL90.PRN	HZ + humid helium [before run: chamber pumped to 745 Torr, then additional HZ flushed in with helium]
1-Aug-90	run 3	painted alum. (20)	none	none	SC01AG90.PRN	HZ + humid helium [before run: chamber pumped to 745 Torr, then additional HZ flushed in with helium]
3-Aug-90	run 1	painted alum. (20)	none	20%	SC03AG90.PRN	HZ + humid helium+ 20% oxygen [before run: chamber heated to 35 deg C and pumped to 5E-5 Torr for 24 hrs, then returned to 20 deg C for this run]
6-Aug-90	run 2	painted alum. (20)	none	20%	SC06AG90.PRN	HZ + humid helium+ 20% oxygen [before run: mixture from previous run sat in the chamber for 3 days, then the chamber was pumped to 745 Torr and additional HZ was flushed in with 80% helium and 20% oxygen]
7-Aug-90	run 3	painted alum. (20)	none	20%	SC07AG90.PRN	HZ + humid helium+ 20% oxygen [before run: chamber pumped to 745 Torr, then additional HZ flushed in with 80% helium and 20% oxygen]

APPENDIX N
SUMMARY 1
 RESULTS FOR NO PLATES
 DATA FILES USING MOD310

DATA FILE	SOS	RMS	S1°	S2°	HZ:S1	HZ:S2	NH3	Prod	G	S1	S2	KS1
SC04MY88.DAT	1.1350	0.1076	0.0265	0.0079	0.0422	0.0000	0.0296	0.0000	1.2103	0.4745	0.9931	0.0744
SC18MY88.DAT	0.0526	0.0193	0.0026	0.0100	0.1386	0.0000	0.0000	0.0807	1.1900	0.5733	0.9910	0.0800
SC20AP88.DAT	17.0000	0.3460	0.1673	0.2425	0.0010	0.0000	0.0011	0.0010	4.0330	0.3337	1.5691	0.0104
SC26AP88.DAT	0.0409	0.0175	0.0177	0.0070	0.0176	0.0907	0.0001	0.0283	1.1696	0.4833	0.9940	0.0085
SC23AG88.DAT	0.0348	0.0241	0.0429	0.0023	0.0383	0.0964	0.0002	0.0000	1.1852	0.4990	1.0048	0.1452
SC24AG88.DAT	0.0574	0.0261	0.0508	0.0035	0.0334	0.0812	0.0003	0.0004	1.2042	0.4932	0.9975	0.1267
SC25AG88.DAT	0.0189	0.0195	0.0001	0.0049	0.0006	0.0753	0.0001	0.0000	1.1852	0.5303	0.9961	0.0004
SC26AG88.DAT	0.0121	0.0156	0.0001	0.0027	0.0001	0.1232	0.0002	0.0001	1.1590	0.5286	1.0021	0.0048
SC27AG88.DAT	0.0369	0.0248	0.0124	0.0008	0.0000	0.0841	0.0001	0.0002	1.2566	0.5253	1.0086	0.0002
SC29AG88.DAT	0.0262	0.0229	0.0000	0.0058	0.0000	0.0535	0.0002	0.0029	1.1751	0.5294	0.9952	0.0000
SC30AG88.DAT	0.0764	0.0391	0.0000	0.0092	0.0002	0.0312	0.0000	0.0003	1.1881	0.5469	0.9918	0.0000

DATA FILE	KS2	k1	k2	k3	k4
SC04MY88.DAT	0.5284	0.0910	0.0003	0.0132	0.0031
SC18MY88.DAT	0.5557	0.0416	0.0374	0.0080	0.0805
SC20AP88.DAT	1.8724	0.1054	0.8503	0.0301	0.0376
SC26AP88.DAT	0.5324	0.0133	0.0340	0.0120	0.0000
SC23AG88.DAT	0.3833	0.2148	0.1318	0.0677	0.1462
SC24AG88.DAT	0.3825	0.2289	0.1113	0.0623	0.1364
SC25AG88.DAT	0.4818	0.1121	0.0470	0.0515	0.1646
SC26AG88.DAT	0.4674	0.0924	0.0845	0.0341	0.1076
SC27AG88.DAT	0.3348	0.0830	0.1129	0.0310	0.1249
SC29AG88.DAT	0.4682	0.1417	0.0795	0.0196	0.1494
SC30AG88.DAT	0.4478	0.1640	0.0831	0.0198	0.1748

APPENDIX N
SUMMARY 2
RESULTS FOR NO PLATES
DATA FILES USING MOD315

DATA FILE	SOS	RMS	S1*	S2*	Hz:S1	Hz:S2	Prod	NH3	G	S1	S2	KS1
SC04MY88.DAT	1.1430	0.1080	0.0176	0.0000	0.0264	0.0181	0.0587	0.0259	1.1638	0.4834	1.1379	0.0007
SC18MY88.DAT	0.4926	0.0589	0.0055	0.0089	0.0770	0.0000	0.0484	0.0507	1.1278	0.4955	1.0983	0.0283
SC20AP88.DAT	41.21	0.5387	0.0043	0.1071	0.0010	0.0010	0.0063	0.0010	3.0133	1.0635	0.9939	1.0284
SC26AP88.DAT	0.5718	0.0653	0.0530	0.0035	0.0812	0.0003	0.0013	0.0004	1.1423	0.4480	1.1078	0.0057
SC23AG88.DAT	0.1159	0.0440	0.0000	0.0000	0.0312	0.0000	0.0936	0.0001	1.1292	0.5547	1.1293	0.0021
SC24AG88.DAT	0.1512	0.0424	0.0000	0.0002	0.0302	0.0003	0.0890	0.0016	1.1525	0.5317	1.1295	0.0026
SC25AG88.DAT	0.0779	0.0274	0.0000	0.0002	0.0001	0.0001	0.1139	0.0001	1.1731	0.5593	1.1633	0.0001
SC28AG88.DAT	0.0612	0.0350	0.0000	0.0038	0.0407	0.0001	0.0633	0.0157	1.1358	0.5354	1.1091	0.0041
SC27AG88.DAT	0.0872	0.0381	0.0000	0.0023	0.0000	0.0001	0.0439	0.0001	1.1782	0.5518	1.1131	0.0090
SC29AG88.DAT	0.0520	0.0322	0.0002	0.0448	0.0323	0.0001	0.0001	0.0000	1.0861	0.5962	1.0562	0.0064
SC30AG88.DAT	0.0952	0.0436	0.0000	0.0601	0.0000	0.0001	0.0000	0.0001	1.1065	0.6142	1.0409	0.0007

DATA FILE	KS2	k1	k2	k3	k4
SC04MY88.DAT	0.0075	0.0034	0.0043	0.0384	0.0007
SC18MY88.DAT	0.2005	0.0128	0.0189	0.0131	0.0067
SC20AP88.DAT	1.4114	0.1084	0.0828	0.6980	0.0336
SC26AP88.DAT	0.3497	0.0077	0.0365	0.0206	0.0080
SC23AG88.DAT	0.3094	0.1783	0.0473	0.0236	0.1663
SC24AG88.DAT	0.2526	0.1349	0.0429	0.0276	0.2044
SC25AG88.DAT	0.0371	0.1202	0.0181	0.0043	0.1896
SC26AG88.DAT	0.3647	0.1343	0.0348	0.0379	0.0848
SC27AG88.DAT	0.3400	0.1457	0.0352	0.0408	0.1729
SC29AG88.DAT	0.3714	0.1406	0.0286	0.0341	0.2300
SC30AG88.DAT	0.3697	0.1654	0.0296	0.0303	0.1692

APPENDIX N
SUMMARY 3
RESULTS FOR NO PLATES
DATA FILES USING MOD350

DATA FILE	SOS	RMS	S1*	HZ:S	NH3	PROD	G	S	KS	K1	K2	K3
SC04MY88.DAT	3.6534	0.1931	0.2014	0.0010	0.0001	0.0002	1.1776	0.7996	1.5540	1.0647	0.7308	0.1162
SC18MY88.DAT	0.1436	0.0318	0.1515	0.0182	0.0017	0.1142	1.1273	0.6495	0.0340	0.0544	0.0153	0.0003
SC20AP88.DAT	8.6840	0.2473	0.0037	0.0172	0.0019	0.0008	5.5649	3.1044	0.9103	0.4309	0.0019	0.0262
SC26AP88.DAT	0.6967	0.0721	0.0075	0.0491	0.0001	0.0001	1.1726	0.6025	0.2637	0.3275	0.0078	0.0035
SC23AG88.DAT	0.0064	0.0104	0.0055	0.0176	0.0000	0.0282	1.0239	0.6815	0.0337	0.1833	0.0806	0.1074
SC24AG88.DAT	0.0111	0.0115	0.0213	0.0000	0.0001	0.0011	1.0133	0.6199	0.0172	0.1811	0.0733	0.0851
SC25AG88.DAT	0.0128	0.0111	0.0322	0.0005	0.0000	0.0070	1.0757	0.6260	0.0087	0.1744	0.0630	0.0722
SC26AG88.DAT	0.0065	0.0114	0.0228	0.0011	0.0002	0.0638	1.0611	0.6716	0.0087	0.1356	0.0412	0.0585
SC27AG88.DAT	0.0060	0.0100	0.0453	0.0023	0.0003	0.0039	1.1272	0.6731	0.0000	0.1474	0.0372	0.0933
SC29AG88.DAT	0.0092	0.0136	0.0471	0.0000	0.0000	0.0121	1.0700	0.5952	0.0001	0.1708	0.0286	0.0826
SC30AG88.DAT	0.0243	0.0220	0.0369	0.0003	0.0008	0.0067	1.0909	0.6182	0.0000	0.1457	0.0369	0.1263

APPENDIX N
SUMMARY 4
RESULTS FOR NO PLATES
DATA FILES USING MOD360

DATA FILE	SOS	RMS	S1*	Hz:S1	Hz:S2	NH3	Prod	G	S1	S2	KS1	K1
SC04MY88.DAT	1.1190	0.1069	0.0013	0.2187	0.0027	0.0096	0.0139	1.4634	0.8002	0.1421	0.6725	0.5128
SC18MY88.DAT	0.1200	0.0291	0.0919	0.0803	0.0356	0.0002	0.0420	1.2352	0.6591	0.1146	0.7761	0.4254
SC20AP88.DAT	12.510	0.2968	0.0016	0.0004	0.0003	0.0005	0.0005	3.7178	1.3018	0.3201	0.0000	0.0195
SC26AP88.DAT	0.1804	0.0367	0.0386	0.1075	0.0004	0.0007	0.0014	1.2116	0.5624	0.1829	0.7143	0.4655
SC23AG88.DAT	0.0240	0.0200	0.0691	0.0806	0.0001	0.0002	0.0007	1.1014	0.5319	0.3784	0.7189	0.4312
SC24AG88.DAT	0.0794	0.0307	0.1507	0.1571	0.0002	0.0010	0.0010	1.1187	0.4503	0.3757	0.6492	0.3063
SC25AG88.DAT	0.0494	0.0218	0.0998	0.1840	0.0020	0.0000	0.0006	1.2418	0.5012	0.3893	0.7336	0.3954
SC26AG88.DAT	0.0211	0.0206	0.0598	0.0256	0.0004	0.0000	0.0006	1.0870	0.5412	0.4009	0.7208	0.4518
SC27AG88.DAT	0.0201	0.0183	0.1045	0.0277	0.0010	0.0010	0.0010	1.1912	0.4965	0.5165	0.7361	0.4120
SC29AG88.DAT	0.0195	0.0197	0.1104	0.0296	0.0010	0.0010	0.0000	1.1287	0.4906	0.4217	0.7367	0.4110
SC30AG88.DAT	0.0356	0.0267	0.1378	0.0603	0.0010	0.0010	0.0000	1.1792	0.4632	0.4818	0.7620	0.4057

DATA FILE	k2	k3	k4
SC04MY88.DAT	0.0083	0.0082	0.3695
SC18MY88.DAT	0.1157	0.0096	0.2103
SC20AP88.DAT	0.0110	0.0030	0.6176
SC26AP88.DAT	0.0109	0.0081	0.3673
SC23AG88.DAT	0.2000	0.0883	0.2298
SC24AG88.DAT	0.1382	0.0987	0.5918
SC25AG88.DAT	0.1374	0.0646	0.3086
SC26AG88.DAT	0.1193	0.0528	0.1904
SC27AG88.DAT	0.1099	0.0687	0.1978
SC29AG88.DAT	0.1330	0.0469	0.2209
SC30AG88.DAT	0.1300	0.0483	0.2274

APPENDIX N
SUMMARY 5
RESULTS FOR NO PLATES
DATA FILES USING MOD361

DATA FILE	SOS	RMS	S1*	HZ:S1	HZ:S2	Prod	NH3	G	S1	S2	KS1	k1
SC04MY88.DAT	1.1180	0.1068	0.0523	0.0001	0.0512	0.0003	0.0428	1.1085	0.4598	0.4465	0.3721	0.0001
SC18MY88.DAT	0.0694	0.0221	0.0243	0.0001	0.0408	0.0001	0.0003	0.9607	0.4767	0.2406	0.3728	0.0011
SC20AP88.DAT	6.7830	0.2186	0.0001	0.0000	0.0216	0.0014	0.0047	5.1513	1.7594	0.2422	0.0019	0.2257
SC26AP88.DAT	0.0538	0.0200	0.0187	0.0000	0.0004	0.0001	0.0002	0.9650	0.4823	0.3726	0.3354	0.0025
SC23AG88.DAT	0.0098	0.0128	0.0001	0.0001	0.0001	0.0000	0.0006	0.9650	0.6182	0.4172	0.1261	0.1273
SC24AG88.DAT	0.0121	0.0120	0.0013	0.0002	0.0000	0.0010	0.0001	0.9955	0.5813	0.4415	0.1225	0.1146
SC25AG88.DAT	0.0166	0.0126	0.0001	0.0002	0.0006	0.0010	0.0001	1.0510	0.5817	0.4226	0.1193	0.1139
SC26AG88.DAT	0.0117	0.0153	0.0009	0.0010	0.0002	0.0010	0.0000	0.9638	0.5226	0.3136	0.0541	0.1079
SC27AG88.DAT	0.0046	0.0087	0.0008	0.0002	0.0002	0.0001	0.0000	1.0972	0.5269	0.2110	0.0160	0.0960
SC29AG88.DAT	0.0106	0.0145	0.0021	0.0010	0.0006	0.0000	0.0010	1.0137	0.5157	0.2736	0.0318	0.0779
SC30AG88.DAT	0.0413	0.0287	0.0019	0.0010	0.0010	0.0010	0.0022	1.0131	0.5212	0.2774	0.0191	0.0799

DATA FILE	k2	k3	k4
SC04MY88.DAT	0.0114	0.1196	0.0436
SC18MY88.DAT	0.0518	0.2598	0.0137
SC20AP88.DAT	0.0030	0.0279	1.4192
SC26AP88.DAT	0.0134	0.0591	0.0174
SC23AG88.DAT	0.0574	0.3315	0.3864
SC24AG88.DAT	0.0536	0.2869	0.3228
SC25AG88.DAT	0.0523	0.2439	0.2621
SC26AG88.DAT	0.0662	0.1012	0.1350
SC27AG88.DAT	0.0966	0.2516	0.1353
SC29AG88.DAT	0.0859	0.3611	0.0614
SC30AG88.DAT	0.0779	0.3122	0.0728

APPENDIX N
SUMMARY 6
RESULTS FOR NO PLATES
DATA FILES USING MOD370

DATA FILE	SOS	RMS	S1*	Hz:S1	Hz:S2	Prod	NH3	G	S1	S2	KS1	K1
SC04MY88.DAT	1.1090	0.1064	0.8840	0.0196	0.0896	0.0006	0.0142	1.1456	0.1160	0.0983	1.1711	0.0001
SC18MY88.DAT	0.1288	0.0301	0.5504	0.0283	0.0469	0.0001	0.0156	1.0761	0.4496	0.1979	1.0181	0.0671
SC20AP88.DAT	44.370	0.5590	1.1207	0.0010	0.0010	0.0010	0.0180	1.8622	0.2906	0.0078	1.1452	0.6713
SC26AP88.DAT	0.1071	0.0283	0.0432	0.0000	0.0009	0.0000	0.0001	0.9600	0.5578	0.0153	0.4262	0.0250
SC23AG88.DAT	0.0254	0.0206	0.0001	0.0068	0.0665	0.0002	0.0010	1.0766	0.6551	0.1054	0.1904	0.1947
SC24AG88.DAT	0.0260	0.0176	0.0000	0.0043	0.0574	0.0000	0.0003	1.0853	0.6451	0.1071	0.1558	0.1408
SC25AG88.DAT	0.0368	0.0188	0.0001	0.0006	0.0303	0.0000	0.0000	1.1058	0.6392	0.1232	0.1471	0.1387
SC26AG88.DAT	0.0455	0.0302	0.0001	0.0670	0.0005	0.0005	0.0002	1.0458	0.6277	0.1539	0.2837	0.1515
SC27AG88.DAT	0.0076	0.0112	0.0001	0.0256	0.0148	0.0000	0.0001	1.1610	0.6591	0.0848	0.0530	0.1099
SC29AG88.DAT	0.0528	0.0325	0.0005	0.0573	0.0004	0.0005	0.0001	1.0928	0.6414	0.1340	0.2094	0.1565
SC30AG88.DAT	0.0214	0.0207	0.0042	0.0240	0.0002	0.0000	0.0000	1.1188	0.6555	0.0975	0.0554	0.1123

DATA FILE	k2	k3	k4
SC04MY88.DAT	0.0257	0.8040	0.1078
SC18MY88.DAT	0.3139	0.1213	0.0063
SC20AP88.DAT	0.8971	0.3281	1.5391
SC26AP88.DAT	0.1762	0.2141	0.3338
SC23AG88.DAT	0.3048	0.2448	0.1677
SC24AG88.DAT	0.2626	0.2441	0.1839
SC25AG88.DAT	0.1510	0.2083	0.2334
SC26AG88.DAT	0.2423	0.1212	0.1058
SC27AG88.DAT	0.1583	0.1706	0.2007
SC29AG88.DAT	0.1972	0.1336	0.1081
SC30AG88.DAT	0.1236	0.1880	0.1693

APPENDIX N
SUMMARY 7
RESULTS FOR NO PLATES
DATA FILES USING MOD375

DATA FILE	SOS	RMS	S1*	Hz:S1	Hz:S2	NH3	Prod	G	S1	S2	KS1	K1
SC04MY88.DAT	1.1200	0.1069	0.3332	0.1213	0.0002	0.0241	0.0010	1.3551	0.8668	0.0137	0.2835	0.3605
SC18MY88.DAT	0.1189	0.0289	0.4612	0.0060	0.0000	0.0001	0.0000	1.0171	0.7388	0.0270	0.0983	0.3024
SC20AP88.DAT	66.250	0.6830	0.7142	0.0010	0.0010	0.0010	0.0010	1.8774	0.4858	0.0431	0.6806	0.1988
SC26AP88.DAT	0.2637	0.0444	0.4844	0.0022	0.0010	0.0001	0.0004	1.0674	0.7156	0.0306	0.1360	0.3202
SC23AG88.DAT	0.0469	0.0280	0.4398	0.0005	0.0007	0.0002	0.0378	1.0025	0.7602	0.2430	0.0582	0.2981
SC24AG88.DAT	0.0502	0.0245	0.4530	0.0002	0.0005	0.0001	0.0105	1.0121	0.7470	0.2314	0.0480	0.2831
SC25AG88.DAT	0.0777	0.0273	0.4578	0.0000	0.0004	0.0002	0.0001	1.0374	0.7422	0.2320	0.0312	0.2654
SC26AG88.DAT	0.0172	0.0185	0.4763	0.0001	0.0000	0.0001	0.0025	1.0061	0.7237	0.2184	0.0776	0.2965
SC27AG88.DAT	0.0694	0.0340	0.4862	0.0006	0.0006	0.0004	0.0000	1.0666	0.7138	0.2407	0.0611	0.2731
SC29AG88.DAT	0.0388	0.0279	0.4790	0.0006	0.0006	0.0003	0.0001	1.0334	0.7210	0.2300	0.0680	0.2861
SC30AG88.DAT	0.0888	0.0421	0.4781	0.0004	0.0004	0.0000	0.0000	1.0486	0.7219	0.2400	0.0499	0.2710

DATA FILE	k2	k3	k4
SC04MY88.DAT	0.2280	0.0123	0.0893
SC18MY88.DAT	0.0218	0.0131	0.1876
SC20AP88.DAT	0.0403	0.1036	0.4551
SC26AP88.DAT	0.0519	0.0147	0.1764
SC23AG88.DAT	0.2377	0.1115	0.0570
SC24AG88.DAT	0.2231	0.1229	0.0670
SC25AG88.DAT	0.2177	0.1208	0.0531
SC26AG88.DAT	0.2116	0.0723	0.1004
SC27AG88.DAT	0.2182	0.0857	0.0986
SC29AG88.DAT	0.2179	0.0463	0.0958
SC30AG88.DAT	0.2178	0.0492	0.1006

APPENDIX N
SUMMARY 8
RESULTS FOR NO PLATES
DATA FILES USING MOD380

DATA FILE	SOS	RMS	HZ:S1	I	NH3	G	k1	k2	k3	S1
SC04MY88.DAT	1.1780	0.1096	0.1093	0.0005	0.2336	1.2916	0.0357	1.0487	1.9307	0.0352
SC18MY88.DAT		diverged								
SC20AP88.DAT		diverged								
SC26AP88.DAT	6.3630	0.2179	0.0010	0.2434	0.0001	0.5333	0.0063	2.0670	1.7504	0.1008
SC23AG88.DAT	0.2787	0.0682	0.1157	0.0003	0.0001	0.8972	0.1331	0.3665	0.3061	0.1596
SC24AG88.DAT	0.2852	0.0583	0.2016	0.0003	0.0000	1.0467	0.1721	0.3525	0.1255	0.1175
SC25AG88.DAT	0.4649	0.0669	0.0859	0.0005	0.0000	0.9289	0.1204	0.3923	0.3298	0.1391
SC26AG88.DAT	0.0951	0.0436	0.0797	0.0010	0.0010	0.9527	0.1988	0.3543	0.0525	0.1435
SC27AG88.DAT	0.2125	0.0595	0.1182	0.0010	0.0186	1.0928	0.1228	0.4331	0.0222	0.2130
SC29AG88.DAT	0.1217	0.0494	0.0778	0.0010	0.0093	1.0109	0.1868	0.3851	0.0216	0.1646
SC30AG88.DAT	0.1906	0.0617	0.0797	0.0010	0.0209	1.0484	0.1551	0.4038	0.0134	0.2063

APPENDIX N
SUMMARY 9
RESULTS FOR NO PLATES
DATA FILES USING MOD385

DATA FILE	SOS	RMS	Hz:S	I	NH3	Prod	G	k1	k2	k3	S	k4
SC04MY88.DAT	1.0990	0.1059	0.0006	0.0001	0.1143	0.0039	1.1917	1.0423	0.0154	0.8897	0.2376	0.6639
SC18MY88.DAT	0.1184	0.0289	0.0084	0.0010	0.0000	0.0138	0.9031	0.2753	0.0227	1.0817	0.0842	0.0100
SC20AP88.DAT		diverged										
SC26AP88.DAT	4.1500	0.1760	0.0819	0.0002	0.0010	0.0010	1.3660	0.3605	0.0558	0.0133	0.1048	0.0407
SC23AG88.DAT	0.2591	0.0657	0.0631	0.0437	0.0214	0.0431	1.1570	0.4372	0.0151	0.6702	0.8145	0.0789
SC24AG88.DAT	1.0200	0.1100	0.1330	0.0118	0.0034	0.0015	0.9172	0.4409	0.0187	0.3418	0.5935	0.0633
SC25AG88.DAT	1.2480	0.1096	0.1089	0.0012	0.0038	0.0036	0.9380	0.4691	0.0197	0.3706	0.5820	0.0688
SC26AG88.DAT	0.2030	0.0637	0.0592	0.0000	0.0115	0.0617	1.0200	0.4408	0.0362	0.3291	0.4818	0.0994
SC27AG88.DAT	0.7855	0.1144	0.1143	0.0000	0.0115	0.0156	1.0098	0.4315	0.0220	0.3411	0.5876	0.0968
SC29AG88.DAT	0.6108	0.1105	0.1354	0.0001	0.0142	0.0271	1.0009	0.4427	0.0182	0.3052	0.5772	0.0822
SC30AG88.DAT	0.7990	0.1264	0.1213	0.0003	0.0314	0.0190	0.9815	0.4039	0.0158	0.3635	0.6035	0.0822

APPENDIX N
SUMMARY 10
RESULTS FOR NO PLATES
DATA FILES USING MOD390

DATA FILE	SOS	RMS	Hz:S	I	NH3	Prod	G	k1	k2	k3	S	k4
SC04MY88.DAT	58.000	0.7693	0.2066	0.4817	0.1951	0.8580	0.6250	0.9056	0.0225	1.1983	0.4128	1.0602
SC18MY88.DAT	0.5768	0.0637	0.1180	0.5088	0.0010	0.4951	1.1538	1.9511	0.0006	2.5451	0.9544	2.4130
SC20AP88.DAT	779.30	2.3430	0.4284	0.0010	0.4496	0.9270	0.8937	1.2574	0.4000	1.9656	0.4365	1.2235
SC26AP88.DAT	29.970	0.4729	0.0002	0.7930	0.0996	1.2667	0.0001	1.1830	0.0770	1.8032	0.6009	1.8766
SC23AG88.DAT	1.6340	0.1650	0.0130	0.3436	0.0755	0.5320	0.8513	1.0653	0.0310	1.0620	0.7128	1.0908
SC24AG88.DAT	2.9120	0.1862	0.0611	0.3228	0.0868	0.5432	0.8710	1.0078	0.0266	1.0518	0.6100	0.9961
SC25AG88.DAT	5.1340	0.2222	0.1408	0.1890	0.0583	0.5306	0.8678	0.8259	0.0252	0.9046	0.3520	0.7739
SC26AG88.DAT	1.0670	0.1461	0.0693	0.2478	0.0398	0.5207	0.9140	0.8831	0.0264	0.9253	0.4009	0.8920
SC27AG88.DAT	1.7640	0.1715	0.0907	0.1994	0.0353	0.5307	0.9256	0.7921	0.0291	0.8425	0.3207	0.8686
SC29AG88.DAT	1.2290	0.1568	0.0610	0.2223	0.0419	0.5615	0.9174	0.8629	0.0276	0.8803	0.3881	0.9089
SC30AG88.DAT	1.6710	0.1828	0.0580	0.1524	0.0585	0.5857	0.9005	0.7989	0.0355	0.8235	0.3352	0.8135

APPENDIX N
SUMMARY 11
RESULTS FOR NO PLATES
DATA FILES USING MOD310

DATA FILE	SOS	RMS	S1*	S2*	Hz:S1	Hz:S2	NH3	Prod	G	S1	S2	KS1
MD18AP90.DAT	0.0112	0.0086	0.0596	0.0082	0.0494	0.0428	0.0285	0.0010	1.2706	0.4798	0.9928	0.0537
MD04MY90.DAT	2.9910	0.1422	0.0113	0.0543	0.2479	0.0010	0.0475	0.0367	1.3871	0.8339	0.9467	0.1882
MD22MY90.DAT	0.0027	0.0052	0.0193	0.0036	0.1558	0.1236	0.0151	0.0007	1.1455	0.4921	0.9974	0.1185
MD23MY90.DAT	0.0170	0.0131	0.0006	0.0032	0.0884	0.1444	0.0243	0.0571	1.1037	0.5071	0.9978	0.0000
MD24MY90.DAT	0.0219	0.0141	0.0004	0.0013	0.0896	0.1666	0.0079	0.0461	1.1005	0.5235	0.9997	0.0000
MD25MY90.DAT	0.0236	0.0144	0.0014	0.0025	0.1387	0.1468	0.0304	0.0504	1.1058	0.5113	0.9985	0.0000
MD31MY90.DAT	0.0640	0.0270	0.0171	0.0078	0.4766	0.0007	0.1479	0.0005	1.4219	0.4839	1.0541	0.3106
MD01JN90.DAT	diverged											
MD04JN90.DAT	0.0072	0.0079	0.0460	0.0032	0.2772	0.0094	0.0575	0.0007	1.3039	0.4691	1.1539	0.3982

DATA FILE	KS2	K1	K2	K3	K4
MD18AP90.DAT	0.4981	0.0639	0.0073	0.0098	0.0056
MD04MY90.DAT	0.4779	0.0788	0.0001	0.0164	0.0176
MD22MY90.DAT	0.4747	0.0999	0.0496	0.1117	0.0970
MD23MY90.DAT	0.5100	0.0944	0.0698	0.0775	0.1278
MD24MY90.DAT	0.4912	0.1183	0.0739	0.0358	0.1306
MD25MY90.DAT	0.4946	0.1145	0.0604	0.0311	0.1280
MD31MY90.DAT	0.5846	0.0487	0.5595	0.5481	0.0000
MD01JN90.DAT	diverged				
MD04JN90.DAT	0.2054	0.0006	0.4630	0.5039	0.0126

APPENDIX N
SUMMARY 12
RESULTS FOR NO PLATES
DATA FILES USING MOD315

DATA FILE	SOS	RMS	S1*	S2*	Hz:S1	Hz:S2	Prod	NH3	G	S1	S2	KS1
MD18AP90.DAT	1.2620	0.0911	0.0019	0.0199	0.0350	0.0083	0.0000	0.0001	1.4075	0.5225	1.1196	0.0941
MD04MY90.DAT	4.3660	0.1717	0.1508	0.0070	0.0112	0.0202	0.0010	0.0010	1.4962	0.3502	1.7656	0.1052
MD22MY90.DAT	0.0003	0.0019	0.0008	0.0000	0.1642	0.0000	0.0621	0.0305	1.0912	0.5138	1.0313	0.2153
MD23MY90.DAT	0.0831	0.0283	0.1191	0.0003	0.1048	0.0001	0.1562	0.0448	1.0782	0.3819	1.0927	0.0004
MD24MY90.DAT	0.0087	0.0089	0.0117	0.0001	0.1967	0.0001	0.0945	0.0649	1.0753	0.4893	1.0718	0.0565
MD25MY90.DAT	0.1672	0.0332	0.0175	0.3599	0.0475	0.0010	0.0015	0.0008	1.1820	0.7029	0.6411	0.0551
MD31MY90.DAT	0.0285	0.0180	0.0001	0.0010	0.0001	0.0009	0.2090	0.1366	1.2277	0.5539	1.1130	0.2300
MD01JN90.DAT	diverged											
MD04JN90.DAT	0.0083	0.0085	0.0006	0.0336	0.0000	0.0268	0.1111	0.0967	1.1793	1.5466	1.4052	0.1445

DATA FILE	KS2	K1	K2	K3	K4
MD18AP90.DAT	0.3823	0.0642	0.0893	0.0084	0.0049
MD04MY90.DAT	0.3365	0.0404	0.1327	0.0075	0.0065
MD22MY90.DAT	0.0288	0.0612	0.0284	0.2340	0.0651
MD23MY90.DAT	0.4061	0.1315	0.0679	0.4196	0.0666
MD24MY90.DAT	0.0450	0.0880	0.0146	0.1954	0.0869
MD25MY90.DAT	0.0148	0.0785	0.0281	0.1338	0.0443
MD31MY90.DAT	0.5675	0.3715	0.5229	0.0001	0.0178
MD01JN90.DAT	diverged				
MD04JN90.DAT	0.3123	0.2198	0.1180	0.0000	0.0003

APPENDIX N
SUMMARY 13
RESULTS FOR NO PLATES
DATA FILES USING MOD350

DATA FILE	SOS	RMS	S1°	HZ:S	NH3	PROD	G	S	kS	k1	k2	k3
MD18AP90.DAT	0.41185	0.05205	0.00012	0.11206	0.00124	0.001	1.30282	0.69637	0.03772	0.07622	0.00585	0.00071
MD04MY90.DAT	0.51048	0.05873	0.00033	0.40063	0.02706	0.00032	1.74256	0.77137	0.14009	0.87013	0.01018	0.00002
MD22MY90.DAT	0.00089	0.00302	0.06517	0.15212	0.01528	0.00004	0.99777	0.68583	0.03715	0.1134	0.10919	0.05499
MD23MY90.DAT	0.01921	0.01359	0.01565	0.20336	0.01358	0.00003	0.98424	0.73535	0.00017	0.1461	0.04738	0.03846
MD24MY90.DAT	0.00941	0.00925	0.04812	0.20183	0.00001	0.00002	0.93065	0.70288	0.00004	0.13108	0.03729	0.06949
MD25MY90.DAT	0.13501	0.0298	0.02289	0.00074	0.00057	0.00003	1.13316	0.72811	0.00001	0.0978	0.03076	0.06597
MD31MY90.DAT	0.00778	0.0094	0.0263	0.0998	0.14008	0.00003	1.25872	1.12781	1.1949	1.39836	0.70838	0.27265
MD01JN90.DAT		diverged										
MD04JN90.DAT	0.0147	0.01128	0.02268	0.03492	0.11346	0.00074	1.12821	0.94281	0.50372	0.84644	0.19374	0.2851

APPENDIX N
SUMMARY 14
RESULTS FOR NO PLATES
DATA FILES USING MOD360

DATA FILE	SOS	RMS	S1'	HZ:S1	HZ:S2	NH3	Prod	G	S1	S2	KS1	k1
MD18AP90.DAT	0.0237	0.0152	0.0135	0.1229	0.0001	0.0008	0.0003	1.4052	0.5806	0.5554	0.4118	0.7364
MD04MY90.DAT	0.0844	0.0239	0.0000	0.2811	0.0000	0.0727	0.0901	1.9676	0.8766	0.0062	0.6543	0.7877
MD22MY90.DAT	0.0002	0.0015	0.0728	0.3111	0.0417	0.0012	0.0064	1.1941	0.4282	0.2550	0.7333	0.4660
MD23MY90.DAT	0.0090	0.0093	0.0163	0.2386	0.0001	0.0031	0.0492	1.0815	0.4893	0.5798	0.6693	0.4451
MD24MY90.DAT	0.0058	0.0073	0.1218	0.2448	0.0070	0.0000	0.0849	1.0440	0.3792	0.5109	0.7580	0.4729
MD25MY90.DAT	0.2172	0.0378	0.1005	0.1395	0.0000	0.0010	0.0000	1.2646	0.4005	0.5354	0.7642	0.4690
MD31MY90.DAT	0.1519	0.0415	0.0008	0.0001	0.2109	0.2686	0.0294	1.3726	1.1215	0.0898	0.6048	0.9744
MD01JN90.DAT		diverged										
MD04JN90.DAT	0.0889	0.0277	0.0001	0.0010	0.2630	0.1206	0.0010	1.2514	0.8449	0.2453	0.5024	0.6533

DATA FILE	k2	k3	k4
MD18AP90.DAT	0.0027	0.0075	0.0004
MD04MY90.DAT	0.1773	0.0077	0.2918
MD22MY90.DAT	0.1523	0.0790	0.2365
MD23MY90.DAT	0.0839	0.0597	0.1466
MD24MY90.DAT	0.1287	0.0419	0.1418
MD25MY90.DAT	0.0820	0.0346	0.1964
MD31MY90.DAT	0.0894	0.2571	0.0004
MD01JN90.DAT		diverged	
MD04JN90.DAT	0.1200	0.1800	0.2703

APPENDIX N
SUMMARY 15
RESULTS FOR NO PLATES
DATA FILES USING MOD361

DATAFILE	SOS	RMS	S1*	Hz:S1	Hz:S2	Prod	NH3	G	S1	S2	KS1	k1
MD18AP90.DAT	0.0059	0.0062	0.4219	0.0002	0.0825	0.0001	0.0001	1.1406	0.6781	0.5167	0.3082	0.0325
MD04MY90.DAT	0.0720	0.0221	1.0823	0.0042	0.8129	0.0380	0.0839	1.9370	0.0177	1.0699	0.9696	0.0000
MD22MY90.DAT	0.0002	0.0016	0.3544	0.0440	0.1558	0.0002	0.0002	1.0329	0.7456	0.4791	0.1146	0.0883
MD23MY90.DAT	0.0165	0.0126	0.3540	0.2194	0.0090	0.0001	0.0404	1.0176	0.7460	0.5671	0.1445	0.0945
MD24MY90.DAT	0.0062	0.0075	0.3024	0.2246	0.0492	0.0002	0.0064	0.9957	0.7976	0.4649	0.0003	0.1169
MD25MY90.DAT	0.1141	0.0274	0.3002	0.0636	0.0000	0.0000	0.0001	1.1786	0.7998	0.4587	0.0000	0.0840
MD31MY90.DAT	0.0006	0.0025	0.1239	0.0630	0.4115	0.1320	0.0417	1.6507	0.9761	0.4964	0.6218	0.9504
MD01JN90.DAT		diverged										
MD04JN90.DAT	0.0069	0.0077	0.3860	0.4837	0.2748	0.4589	0.2709	1.5401	0.8698	0.2748	0.3394	0.9158

DATAFILE	k2	k3	k4
MD18AP90.DAT	0.0049	0.1301	0.0476
MD04MY90.DAT	0.0005	0.4382	0.0084
MD22MY90.DAT	0.0467	0.1402	0.1682
MD23MY90.DAT	0.0918	0.0693	0.1236
MD24MY90.DAT	0.0405	0.0744	0.1372
MD25MY90.DAT	0.0360	0.1061	0.0895
MD31MY90.DAT	0.4422	0.0011	1.1280
MD01JN90.DAT		diverged	
MD04JN90.DAT	1.1657	0.3949	0.5349

APPENDIX N
SUMMARY 16
RESULTS FOR NO PLATES
DATA FILES USING MOD370

DATAFILE	SOS	RMS	S1*	HZ:S1	HZ:S2	Prod	NH3	G	S1	S2	KS1	k1
MD18AP90.DAT	0.0189	0.0353	0.5614	0.0001	0.0000	0.0003	0.1188	1.0518	0.0586	0.3491	0.7460	0.2990
MD04MY90.DAT	1.2981	0.1039	1.3285	0.0000	0.0235	0.0199	0.3616	1.5063	0.4715	0.3997	0.8146	0.2707
MD22MY90.DAT	0.0077	0.0088	0.9608	0.2440	0.2449	0.0018	0.0336	1.3535	0.8393	0.2909	1.1106	0.1801
MD23MY90.DAT	0.0110	0.0103	0.9156	0.3987	0.1532	0.0001	0.0059	1.2935	0.8844	0.2118	1.1079	0.1249
MD24MY90.DAT	0.0284	0.0161	0.9071	0.4468	0.1542	0.0001	0.0001	1.2738	0.8929	0.1881	1.1086	0.1237
MD25MY90.DAT	0.1573	0.0322	0.1486	0.0010	0.0010	0.0010	0.0010	1.0852	0.7514	0.2674	0.0191	0.0700
MD31MY90.DAT	0.2206	0.0501	0.5285	0.0005	0.0655	0.0006	0.3364	1.5005	1.2615	0.2552	1.5764	0.4624
MD01JN90.DAT	diverged											
MD04JN90.DAT	0.1016	0.0296	0.0080	0.0010	0.0984	0.0002	0.0018	0.9646	0.9851	0.4594	0.2725	0.3016

DATAFILE	k2	k3	k4
MD18AP90.DAT	0.0604	0.1387	0.0027
MD04MY90.DAT	0.2576	0.4212	0.0033
MD22MY90.DAT	0.5332	0.2692	0.0546
MD23MY90.DAT	0.5395	0.0909	0.0790
MD24MY90.DAT	0.5236	0.1027	0.0567
MD25MY90.DAT	0.0611	0.0862	0.1151
MD31MY90.DAT	2.7204	2.4370	0.1087
MD01JN90.DAT	diverged		
MD04JN90.DAT	0.1327	0.0001	4.5726

APPENDIX N
SUMMARY 17
RESULTS FOR NO PLATES
DATA FILES USING MOD375

DATA FILE	SOS	RMS	S1*	Hz:S1	Hz:S2	NH3	Prod	G	S1	S2	KS1	k1
MD18AP90.DAT	0.1399	0.0303	0.1286	0.0542	0.0375	0.0007	0.0010	1.3121	0.7714	0.0096	0.4345	0.4491
MD04MY90.DAT	0.1527	0.0321	0.3152	0.5393	0.0010	0.0413	0.0281	1.8771	1.5348	0.0312	0.7545	0.3414
MD22MY90.DAT	0.0002	0.0016	0.7848	0.3671	0.0133	0.0000	0.1697	1.3795	1.0652	0.3828	0.3130	0.2123
MD23MY90.DAT	0.0031	0.0055	0.7761	0.4134	0.1210	0.0057	0.1011	1.3842	1.0739	0.2203	0.2638	0.0849
MD24MY90.DAT	0.0096	0.0093	0.8830	0.2320	0.1425	0.0001	0.2155	1.3133	0.9670	0.3016	0.2842	0.2491
MD25MY90.DAT	0.4148	0.0522	0.6516	0.0000	0.0007	0.0000	0.0010	1.0807	1.0485	0.5555	0.8598	0.1309
MD31MY90.DAT	0.0011	0.0036	0.8177	0.8541	0.0010	0.0516	0.2606	2.1600	1.0323	0.6162	0.3752	0.5505
MD01JN90.DAT		diverged										
MD04JN90.DAT	0.0142	0.0111	0.9629	0.3246	0.0010	0.0312	0.0673	1.3278	0.7371	0.5901	0.0697	0.0334

DATA FILE	k2	k3	k4
MD18AP90.DAT	0.5426	0.0092	0.0517
MD04MY90.DAT	0.0020	0.0099	0.0591
MD22MY90.DAT	0.1061	0.0745	0.0065
MD23MY90.DAT	0.3241	0.0424	0.1114
MD24MY90.DAT	0.2548	0.0667	0.0691
MD25MY90.DAT	0.0785	0.8350	0.0951
MD31MY90.DAT	1.2353	0.4891	0.0068
MD01JN90.DAT		diverged	
MD04JN90.DAT	0.6519	0.4608	0.0152

APPENDIX N
SUMMARY 18
RESULTS FOR NO PLATES
DATA FILES USING MOD380

DATA FILE	SOS	RMS	Hz:S1	I	NH3	G	k1	k2	k3	S1
MD18AP90.DAT		diverged								
MD04MY90.DAT		diverged								
MD22MY90.DAT	0.0135	0.0117	0.0726	0.0001	0.0001	0.9228	0.1226	1.4825	1.1882	0.1331
MD23MY90.DAT	0.0153	0.0121	0.0202	0.0001	0.0049	0.7338	0.2029	1.4316	0.7669	0.1300
MD24MY90.DAT	0.0164	0.0122	0.2181	0.0330	0.0169	1.1031	0.0341	2.1572	0.0252	0.6225
MD25MY90.DAT	0.1522	0.0316	0.0254	0.0001	0.0000	1.1280	0.1008	0.0258	0.5724	0.7186
MD31MY90.DAT	0.0248	0.0168	0.5244	0.0003	0.1130	1.5129	0.3249	2.2719	1.2743	0.0234
MD01JN90.DAT	0.1026	0.0252	0.2795	0.0010	0.0652	0.9050	0.0562	1.4264	0.1974	0.2941
MD04JN90.DAT	0.0069	0.0077	0.0976	0.2751	0.0548	1.3726	0.5269	0.0000	0.5276	0.5357

**APPENDIX N
SUMMARY 19
RESULTS FOR NO PLATES
DATA FILES USING MOD385**

DATA FILE	SOS	RMS	Hz:S	I	NH3	Prod	G	k1	k2	k3	S	k4
MD18AP90.DAT		diverged										
MD04MY90.DAT		diverged										
MD22MY90.DAT	0.2603	0.0515	0.1573	0.0885	0.0187	0.0164	1.0175	0.6123	0.0473	0.2634	0.4101	0.0866
MD23MY90.DAT	0.0099	0.0098	0.1046	0.1016	0.0303	0.0041	0.9996	0.5883	0.1194	0.0927	0.3043	0.2091
MD24MY90.DAT	0.0314	0.0169	0.1752	0.0352	0.0172	0.0334	0.9633	0.5207	0.0706	0.1345	0.3952	0.2857
MD25MY90.DAT		diverged										
MD31MY90.DAT	0.8511	0.0983	0.0101	0.4261	0.2751	0.0100	1.2406	0.9192	0.0185	0.1620	0.8416	0.0101
MD01JN90.DAT	0.1628	0.0317	0.0089	0.2529	0.0513	0.0074	0.9371	0.6342	0.0280	0.2039	0.6694	0.0046
MD04JN90.DAT	0.3210	0.0526	0.1405	0.6817	0.2471	0.0623	1.1256	0.7284	0.0922	0.0613	0.7145	0.0352

**APPENDIX N
SUMMARY 20
RESULTS FOR NO PLATES
DATA FILES USING MOD390**

DATA FILE	SOS	RMS	Hz:S	I	NH3	Prod	G	k1	k2	k3	S	k4
MD18AP90.DAT		diverged										
MD04MY90.DAT		diverged										
MD22MY90.DAT	0.3327	0.0583	0.0187	0.2514	0.0383	0.1302	0.8127	0.9867	0.0208	1.2344	0.8303	1.0003
MD23MY90.DAT	0.0049	0.0069	0.0613	0.0595	0.0000	0.0015	0.8693	0.7473	0.0348	0.9796	0.5416	0.7292
MD24MY90.DAT	0.0247	0.0150	0.0350	0.0020	0.0037	0.1372	0.7645	0.8549	0.0333	0.9375	0.7049	1.0173
MD25MY90.DAT	0.3016	0.0445	0.0504	0.1523	0.0058	0.3218	1.1609	2.6873	0.0086	2.3898	0.1977	2.6825
MD31MY90.DAT	2.4273	0.1661	0.4023	0.4526	0.3131	0.1419	1.2581	1.0123	0.0085	0.6679	0.2727	1.6555
MD01JN90.DAT		diverged										
MD04JN90.DAT	0.4764	0.0641	0.2368	0.2329	0.0593	0.0490	1.1549	1.0185	0.0396	1.0658	0.8057	1.0882

APPENDIX O
SUMMARY I
RESULTS FOR TEFLON COATED ALUMINUM PLATES
DATA FILES USING MOD310

DATA FILE	SOS	RMS	S1*	S2*	Hz:S1	Hz:S2	NH3	Prod	G	S1	S2	KS1
SC01JN89.DAT	0.0010	0.0037	0.0032	0.0038	0.1568	0.2025	0.0006	0.1102	1.0454	0.5028	0.9972	0.0572
SC02JN89.DAT	0.0654	0.0258	0.0010	0.0010	0.0000	0.0000	0.0544	0.0000	1.2449	0.5000	1.0000	0.1200
SC09MY89.DAT	0.6517	0.0777	0.3389	0.4052	0.6468	0.0010	0.0156	0.4651	1.2839	0.3620	0.0010	0.2501
SC18MY89.DAT	0.0068	0.0097	0.0044	0.0008	0.0902	0.1478	0.0151	0.0003	1.1328	0.5078	1.0002	0.0408

DATA FILE	KS2	K1	K2	K3	K4
SC01JN89.DAT	0.4995	0.0671	0.0524	0.0372	0.0840
SC02JN89.DAT	0.5000	0.0540	0.0800	0.0300	0.0180
SC09MY89.DAT	0.6825	0.1910	0.2865	0.0381	1.0013
SC18MY89.DAT	0.4731	0.0809	0.0728	0.0415	0.0947

APPENDIX O
SUMMARY 2

RESULTS FOR TEFLON COATED ALUMINUM PLATES
DATA FILES USING MOD315

DATA FILE	SOS	RMS	S1*	S2*	Hz:S1	Hz:S2	Prod	NH3	G	S1	S2	KS1
SC01JN89.DAT	0.0163	0.0147	0.0058	0.0009	0.1951	0.0000	0.1334	0.1472	1.0386	0.5952	1.1077	0.0440
SC02JN89.DAT	0.0158	0.0127	0.0052	0.0030	0.0044	0.0240	0.0000	0.0001	1.2211	0.6019	1.0980	0.0006
SC09MY89.DAT	1.9350	0.1339	0.0456	0.0017	0.0726	0.0002	0.0030	0.0043	1.2280	0.5554	1.2131	0.1138
SC18MY89.DAT	0.0199	0.0166	0.0006	0.0000	0.1303	0.0014	0.0396	0.0585	1.1071	0.6063	1.1312	0.1405

DATA FILE	KS2	k1	k2	k3	k4
SC01JN89.DAT	0.2498	0.0435	0.0245	0.0876	0.0050
SC02JN89.DAT	0.1838	0.0785	0.0147	0.1396	0.0573
SC09MY89.DAT	0.0525	0.0008	0.0490	0.0185	0.0071
SC18MY89.DAT	0.1285	0.1187	0.0222	0.0808	0.0484

APPENDIX O
SUMMARY 3

RESULTS FOR TEFLON COATED ALUMINUM PLATES

DATA FILES USING MOD350

DATA FILE	SOS	RMS	S1°	HZ:S	NH3	PROD	G	S	KS	K1	K2	K3
SC01JN89.DAT	0.0083	0.0111	0.0682	0.2535	0.0003	0.0196	1.0864	1.0328	1.2549	1.3893	0.0179	0.0381
SC02JN89.DAT	0.0724	0.0272	0.3597	0.0579	0.0045	0.0010	1.3574	0.7413	1.2553	1.1725	0.1588	0.2366
SC09MY89.DAT	2.0829	0.1389	0.0647	0.0271	0.0083	0.0307	1.4377	1.0363	1.1995	1.3385	0.0323	0.0040
SC18MY89.DAT		diverged										

APPENDIX O
SUMMARY 4
RESULTS FOR TEFLON COATED ALUMINUM PLATES

DATA FILES USING MOD360

DATA FILE	SOS	RMS	S1*	Hz:S1	Hz:S2	NH3	Prod	G	S1	S2	KS1	K1
SC01JN89.DAT	0.0021	0.0052	0.0747	0.1972	0.1111	0.0002	0.1345	1.0641	0.6763	0.3045	0.7784	0.4634
SC02JN89.DAT	0.0210	0.0146	0.1841	0.0717	0.0000	0.0297	0.0000	1.3299	0.5669	0.3312	0.8021	0.3349
SC09MY89.DAT	0.0476	0.0210	0.0003	0.4449	0.0749	0.0158	0.0286	1.8458	1.1315	0.0003	0.5375	0.7874
SC18MY89.DAT	0.0025	0.0059	0.1110	0.1324	0.0167	0.0002	0.0666	1.1259	0.6400	0.3311	0.7876	0.4213

DATA FILE	K2	K3	K4
SC01JN89.DAT	0.1264	0.0257	0.2144
SC02JN89.DAT	0.0992	0.0996	0.2168
SC09MY89.DAT	0.0404	0.0153	0.2518
SC18MY89.DAT	0.1287	0.0430	0.2217

APPENDIX O
SUMMARY 5
RESULTS FOR TEFLON COATED ALUMINUM PLATES
DATA FILES USING MOD361

DATA FILE	SOS	RMS	S1*	Hz:S1	Hz:S2	Prod	NH3	G	S1	S2	KS1	k1
SC01JN89.DAT	0.0124	0.0128	0.3827	0.1408	0.1984	0.0001	0.0001	0.9185	0.7173	0.2755	0.2478	0.1163
SC02JN89.DAT	0.0345	0.0188	0.3941	0.0001	0.0133	0.0010	0.0269	1.2757	0.7059	0.1755	0.2485	0.0977
SC09MY89.DAT		diverged										
SC18MY89.DAT	0.0018	0.0051	0.3155	0.0431	0.2344	0.0000	0.0000	1.1223	0.7845	0.2334	0.0339	0.1420

DATA FILE	k2	k3	k4
SC01JN89.DAT	0.9061	0.1068	0.0338
SC02JN89.DAT	0.7510	0.1869	0.1537
SC09MY89.DAT		diverged	
SC18MY89.DAT	0.8688	0.0739	0.0488

APPENDIX O
SUMMARY 6
RESULTS FOR TEFLON COATED ALUMINUM PLATES

DATA FILES USING MOD370

DATA FILE	SOS	RMS	S1*	Hz:S1	Hz:S2	Prod	NH3	G	S1	S2	kS1	k1
SC01JN89.DAT	0.0010	0.0036	0.8799	0.3326	0.1893	0.1434	0.0002	1.2199	0.9201	0.2070	1.1101	0.0932
SC02JN89.DAT	0.0184	0.0137	0.9769	0.1689	0.0155	0.0001	0.0306	1.4161	0.8231	0.2332	1.1019	0.1793
SC09MY89.DAT	7.5590	0.2646	0.6139	0.0010	0.0493	0.0294	0.0039	0.6763	0.4861	0.3102	1.1621	0.1671
SC18MY89.DAT	0.0060	0.0091	0.6139	0.0010	0.0493	0.0294	0.0039	0.6763	0.4861	0.3102	1.1621	0.1671

DATA FILE	k2	k3	k4
SC01JN89.DAT	0.7237	0.1820	0.0352
SC02JN89.DAT	0.4553	0.1090	0.1021
SC09MY89.DAT	0.0209	0.4422	0.1540
SC18MY89.DAT	0.0209	0.4422	0.1540

APPENDIX O
SUMMARY 7
RESULTS FOR TEFLON COATED ALUMINUM PLATES
DATA FILES USING MOD375

DATA FILE	SOS	RMS	S1*	Hz:S1	Hz:S2	NH3	Prod	G	S1	S2	kS1	k1
SC01JN89.DAT	0.0012	0.0040	0.7941	0.2752	0.1952	0.0000	0.2774	1.3013	1.0559	0.2087	0.7758	0.6156
SC02JN89.DAT	0.0156	0.0126	0.9859	0.2076	0.0345	0.0258	0.0009	1.4659	0.8641	0.2626	0.1211	0.0460
SC09MY89.DAT	0.3877	0.0599	0.4222	0.3095	0.0004	0.0228	0.0000	1.5815	1.4278	0.0001	0.3787	0.4308
SC18MY89.DAT	0.0057	0.0089	0.8442	0.2083	0.0932	0.0001	0.1846	1.3532	1.0058	0.2928	0.3020	0.2819

DATA FILE	k2	k3	k4
SC01JN89.DAT	0.1504	0.0301	0.0259
SC02JN89.DAT	0.2900	0.0888	0.1906
SC09MY89.DAT	0.1895	0.0216	0.0616
SC18MY89.DAT	0.2184	0.0692	0.0335

APPENDIX O
SUMMARY 8
RESULTS FOR TEFLON COATED ALUMINUM PLATES
DATA FILES USING MOD380

DATA FILE	SOS	RMS	HZ:S1	I	NH3	G	K1	K2	K3	S1
SC01JN89.DAT	0.0066	0.0093	0.0093	0.0001	0.0000	0.5290	0.0499	1.6483	0.7876	0.3142
SC02JN89.DAT	0.0149	0.0123	0.0847	0.0200	0.0369	1.3444	0.0571	1.3403	0.1622	0.3970
SC09MY89.DAT	1.8280	0.1301	0.3687	0.0007	0.0006	1.8997	0.0247	1.7576	1.8200	0.0524
SC18MY89.DAT	0.0564	0.0280	0.0000	0.0001	0.0001	0.7242	0.1526	1.4205	0.8723	0.1042

**APPENDIX O
SUMMARY 9**

**RESULTS FOR TEFLON COATED ALUMINUM PLATES
DATA FILES USING MOD385**

DATA FILE	SOS	RMS	Hz:S	I	NH3	Prod	G	k1	k2	k3	S	k4
SC01JN89.DAT	0.0026	0.0058	0.1863	0.0273	0.0097	0.0102	0.7901	0.5684	0.0472	0.2108	0.3178	0.2597
SC02JN89.DAT	0.0562	0.0240	0.0441	0.0596	0.0409	0.1299	1.4101	1.5859	0.3997	1.0135	0.1509	1.2091
SC09MY89.DAT	diverged											
SC18MY89.DAT	0.0755	0.0324	0.1174	0.0147	0.0140	0.0216	1.0117	0.5863	0.0388	0.2583	0.4463	0.2568

**APPENDIX O
SUMMARY 10**

**RESULTS FOR TEFLON COATED ALUMINUM PLATES
DATA FILES USING MOD390**

DATA FILE	SOS	RMS	Hz:S	I	NH3	Prod	G	k1	k2	k3	S	k4
SC01JN89.DAT	0.0094	0.0111	0.0548	0.0403	0.0004	0.0399	0.6505	1.0024	0.0167	1.1773	0.8089	1.0672
SC02JN89.DAT	0.5417	0.0744	0.0001	0.0420	0.0557	0.0279	1.0625	0.8114	0.0176	0.9153	0.6104	0.9271
SC09MY89.DAT	32.82	0.5512	0.2221	1.2805	0.0677	0.3985	0.0024	2.0677	0.5488	3.1128	0.9388	1.4254
SC18MY89.DAT	0.4728	0.0810	0.0001	0.2158	0.0288	0.2265	0.6384	1.0387	0.0168	1.1978	0.8812	1.1646

APPENDIX P
SUMMARY 1
RESULTS FOR BLACK IRON PLATES
DATA FILES USING MOD310

DATA FILE	SOS	RMS	S1*	S2*	Hz:S1	Hz:S2	NH3	Prod	G	S1	S2	KS1
SC04JA90.DAT	0.0064	0.0116	0.0153	0.0369	0.0008	0.0640	0.0009	0.1624	0.9501	0.4857	1.0015	0.1083
SC05JA90.DAT	0.0508	0.0376	0.0029	0.0009	0.0920	0.0423	0.0100	0.0811	1.1416	0.5007	1.0178	0.1423
SC08JA90.DAT			unusable									
CA09JA90.DAT	0.0604	0.0465	0.0944	0.0000	0.1651	0.0010	0.1411	0.3202	1.4826	0.4066	1.4387	0.4043
CB09JA90.DAT			unusable									
CA11JA90.DAT	0.0098	0.0098	0.1039	0.0010	0.3476	0.0000	0.0101	0.1585	1.1695	0.4535	1.1322	0.1699
CB11JA90.DAT	0.1107	0.0299	0.0005	0.0002	0.2827	0.0001	0.1643	0.0001	1.3996	0.5646	1.0339	0.1151
CA12JA90.DAT	0.0369	0.0312	0.0017	0.0012	0.4346	0.0000	0.0003	0.2068	1.3308	0.7279	1.2010	0.1003
CB12JA90.DAT	0.0819	0.0453	0.0112	0.0010	0.1898	0.0012	0.3486	0.1549	1.1708	0.5589	1.1193	0.1673
CA16JA90.DAT			diverged									
CB16JA90.DAT	0.0055	0.0087	0.0010	0.0006	0.1949	0.0544	0.1950	0.0935	1.1554	3.7082	2.7139	5.2731

DATA FILE	KS2	K1	K2	K3	K4
SC04JA90.DAT	1.1746	0.0585	0.8859	0.0411	0.2108
SC05JA90.DAT	0.4211	0.0834	0.1724	0.0022	0.0000
SC08JA90.DAT			unusable		
CA09JA90.DAT	0.7564	0.0900	1.4420	0.1833	0.0041
CB09JA90.DAT			unusable		
CA11JA90.DAT	0.5902	0.1435	0.6410	0.4661	0.0003
CB11JA90.DAT	0.4852	0.3979	0.3349	0.4842	0.0517
CA12JA90.DAT	0.4576	0.5461	0.8048	0.5663	0.0008
CB12JA90.DAT	0.5638	0.3611	0.6323	0.0013	0.0015
CA16JA90.DAT			diverged		
CB16JA90.DAT	2.5488	0.4278	0.2375	5.1529	0.1312

APPENDIX P
SUMMARY 2
RESULTS FOR BLACK IRON PLATES
DATA FILES USING MOD315

DATA FILE	SOS	RMS	S1*	S2*	HZ:S1	HZ:S2	Prod	NH3	G	S1	S2	KS1
SC04JA90.DAT	0.0066	0.0117	0.0111	0.0174	0.0007	0.0001	0.2415	0.2017	1.1372	0.5375	0.9836	0.5327
SC05JA90.DAT	0.0508	0.0376	0.0001	0.0213	0.0254	0.0109	0.1107	0.0737	1.1336	0.5314	0.9797	0.1704
SC08JA90.DAT			unusable									
CA09JA90.DAT	0.0472	0.0410	0.0005	0.0520	0.0000	0.0013	0.4928	0.1786	1.5851	0.8262	0.9490	0.8248
CB09JA90.DAT			unusable									
CA11JA90.DAT	0.0097	0.0097	0.0001	0.0023	0.0000	0.0000	0.3004	0.2175	1.1631	0.5856	1.0566	0.2769
CB11JA90.DAT	0.1050	0.0291	0.0010	0.0016	0.0098	0.1375	0.1542	0.0101	1.2773	0.6405	1.0573	0.2021
CA12JA90.DAT	0.0750	0.0444	0.0002	0.0080	0.0008	0.0002	0.3022	0.1895	1.1203	0.6150	1.0371	0.1716
CB12JA90.DAT	0.0135	0.0183	0.0006	0.0032	0.0000	0.1969	0.2861	0.1655	1.1266	0.6294	1.1071	0.2395
CA16JA90.DAT			diverged									
CB16JA90.DAT	0.0500	0.0260	0.0009	0.0000	0.0002	0.1733	0.2839	0.1472	1.1065	0.6250	1.1139	0.3491

DATA FILE	KS2	K1	K2	K3	K4
SC04JA90.DAT	0.6175	0.7608	0.0038	0.2541	0.2011
SC05JA90.DAT	0.6947	0.2878	0.0007	0.0001	0.0179
SC08JA90.DAT			unusable		
CA09JA90.DAT	1.5928	1.1704	0.3687	0.0001	0.0248
CB09JA90.DAT			unusable		
CA11JA90.DAT	0.3572	0.5112	0.1932	0.0855	0.0125
CB11JA90.DAT	0.0829	0.5954	0.1585	0.1784	0.2230
CA12JA90.DAT	0.6908	0.7479	0.4661	0.0228	0.0065
CB12JA90.DAT	0.6388	0.5991	0.5996	0.0263	0.0037
CA16JA90.DAT			diverged		
CB16JA90.DAT	0.8118	0.6336	0.6729	0.0272	0.0011

APPENDIX P
SUMMARY 3
RESULTS FOR BLACK IRON PLATES
DATA FILES USING MOD350

DATA FILE	SOS	RMS	S1*	HZ:S	NH3	PROD	G	S	KS	k1	k2	k3
SC04JA90.DAT	0.0072	0.0123	0.0005	0.1384	0.0002	0.2240	1.0208	1.7186	0.6582	0.2779	0.0071	0.0963
SC05JA90.DAT	0.0484	0.0367	0.0004	0.1238	0.0106	0.4792	1.4624	0.8006	1.0402	0.6178	0.0037	2.1788
SC08JA90.DAT		unusable	8 pts.									
CA09JA90.DAT	0.0451	0.0401	0.4674	0.6601	0.1857	0.4713	1.2980	1.1300	1.7648	1.3975	1.0610	2.1780
CB09JA90.DAT		unusable	noisy									
CA11JA90.DAT	0.0082	0.0090	0.0001	0.1922	0.0014	0.1630	0.9916	1.9999	0.6664	0.2405	4.1128	1.9740
CB11JA90.DAT	0.0945	0.0276	0.0012	0.0633	0.1880	0.0000	1.1674	0.9865	0.4159	0.5589	1.2966	1.0742
CA12JA90.DAT	0.0335	0.0297	0.0087	0.4174	0.0001	0.0633	1.2374	1.0940	1.6254	1.2520	1.2280	1.9357
CB12JA90.DAT	0.0033	0.0090	0.1887	0.2042	0.2251	0.0010	0.9435	2.4602	2.9117	0.7115	5.2494	1.1801
CA16JA90.DAT		diverged										
CB16JA90.DAT	0.0733	0.0315	0.8849	0.0005	0.5687	0.1000	1.2706	4.8766	2.5351	0.5357	0.4084	0.0300

APPENDIX P
SUMMARY 4
RESULTS FOR BLACK IRON PLATES
DATA FILES USING MOD360

DATA FILE	SOS	RMS	S1*	HZ:S1	HZ:S2	NH3	PROD	G	S1	S2	KS1	k1
SC04JA90.DAT	0.0063	0.0012	0.0009	0.1182	0.1577	0.0002	0.0868	1.0794	0.6811	1.1278	0.7235	1.2511
SC05JA90.DAT	0.0512	0.0377	0.0170	0.0730	0.0664	0.0097	0.0571	1.1357	0.4840	0.9987	0.7168	0.5227
SC08JA90.DAT	unusable 8 data pts.											
CA09JA90.DAT	0.0776	0.0526	0.0010	0.0010	0.0001	0.1492	0.3261	1.2276	1.2324	0.9421	0.7918	1.2234
CB09JA90.DAT	too noisy											
CA11JA90.DAT	0.0089	0.0093	0.1775	0.0851	0.0017	0.0149	0.4063	1.1599	0.6388	0.9104	1.4448	1.2272
CB11JA90.DAT	0.1030	0.0288	0.0005	0.2760	0.0001	0.1579	0.0000	1.3905	0.6988	1.0153	0.5424	0.5116
CA12JA90.DAT	0.0298	0.0280	0.0568	0.0070	0.0910	0.0001	0.3301	1.1123	1.0638	0.9724	0.9384	1.2449
CB12JA90.DAT	0.0237	0.0243	0.0019	0.3078	0.0005	0.2618	0.2536	1.2863	1.0528	0.9486	0.9816	1.2694
CA16JA90.DAT	0.0063	0.0177	0.0003	0.2003	0.0001	0.0005	0.2770	1.1556	0.7783	1.1012	0.6751	0.7430
CB16JA90.DAT	0.0565	0.0276	0.0074	0.0002	0.0260	0.5646	0.0375	1.1728	0.9369	1.8066	1.4932	1.4139

DATA FILE	k2	k3	k4
SC04JA90.DAT	0.0949	0.0027	0.0169
SC05JA90.DAT	0.0648	0.0028	0.0149
SC08JA90.DAT	unusable 8 data pts.		
CA09JA90.DAT	0.1610	0.0003	0.0637
CB09JA90.DAT	too noisy		
CA11JA90.DAT	0.2250	1.0573	0.0509
CB11JA90.DAT	0.2868	0.5788	0.0274
CA12JA90.DAT	0.0746	1.4383	0.0790
CB12JA90.DAT	0.0002	0.9078	0.1296
CA16JA90.DAT	0.6114	0.5178	0.0240
CB16JA90.DAT	0.1571	0.2918	0.0006

APPENDIX P
SUMMARY 5
RESULTS FOR BLACK IRON PLATES
DATA FILES USING MOD361

DATA FILE	SOS	RMS	S1*	HZ:S1	HZ:S2	PROD	NH3	G	S1	S2	KS1	k1
SC04JA90.DAT	0.0065	0.0116	0.8074	0.1376	0.0498	0.0043	0.0002	0.9027	1.4926	0.5952	0.7034	0.2272
SC05JA90.DAT	0.0518	0.0379	1.0690	0.0004	0.0001	0.0982	0.0056	1.0150	1.2310	0.6055	0.3220	0.8120
SC08JA90.DAT		unsuable 8 pts.										
CA09JA90.DAT	0.0998	0.0597	0.5465	0.0010	0.0937	0.2227	0.1521	1.1157	1.7535	0.4967	0.2975	0.9980
CB09JA90.DAT		too noisy										
CA11JA90.DAT	0.0115	0.0106	0.5400	0.0899	0.1236	0.1444	0.0002	0.9863	1.7600	0.7756	0.3226	0.3447
CB11JA90.DAT	0.1120	0.0301	0.9302	0.0004	0.2672	0.0001	0.1662	1.4018	1.3698	0.7423	0.2713	0.7998
CA12JA90.DAT	0.0467	0.0351	0.6632	0.0010	0.4644	0.1502	0.0005	1.2358	1.6368	0.7328	0.2499	0.8993
CB12JA90.DAT	0.0059	0.0122	0.9218	0.0379	0.3188	0.0007	0.1422	1.0434	1.3782	1.0983	3.2844	0.8480
CA16JA90.DAT	0.0042	0.0146	0.8015	0.1505	0.0602	0.0958	0.0000	0.9900	1.4985	1.6262	1.7920	1.3719
CB16JA90.DAT	0.0089	0.0110	0.8561	0.0000	0.4253	0.0003	0.1247	1.1482	1.4439	0.3979	1.3021	1.7651

DATA FILE	k2	k3	k4
SC04JA90.DAT	0.1236	3.6214	0.0071
SC05JA90.DAT	0.1444	0.0000	0.0754
SC08JA90.DAT		unsuable 8 pts.	
CA09JA90.DAT	0.1293	0.0040	0.1039
CB09JA90.DAT		too noisy	
CA11JA90.DAT	0.1703	0.0007	1.8165
CB11JA90.DAT	0.5039	0.0806	0.4511
CA12JA90.DAT	0.4852	0.0000	0.6163
CB12JA90.DAT	0.2578	8.1798	6.7905
CA16JA90.DAT	0.3298	1.0902	1.5579
CB16JA90.DAT	0.7184	0.1908	2.2283

APPENDIX P
SUMMARY 6
RESULTS FOR BLACK IRON PLATES
DATA FILES USING MOD370

DATA FILE	SOS	RMS	S1*	HZ:S1	HZ:S2	PROD	NH3	G	S1	S2	KS1	K1
SC04JA90.DAT	0.0083	0.0132	0.2892	0.0000	0.0002	0.0000	0.0002	0.6427	1.3905	0.0658	1.2773	0.5563
SC05JA90.DAT	0.1902	0.0382	0.3858	0.0000	0.0000	0.0010	0.0000	0.7809	0.6142	0.0740	0.9040	0.6552
SC08JA90.DAT		8 pts										
CA09JA90.DAT	0.0483	0.0415	0.0002	0.0010	0.0006	0.6313	0.1475	1.7827	1.4053	0.0004	0.8355	1.5175
CB09JA90.DAT		usable 8 pts										
CA11JA90.DAT	0.0950	0.0276	0.2287	0.0010	0.0002	0.0010	0.0001	0.8736	0.7714	0.2211	0.4173	0.9372
CB11JA90.DAT	0.1066	0.0293	0.0332	0.0000	0.4434	0.0001	0.1534	1.5533	0.6368	0.3542	0.6053	0.7849
CA12JA90.DAT	0.0415	0.0331	0.3030	0.0010	0.1352	0.0004	0.0001	0.8091	0.6470	1.0006	2.2762	1.7242
CB12JA90.DAT	0.0522	0.0361	2.5490	0.0009	0.2093	0.0436	0.3122	0.9082	0.0006	0.9394	25.8319	2.1125
CA16JA90.DAT	0.0064	0.0179	0.0003	0.0001	0.3687	0.2830	0.0002	1.3273	1.2264	0.6561	0.5126	1.2209
CB16JA90.DAT	0.0045	0.0078	0.0304	0.0094	0.3814	0.1863	0.1498	1.3876	0.9316	0.2537	2.6545	2.1037

DATA FILE	k2	k3	k4
SC04JA90.DAT	0.1496	0.4717	0.3267
SC05JA90.DAT	0.1934	0.2703	0.2660
SC08JA90.DAT		usable 8 pts	
CA09JA90.DAT	0.2958	0.0192	0.0040
CB09JA90.DAT		too noisy	
CA11JA90.DAT	0.8553	0.4095	4.9105
CB11JA90.DAT	0.3863	0.5486	0.3657
CA12JA90.DAT	1.4013	0.0018	0.9303
CB12JA90.DAT	1.4976	1.2209	0.4001
CA16JA90.DAT	0.5508	0.5345	0.5477
CB16JA90.DAT	0.2656	0.0021	3.9286

APPENDIX P
SUMMARY 7
RESULTS FOR BLACK IRON PLATES
DATA FILES USING MOD375

DATA FILE	SOS	RMS	S1*	HZ:S1	HZ:S2	PROD	NH3	G	S1	S2	KS1	K1
SC04JA90.DAT	0.0066	0.0118	1.3488	0.0001	0.1157	0.0000	0.0089	0.8173	1.7511	0.4960	2.3068	0.7492
SC05JA90.DAT	0.0512	0.0377	1.5217	0.0029	0.0623	0.2739	0.0011	0.9814	1.5783	0.4031	1.9153	0.4388
SC08JA90.DAT		unusable 8 pts.										
CA09JA90.DAT	0.1030	0.0606	0.7649	0.0008	0.2852	0.0223	0.1090	1.4772	3.1895	0.0013	7.8315	3.4443
CB09JA90.DAT		too noisy										
CA11JA90.DAT	0.0084	0.0091	0.9734	0.3928	0.1906	0.0000	0.2358	1.4717	1.0267	0.6037	0.1620	0.3961
CB11JA90.DAT	0.1027	0.0288	0.7244	0.4171	0.0001	0.1502	0.0857	1.6126	1.2756	0.7756	0.4970	0.5959
CA12JA90.DAT	0.1833	0.0695	1.9562	0.0644	0.0221	0.1045	0.0009	0.7867	1.0438	1.1534	22.6271	1.2436
CB12JA90.DAT	0.0053	0.0115	1.0429	0.2803	0.0000	0.1618	0.0008	0.9700	1.9572	0.5302	2.0029	1.0444
CA16JA90.DAT	0.0071	0.0188	0.5932	0.4808	0.0006	0.0004	0.4090	1.5469	1.4068	0.9292	0.4985	0.6116
CB16JA90.DAT	0.0184	0.0158	0.6194	0.2780	0.0003	0.1141	0.0001	1.0123	2.1550	0.9697	12.0598	2.2048

DATA FILE	k2	k3	k4
SC04JA90.DAT	1.3411	0.0164	0.0170
SC05JA90.DAT	0.4922	16.4290	0.0439
SC08JA90.DAT		unusable 8 pts.	
CA09JA90.DAT	0.7724	0.8756	0.3191
CB09JA90.DAT		too noisy	
CA11JA90.DAT	1.1401	0.5392	0.0189
CB11JA90.DAT	0.4359	0.4032	0.0379
CA12JA90.DAT	1.2300	0.0408	0.6596
CB12JA90.DAT	0.5444	6.6107	0.0054
CA16JA90.DAT	0.7498	0.4122	0.0253
CB16JA90.DAT	0.3527	4.1728	0.0003

APPENDIX P
SUMMARY 8
RESULTS FOR BLACK IRON PLATES
DATA FILES USING MOD380

DATA FILE	SOS	RMS	Hz:S1	I	NH3	G	K1	K2	K3	S1
SC04JA90.DAT	0.0066	0.0012	0.2668	0.0001	0.0012	0.9527	1.8387	0.0135	0.0974	0.6740
SC05JA90.DAT	0.0536	0.0386	0.1248	0.0001	0.0094	1.1013	1.9658	0.0496	0.0025	0.3644
SC08JA90.DAT		unusable 8pts								
CA09JA90.DAT	0.0935	0.0578	0.0004	0.0443	0.1407	0.8405	1.4298	0.3002	0.0017	1.1436
CB09JA90.DAT		too noisy								
CA11JA90.DAT	0.0086	0.0092	0.1862	0.2543	0.0000	1.1036	1.7422	0.0736	0.7856	0.3344
CB11JA90.DAT	0.1004	0.0285	0.2472	0.4058	0.1382	1.7524	0.3269	0.0050	0.5670	0.8165
CA12JA90.DAT	0.0414	0.0330	0.1032	0.1306	0.0002	0.9926	3.2547	0.2355	50.4754	0.5648
CB12JA90.DAT	0.0024	0.0078	0.3599	0.4388	0.1922	1.5678	3.6788	0.0168	2.2149	0.2545
CA16JA90.DAT	0.0069	0.0186	0.0104	0.3011	0.0002	1.0226	1.9588	0.1444	0.6769	0.6803
CB16JA90.DAT	0.0098	0.0115	0.0001	0.0526	0.5967	1.3077	2.7257	0.0318	0.2509	0.7686

APPENDIX P
SUMMARY 9
RESULTS FOR BLACK IRON PLATES
DATA FILES USING MOD385

DATA FILE	SOS	RMS	Hz:S1	I	NH3	PROD	G	k1	k2	k3	S1	k4
SC04JA90.DAT	0.0204	0.0206	0.2020	0.0047	0.0211	0.0171	0.9241	1.7231	0.0109	1.2305	0.6836	0.0960
SC05JA90.DAT	0.8539	0.1540	0.2680	0.0143	0.0872	0.0508	1.1362	0.7466	0.0091	1.2670	0.8450	0.1646
SC08JA90.DAT	unusable 8 pts											
CA09JA90.DAT	0.1731	0.0786	0.0010	0.1955	0.0091	0.0010	1.1441	3.8930	0.1987	1.1275	0.7188	1.2836
CB09JA90.DAT	too noisy											
CA11JA90.DAT	0.0526	0.0227	0.0561	0.2212	0.0010	0.0002	0.8447	0.5249	0.1061	0.9325	0.7071	0.0015
CB11JA90.DAT	diverged											
CA12JA90.DAT	0.0955	0.0501	0.0710	0.6076	0.0000	0.0007	1.3379	1.1552	0.2469	0.7412	0.6619	0.7339
CB12JA90.DAT	0.0063	0.0126	0.0073	0.4713	0.1959	0.0175	1.2023	1.7948	0.0000	2.0248	0.8034	0.0809
CA16JA90.DAT	0.0119	0.0244	0.0001	0.4687	0.0000	0.0001	1.0895	0.1804	0.3926	0.6152	1.1654	0.2510
CB16JA90.DAT	0.7129	0.0981	0.0605	0.6795	0.1922	0.0100	1.6910	1.6228	0.0080	0.8374	1.1506	0.0361

APPENDIX P
SUMMARY 10
RESULTS FOR BLACK IRON PLATES
DATA FILES USING MOD390

DATA FILE	SOS	RMS	HZ:S1	I	NH3	PROD	G	S1	k1	k2	k3	k4
SC04JA90.DAT	0.0800	0.0408	0.0695	0.0031	0.0406	0.2874	0.8705	1.5881	0.1723	0.0479	0.1153	0.0212
SC05JA90.DAT	0.0518	0.0379	0.0010	0.0413	0.0010	0.4275	1.3629	0.3210	0.2336	0.0785	0.7841	0.1797
SC08JA90.DAT	only 8 data pts.											
CA09JA90.DAT	0.1631	0.0763	0.0010	0.2910	0.0358	0.4644	1.2159	0.2705	0.2889	0.0389	0.6269	0.0650
CB09JA90.DAT	too noisy											
CA11JA90.DAT	0.0688	0.0260	0.0117	0.3354	0.0329	0.0000	0.0321	0.7254	0.4199	0.1373	0.3549	0.1365
CB11JA90.DAT	0.2681	0.0465	0.0004	0.4176	0.0309	0.0008	1.3298	0.4610	0.2907	0.0378	0.7265	0.2322
CA12JA90.DAT	0.1697	0.0668	0.0001	0.2102	0.1194	0.0002	0.9368	1.5489	0.6921	0.1068	0.0695	0.0532
CB12JA90.DAT	0.0351	0.0296	0.0010	0.6751	0.2011	0.0010	1.2726	0.3972	0.2710	0.0910	0.6653	0.1555
CA16JA90.DAT	0.0314	0.0390	0.0000	0.4100	0.0175	0.0343	1.0414	0.8899	0.7339	0.0447	0.2310	0.0424
CB16JA90.DAT	0.3436	0.0681	0.0943	0.0500	0.3594	0.0001	0.8879	1.5648	0.4541	0.1336	0.0565	0.0677

APPENDIX Q
SUMMARY 1
RESULTS FOR CORRODED ALUMINUM PLATES
DATA FILES USING MOD310

DATA FILE	SOS	RMS	S1*	S2*	HZ:S1	HZ:S2	NH3	Prod	G	S1	S2	KS1
CA07MR90.DAT	0.0358	0.0154	0.0134	0.0010	0.1063	0.0010	0.0560	0.0053	1.4530	0.5189	1.1738	0.3119
CB15MR90.DAT	0.0014	0.0057	0.0131	0.0001	0.3089	0.0964	0.0554	0.1068	1.0971	0.4879	1.0009	0.1928
CA16MR90.DAT	0.0005	0.0026	0.0042	0.0266	0.3232	0.0090	0.0000	0.0572	1.2261	0.4968	0.9744	0.0609
CA23MR90.DAT	0.4308	0.0834	0.0005	0.0010	0.0007	0.0010	0.1868	0.2888	1.5418	0.6662	1.5507	0.2106
CA26MR90.DAT	0.2540	0.0550	0.0131	0.0010	0.3819	0.0010	0.0774	0.2294	1.3821	0.4988	1.3114	0.2079
CB26MR90.DAT	0.1238	0.0384	0.0308	0.0002	0.4788	0.0010	0.2248	0.0203	1.4528	0.4702	1.1886	0.2950
CA27MR90.DAT	0.0711	0.0222	0.0206	0.0058	0.5756	0.0010	0.3103	0.0012	1.7530	0.4804	1.1651	0.3012
CB27MR90.DAT	0.1589	0.0399	0.0032	0.0204	0.5600	0.0010	0.4434	0.0010	1.9348	0.5230	1.0471	0.2958
CC27MR90.DAT	0.2877	0.0498	0.0096	0.0033	0.5764	0.0010	0.5635	0.0010	2.0168	0.5638	1.1193	0.5702
CA29MR90.DAT	0.0090	0.0087	0.0014	0.6191	0.3541	0.0079	0.0699	0.0019	1.3123	2.4127	3.9748	2.4914
CB29MR90.DAT	0.0089	0.0088	0.0146	0.8214	0.4708	0.0000	0.4778	0.0002	1.8163	2.4241	3.4780	2.5017
CC29MR90.DAT	0.0879	0.0275	0.0482	4.5947	0.1649	0.0001	0.8342	0.0000	2.0123	5.1860	1.6493	5.2286

DATA FILE	KS2	k1	k2	k3	k4
CA07MR90.DAT	0.5443	0.1073	0.6949	0.1163	0.0021
CB15MR90.DAT	0.5062	0.0087	0.0971	0.0290	0.0042
CA16MR90.DAT	0.7793	0.0215	0.0092	0.0161	0.0829
CA23MR90.DAT	0.5831	0.5325	1.4032	0.0025	0.0005
CA26MR90.DAT	0.6670	0.0984	1.0724	0.4675	0.0012
CB26MR90.DAT	0.6404	0.0720	0.8828	0.5050	0.0017
CA27MR90.DAT	0.6532	0.0909	0.8673	0.7078	0.0117
CB27MR90.DAT	0.6226	0.2594	0.6622	0.5842	0.0006
CC27MR90.DAT	0.5753	0.3942	0.2203	0.4269	0.0835
CA29MR90.DAT	5.0014	0.2957	0.3863	5.0499	0.0002
CB29MR90.DAT	5.5706	0.3332	0.3448	16.8868	0.0495
CC29MR90.DAT	28.2224	0.6038	0.3420	3.0599	0.0005

APPENDIX Q
SUMMARY 2
RESULTS FOR CORRODED ALUMINUM PLATES
DATA FILES USING MOD315

DATA FILE	SOS	RMS	S1*	S2*	HZ:S1	HZ:S2	Prod	NH3	G	S1	S2	KS1
CA07MR90.DAT	0.2460	0.0405	0.0010	0.0615	0.0010	0.0000	0.1816	0.0422	1.3504	1.1239	1.2774	0.2214
CB15MR90.DAT	0.0003	0.0027	0.1212	0.1511	0.2019	0.0195	0.1182	0.1548	1.0069	0.3897	0.8499	0.2157
CA16MR90.DAT	0.0392	0.0244	0.1336	0.2013	0.0844	0.0002	0.0226	0.1675	1.1143	0.3674	0.7997	0.0593
CA23MR90.DAT	0.2061	0.0577	0.0010	0.0079	0.0004	0.0005	0.0940	0.0895	1.4055	5.6686	3.0599	1.7066
CA26MR90.DAT	0.1911	0.0477	0.0000	0.0353	0.0002	0.0000	0.3304	0.0840	1.0962	0.6923	1.0175	0.5614
CB26MR90.DAT	0.0158	0.0137	0.0003	0.0001	0.0003	0.0866	0.4357	0.1403	1.5790	0.6736	1.2124	0.5971
CA27MR90.DAT	0.0371	0.0161	0.0011	0.0867	0.0010	0.2409	0.3108	0.0901	1.5848	0.6812	1.2005	0.5668
CB27MR90.DAT	0.0668	0.0259	0.0000	0.0000	0.0000	0.3111	0.2042	0.0000	1.6078	0.6651	1.2027	0.5699
CC27MR90.DAT	0.0241	0.0144	0.1106	0.0060	0.0001	0.5021	0.1385	0.0581	1.7858	0.5881	1.1333	0.6976
CA29MR90.DAT	0.0082	0.0083	0.0017	0.0000	0.0039	0.0589	0.1198	0.1200	1.1880	3.5152	4.0026	2.4700
CB29MR90.DAT	0.0090	0.0088	0.0113	0.0000	0.0000	0.4357	0.0457	0.0405	1.4089	3.8191	3.7539	1.2648
CC29MR90.DAT	0.0350	0.0174	0.1748	0.1974	0.0001	0.6106	0.0010	0.0001	1.7174	5.3630	4.1163	6.2280

DATA FILE	KS2	K1	K2	K3	K4
CA07MR90.DAT	0.6030	0.1563	0.1121	0.0091	0.0001
CB15MR90.DAT	0.2460	0.0460	0.0616	0.0387	0.0000
CA16MR90.DAT	0.3219	0.0375	0.0551	0.0401	0.2075
CA23MR90.DAT	1.1826	0.6389	0.2597	0.0621	0.0161
CA26MR90.DAT	1.0323	0.9685	0.6077	0.0216	0.0153
CB26MR90.DAT	1.0368	0.8190	0.4449	0.0002	0.0000
CA27MR90.DAT	0.7328	0.9095	0.4772	0.0034	0.1481
CB27MR90.DAT	0.8337	0.9266	0.5987	0.0002	0.2006
CC27MR90.DAT	0.4478	0.2046	0.2994	0.0264	1.2355
CA29MR90.DAT	1.3193	0.4566	0.3873	0.0002	0.0001
CB29MR90.DAT	0.9148	0.5041	0.3687	0.0000	0.0001
CC29MR90.DAT	1.8826	0.6075	0.3920	1.6607	0.0010

APPENDIX Q
SUMMARY 3

RESULTS FOR CORRODED ALUMINUM PLATES

DATA FILES USING MOD350

DATA FILE	SOS	RMS	S1*	HZ:S	NH3	PROD	G	S	KS	K1	K2	K3
CA07MR90.DAT	0.3528	0.0485	0.0315	0.0903	0.0051	0.0010	1.2051	0.4695	0.0002	0.4949	0.5903	0.7362
CB15MR90.DAT	0.0047	0.0071	0.0002	0.2656	0.0457	0.0983	0.9527	0.8377	0.7130	0.1753	0.0557	0.0265
CA16MR90.DAT	0.0476	0.0269	0.1510	0.8392	0.0751	0.1065	1.1091	0.3506	0.0003	0.2248	0.8049	0.1648
CA23MR90.DAT	0.4919	0.0891	0.0003	0.5608	0.0002	0.0010	1.3614	1.0292	0.6542	1.3028	0.9261	1.2272
CA26MR90.DAT	0.3249	0.0622	0.0001	0.5572	0.0004	0.0001	1.1259	0.7194	0.5347	1.0500	0.6912	0.7371
CB26MR90.DAT	0.0086	0.0101	0.0010	0.2646	0.1586	0.0001	1.2909	0.8913	1.0514	1.9924	1.2248	1.1048
CA27MR90.DAT	0.0178	0.0111	0.0001	0.1777	0.3556	0.0010	1.4521	0.8913	0.3810	1.2835	0.7132	0.7861
CB27MR90.DAT	0.0287	0.0169	0.0002	0.0004	0.5279	0.0010	1.6094	0.9121	0.3005	1.6690	0.8928	1.1895
CC27MR90.DAT	0.0660	0.0241	0.0204	0.1591	0.6288	0.0010	1.8713	0.5486	0.9006	0.2968	0.3049	0.1496
CA29MR90.DAT	0.0739	0.0249	0.0021	0.9232	0.1021	0.0010	1.7033	0.7947	0.8697	1.3017	1.2697	0.8685
CB29MR90.DAT	0.1592	0.0371	0.0010	0.7823	0.5581	0.0010	1.9499	1.0900	0.7587	1.3890	1.1101	0.8392
CC29MR90.DAT	0.0985	0.0294	0.0010	0.4897	0.8344	0.0127	2.3003	1.5512	1.0234	1.8888	0.4491	0.0895

APPENDIX Q
SUMMARY 4
RESULTS FOR CORRODED ALUMINUM PLATES
DATA FILES USING MOD360

DATA FILES	SOS	RMS	S1*	HZ:S1	HZ:S2	NH3	PROD	G	S1	S2	ks1	k1
CA07MR90.DAT	0.2679	0.0423	0.1796	0.0010	1.4228	0.0126	0.0603	2.6492	1.7648	0.9440	2.5597	0.3829
CB15MR90.DAT	0.0033	0.0084	0.2513	0.3049	0.2688	0.1378	0.0474	1.0889	0.5563	0.4561	0.8114	0.7382
CA16MR90.DAT	0.0016	0.0049	0.4496	0.1274	0.3719	0.0007	0.3407	1.8104	1.0514	0.8032	1.5013	0.4761
CA23MR90.DAT	0.4040	0.0807	0.0010	0.0010	0.0010	0.1004	0.3783	1.4693	1.5794	0.9013	1.3592	1.5918
CA26MR90.DAT	0.1677	0.0447	0.0007	0.0042	0.0006	0.1004	0.4234	1.3099	1.3206	0.6876	1.0483	1.5652
CB26MR90.DAT	0.1603	0.0437	0.0200	0.0006	0.0001	0.2627	0.2560	1.2647	1.0083	0.6861	1.1554	1.2886
CA27MR90.DAT	0.0787	0.0234	0.0030	0.0550	0.0000	0.3863	0.0264	1.3956	1.0097	0.6773	0.9298	1.0884
CB27MR90.DAT	0.0822	0.0287	0.0010	0.0002	0.0000	0.5405	0.0011	1.6472	1.1473	0.6721	0.9709	1.2693
CC27MR90.DAT	0.0801	0.0265	0.1970	0.1420	0.1157	0.6193	0.0001	2.0745	1.3040	0.9112	1.1103	1.5498
CA29MR90.DAT	0.0177	0.0121	0.0000	0.2709	0.0119	0.0786	0.0707	1.2415	1.1410	0.5551	2.9631	1.7511
CB29MR90.DAT	0.0177	0.0121	0.0000	0.2709	0.0119	0.0786	0.0707	1.2415	1.1410	0.5551	2.9631	1.7511
CC29MR90.DAT	0.0972	0.0292	0.0012	0.3759	0.0001	0.8364	0.0231	2.2184	1.5715	0.8901	1.2561	1.8351

DATA FILES	k2	k3	k5
CA07MR90.DAT	0.1515	0.3698	0.1164
CB15MR90.DAT	0.0255	0.0317	0.0000
CA16MR90.DAT	0.0007	0.0234	0.0297
CA23MR90.DAT	0.1224	0.3929	0.0140
CA26MR90.DAT	0.0013	0.2479	0.1049
CB26MR90.DAT	0.0797	0.7444	0.0487
CA27MR90.DAT	0.1884	0.9789	0.0000
CB27MR90.DAT	0.1923	0.9903	0.0010
CC27MR90.DAT	0.1925	0.8446	0.0005
CA29MR90.DAT	0.0672	4.5924	0.0021
CB29MR90.DAT	0.6718	4.5925	0.0021
CC29MR90.DAT	0.0001	0.6110	0.0030

APPENDIX Q
SUMMARY 5
RESULTS FOR CORRODED ALUMINUM PLATES
DATA FILES USING MOD360

DATA FILE	SOS	RMS	S1*	HZ:S1	HZ:S2	PROD	NH3	G	S1	S2	KS1
CA07MR90.DAT											
CB15MR90.DAT	0.0008	0.0029	1.0987	0.2478	0.1423	0.1764	0.1255	1.0286	1.3468	0.1360	0.1905
CA16MR90.DAT	0.0039	0.0077	0.7996	0.1077	0.1934	0.0000	0.0001	1.1046	0.5004	0.1700	0.5983
CA23MR90.DAT	0.2573	0.0644	0.7950	0.0000	0.0000	0.8742	0.1042	2.3447	0.5050	1.4382	0.5890
CA26MR90.DAT	0.0491	0.0242	0.6474	0.0001	0.1698	1.1031	0.0771	2.4999	0.6526	1.1993	0.4938
CB26MR90.DAT	0.0777	0.0304	0.5480	0.0000	0.0015	0.4036	0.2777	1.7315	0.7520	0.9409	0.5499
CA27MR90.DAT	0.0276	0.0139	0.5142	0.0003	0.0680	0.0010	0.3808	1.3607	4.2264	0.5312	0.7491
CB27MR90.DAT	0.1362	0.0369	0.5068	0.0789	0.0010	0.0010	0.4792	1.7390	0.7932	0.8508	0.5779
CC27MR90.DAT	0.0299	0.0162	0.6593	0.0001	0.7576	0.0771	0.5332	2.3975	1.6407	0.7771	0.1159
CA29MR90.DAT	0.0901	0.0274	0.2141	0.0010	0.8179	0.0284	0.1704	1.6911	1.3910	0.3030	0.9318
CB29MR90.DAT	0.4077	0.0593	0.0313	0.0006	0.4751	0.0001	0.7511	1.9099	1.1687	0.6646	0.8853
CC29MR90.DAT	0.1048	0.0303	0.9631	0.0010	0.6807	0.2265	0.8307	2.6580	1.3370	1.2611	1.0894

DATA FILE	k1	k2	k3	k4
CA07MR90.DAT				
CB15MR90.DAT	0.5400	0.4489	0.0872	0.0745
CA16MR90.DAT	0.0397	1.1594	0.0253	0.0424
CA23MR90.DAT	0.0124	2.7757	0.2189	0.1638
CA26MR90.DAT	0.0180	3.2577	0.0406	0.1345
CB26MR90.DAT	0.1443	2.3063	0.0695	0.1211
CA27MR90.DAT	0.0441	3.7270	2.2239	2.9833
CB27MR90.DAT	0.1826	2.2384	0.1926	0.3691
CC27MR90.DAT	0.5425	0.6030	0.0000	0.7137
CA29MR90.DAT	1.0985	0.5200	0.0010	0.9785
CB29MR90.DAT	0.8484	0.5305	0.0022	0.0002
CC29MR90.DAT	0.7613	2.0026	0.0479	0.3731

APPENDIX Q
SUMMARY 6
RESULTS FOR CORRODED ALUMINUM PLATES
DATA FILES USING MOD370

DATA FILE	SOS	RMS	S1'	HZ:S1	HZ:S2	Prod	NH3	G	S1	S2	KS1	K1
CA07MR90.DAT	0.0267	0.0132	0.4544	0.7949	0.0359	0.4335	0.0003	1.9782	1.2356	0.1461	2.1243	1.7499
CB15MR90.DAT	0.0061	0.0081	0.3010	0.3275	0.1071	0.0655	0.0405	1.1621	2.2677	0.0704	1.2215	0.2073
CA16MR90.DAT	0.0008	0.0004	0.4489	0.1455	0.0077	0.7512	0.0010	2.1141	1.2411	0.1519	2.1414	1.7476
CA23MR90.DAT	0.1658	0.0535	0.0002	0.0082	0.1199	0.0611	0.1920	1.5275	3.0485	0.3928	1.9671	1.9025
CA26MR90.DAT	0.0073	0.0095	0.0213	0.2377	0.2325	0.1240	0.0001	1.5117	2.6643	4.3357	3.8134	1.9902
CB26MR90.DAT	0.0238	0.0168	0.2256	0.1175	0.4162	0.4924	0.1257	2.1605	1.4644	0.1296	2.0497	1.6925
CA27MR90.DAT	0.0095	0.0081	0.4617	0.4062	0.5453	0.0433	0.2860	2.2207	1.2283	0.1297	1.9205	1.4233
CB27MR90.DAT	0.0226	0.0150	0.4010	0.2450	0.6427	0.0005	0.3699	2.4253	1.2890	0.1474	2.0636	1.6358
CC27MR90.DAT	0.0653	0.0237	0.4425	0.2529	0.7036	0.0010	0.4747	2.6255	1.2475	0.1932	2.0744	1.6306
CA29MR90.DAT	0.0040	0.0063	1.4725	0.4213	0.5638	0.0536	0.5568	1.6070	1.8940	0.2222	4.0264	1.4177
CB29MR90.DAT	0.0451	0.0197	0.4045	0.0000	0.8236	0.3062	0.5190	2.4919	1.2855	0.1298	2.0993	1.6866
CC29MR90.DAT	0.0512	0.0212	0.4141	0.0010	1.0038	0.0370	0.7094	2.6523	1.2759	0.1298	2.0795	1.6440

DATA FILE	K2	K3	K4
CA07MR90.DAT	0.1028	0.3665	1.5005
CB15MR90.DAT	0.1502	0.0001	0.2313
CA16MR90.DAT	0.0198	0.0218	1.4337
CA23MR90.DAT	0.2332	0.0001	0.0210
CA26MR90.DAT	0.0012	0.0505	2.5505
CB26MR90.DAT	0.0001	0.6421	1.5592
CA27MR90.DAT	0.0001	1.5041	1.1812
CB27MR90.DAT	0.0055	0.8795	1.3130
CC27MR90.DAT	0.0933	0.8342	1.4754
CA29MR90.DAT	0.0662	0.0001	2.6479
CB29MR90.DAT	0.0001	0.3085	1.5487
CC29MR90.DAT	0.0001	0.3600	1.5377

APPENDIX Q
SUMMARY 7
RESULTS FOR CORRODED ALUMINUM PLATES
DATA FILES USING MOD375

DATA FILE	SOS	RMS	S1'	Hz:S1	Hz:S2	NH3	PROD	G	S1	S2	KS1	k1
CA07MR90.DAT	0.1886	0.0355	1.2050	0.0002	0.3861	0.0131	0.0843	1.6893	1.7205	0.7255	1.1802	0.6304
CB15MR90.DAT	0.0014	0.0039	0.8998	0.0010	0.0011	0.0103	0.0014	1.6857	2.0602	1.0378	7.3513	0.8352
CA16MR90.DAT	0.0079	0.0077	0.8379	0.1003	0.1912	0.0000	0.0000	1.2053	1.0471	0.3558	0.6951	1.8484
CA23MR90.DAT	0.3238	0.0723	1.4240	0.3897	0.0084	0.0322	0.0476	1.9486	1.5013	0.8434	1.4729	1.0268
CA26MR90.DAT	0.0072	0.0095	0.7141	0.0793	0.4243	0.0000	0.0972	1.5843	2.2359	0.8483	6.0624	0.9655
CB26MR90.DAT	0.0124	0.0088	0.9641	0.2128	0.3460	0.1797	0.0572	1.6592	1.9859	0.7494	1.5531	0.6484
CA27MR90.DAT	0.0292	0.0143	0.5889	0.4297	0.0001	0.3005	0.0016	1.7061	1.3111	0.5788	1.7398	1.3544
CB27MR90.DAT	0.0066	0.0018	0.9143	0.3443	0.0138	0.4359	0.0095	1.8381	2.0357	0.7293	1.2699	0.6676
CC27MR90.DAT	0.0445	0.0198	0.9237	0.4535	0.0075	0.5989	0.0017	2.0741	2.0023	0.7741	0.9306	0.6723
CA29MR90.DAT	0.0067	0.0075	0.4718	0.3697	0.1339	0.1099	0.0640	1.6135	1.6282	0.3533	7.9620	2.7777
CB29MR90.DAT	0.0217	0.0096	0.3156	0.3698	0.0002	0.5190	0.0184	1.9127	1.7844	0.2487	6.2887	3.2801
CC29MR90.DAT	0.0096	0.0092	1.2312	0.9820	0.5750	0.9773	0.1273	2.6927	2.2132	0.4562	2.5457	2.3061

DATA FILE	k2	k3	k4
CA07MR90.DAT	0.3858	2.5005	0.0022
CB15MR90.DAT	10.1119	0.3162	0.0023
CA16MR90.DAT	0.0070	0.0408	0.0017
CA23MR90.DAT	1.6274	1.6912	0.0001
CA26MR90.DAT	11.0695	3.7303	0.0448
CB26MR90.DAT	2.3736	3.3155	0.0001
CA27MR90.DAT	1.9956	1.1903	0.0272
CB27MR90.DAT	0.4739	3.0608	0.0003
CC27MR90.DAT	0.3529	1.6050	0.0000
CA29MR90.DAT	5.2681	2.6646	0.0018
CB29MR90.DAT	1.8872	2.7597	0.0096
CC29MR90.DAT	1.7855	2.4003	0.0002

APPENDIX Q
SUMMARY 8
RESULTS FOR CORRODED ALUMINUM PLATES

DATA FILES USING MOD380

DATA FILE	SOS	RMS	H _z :S1	I	NH3	G	k1	k2	k3	S1
CA07MR90.DAT	1.2958	0.0929	0.3126	0.0010	0.0010	1.1770	3.3189	0.5675	1.2035	0.0116
CB15MR90.DAT	0.0006	0.0024	0.1053	0.0719	0.0018	0.7206	0.0504	0.4970	0.6826	0.0734
CA16MR90.DAT	0.0178	0.0164	0.0855	0.0007	0.0294	0.9814	0.5607	0.7137	1.1131	0.0069
CA23MR90.DAT	0.0453	0.0280	0.0003	0.2309	0.0002	1.5118	7.2594	0.0143	5.8677	0.8044
CA26MR90.DAT	0.0072	0.0095	0.1515	0.2238	1.3453	8.2555	0.0271	0.0000	2.6157	0.6182
CB26MR90.DAT	0.0150	0.0097	0.2912	0.4062	0.1477	1.7213	1.7379	0.0000	1.7237	0.5175
CA27MR90.DAT	0.0121	0.0092	0.0001	0.5431	0.2822	1.7817	1.0532	0.0000	1.2263	0.1845
CB27MR90.DAT	0.0167	0.0129	0.0435	0.6540	0.3911	2.2085	0.6959	0.0002	1.0516	0.2591
CC27MR90.DAT	0.0269	0.0154	0.0576	0.7497	0.5103	2.3814	0.4359	0.0002	1.0371	0.1590
CA29MR90.DAT	0.0046	0.0062	0.4750	0.5589	0.0850	2.0272	4.1322	0.0068	2.5376	0.3314
CB29MR90.DAT	0.0148	0.0079	0.3701	0.8062	0.4755	2.5786	2.0743	0.0285	2.2482	0.1334
CC29MR90.DAT	0.0291	0.0160	0.0001	1.2699	0.6668	2.8038	0.5024	0.4332	1.1807	0.0001

APPENDIX Q
SUMMARY 9
RESULTS FOR CORRODED ALUMINUM PLATES

DATA FILES USING MOD385

DATA FILE	SOS	RMS	Hz:S1	I	NH3	Prod	G	K1	K2	K3	S1	K4
CA07MR90.DAT	1.0410	0.0833	0.0019	0.0894	0.0367	0.0015	1.2338	1.1106	0.0034	0.4531	0.7986	0.0682
CB15MR90.DAT	0.0032	0.0059	0.0216	0.1975	0.0385	0.0004	0.8240	1.0108	0.0003	0.0800	0.3293	0.0164
CA16MR90.DAT	1.1704	0.1332	0.4427	0.2812	0.1281	0.2825	1.4476	1.3004	0.0008	0.6037	0.5834	0.1972
CA23MR90.DAT	diverged											
CA26MR90.DAT	1.3631	0.1274	0.0071	0.0007	0.2249	0.0276	0.7567	3.6040	0.1988	1.4573	0.9110	1.5475
CB26MR90.DAT	0.3225	0.0620	0.0010	0.3919	0.2757	0.0010	1.3092	1.1246	0.0700	0.2526	0.9827	0.0100
CA27MR90.DAT	0.0582	0.0201	0.0004	0.5880	0.3007	0.0045	1.8366	0.9518	0.0066	0.8350	1.3080	0.0009
CB27MR90.DAT	6.6670	0.2582	0.0039	0.3367	0.4416	0.0020	1.2639	1.0004	0.0714	0.2064	1.0476	0.0138
CC27MR90.DAT	5.2689	0.2150	0.0036	0.4489	0.5584	0.0020	1.2544	0.9448	0.2417	0.0283	0.4695	0.1825
CA29MR90.DAT	1.8150	0.1230	0.0025	0.6186	0.3477	0.0018	1.3412	1.2767	0.0711	0.3885	0.9668	0.0116
CB29MR90.DAT	8.7655	0.2749	0.0043	0.4991	0.6052	0.0021	1.2133	1.1485	0.0724	0.1840	0.9152	0.0146
CC29MR90.DAT	7.3890	0.2191	0.0010	0.2487	0.7455	0.0010	1.3382	1.1784	0.0600	0.0929	0.5680	0.0100

**APPENDIX Q
SUMMARY 10**

RESULTS FOR CORRODED ALUMINUM PLATES

DATA FILES USING MOD390

DATA FILE	SOS	RMS	Hz:S1	I	NH3	Prod	G	S	K1	K2	K3	K4
CA07MRAM		no fit										
CB15MR90.DAT	2.8946	0.2565	0.0447	0.0050	0.0179	0.3095	0.0002	1.4504	3.4248	1.1507	1.8079	1.2879
CA16MR90.DAT		no fit										
CA23MR90.DAT	0.5268	0.0922	0.1860	0.4099	0.1002	0.2446	2.0338	0.6591	1.5575	0.0856	0.6225	0.0029
CA26MR90.DAT	3.0268	0.1897	0.0000	0.3744	0.0285	0.1380	1.9969	0.6256	1.9895	0.1965	0.7649	0.2225
CB26MR90.DAT	0.0129	0.0124	0.1792	0.4239	0.1676	0.3053	2.0105	0.1553	1.4786	0.0010	1.1982	0.0010
CA27MR90.DAT	8.3677	0.2411	0.3178	0.5216	0.3060	0.0019	1.7602	0.5919	1.1397	0.0172	0.8175	0.0594
CB27MR90.DAT		no fit										
CC27MR90.DAT		no fit										
CA29MR90.DAT	0.1993	0.0408	0.4246	0.6555	0.2565	0.2187	2.2410	0.0007	1.8051	0.0849	0.9384	0.0769
CB29MR90.DAT	5.9569	0.2266	0.2727	0.6620	0.6417	0.0010	1.9212	0.2173	1.4582	0.0322	0.8121	0.0334
CC29MR90.DAT		no fit										

APPENDIX R
SUMMARY 1
RESULTS FOR PAINTED ALUMINUM PLATES
DATA FILES USING MOD310

DATA FILE	SOS	RMS	S1*	S2*	Hz:S1	Hz:S2	NH3	Prod	G	S1	S2	KS1
SC19JL90.DAT	0.0005	0.0022	0.0339	0.0007	0.2812	0.1933	0.0085	0.1961	1.0526	0.4844	1.0045	0.2194
SC20JL90.DAT	diverged											
SC25JL90.DAT	0.0103	0.0094	0.0550	0.0003	0.1662	0.0133	0.0003	0.0258	1.1687	0.4645	1.0421	0.2181
SC26JL90.DAT	0.0175	0.0126	0.0740	0.0023	0.2096	0.0335	0.0281	0.0006	1.1650	0.4425	1.0463	0.2038
SC27JL90.DAT	0.0001	0.0011	0.0150	0.0007	0.1620	0.1512	0.0027	0.1336	1.0530	0.4937	1.0097	0.2194
SC30JL90.DAT	0.0001	0.0011	0.0149	0.0007	0.1620	0.1512	0.0027	0.1336	1.0530	0.4937	1.0097	0.2194
SC31JL90.DAT	0.0432	0.0181	0.0001	0.0004	0.0000	0.0868	0.0010	0.0746	1.1219	0.5152	1.0042	0.0455
SC01AG90.DAT	0.0348	0.0162	0.0000	0.0008	0.0002	0.1057	0.0003	0.0875	1.1060	0.5138	1.0021	0.0334
SC03AG90.DAT	0.0003	0.0017	0.0968	0.0218	0.2503	0.0762	0.0021	0.1018	1.1174	0.4068	0.9877	0.1265
SC06AG90.DAT	0.0010	0.0030	0.0668	0.0020	0.1907	0.0707	0.0062	0.0611	1.1182	0.4495	1.0457	0.2403
SC07AG90.DAT	0.0075	0.0090	0.0554	0.0001	0.1844	0.1350	0.0119	0.0568	1.0943	0.4618	1.0316	0.1898

DATA FILE	KS2	k1	k2	k3	k4
SC19JL90.DAT	0.4172	0.0795	0.0833	0.0212	0.1758
SC20JL90.DAT	0.4842	0.1277	0.1346	0.0275	0.0693
SC25JL90.DAT	diverged				
SC26JL90.DAT	0.4061	0.1308	0.2700	0.1801	0.1473
SC27JL90.DAT	0.4270	0.0410	0.3015	0.2122	0.1471
SC30JL90.DAT	0.4061	0.0094	0.1066	0.1087	0.1108
SC31JL90.DAT	0.5209	0.1168	0.1571	0.0160	0.0993
SC01AG90.DAT	0.5227	0.0969	0.1335	0.0143	0.1080
SC03AG90.DAT	0.7132	0.1173	0.2403	0.4550	0.0000
SC06AG90.DAT	0.3767	0.0002	0.2545	0.2323	0.1552
SC07AG90.DAT	0.3958	0.0084	0.2148	0.1399	0.1937

APPENDIX R
SUMMARY 2
RESULTS FOR PAINTED ALUMINUM PLATES
DATA FILES USING MOD315

DATA FILE	SOS	RMS	S1*	S2*	HZ:S1	HZ:S2	Prod	NH3	G	S1	S2	KS1
SC19JL90.DAT	0.0002	0.0013	0.0000	0.3137	0.2149	0.0000	0.1465	0.1674	0.9988	0.7656	0.6873	0.1407
SC20JL90.DAT	0.0001	0.0008	0.0394	0.4036	0.2592	0.0028	0.1621	0.1971	0.9556	0.5508	0.5974	0.1039
SC25JL90.DAT	0.0039	0.0051	0.0002	0.1167	0.1724	0.0000	0.1200	0.1356	1.0386	0.8236	0.8843	0.0730
SC26JL90.DAT	0.0226	0.0123	0.0001	0.1636	0.0619	0.0000	0.0604	0.0569	1.1383	1.4522	0.8374	0.3963
SC27JL90.DAT	0.0293	0.0140	0.0010	0.0271	0.0733	0.0000	0.0742	0.0726	1.1246	1.3967	1.0252	0.4164
SC30JL90.DAT	0.0003	0.0014	0.0010	0.2526	0.1762	0.0000	0.1211	0.1372	1.0347	0.7705	0.7484	0.2893
SC31JL90.DAT	0.0007	0.0023	0.0309	0.3309	0.2323	0.0000	0.1437	0.1766	0.9798	0.5377	0.6701	0.0683
SC01AG90.DAT	0.0014	0.0032	0.0277	0.3453	0.2328	0.0000	0.1438	0.1781	0.9775	0.5404	0.6557	0.0610
SC03AG90.DAT	0.0012	0.0029	0.0001	0.0013	0.1376	0.0001	0.1219	0.1302	1.0693	1.1470	1.2697	0.5774
SC06AG90.DAT	0.0035	0.0049	0.0003	0.0421	0.1153	0.0001	0.0956	0.1010	1.0856	1.1543	0.9605	0.0986
SC07AG90.DAT	0.0272	0.0135	0.0003	0.1523	0.1338	0.0000	0.1072	0.1145	1.0678	1.1025	0.8487	0.0858

DATA FILE	KS2	k1	k2	k3	k4
SC19JL90.DAT	0.1315	0.0903	0.0452	0.0491	0.0044
SC20JL90.DAT	0.0036	0.0610	0.0317	0.0458	0.0111
SC25JL90.DAT	0.0613	0.0962	0.0646	0.0708	0.0007
SC26JL90.DAT	0.0218	0.1852	0.0599	0.1235	0.1270
SC27JL90.DAT	0.2749	0.1804	0.0824	0.1290	0.1152
SC30JL90.DAT	0.0979	0.0921	0.0517	0.0741	0.0003
SC31JL90.DAT	0.0822	0.0592	0.0406	0.0591	0.0220
SC01AG90.DAT	0.0717	0.0597	0.0386	0.0621	0.0241
SC03AG90.DAT	0.1628	0.1486	0.1024	0.0501	0.0259
SC06AG90.DAT	0.2531	0.1398	0.0741	0.0514	0.0038
SC07AG90.DAT	0.1691	0.1344	0.0628	0.0351	0.0000

APPENDIX R
SUMMARY 3

RESULTS FOR PAINTED ALUMINUM PLATES

DATA FILES USING MOD350

DATA FILE	SOS	RMS	S1*	HZ:S	NH3	PROD	G	S	KS	k1	k2	k3
SC19JL90.DAT	0.0002	0.0015	0.0008	0.2684	0.0050	0.1761	0.9167	0.8190	0.2096	0.1186	0.1687	0.1280
SC20JL90.DAT	0.0001	0.0008	0.0509	0.2982	0.0040	0.2539	0.8893	0.6593	0.0800	0.0791	0.0723	0.1133
SC25JL90.DAT	0.0025	0.0040	0.0286	0.2549	0.0046	0.1207	0.9937	1.0166	0.1859	0.1278	0.2095	0.1061
SC26JL90.DAT	0.0162	0.0118	0.0001	0.1463	0.0001	0.0070	1.0611	0.9593	0.0766	0.1244	0.3066	0.5252
SC27JL90.DAT	0.0209	0.0138	0.0000	0.2523	0.0366	0.0001	1.1613	1.4353	0.4317	0.2030	0.0927	0.1584
SC30JL90.DAT	0.0007	0.0023	0.0001	0.2399	0.0069	0.1297	0.9665	0.8008	0.2245	0.1159	0.1095	0.0812
SC31JL90.DAT	0.0002	0.0013	0.0214	0.2646	0.0021	0.2245	0.9188	0.6352	0.0701	0.0755	0.1239	0.1006
SC01AG90.DAT	0.0007	0.0023	0.0042	0.2839	0.0001	0.2018	0.9098	0.6509	0.0709	0.0802	0.0745	0.0817
SC03AG90.DAT	0.0020	0.0043	0.0001	0.2667	0.0157	0.0001	1.0603	1.3436	0.4576	0.1878	0.0983	0.1642
SC06AG90.DAT	0.0027	0.0042	0.0154	0.2570	0.0154	0.0002	1.0567	1.4321	0.5102	0.1898	0.1018	0.1607
SC07AG90.DAT	0.0270	0.1323	0.1004	0.2336	0.0047	0.0150	0.9628	1.0059	0.1659	0.1228	0.1459	0.3408

APPENDIX R
SUMMARY 4
RESULTS FOR PAINTED ALUMINUM PLATES
DATA FILES USING MOD360

DATA FILE	SOS	RMS	S1*	HZ:S1	HZ:S2	NH3	Prod	G	S1	S2	KS1	K1
SC19JL90.DAT	0.0004	0.0016	0.1487	0.3345	0.3375	0.0451	0.0923	1.0566	0.4849	1.0009	0.6210	0.4288
SC20JL90.DAT	0.0001	0.0010	0.1893	0.2917	0.3921	0.0334	0.1084	1.0093	0.4810	0.8601	1.7006	0.4641
SC25JL90.DAT	0.0027	0.0042	0.1644	0.3110	0.3192	0.1377	0.0746	1.0873	0.4867	0.9781	0.3094	0.3471
SC26JL90.DAT	0.0118	0.0101	0.2176	0.3095	0.4794	0.1737	0.0333	1.1576	0.5296	1.2498	0.3984	0.5061
SC27JL90.DAT	0.0210	0.0138	0.2160	0.3210	0.4833	0.1866	0.0308	1.1680	0.5371	1.2980	0.8481	0.7155
SC30JL90.DAT	0.0007	0.0021	0.1999	0.2920	0.2881	0.0759	0.0734	1.0840	0.4921	0.8406	0.9037	0.5088
SC31JL90.DAT	0.0004	0.0018	0.1890	0.2943	0.3783	0.0598	0.0870	1.0430	0.4834	0.8300	1.3930	0.5086
SC01AG90.DAT	0.0008	0.0024	0.1765	0.2836	0.4053	0.0573	0.0870	1.0392	0.4602	0.8551	1.1153	0.3828
SC03AG90.DAT	0.0066	0.0066	0.2214	0.3637	0.2106	0.2648	0.0623	1.1057	0.5859	0.6930	0.7708	0.7871
SC06AG90.DAT	0.0049	0.0056	0.2094	0.3194	0.3697	0.1404	0.0532	1.1244	0.5349	1.1978	0.5022	0.5565
SC07AG90.DAT	0.0086	0.0096	0.0369	0.1461	0.1036	0.0189	0.1029	1.0914	0.4642	1.0060	0.7205	0.5168

DATA FILE	K2	K3	K4
SC19JL90.DAT	0.0807	0.0252	0.0003
SC20JL90.DAT	0.0666	0.0125	0.0000
SC25JL90.DAT	0.0778	0.1137	0.0049
SC26JL90.DAT	0.1086	0.1207	0.0000
SC27JL90.DAT	0.1162	0.1079	0.0001
SC30JL90.DAT	0.0653	0.0504	0.0001
SC31JL90.DAT	0.0629	0.0228	0.0002
SC01AG90.DAT	0.0664	0.0214	0.0001
SC03AG90.DAT	0.0551	0.2699	0.0001
SC06AG90.DAT	0.1010	0.1164	0.0000
SC07AG90.DAT	0.1385	0.0976	0.0000

APPENDIX R
SUMMARY 5

RESULTS FOR PAINTED ALUMINUM PLATES

DATA FILES USING MOD361

DATA FILE	SOS	RMS	S1*	HZ:S1	HZ:S2	Prod	NH3	G	S1	S2	KS1	K1
SC19JL90.DAT	0.0004	0.0015	1.2046	0.2234	0.2323	0.2179	0.0462	0.9689	1.4326	0.4659	0.6329	0.3798
SC20JL90.DAT	0.0001	0.0010	1.2937	0.2324	0.2374	0.2324	0.0346	0.9216	1.5261	0.4225	1.1589	0.4359
SC25JL90.DAT	0.0025	0.0041	1.1712	0.1838	0.2705	0.1715	0.1384	1.0123	1.3683	0.5076	0.4599	0.3479
SC26JL90.DAT	0.0204	0.0133	1.2459	0.0652	0.6541	0.0651	0.1844	1.1266	1.3124	0.8777	0.6548	0.1428
SC27JL90.DAT	0.0287	0.0162	1.2331	0.0841	0.6188	0.0839	0.1984	1.1402	1.3282	0.7694	0.3950	0.1692
SC30JL90.DAT	0.0003	0.0013	1.0532	0.2179	0.1859	0.1742	0.0752	1.0126	1.3229	0.2659	0.1056	0.3279
SC31JL90.DAT	0.0008	0.0024	0.5528	0.3891	0.4191	0.1101	0.0618	1.2007	0.9419	1.0460	1.2421	0.3332
SC01AG90.DAT	0.0009	0.0026	0.5097	0.3938	0.4277	0.1118	0.0592	1.1975	0.9042	1.0691	0.4417	0.2274
SC03AG90.DAT	0.0014	0.0030	1.1756	0.1813	0.2907	0.0902	0.2527	1.0272	1.3701	0.4453	0.4588	0.3679
SC06AG90.DAT	0.0047	0.0055	1.2016	0.1741	0.3487	0.1647	0.1416	1.0785	1.3965	0.5268	0.4383	0.2991
SC07AG90.DAT	0.0203	0.0142	1.2596	0.1657	0.3763	0.1551	0.1204	1.0043	1.4253	0.6567	1.2272	0.3753

DATA FILE	K2	K3	K4
SC19JL90.DAT	0.0991	0.6118	0.0451
SC20JL90.DAT	0.1062	0.7956	0.0196
SC25JL90.DAT	0.0953	0.6149	0.1724
SC26JL90.DAT	0.2767	1.5582	0.0558
SC27JL90.DAT	0.3177	7.1939	0.0558
SC30JL90.DAT	0.0337	0.0652	0.0974
SC31JL90.DAT	0.0439	0.0001	0.0183
SC01AG90.DAT	0.0460	0.0001	0.0174
SC03AG90.DAT	0.1304	0.0000	0.5410
SC06AG90.DAT	0.1368	0.9515	0.1113
SC07AG90.DAT	0.1617	0.4620	0.0664

APPENDIX R
SUMMARY 6
RESULTS FOR PAINTED ALUMINUM PLATES
DATA FILES USING MOD370

DATA FILE	SOS	RMS	SI*	HZ:S1	HZ:S2	Prod	NH3	G	S1	S2	KS1	k1
SC19JL90.DAT	0.0002	0.0010	0.2787	0.3951	0.3474	0.3372	0.0435	1.3763	0.7028	0.2779	0.3104	0.3154
SC20JL90.DAT	0.0000	0.0008	0.3263	0.3766	0.4115	0.3451	0.0333	1.3520	0.7055	0.3823	0.3986	0.3186
SC25JL90.DAT	0.0026	0.0041	0.2782	0.3445	0.3609	0.2944	0.1344	1.3877	0.6659	0.3826	0.2704	0.2600
SC26JL90.DAT	0.0134	0.0108	0.4256	0.3323	0.4831	0.3228	0.1783	1.4821	0.7598	0.3576	0.4945	0.3989
SC27JL90.DAT	0.0235	0.0146	0.3630	0.4151	0.4733	0.2426	0.1929	1.4723	0.7914	0.3505	0.3009	0.3903
SC30JL90.DAT	0.0003	0.0015	0.3315	0.3610	0.3359	0.3426	0.1293	1.4112	0.6940	0.2093	0.2887	0.2769
SC31JL90.DAT	0.0002	0.0013	0.3408	0.3467	0.4128	0.3329	0.0601	1.3790	0.6883	0.3635	0.4229	0.3101
SC01AG90.DAT	0.0007	0.0023	0.3211	0.3584	0.4148	0.3333	0.0570	1.3720	0.6817	0.3684	0.3392	0.2809
SC03AG90.DAT	0.0026	0.0042	0.4128	0.3409	0.3644	0.2293	0.2581	1.4100	0.7601	0.1745	0.6529	0.4141
SC06AG90.DAT	0.0025	0.0041	0.2284	0.4772	0.3094	0.2464	0.1366	1.4221	0.7826	0.2578	0.1860	0.3604
SC07AG90.DAT	0.0181	0.0135	0.3218	0.4099	0.3386	0.3647	0.1149	1.4221	0.7479	0.2328	0.3173	0.3505

DATA FILE	k2	k3	k4
SC19JL90.DAT	0.3823	0.3130	0.0215
SC20JL90.DAT	0.7198	0.2073	0.0084
SC25JL90.DAT	0.0117	0.3351	0.0976
SC26JL90.DAT	0.5808	0.5719	0.0726
SC27JL90.DAT	0.4246	0.0795	0.0714
SC30JL90.DAT	0.1987	0.2521	0.0340
SC31JL90.DAT	0.6181	0.2679	0.0148
SC01AG90.DAT	0.5572	0.2125	0.0139
SC03AG90.DAT	0.0361	0.0666	0.2545
SC06AG90.DAT	0.0175	0.0768	0.1152
SC07AG90.DAT	0.1610	0.3865	0.0542

APPENDIX R
SUMMARY 7
RESULTS FOR PAINTED ALUMINUM PLATES
DATA FILES USING MOD375

DATA FILE	SOS	RMS	S1*	Hz:S1	Hz:S2	NH3	Prod	G	S1	S2	KS1	k1
SC19JL90.DAT	0.0205	0.0134	1.7462	0.0515	0.4131	0.0515	0.0535	0.7183	1.7977	0.5290	4.3409	0.9250
SC20JL90.DAT	0.0001	0.0009	1.8353	0.0645	0.4325	0.0320	0.0428	0.7566	1.8998	0.4363	10.8628	1.1520
SC25JL90.DAT	0.0065	0.0065	1.6074	0.1738	0.3057	0.1262	0.0743	0.9247	1.7811	0.4110	2.5926	0.8384
SC26JL90.DAT	0.0371	0.0179	1.7331	0.1487	0.3985	0.1421	0.1593	0.9874	1.8818	0.5534	3.1490	1.0067
SC27JL90.DAT	0.0166	0.0123	1.7401	0.1824	0.4062	0.1706	0.1008	1.0094	1.9226	0.4601	3.0694	1.0746
SC30JL90.DAT	0.0003	0.0013	1.5214	0.1223	0.3403	0.0725	0.0137	0.9081	1.6437	0.3967	1.7803	0.3914
SC31JL90.DAT	0.0012	0.0030	1.7572	0.0707	0.3916	0.0536	0.0678	0.8072	1.8279	0.4090	3.8664	0.9581
SC01AG90.DAT	0.0007	0.0032	1.7217	0.0449	0.4080	0.0308	0.0519	0.8192	1.7667	0.4121	4.7824	0.8392
SC03AG90.DAT	0.0030	0.0053	1.7143	0.3087	0.2624	0.2822	0.0004	1.0102	2.0230	0.4558	2.7896	1.2806
SC06AG90.DAT	0.0035	0.0058	1.7437	0.1558	0.3929	0.1436	0.0464	0.9026	1.8995	0.6665	3.6844	1.1444
SC07AG90.DAT	0.0183	0.0135	1.6779	0.1297	0.4056	0.1066	0.0330	0.8654	1.8076	0.6463	7.2091	0.9968

DATA FILE	K2	K3	K4
SC19JL90.DAT	0.2314	1.2760	0.0111
SC20JL90.DAT	0.4973	0.0734	0.0111
SC25JL90.DAT	0.2490	0.2389	0.0654
SC26JL90.DAT	0.2299	0.4370	0.1226
SC27JL90.DAT	0.4026	0.3915	0.0644
SC30JL90.DAT	0.4530	0.1688	0.0093
SC31JL90.DAT	0.2113	0.1364	0.0198
SC01AG90.DAT	0.4463	0.2174	0.0267
SC03AG90.DAT	0.1712	0.3682	0.0001
SC06AG90.DAT	0.2468	0.3893	0.0228
SC07AG90.DAT	0.3078	0.2600	0.0119

APPENDIX R
SUMMARY 8
RESULTS FOR PAINTED ALUMINUM PLATES
DATA FILES USING MOD380

DATA FILE	SOS	RMS	Hz:S1	I	NH3	G	k1	k2	k3	S1
SC19JL90.DAT	0.0089	0.0077	0.0951	0.0615	0.0586	0.4552	1.4542	0.3805	4.4320	0.0575
SC20JL90.DAT	0.0058	0.0087	0.0632	0.0437	0.0431	0.3315	1.8462	0.2701	9.6475	0.0299
SC25JL90.DAT	0.0059	0.0062	0.1505	0.1367	0.1342	0.6545	0.3211	1.5403	8.6474	0.1417
SC26JL90.DAT	0.1519	0.0362	0.2768	0.2156	0.2092	0.8075	1.3417	0.4751	4.5370	0.1003
SC27JL90.DAT	0.1308	0.0345	0.2840	0.2297	0.2235	0.8407	1.3237	0.5127	4.5205	0.0907
SC30JL90.DAT	0.0287	0.0152	0.1423	0.1326	0.1307	0.6158	1.4296	0.8249	4.1779	0.0215
SC31JL90.DAT	0.6481	0.0701	0.0003	0.0000	0.0003	0.6899	0.4348	1.1237	2.1558	0.0487
SC01AG90.DAT	0.0042	0.0056	0.0771	0.0665	0.0656	0.4110	1.4456	0.5878	7.0236	0.0232
SC03AG90.DAT	0.0306	0.0142	0.3119	0.2496	0.2480	0.9906	0.7085	0.3850	15.7530	0.1031
SC06AG90.DAT	0.0119	0.0106	0.7302	0.1629	0.1591	1.1991	1.0070	0.0327	4.9065	0.6086
SC07AG90.DAT	0.0679	0.0261	0.2107	0.1531	0.1476	0.6669	1.4117	0.4092	4.3302	0.0928

APPENDIX R
SUMMARY 9
RESULTS FOR PAINTED ALUMINUM PLATES
DATA FILES USING MOD385

DATA FILE	SOS	RMS	HZ:S	I	NH3	Prod	G	k1	k2	k3	S	k4
SC19JL90.DAT	0.0163	0.0119	0.3263	0.1360	0.0940	0.0337	0.7506	1.5480	0.0273	1.0926	0.4425	0.4206
SC20JL90.DAT	0.0649	0.0292	0.2505	0.1320	0.0823	0.0357	0.6981	1.5760	0.0398	1.0872	0.3605	0.0007
SC25JL90.DAT	0.2001	0.0360	0.4082	0.2483	0.1685	0.0401	1.1111	1.7280	0.0773	1.2260	0.6148	0.0318
SC26JL90.DAT	2.4630	0.1457	0.4912	0.3615	0.2442	0.0804	1.1710	1.7890	0.0620	1.2935	0.8061	0.1403
SC27JL90.DAT	1.3380	0.1103	0.4727	0.3455	0.2539	0.0550	1.1547	1.7710	0.0620	1.2734	0.7735	0.1150
SC30JL90.DAT	0.3058	0.0446	0.3931	0.2109	0.1288	0.0506	1.1222	1.7360	0.0671	1.2315	0.5716	0.0386
SC31JL90.DAT	0.0313	0.0154	0.1877	0.1630	0.0908	0.0619	0.7394	1.5610	0.0436	1.0349	0.3323	0.4554
SC01AG90.DAT	0.0061	0.0068	0.2393	0.1353	0.0703	0.0560	0.7175	1.5530	0.0386	1.0099	0.3545	0.5941
SC03AG90.DAT	0.0154	0.0121	0.1962	0.3715	0.3185	0.0244	1.0645	1.7070	0.0665	1.2315	0.5414	0.0931
SC06AG90.DAT	0.2129	0.0448	0.4444	0.2996	0.2160	0.0494	1.1397	1.7540	0.0618	1.2536	0.7044	0.0885
SC07AG90.DAT	0.0863	0.0294	0.4640	0.2287	0.1620	0.0378	1.1019	1.7290	0.0549	1.2338	0.6574	0.0739

APPENDIX R
SUMMARY 10
RESULTS FOR PAINTED ALUMINUM PLATES

DATA FILES USING MOD390

DATA FILE	SOS	RMS	Hz:S	I	NH3	Prod	G	K1	K2	K3	S	K4
SC19JL90.DAT	3.3886	0.1724	0.0000	0.1991	0.3925	0.4452	0.1265	0.0287	3.9535	5.2332	7.2432	4.0838
SC20JL90.DAT		no fit										
SC25JL90.DAT		no fit										
SC26JL90.DAT		no fit										
SC27JL90.DAT		no fit										
SC30JL90.DAT		no fit										
SC31JL90.DAT		no fit										
SC01AG90.DAT		no fit										
SC03AG90.DAT		no fit										
SC06AG90.DAT		no fit										
SC07AG90.DAT	0.0917	0.0312	0.0074	0.0854	0.0101	0.0505	0.6904	0.8690	0.0775	0.7853	1.3076	1.1279

The models with numbers listed here were also very poor.

APPENDIX S

REPRESENTATIVE MODEL FITS -- PLOTS FOR HYDRAZINE AND AMMONIA (SINGLE, SELECTED RUNS)

The following figures illustrate the best fits for representative data sets with variation on chamber conditions and type of available reactive surface sites. The models which yielded the best results were chosen based on SOS and RMS values. Examples of fits by all models are not shown. Certain models consistently gave poor fits and were never able to give the "best" fit for any of the data sets.

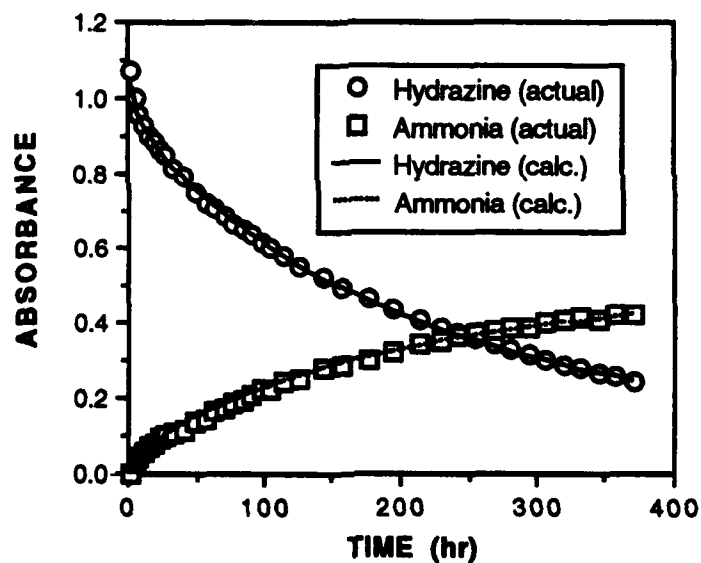


Figure S1. Model (MOD361) Fits for Hydrazine and Ammonia for the Run Conducted on 18 Apr 90 (Dry Helium, no Plates)

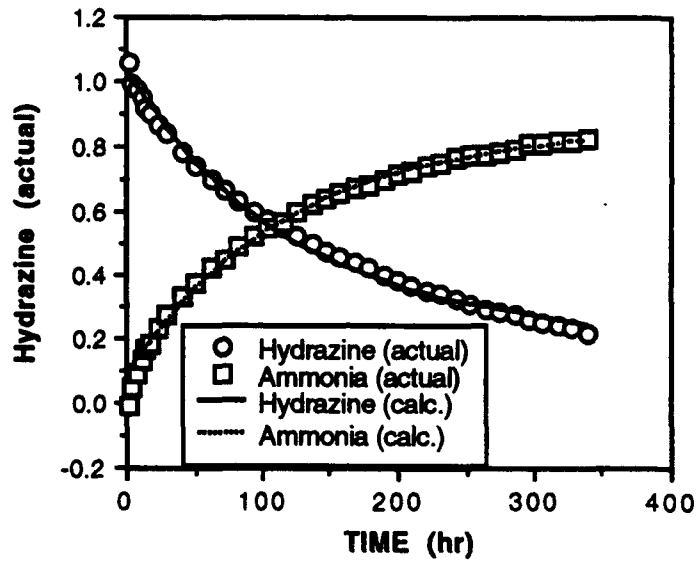


Figure S2 Model (MOD361) Fits for Hydrazine and Ammonia for the Run Conducted on 18 Apr 90 (Dry Helium, no Plates)

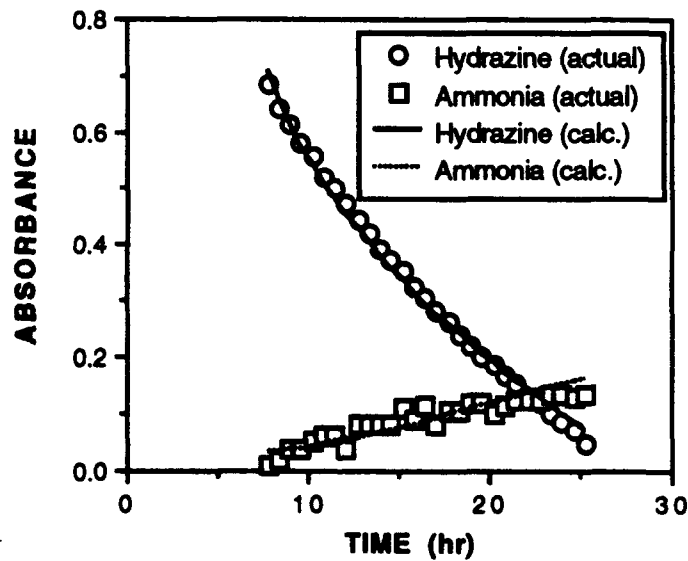


Figure S3. Model (MOD310) Fits for Hydrazine and Ammonia for the Run Conducted on 25 May 90 (80 Percent Dry Helium and 20 Percent Oxygen, No Plates)

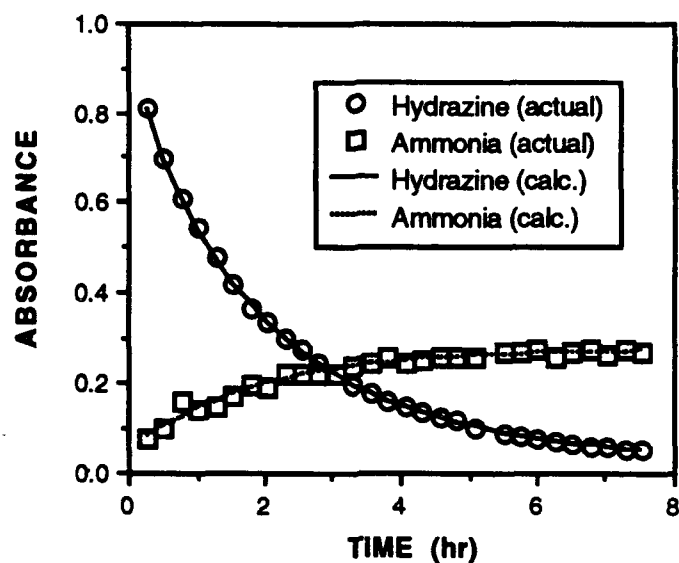


Figure S4. Model (MOD361) Fits for Hydrazine and Ammonia for the Run Conducted on 04 Jun 90 (80 Percent Humid Helium and 20 Percent Oxygen, No Plates)

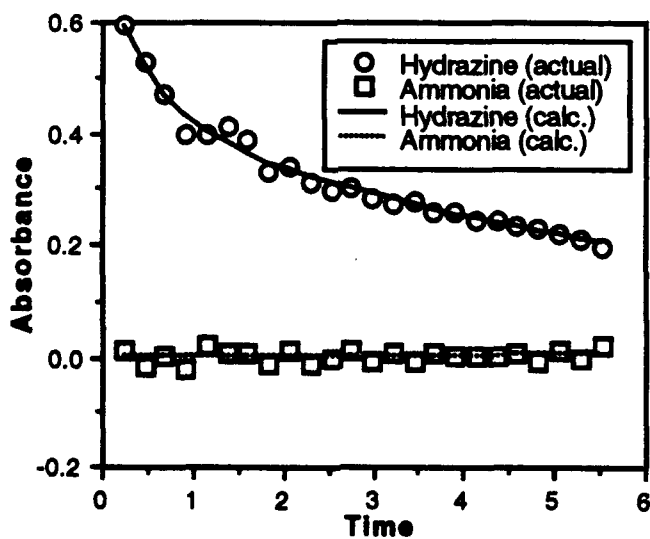


Figure S5. Model (MOD370) Fits for Hydrazine and Ammonia for the Run Conducted on 16 Jan 90 (80 Percent Humid Helium and 20 Percent Oxygen, with 19 Black Iron Plates)

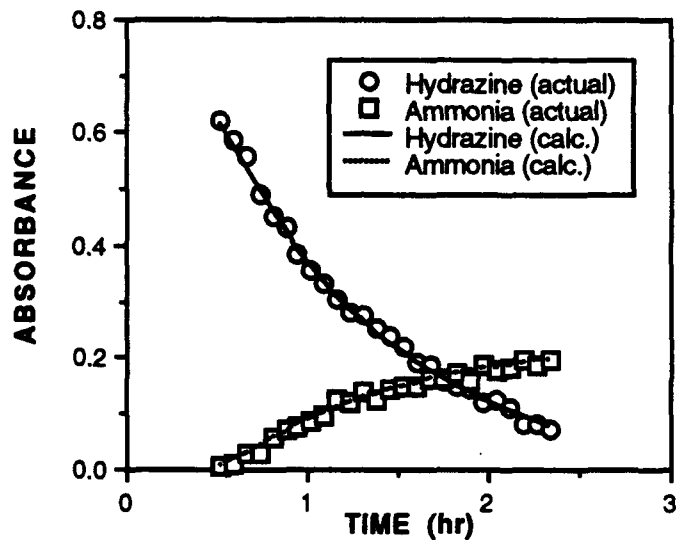


Figure S6. Model (MOD370) Fits for Hydrazine and Ammonia for the Run Conducted on 20 Jul 90 (80 Percent Dry Helium and 20 Percent Oxygen, with 20 Painted Aluminum Plates)

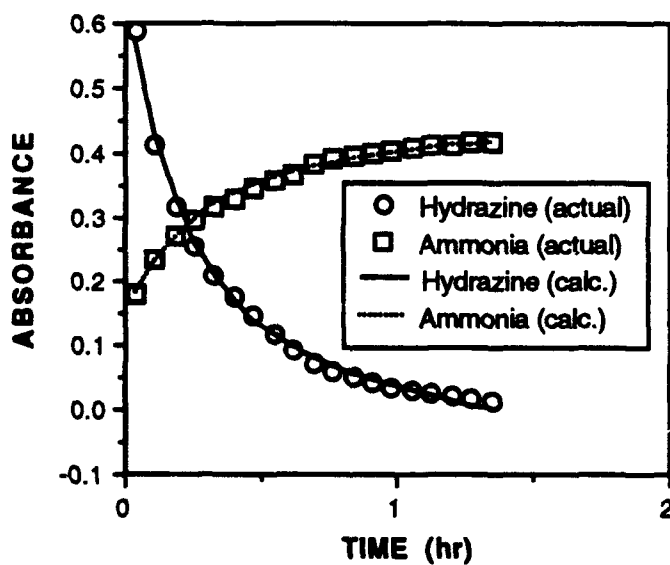


Figure S7. Model (MOD360) Fits for Hydrazine and Ammonia for the Run Conducted on 04 Jan 90 (80 Percent Dry Helium and 20 Percent Oxygen, with 19 Black Iron Plates)

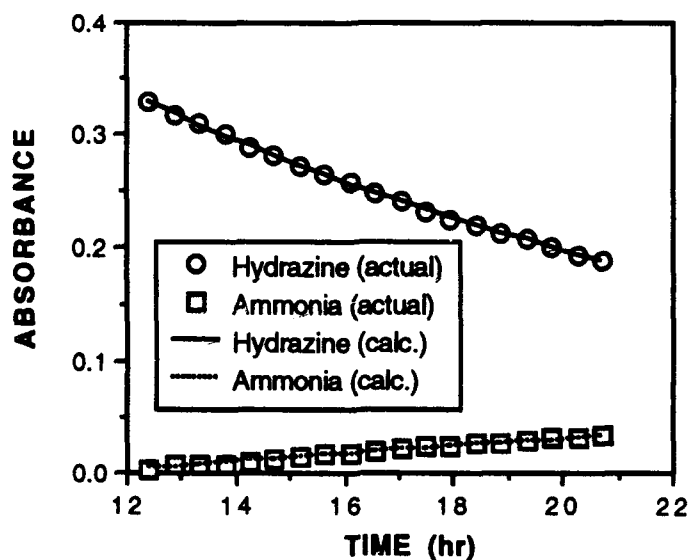


Figure S8 Model (MOD350) Fits for Hydrazine and Ammonia for the Run Conducted on 11 Jan 90 (80 Percent Dry Helium and 20 Percent Oxygen, with 19 Black Iron Plates)

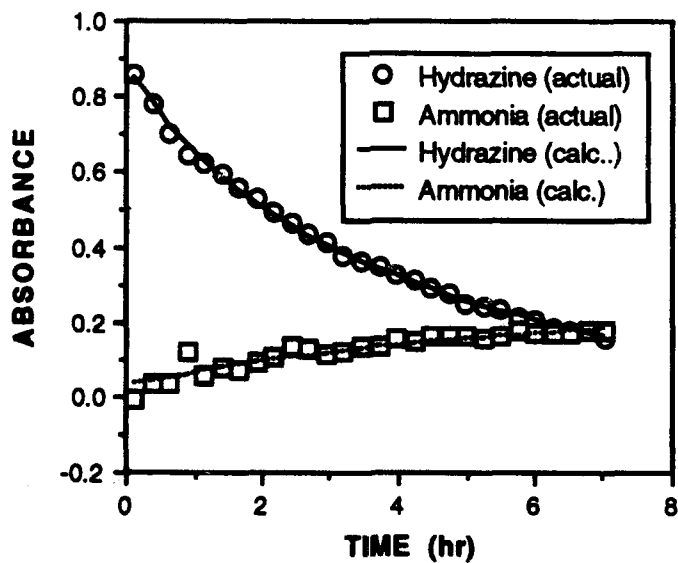


Figure S9. Model (MOD310) Fits for Hydrazine and Ammonia for the Run Conducted on 27 Jul 90 (80 Percent Dry Helium and 20 Percent Oxygen, with 20 Painted Aluminum Plates)

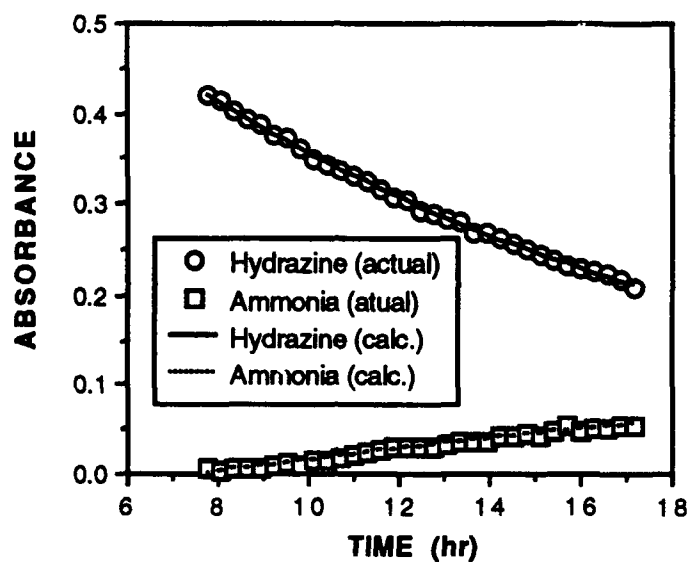


Figure S10. Model (MOD350) Fits for Hydrazine and Ammonia for the Run Conducted on 01 Aug 90 (Humid Helium 20 Painted Aluminum Plates)

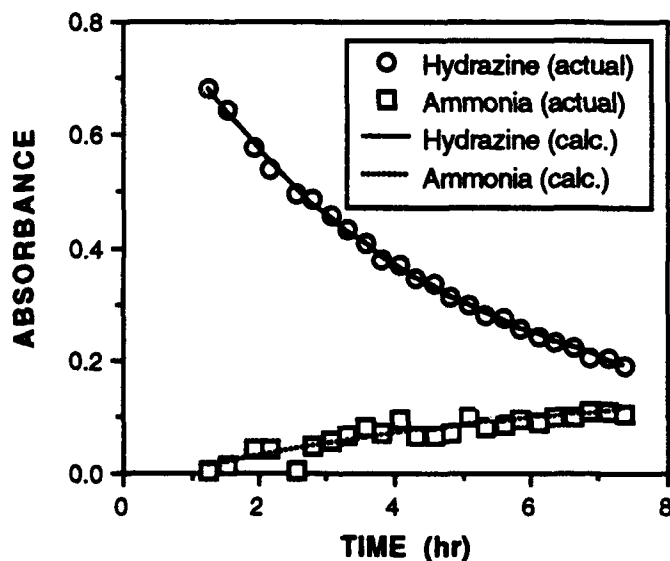


Figure S11 Model (MOD310) Fits for Hydrazine and Ammonia for the Run Conducted on 07 Aug 90 (80 Percent Humid Helium and 20 Percent Oxygen, with 20 Painted Aluminum Plates)

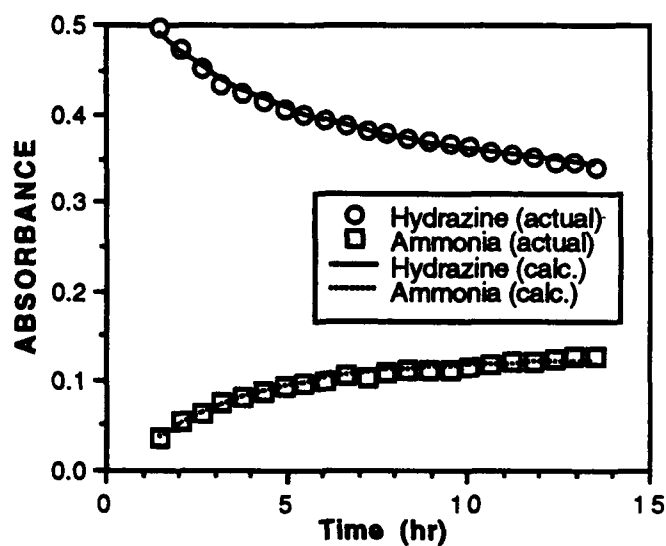


Figure S12. Model (MOD315) Fits for Hydrazine and Ammonia for the Run Conducted on 15 Mar 90 (Dry Helium and 1 Corroded Aluminum Plate)

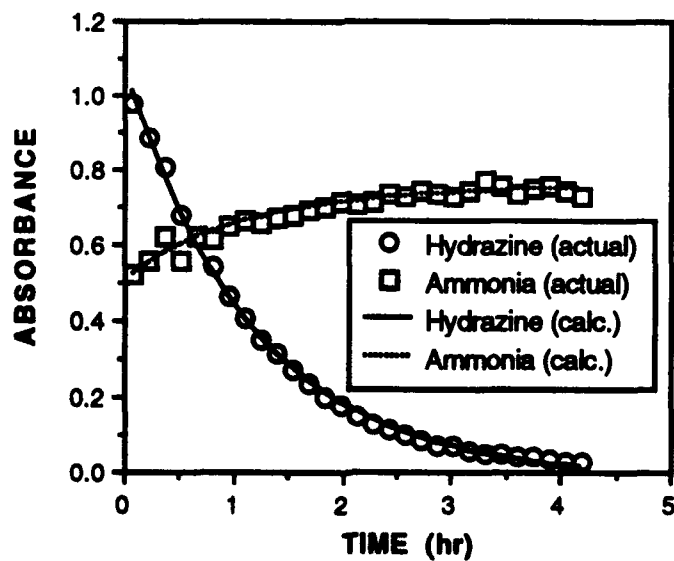


Figure S13. Model (MOD315) Fits for Hydrazine and Ammonia for the Run Conducted on 27 Mar 90 (80 Percent Dry Helium and 20 Percent Oxygen, with 1 Corroded Aluminum Plate)

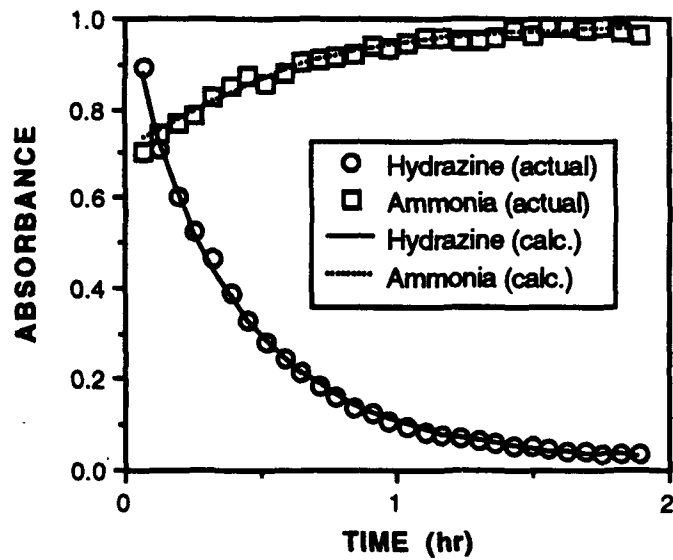


Figure S14. Model (MOD375) Fits for Hydrazine and Ammonia for the Run Conducted on 29 Mar 90 (80 Percent Humid Helium and 20 Percent Oxygen, with 1 Corroded Aluminum Plate)


```

c
c e1 = x8-x1-x2
c dx(1)/dt = k1*(x4-x1)(s1-x1+x2) = x5 * (x4-x1) * e1
c dx(2)/dt = k2*(x1-x2) = x6 * x1-x2)
c dx(3)/dt = k3*(x2-x3) = x7 * (x2-x3)
c
c y = x4-x2-x3-x1 (Hydrazine measured)
c y2 = x(3) NH3
c
c
c for two error estimation the second state x(3) is also measured
c-----
C WITH MICROSOFT F77 LIMITATIONS 5/24/89 AT TAFB
C$NOTRUNCATE or and comment IMPLICIT NONE in every module and routine
C MODIFIED 2/8/89 TO USE GIL FORM OF INTEGRATION
C MODIFIED TO INCLUDE NORMAL EQUATION SOLUTIONS
c nov 15, 1988 modified number of points, so as to take
c different number of steps between points
c DOUBLE precision
c2345678912345678921234567893123456789412345678951234567896123456789712
    implicit none
    integer*4 m,n,p,max_points
    integer*4 no_iterations
    integer*4 NUM_STATE, NUM_PARAM
    integer*4 NUM_MEASU, NUM_DATAP
    integer*4 max_inject
c *****
c * THE NUM_STATE & NUM_PARAM MUST BE DEFINED FOR EACH NEW MODEL *
c *****
    PARAMETER (NUM_STATE = 4)
    PARAMETER (NUM_PARAM = 4)
c experimental
c
c *****
c * M & N MUST BE DEFINED FOR EACH NEW MODEL *
c *****
    parameter (m = 8)
c m = then number of state variable plus number of parameters to estimate
    parameter (n = 9)
c n = number of states (m) plus 1
    parameter (p = 2)
c p = number of measurement variables, 2 for two measurements 12/30/89
    parameter (max_inject = 2 )
c *****
c * MAX_POINTS MUST BE DEFINED FOR EACH NEW MODEL *
c *****
    parameter (max_points = 90)
    logical with_invert, with_weight, with_noise
    logical partials
    integer*4 i,j,data_point
    integer*4 steps, loops
    real*8 zsigma,zbar
    real*8 noise(max_points+1,P), work_noise(max_points+1)
    real*8 state( m,n)

```

```

real*8 state_jacobian( num_state, num_state)
real*8 param_jacobian( num_state, num_param)
real*8 start_state( m)
c          system is the states plus state Jacobian
c          (partials) and parameter Jacobian (partials)
real*8 y( max_points+1, p)
real*8 yhat( max_points+1, p)
real*8 delta, t
real*8 s0, std_dev
c s0 is a initial condition constant
c st_dev is the std deviation of the measurement errors
real*8 weight( p*max_points, p*max_points)
real*8 tt( max_points+1)
real*8 ttold
real*8 a( p*max_points, m)
real*8 at( m, p*max_points)
real*8 error( p*max_points, 1)
real*8 HOLD_a( p*max_points, m)
real*8 HOLD_at( m, p*max_points)
real*8 HOLD_error( p*max_points, 1)
real*8 atw( m, p*max_points)
real*8 gamma_inv( m, m)
real*8 gat( m, p*max_points)
real*8 gatw( m, p*max_points)
real*8 delx( m, 1)
real*8 sum_error_sq
real*8 dt, rms
c z is real number work space, rcond is an estimate of the condition
c of the matrix to invert
real*8 z( m), rcond
c kpvt is the pivot information for inverse
integer*4 kvpt( m)
integer*4 cond
c
c modified 2/20/89 to include Singular Value Decomposition
logical with_svd
real*8 svdW( p*max_points)
real*8 svdU( p*max_points, m)
real*8 svdUt( m, p*max_points)
real*8 svdV( m, m)
real*8 svdS( m)
real*8 svdE( m)
real*8 svdSplus( m, m)
real*8 svdVS( m, m)
real*8 svdAplus( m, p*max_points)
integer*4 svdJOB
integer*4 svdINFO
c modified 3/5/89 to solve the Marquardt algorithm
real*8 marqLamda
real*8 ORIGLamda
real*8 marqSumSq( 6)
real*8 marqRMS( 6)
c-----
c 06/05/89 added to inner loop from marqstoneidsd4c.for

```

```

real*8 oldmarqSumSq
integer*4 inner_loop
c-----
real*8 marqV
real*8 marqMean( m)
real*8 marqSigma( m)
real*8 marqSigmaSq( m)
real*8 marqB( p*max_points)
real*8 marqDeltaSumSq
real*8 marqEpsilon(2)
real*8 marqState( m,1)
c-----
character*40 ptsfile
character*40 initfile
character*40 outfile
character*40 parfile
character*40 endfile
character*4 extension
character*40 newfile
character*40 eigfile
character*1 string
integer*4 location
c-----
c FOR SIZE INDEPENDENT INTEGRATION
real*8 left1( M,N)
real*8 left2( M,N)
real*8 right1(M,N)
real*8 right2(M,N)
real*8 temp( M,N)
c-----
c FOR SEQUENTIAL RUNS
integer*4 no_injections
real*8 inject_time( max_inject)
real*8 concentration( max_inject)
real*8 s0_original
logical sequential
c-----
integer*4 marqLoop_count
integer*4 lamda
logical TRUE, FALSE
logical marqDone
c-----
integer*4 repeat
c-----
c FOR EIGENVALUES AND EIGENVECTORS CALC
real*8 eigenvalues( m)
real*8 eigenvectors( m,m)
real*8 eigennorms( m)
real*8 fv1( m) ! temporary storage for eigenvalue calc
real*8 fv2( m) ! temporary storage for eigenvalue calc
integer*4 eigen_ierr ! on return, 0 if ok, not 0 for jth eigenvalue
integer*4 matz ! if zero eigenvalues only, not zero both
c-----
logical force_zero

```

```

c-----
      real*8 store_Lamda( 4)
      real*8 hold_state( m)
      real*8 end_state( m)
      real*8 hold_end( m,4)
      real*8 hold_deltax( m,4)
      real*8 lamdaMAX
      logical scale_it
c-----
      TRUE = .TRUE.
      FALSE = ( .not. TRUE)
c
      marqDone = FALSE
      lamdaMAX= 1.0d5
      cond = 1
c cond is condition number check flag, 1 means with condition checking
c 0 means withOUT condition checking
c
c-----
c
c      read in the initial conditions and logical flags
      print *, 'For the initial conditions '
      call GETFILN( initfile)

c      initialize state variables
      call INIT_STATE( state, m,n,delta,s0, std_dev,
& with_invert, with_weight,
& zsigma, zbar, with_noise,
& with_svd,
& marqV, marqLamda, marqEpsilon,
& initfile,
& NO_ITERATIONS, partials,
& sequential, no_injections, inject_time, concentration,
& max_inject, num_datap,
& force_zero, scale_it)
      s0_original = s0
      repeat = m
      NUM_MEASU = P

c-----
c
c      initialize weight matrix
      if (with_weight) then
          call ICOVAR( weight, p*max_points, p*max_points, std_dev,
& num_measur* num_datap)
      endif
c      read in the time and data points
      print *, 'For real time data points'
      call GETFILN( ptsfile)
      call GETRTDATA( tt, y, max_points, p, ptsfile, num_datap,
& num_measur)
c
c-----
c      add noise if requested

```

```

    if ( with_noise) then
      call ADDNOISE( y, zsigma, zbar, noise, max_points, p,
&                work_noise, NUM_DATAP, NUM_MEASU)
    endif
c
c-----
c  form several new files for output of calculated data
  string = '.'
  call FINDSUBSTRING( ptsfile, string, location)
  extension = '.par'
  call FORMEXTENSION( ptsfile, extension, location, parfile)
  print *, 'A file ',parfile,' will be opened for ',
&        'estimated parameters '
c
  string = '.'
  call FINDSUBSTRING( ptsfile, string, location)
  extension = '.out'
  call FORMEXTENSION( ptsfile, extension, location, outfile)
  print *, 'A file ',outfile,' will be opened for ',
&        'estimated initial data points'
  string = '.'
  call FINDSUBSTRING( ptsfile, string, location)
  extension = '.end'
  call FORMEXTENSION( ptsfile, extension, location, endfile)
  print *, 'A file ',endfile,' will be opened for ',
&        'estimated final data points'
c
c-----
c
  marqSumSq( 1) = 0.0d0
  marqSumSq( 2) = 0.0d0
  marqSumSq( 3) = 0.0d0
  marqSumSq( 4) = 0.0d0
  marqSumSq( 5) = 0.0d0
  marqSumSq( 6) = 0.0d0
  marqLoop_count = 1
  LOOPS = 0
C-----
C  OPEN ending estimates FILE
  open( unit = 21, file= endfile, status='new')
C  OPEN AND WRITE INITIAL VALUES TO PARAMETER FILE
  open( unit = 18, file= parfile, status='new')
  write( 18, 202) sum_error_sq, rms
  write( 18, 203) (state(i,1),i=1, REPEAT)
c  write( 18, 203) (state(i,1),i=1, REPEAT/2)
c  write( 18, 203) (state(i,1),i=(repeat/2+1), REPEAT)
202  format( 2E11.4)
203  format( 15f10.4)
c203  format( 15f10.4, 2E11.4)
c-----
  ORIGLamda = marqLamda
  do 1000, i= 1, REPEAT
    hold_state( i) = state( i,1)
1000  CONTINUE

```



```

& error, num_datap*num_m measu, 1)
c decrease LAMDA and calculate new DELTA X
  marqLamda = marqlamda / marqV
  store_lamda( 2) = marqLamda
  print *, 'lamda for 2nd calculation = ', marqLamda
c calculate DELTA X based upon the new values of LAMDA
  call DGEAXEB( with_invert, with_weight,
& i, j, s0, std_dev, weight,
& a, at, atw, gamma_inv,
& gat, gatw, error, delx,
& z, rcond, kvpt, cond,
& with_svd, svdW, svdU,
& svdUt, svdV, svdS,
& svdE, svdSplus, svdVS,
& svdAplus, svdJOB, svdINFO,
& marqLamda, marqV,
& marqMean, marqSigma, marqSigmaSq, marqB,
& m, n, p, max_points,
& NUM_STATE, NUM_PARAM, NUM_MEASU, NUM_DATAP, scale_it)
c hold the DELTA X values until we see which SOS is least
c and store final integrated state
  do 1042, i = 1, REPEAT
    hold_deltax( i,2) = delx( i,1)
  c    print *, 'delta x for decreased lamda= ', delx( i,1)
    state( i,1) = hold_state( i) + delx( i,1)
    if (force_zero ) then
      if (state( i,1) .lt. 0.0) then
        state( i,1) = hold_state( i)
      endif
    endif
  endif
1042  CONTINUE
c-----
c-----
c calculate first SOS with nominal values of X for STATES ONLY
  sum_error_sq = 0.0d0
  call DGSPDEQ( data_point, steps, loops,
& state, y, delta, t, s0,
& tt, ttold, error,
& delx, sum_error_sq, dt, rms,
& m, n, p, max_points,
& LEFT1, LEFT2, RIGHT1, RIGHT2, TEMP,
& NUM_STATE, NUM_PARAM,
& sequential, no_injections, inject_time, concentration,
& max_inject, s0_original, num_m measu, num_datap, yhat)
c-----
c-----
c store final state
  do 1052, i = 1, REPEAT
    hold_end( i,2) = state( i,1)
1052  CONTINUE
  marqSumSq( 2) = sum_error_sq
  marqRMS( 2) = rms
  print *, 'sum errors squared = ', sum_error_sq
  print *, 'rms of the errors = ', rms

```



```

do 3014, i= 1, REPEAT
  state( i,1) = hold_state( i)
3014 CONTINUE
  call DGEMTCP( HOLD_at, m, p*max_points,
&               at, m, num_datap*num_m measu)
  call DGEMTCP( HOLD_a, p*max_points, m,
&               a, num_datap*num_m measu, m)
  call DGEMTCP( HOLD_error, p*max_points, 1,
&               error, num_datap*num_m measu, 1)
c increase LAMDA from previous gradient and calculate new DELTA X
  marqLamda = store_lamda( 4) * marqV
  store_lamda( 4) = marqLamda
  print *, 'lamda for inner loop calculation = ', marqLamda
c calculate DELTA X based upon the new values of LAMDA
  call DGEAXEB( with_invert, with_weight,
&               i, j, s0, std_dev, weight,
&               a, at, atw, gamma_inv,
&               gat, gatw, error, delx,
&               z, rcond, kvpt, cond,
&               with_svd, svdW, svdU,
&               svdUt, svdV, svdS,
&               svdE, svdSplus, svdVS,
&               svdAplus, svdJOB, svdINFO,
&               marqLamda, marqV,
&               marqMean, marqSigma, marqSigmaSq, marqB,
&               m, n, p, max_points,
&               NUM_STATE, NUM_PARAM, NUM_MEASU, NUM_DATAP, scale_it)
c hold the DELTA X values until we see which SOS is least
c and store final integrated state
c and then set state to NEW initial state
  do 1044, i = 1, REPEAT
    hold_deltax( i,4) = delx( i,1)
c    print *, 'delta x for increased lamda= ', delx( i,1)
    state( i,1) = hold_state( i) + delx( i,1)
    if (force_zero ) then
      if (state( i,1) .lt. 0.0) then
        state( i,1) = hold_state( i)
      endif
    endif
  endif
1044 CONTINUE
c -----
c -----
c calculate SOS with new values of X for STATES ONLY
  sum_error_sq = 0.0d0
  call DGSPDEQ( data_point, steps, loops,
&               state, y, delta, t, s0,
&               tt, ttold, error,
&               delx, sum_error_sq, dt, rms,
&               m, n, p, max_points,
&               LEFT1, LEFT2, RIGHT1, RIGHT2, TEMP,
&               NUM_STATE, NUM_PARAM,
&               sequential, no_injections, inject_time, concentration,
&               max_inject, s0_original, num_m measu, num_datap, yhat)
c -----

```



```

DO 5000 i = 1, NUM_DATAP
    write( 20, 201) tt( i+1),
&        ( y( i+1, j),j=1,num_m measu ),
&        (yhat( i, j),j=1,num_m measu ),
&        ( (y( i+1, j)- yhat( i,j) ),j=1,num_m measu )
201 format ( f10.4, 3( 15f10.5))
5000 CONTINUE
    close (unit=20)

```

c-----

```

c   FOR EIGENVALUES AND EIGENVECTORS OF FINAL COVARIANCE MATRIX
c   request both eigenvalues and eigenvectors
    if( with_invert) then
        string = '.'
        call FINDSUBSTRING( ptsfile, string, location)
        extension = '.eig'
        call FORMEXTENSION( ptsfile, extension, location, eigfile)
        print *, 'A file ', eigfile, ' will be opened for ',
&        'eigenvalues of final covariance'
        matz = 1
        open( unit = 20, file= eigfile, status='new')
        call RS( m, m, gamma_inv, eigenvalues, matz, eigenvectors,
&        fv1, fv2, eigen_ierr)
        print *, 'the eigenvalues of A are...'
        write( 6, 15) ( eigenvalues(i), i=1, m)
        write( 20,15) ( eigenvalues(i), i=1,m)
        print *, 'the eigenvectors of A in column form are...'
        do i=1, m
            write( 6,15) (eigenvectors(i,j), j=1, m)
            write( 20,15) (eigenvectors(i,j), j=1, m)
        enddo
        call vecnorm( eigenvectors, m, m, eigennorms)
        print *, 'the eigenvector norms of A are...'
        write( 6, 15) ( eigennorms(i), i=1, m)
        write( 20, 15) ( eigennorms(i), i=1, m)
        close( unit=20)
    else
        print *, 'inverse of covariance not formed, so no eigenvalues'
    endif
    stop
end
subroutine wrt_state( end_state, state, sum_error_sq, rms,
&        m, repeat)
    implicit none
    integer*4 m, repeat, i
    real*8 state( m, m+1)
    real*8 end_state( m)
    real*8 sum_error_sq
    real*8 rms
c   write ending states and convergence criterion to endfile
    write( 21, 202) sum_error_sq, rms
    write( 21, 203) (end_state(i),i=1, REPEAT)
c   write beginning states and convergence criterion to parfile
    write( 18, 202) sum_error_sq, rms

```

```

        write( 18, 203) (state(i,1),i=1, REPEAT)
202  format( 2E11.4)
203  format( 15f10.4)
c203  format( 15f10.4, 2E11.4)
c-----
c      write( 6,12) (state(i,1),i=1, REPEAT)
12   format( 15f10.5)
      return
      end
      subroutine vecnorm( matrix, row, col, norms)
      implicit none
      integer*4 i,j
      integer*4 row
      integer*4 col
      real*8 matrix( row, col)
      real*8 norms( col)
      do i=1, col
         norms( i) = 0.0d0
         do j=1, row
            norms( i) = norms( i) + matrix( i,j)**2
         enddo
         norms( i) = DSQRT( norms( i))
      enddo
      return
      end

c-----
c the following routines MAY BE APPLICATION SPECIFIC
c and are associated with a FOUR PARAMETER estimation
c of the 2ND order CATALYTIC adsorption loss equations
c WITH estimation of the initial concentration of HZ
c-----
      subroutine extract_a2( a, rows, m, data_point, state,
&                          n, at,
&                          NUM_STATE, NUM_PARAM, num_measu)
      implicit none
c-----
c This routine extracts the proper form of the jacobian matrix
c based upon the partial of the measurement with respect to the
c states. It is symbolically the partial of H (the algebraic form
c of the measurement) with respect to X (the states, and the
c parameters). If the measurment was nonlinear in the states,
c this subroutine would include nonlinear terms.
c
c      functions called          none
c      subroutines called       none
c-----
      integer*4 NUM_STATE, NUM_PARAM
      integer*4 NUM_MEASU
      integer*4 rows
      integer*4 m
      integer*4 data_point
      integer*4 n
      integer*4 j,i

```

```

      real*8    a( rows,m)
      real*8    state( m,n)
      real*8    at( m,rows)
      integer*4 pointer
      pointer = num_m measu*( data_point -1) +1
c     pointer will advance 1,2,3,4,... if num_m measu = 1
c     pointer will advance 1,3,5,7,... if num_m measu = 2
c     so if two measurements, for the second measurement
c     the proper extraction would be a( pointer+1,1)
      do 100,j = 1, NUM_STATE
c-----
c       edit a to reflect model
c     *****
c     *   A MUST BE DEFINED FOR EACH NEW MODEL   *
c     *****
c
      A( pointer, j) = -STATE( 1, j+1)-state( 2, j+1)
      &
      &               -state( 3,j+1)
      &
      &               +state( 4, j+1)
c for the second measurement
      A( pointer+1, j) = STATE( 3, j+1)

c experimental
c-----
      do 110 i=0, (num_m measu-1)
        AT(j, pointer+i)= A( pointer+i, j)
c for the second measurement
110      continue
c       AT(j, pointer+1)= A( pointer+1, j)
100      CONTINUE
      do 200, j = 1, NUM_PARAM
c-----
c       edit a to reflect model
      A( pointer, j+NUM_STATE ) = -STATE( 3, j+NUM_STATE+1)
      &
      &               -STATE( 1, j+NUM_STATE+1)
      &
      &               -state( 2, j+Num_State+1)
      &
      &               +state( 4, j+Num_State+1)
c for the second measurement
      A( pointer+1, j+NUM_STATE ) = STATE( 3, j+NUM_STATE+1)
c-----
      do 210 i=0, (num_m measu-1)
        AT(j+NUM_STATE, pointer+i) = A( pointer+i, j+NUM_STATE )
210      continue
c for the second measurement
c       AT(j+NUM_STATE, pointer+1) = A( pointer+1, j+NUM_STATE )
200      CONTINUE
      return
      end

c-----
c the following routines are APPLICATION SPECIFIC
c and are associated with a five PARAMETER estimation
c of the 2ND order irreversible oxidation equations
c WITH estimation of the initial concentration of HZ

```

```

c-----
      subroutine form_error( error, e_rows, e_cols, data_point,
&                          y, y_rows, y_cols, state, m, n,
&                          sum_error_sq, s0, NUM_MEASU, yhat)
c-----
c This routine forms the error between the measurement(s) an
c the estimated output of the alegbraic equation y = function
c (of states and parameters). The sum of the errors is also
c calculated.
c
c   functions called          none
c   subroutines called       none
c-----
      implicit none
      integer*4 num_measur
      integer*4 e_rows, e_cols
      integer*4 y_rows, y_cols
      integer*4 m,n,i
      integer*4 data_point
      real*8    error( e_rows, e_cols)
      real*8    y( y_rows, y_cols)
      real*8 yhat( y_rows, y_cols)
      real*8    state( m,n)
      real*8    sum_error_sq
      real*8    s0
      integer*4 pointer
c   e(i) = y -yhat = y - ( x4 - x1 - x3)
c   e( i+1) = x2 - x2hat
      pointer = num_measur*( data_point -1) +1
c   pointer will advance 1,2,3,4,... if num_measur = 1
c   pointer will advance 1,3,5,7,... if num_measur = 2
c   so if two measurements, for the second measurement
c   the proper error would be error( pointer+1,1)
c   the second measurement for the same sample time is y( i,2)
c-----
c   edit yhat to reflect model
c *****
c *   YHAT MUST BE DEFINED FOR EACH NEW MODEL   *
c *****
c
      yhat( data_point, 1) = state( 4,1)- state( 3,1)- state( 2,1)
&                          - state( 1,1)
      yhat( data_point, 2) = state( 3,1)
c-----
      do 100 i= 0, ( num_measur -1)
          error( pointer+i ,1) = y( data_point+1,1+i)
&                          - yhat( data_point ,1+i)
100    continue
c   error( pointer+1, 1) = y( data_point+1, 2)
c   &                          - yhat( data_point ,2)
      do 110 i= 0, ( num_measur -1)
          sum_error_sq = sum_error_sq + error( pointer+i,1)**2
110    continue
c   &                          + error( pointer,1)**2

```

```

c      &          + error( pointer+1,1)**2
      return
      end

      subroutine jacobian( x, m, n, a, b, s0,
& num_state, num_par, partials)
c-----
c This routine defines the partial of the differential equations
c with respect to the states and the unknown parameters. This routine
c is absolutely required if the partials are required for explicit
c calculation. The jacobian can be numerically evaluated for
c "nice" equations with smooth derivatives. It is a significant
c savings in time to use explicitly defined partials.
c
c      functions called          none
c      subroutines called       none
c
c This specific routine is for the catalytic adsorption model
c  $dx(1)/dt = k1(g-x(1)(s-x(1)+x(2) -km1(x(1)-x(2))$ 
c  $dx(2)/dt = k2(x(1)-x(2))$ 
c  $y = g-x(1)-x(2)$ 
c-----
      implicit none
      logical partials
      integer*4 m,n
      integer*4 NUM_STATE, NUM_PAR
      real*8 x( m,n)
c s0 is an initial condition
      real*8 e1,e2,e3
      real*8 a( num_state, num_state)
      real*8 b( num_state, num_par)
      real*8 s0
      if ( partials) then
c-----
c      edit to reflect model
c      e1 = 0.0d0
c      e2 = 0.0d0
c      e3 = 0.0d0
c      a(1,1) = -x( 3,1)*( e1 +e2) -x( 4,1)
c      a(1,2) =  x( 3,1)*( e1 )   +x( 4,1)
c      a(2,1) =  x( 6,1)
c      a(2,2) = -x( 6,1)
c      b(1, 1) = e1 * e2
c      b(1, 2) = -e3
c      b(1, 3) = x( 3,1) * e1
c      b(1, 4) = 0.0d0
c      b(1, 5) = x( 4,1)* e2
c      b(2, 1) = 0.0d0
c      b(2, 2) = 0.0d0
c      b(2, 3) = 0.0d0
c      b(2, 4) = e3
c      b(2, 5) = 0.0d0
      else
      print *, 'Partials not defined for this model...'

```

```

        stop
    endif
c-----
    RETURN
    end

    REAL*8 FUNCTION FUNCOFX( x, t, m, n, xd, s0,j)
c-----
c This routine defines the function for the differential equations
c in question. It is absolutely required for explicit model
c calculation.
c
c     functions called      none
c     subroutines called   none
c
c-----
    implicit none
    integer*4 m,n
    integer*4 j
    real*8 x( m,n), xd( m,n),t
    real*8 e1
c s0 is initial conditions
c *****
c *   FUNCOFX MUST BE DEFINED FOR EACH NEW MODEL   *
c *****

    real*8 s0
    e1 = x( 8,1) - x( 1,1) + x( 2,1)

    if ( j .eq. 1) then
        funcofx = x( 5,1) * (x( 4,1) - x( 1,1))* e1

    elseif ( j .eq. 2) then
        funcofx = x( 6,1) * (x( 1,1) - x(2,1))

    elseif ( j .eq. 3) then
        funcofx = x( 7 ,1) * (x(2,1) - x(3,1))

    else
c experimental
c     print *, 'Improper function number called in FUNCOFX...'
c     stop
c 7/17/89 since x(4) is now a "state", must provide for its function
        funcofx = 0.0d0
    endif
    RETURN
    END

    subroutine seq_inject( no_injections, inject_time,
&         concentration, delta, s0, state, m,n, time,
&         max_inject, s0_original,
&         NUM_STATE, NUM_PARAM)
c-----
c This routine sets the value of s0 to that defined in the

```

```
c input data file at a specified time also specified in the
c input data file. In the method defined by f. wiseman, the
c actual value of s0 is set to a value that is increased by the
c current value of the states in the output equation.
```

```
c
```

```
c     functions called none
c     subroutines called none
```

```
c
```

```
c This specific routine is for 2nd order irreversible oxidation
c dx(1)/dt = a2*(a1-x(1)-x(3))*(a5-x(1)+x(2))
c dx(2)/dt = a3*(x(1)-x(2))
c dx(3)/dt = a4*(a1-x(1)-x(3))*(x(2)-x(3))
c y = a1-x(1)-x(3)
C UNUSED AT THIS TIME!
```

```
c-----
```

```
implicit none
integer*4 j, m, n
INTEGER*4 NUM_STATE, NUM_PARAM
integer*4 no_injections
integer*4 max_inject
real*8 state( m,n)
real*8 s0, delta, s0_original
real*8 inject_time( max_inject)
real*8 concentration(max_inject)
real*8 time
if ( time .lt. inject_time( 1) )then
    s0 = s0_original
else
    do 100 j = 1, no_injections
        if (( time .ge. inject_time( j) ).and.
&          ( time .lt. inject_time( j) + delta)) then
            s0 = concentration( j) + state( 1,1) +state( 3,1)
        endif
100    continue
endif
C    print *, time, s0
return
end
```